2004 Atomic, Molecular and Optical Sciences

Research Meeting

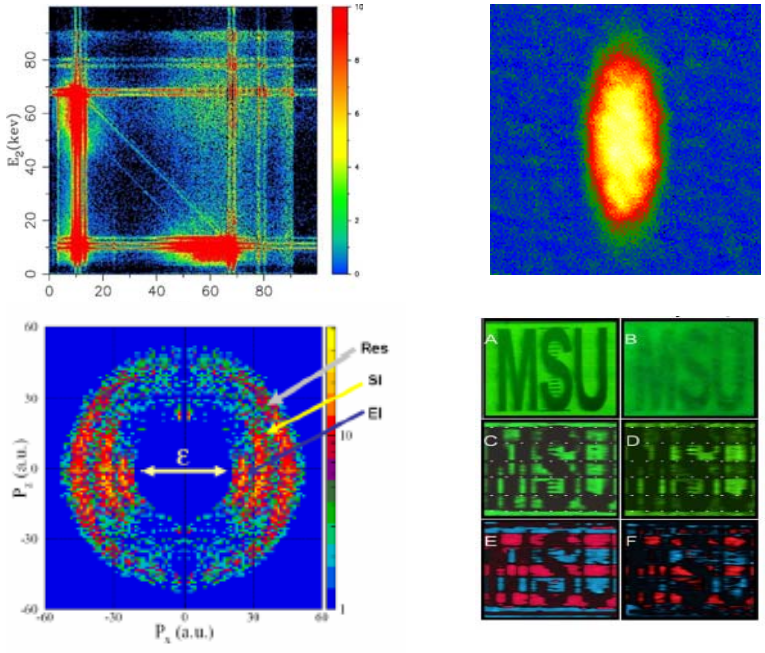

Airlie Conference Center
Warrenton, Virginia
September 12-15, 2004

Sponsored by:
U.S. Department of Energy
Office of Basic Energy Sciences
Chemical Sciences, Geosciences & Biosciences Division

This document was produced under contract number DE-AC05-00OR22750 between the U.S. Department of Energy and Oak Ridge Associated Universities.

Foreword

This volume summarizes the scientific content of the 2004 Research Meeting of the Atomic, Molecular and Optical Sciences (AMOS) Program sponsored by the U. S. Department of Energy (DOE), Office of Basic Energy Sciences (BES). This meeting is held annually for the DOE laboratory and university principal investigators within the BES AMOS Program in order to facilitate scientific interchange among the PIs and to promote a sense of program identity. The 2004 meeting will be highlighted by plenary speakers from several areas that are currently of intense scientific interest, namely, phenomena that take place at an attosecond time scale, the collision of low energy electrons with large molecules, and production of ultracold molecules.

While the BES AMOS Program funding has been essentially constant, we did add three new projects to the program, two theoretical and one experimental. We depict the path of diversity of the program on the front cover of this book with examples chosen from your abstracts. I apologize in advance for all the lovely examples that had to be omitted owing to lack of space. Beginning in the upper left hand corner and proceeding clockwise we have an illustration of two-photon decay of K-shell vacancies in gold following photoionization with synchrotron radiation from Argonne's Advanced Photon Source. The diagonal features corresponding to constant sum energy are due to two-photon decays filling the K vacancy. The next picture is a snapshot of a cloud of ultra cold ^{6}Li atoms experiencing oscillations near a Feshbach resonance to test pairing behavior of the atoms in the cloud. This is followed by an example where coherent control principles are used to achieve functional imaging through scattering by biological tissue (see page 144 in the abstract book for details). Finally, the last illustration is a momentum image of proton pairs produced in the double-ionization of H_2 by 12 fs, 3 x 10^{14} W/cm^2 laser pulses.

This is the program I was to shepherd for a little over a year until a permanent replacement could be found. What a pleasure it has been for me to work with all of you and to celebrate the outstanding contributions that you have made during the past year. I have learned a lot and thank you for your patience. Your new program manager, Michael Casassa, has joined the team, and I know you will enjoy working with him to make this an even more exceptional program. Finally, I want to thank all of you who have given of your valuable time toward the review of colleagues' proposals, either by mail review of grant applications or on-site reviews of multi-PI programs. Thorough and thoughtful reviews are absolutely vital to the continued scientific health and growth of the BES AMOS Program.

I gratefully acknowledge the contributions of this year’s speakers, particularly those not supported by the BES AMOS program, for their investment of time and for their willingness to share their ideas with the meeting participants. Thanks also to the staff of the Oak Ridge Institute of Science and Education, in particular Sophia Kitts, and Kellye Sliger, and the Airlie Conference Center for assisting with logistical aspects of the meeting. Last but not least I want to thank Eric Rohlfing and the rest of the members of the Chemical Sciences, Biosciences, and Geosciences Division for the pleasure of working with them and making my stay here most memorable and enjoyable.

David L. Ederer, Program Manager
Atomic, Molecular and Optical Sciences
Chemical Sciences, Geosciences and Biosciences Division
Office of Basic Energy Sciences
August 2004

Agenda

Agenda
U. S. Department of Energy
Office of Basic Energy Sciences
2004 Meeting of the Atomic, Molecular and Optical Sciences Program

Sunday, September 12

3:00-6:00 pm	**** Registration ****
6:00 pm	**** Reception (No Host) ****
7:00 pm	**** Dinner ****

Monday, September 13

7:00 am	**** Breakfast ****
8:00 am	*Introductory Remarks* **Michael Casassa**, BES/DOE
Session I	Chair: **Dave Ederer**
8:15 am	*Attosecond Physics Comes of Age* **Ferenc Krausz**, Max-Planck Institute for Quantum Optics, Garching
9:15 am	*Ultrafast X-Ray Coherent Control* **Phil Bucksbaum**, University of Michigan
9:45 am	*K Shell Photoionization of Singly Ionized Kr in a Synchrotron-Laser Pump-Probe Experiment* **Steve Southworth**, Argonne National Laboratory
10:15 am	**** Break ****
10:45 am	*Attosecond Atomic and Molecular Dynamics -- Some Theoretical Questions and Answers* **Chii-Dong Lin**, Kansas State University
11:15 am	*Laser-Produced Coherent X-Ray Sources* **Don Umstadter**, University of Michigan
11:45 am	*Rescattering ionization of small molecules in intense laser fields* **Lew Cocke**, Kansas State University
12:15 pm	**** Lunch ****
5:00 pm	**** Reception in Honor of New National Academy Members **** **** Margaret Murnane and Phil Bucksbaum **** and **Debbie Jin winner of a John D. and Catherine T. MacArthur Fellowship** (no host)
6:30 pm	**** Dinner ****

Session II Chair: **Steve Lundeen**

7:30 pm *Probing Dynamics and Structure in Atoms, Molecules and Negative Ions Using the Advanced Light Source*
Nora Berrah, Western Michigan University

8:00 pm *Properties of Transition Metal Atoms and Ions*
Don Beck, Michigan Technological University

8:30 pm *Mode-Specific Polyatomic Photoionization far from Threshold: Molecular Physics at Third Generation Light Sources*
Erwin Poliakoff, Louisiana State University

9:00 pm *Photoabsorption by Atoms and Ions*
Steve Manson, Georgia State University

Tuesday, September 14

7:00 am **** Breakfast ****

Session III Chair: **Vince McKoy**

8:00 am *Low energy electron interactions with condensed organic and biological molecules including DNA*
Léon Sanche, Université de Sherbrooke

9:00 am *Theoretical Studies of Resonant Electron-Polyatomic Collisions*
Anne Orel, University of California, Davis

9:30 am *Electron-Atom and Electron-Molecule Collision Processes*
Bill McCurdy, Lawrence Berkeley National Laboratory

10:00 am **** Break ****

10:30 am *Low-Energy Electron Interactions with Complex Targets*
Thom Orlando, Georgia Tech

11:00 am *Dynamics of Few-Body Atomic Processes*
Anthony F. Starace, University of Nebraska

11:30 am *Structure and Dynamics of Atoms, Ions, Molecules, and Surfaces: Molecular Dynamics with Ion and Laser Beams*
Itzik Ben-Itzhak, Kansas State University

12:00 pm **** Lunch ****

Session IV Chair: **Harvey Gould**

3:30 pm *Cooling of Molecules by a Single Inelastic Collision*
David W. Chandler, Sandia National Laboratory

4:30 pm *Ultracold Molecules: Physics in the Quantum Regime*
John Doyle, Harvard University

5:00 pm *Resonant Interactions in Quantum Degenerate Bose and Fermi Gases*
Murray Holland, University of Colorado

5:30 pm *Theoretical Investigations of Atomic Collision Physics*
Alex Dalgarno, Harvard University

6:00 pm **** Reception (No Host) ****

7:00 pm **** Dinner ****

Wednesday, September 15

7:00 am **** Breakfast ****

Session V Chair: **Linda Young**

8:00 am *Optical Two-Dimensional Fourier Transform Spectroscopy of Disordered Semiconductor Quantum Wells and Quantum Dots*
Steve Cundiff, JILA/University of Colorado

8:30 am *Enhanced, Ultrafast, Coherent, and Active Nanoplasmonics*
Mark Stockman, Georgia State University

9:00 am *Multiparticle Processes and Interfacial Interactions in Nanoscale Systems Built from Nanocrystal Quantum Dots*
Victor Klimov, Los Alamos National Laboratory

9:30 am *Measurement of Electron Impact Excitation Cross Sections of Highly Ionized Ions*
Gus Smith, Morehouse College

10:00 am **** Break ****

10:30 am *Electron/Photon Interactions with Atoms/Ions*
Alfred Msezane Clark Atlanta University

11:00 am *Two photon transitions*
Bob Dunford, Argonne National Laboratory

11:30 am *Recent Progress and New Opportunities for Ion-Atom Merged Beams at MIRF*
Charles Havener, Oak Ridge National Laboratory

12:00 pm *Closing Remarks*
Dave Ederer, BES/DOE

12:10 pm **** Lunch ****

Table of Contents

Invited Presentation (Ordered by Agenda)

Attosecond Physics Comes of Age
Ferenc Krausz ***1***

Ultrafast X-Ray Coherent Control
P.H. Bucksbaun and D. A. Reis ***2***

K-Shell Photoionization of Singly Ionized Kr in a Synchrotron-Laser Pump-Probe Experiment
S. H. Southworth, R. W. Dunford, D. L. Ederer, E. P. Kanter, B. Krässig, and L. Young ***7***

Theoretical Studies of Interactions of Atoms, Molecules, and Surfaces
C.D. Lin ***8***

Laser-Produced Coherent X-Ray Sources
Donald Umstadter ***12***

Structure and Dynamics of Atoms, Ions, Molecules, and Surfaces: Atomic Physics with Ion Beams, Lasers, and Synchrotron Radiation
C.L. Cocke ***16***

Probing Dynamics and Structure in Atoms, Molecules, and Negative Ions Using the Advanced Light Source
Nora Berrah ***20***

Properties of Transition Metal Atoms and Ions
Donald Beck ***24***

Mode-Specific Polyatomic Photoionization Far from Threshold: Molecular Physics at Third Generation Light Sources
Erwin Poliakaff ***28***

Photoabsorption by Atoms and Ions
Steven Manson ***29***

Low Energy Electron Interactions with Condensed Organic and Biological Molecules, including DNA
Léon Sanche ***33***

Theoretical Studies of Resonant Electron-Polyatomic Collisions
A.E. Orel… ***34***

Electron-Atom and Electron-Molecule Collision Processes
C.W. McCurdy and T.N. Reseigno ***36***

Low-Energy Electron Interactions with Complex Targets
Thomas Orlando ***40***

Dynamics of Few-Body Atomic Processes
Anthony Starace ***43***

Structure and Dynamics of Atoms, Ions, Molecules, and Surfaces: Molecular Dynamics with Ions and Laser Beams
Itzik Ben-Itzhak ***47***

Optical Trapping of Collisionally Cooled Molecules
David Chandler, James Valentini, and Mike Ellioff ***49***

Ultracold Molecules: Physics in the Quantum Regime
John Doyle ***51***

Resonant Interactions in Quantum Degenerate Bose and Fermi Gases
Murray Holland ***52***

Theoretical Investigations of Atomic Collision Physics
A. Dalgarno ***56***

Optical Two-Dimensional Fourier Transform Spectroscopy of Disordered Semiconductor Quantum Wells and Quantum Dots
Steven Cundiff ***60***

Femtosecond and Attosecond Laser-Pulse Energy Transformation and Concentration in Nanostructured Systems
Mark Stockman ***63***

Multiparticle Processes and Interfacial Interactions in Nanoscale Systems Built from Nanocrystal Dots
Victor Klimov ***67***

Measurement of Electron Impact Excitation Cross Sections of Highly Ionized Ions
A. J. Smith and D. L. Robbins ***71***

Electron/Photon Interactions with Atoms/Ions
Alfred Msezane ***74***

Two-Photon Decay
R. W. Dunfrod, E. P. Kanter, B Krässig, S. H. Southworth, L. Young, P.H. Mokler, and Th. Stöhlker ***78***

Recent Progress and New Opportunities for Ion-Atom Merged Beams at MIRF
C. C. Havener and R. Rejoub ***79***

Research Summaries (Multi-PI Programs by Institution)

AMO Physics at Argonne National Laboratory
R. W. Dunford, E. P. Kanter, B. Krässig, S. H. Southworth, L. Young ***.....81***

Structure and Dynamics of Atoms, Ions, Molecules, and Surfaces: Electronic Excitation of Highly Charged Ions and Nanotubes
P. Richard**.....89**

Attosecond Pulses and Femtosecond X-Ray Streak Camera
Zenghu Chang**.....93**

MOTRIMS Experiments at Kansas State University
B. D. DePaolat**.....97**

Laser Coulomb Explosion Imaging of Small Molecules
Igor Litvinyuk**.....101**

Time-Dependent Treatment of Three-Body Systems In Intense Laser Fields
B.D. Esry **.....103**

Interactions of Ions and Photons with Surfaces, and Molecules
Uwe Thumm**.....107**

Inner-Shell Photoionization of Atoms and Small Molecules at the Advanced Light Source
A. Belkacem, M. Prior and M. Hertlein**.....111**

Slow Molecules
Harvey Gould **.....115**

Femtosecond X-ray Beamline for Studies of Structural Dynamics
Robert W. Schoenlein **.....118**

Atomic and Molecular Physics Research at Oak Ridge National Laboratory
David R. Schultz**.....122**

Research Summaries (Single-PI Grants by PI)

Molecular Structure and Electron-Driven Dissociation and Ionization
Kurt H. Becker and Vladimir Tarnovsky**.....135**

Bose and Fermi Gases with Strong Anisotrpic Interactions
John Bohn**.....139**

Atomic and Molecular Physics in Strong Fields
Shih-I Chu ***142***

Coherent Control of Multiphoton Transitions in the Gas and Condensed Phases With Ultrashort Shaped Pulses
Marcus Dantus ***146***

Generation and Characterization of Attosecond Pulses
L. F. DiMauro, K. C. Kulander, I. A. Walmsley, and R. Boyd ***149***

High Intensity Laser Drive Explosions of Homo-nuclear and Hetero-Nuclear Molecular Clusters
Todd Ditmire ***153***

Reaction and Fragmentation Interferometry
James Feagin ***158***

Studies of Autoionizing States Relevant to Dielectronic Recombination
T. F. Gallagher ***162***

Experiments in Molecular Optics
Robert Gordon ***165***

Experiments in Ultracold Collisions
Phillip Gould ***168***

Physics of Correlated Systems
Chris Greene ***171***

Chemistry with Ultracold Molecules
Dudley Herschbach ***174***

Exploring Quantum Degenerate Bose-Fermi Mixtures
Deborah Jin ***177***

Using Intense Short Laser Pulses to Manipulate and View Molecular Dynamics
Robert R. Jones ***181***

Physics of Low-Dimensional Bose-Einstein Condensates
Eugene Kolomeisky ***185***

Ion/Excited-Atom Collision Studies with Rydberg Target and a CO_2 Laser
Stephen Lundeen ***189***

Theory of Fragmentation and Rearrangement Processes in Ion-Atom Collisions
J. H. Macek ***193***

Electron Driven Processes in Polyatomic Molecules
Vincent McKoy ***197***

Ultrafast Atomic and Molecular Optics at Short Wavelengths
Henry Kapteyn and Margaret Murnane ***201***

Theory and Simulations of Ultrafast Nonlinear X-Ray Spectroscopy of Molecules
Shaul Mukamel and Luke Campbell ***205***

Ultrafast Coherent Soft X-Rays: A Novel Tool for Spectroscopy of Collective Behavior in Complex Materials
Keith Nelson ***209***

Localized Photoemission from Gold Nanostructures and Electromagnetic Friction
Lukas Novotny ***213***

Energetic Photon and Electron Interactions with Positive Ions
Ronald Phaneuf ***217***

Control of Molecular Dynamics: Algorithms for Design and Implementation
Herschel Rabitz and Tak-San Ho ***221***

Cold Rydberg Atom Gases and Plasmas in Strong Magnetic Fields
G. Raithel ***225***

A Dual Bose-Einstien Condensate: Towards the Formation of Heteronuclear Molecules
Chandra Raman ***229***

Atomic Physics Based Simulations of Ultra-Cold Plasmas
F. Robicheaux ***233***

Ultrafast Tabletop Laser Pump—X-Ray Probe Measurement of Solvated $Fe(Cn)_6^{4-}$
Taewoo Lee, Frank Benesch, Yan Jiang, and Christoph G. Rose-Petruck ***237***

Development and Utilization of Bright Tabletop Sources of Coherent Soft X-ray Radiation
Jorge Rocca, Henry Kapteyn, and Carmen Menoni ***240***

New Directions in Intense-Laser Alignment
Tamar Seideman ***244***

Inner-Shell Electron Spectroscopy and Chemical Properties of Atoms and Small Molecules
T. Darrah Thomas ***248***

Quantum Dynamics of Ultracold Fermionic Vapors
John E. Thomas ***252***

Invited Presentations

(ordered by agenda)

Attosecond Physics Comes of Age

Ferenc Krausz

Photonics Institute, Vienna University of Technology, Gusshausstr. 27/387, A-1040 Wien, Austria, Max Planck Institute for Quantum Optics, D-85748, Garching, Germany
Email: ferenc.krausz@mpq.mpg.de

Abstract

Atoms exposed to a few oscillations cycles of intense visible or near-infrared light are able to emit a single electron and X-ray photon wavepacket of sub-femtosecond duration. Precise control of these sub-femtosecond wavepackets have recently been achieved by full control of the electromagnetic field in few-cycle light pulses. Sub-femtosecond X-ray pulses along with intense, synchronized, few-cycle laser pulses offer an attosecond-resolution sampling system for both characterizing the pulses themselves (attosecond diagnostics) and tracing atomic (or molecular) processes (attosecond spectroscopy) in time-resolved measurements. Proof-of-principle attosecond experiments will be presented.

Ultrafast X-Ray Coherent Control

P.H. Bucksbaum* and D. A. Reis

FOCUS Center and Department of Physics, University of Michigan.†

(Dated: August 20, 2004)

This is a program to develop ultrafast x-ray physics at synchrotrons and linear accelerators. The research is carried out at the Advanced Photon Source sector 7, with the MHATT-CAT collaboration; and at the Stanford Linear Accelerator Center, with the SPPS collaboration. This 3-year renewal will overlap the concluding period of SPPS, and the construction period for LCLS. Our research will develop the ultrafast physics techniques on this machine, and the associated work on existing 3rd generation machines.

I. INTRODUCTION

This is a program to develop ultrafast x-ray physics at synchrotrons and linear accelerators. The research is carried out at the Advanced Photon Source sector 7, with the MHATT-CAT collaboration; and at the Stanford Linear Accelerator Center, with the SPPS collaboration. There are three aspects to developing ultrafast science at electron accelerators: (1) Source development; (2) development of techniques to use the source; (3) development of new science at the source.

Our program is presently developing three approaches to the source and techniques problems. The first approach is an ultrafast x-ray switch, based on coherent control of high amplitude phonons in Bragg scattering mirrors or filters. A switch based on the highest frequency optical phonons could in principle create x-rays as short as 12 fs. The switch has been demonstrated to have 30 ps turn-on time using lower-frequency acoustic phonons. However, recent results of melting experiments at SPPS indicate that reversible structural phase transitions can change the intensity of a diffracted x-ray beam in under 1 ps, and this may lead to methods for much faster switches. In the next grant period, we will continue to develop these. The experiments will make use of a laser upgrade program underway at our beam line at the APS (see page **??**)

A second approach is to use an x-ray streak camera with approximately 1 ps resolution to observe transient phenomena illuminated by the 100 ps APS x-ray beam. Our streak camera uses the meander plate technique invented by Zenghu Chang [1]. There are some ideas that may shorten the resolution to a fraction of a picosecond. This streak camera will become part of the suite of equipment available at our APS beamline.

Alternatively, we can compress highly relativistic electrons in a linear accelerator, where bunch lengths can be shortened to less than 100 fs. When these ultrashort electron bunches travel through an undulator, they produce ultrafast pulses of x-rays. We have recently demonstrated this as part of the Sub-Picosecond Pulse Source (SPPS) experiment at the

*Electronic address: phb@umich.edu

†URL: http://www.umich.edu/~focuspfc

Stanford Linear Accelerator Center (SLAC). SPPS will continue for the first part of our next grant period, and we are committed to continue to develop ultrafast x-ray physics there.

Our success at the SPPS in electro-optic timing of the x-rays has created the possibility of real ultrafast pump-probe experiments. In our next grant period, we plan to devote considerable effort to developing the techniques that will make this a reality.

Advanced ideas Electron bunching may also be possible at synchrotron storage rings [2]. Developing this technique is outside the resources of this grant; however, through a number of workshops, and discussions with management accelerator physicists, we have been actively trying to generate interest at the APS to pursue this route. Similarly, we plan on continuing our activities to help develop ideas for new source development, whether this be for LCLS at SLAC, LUX at Berkeley, or elsewhere.

The science applications that we feel we can study in the next period are as follows:

- Optical Phonon dynamics in solids, at APS and SPPS
- Ultrafast X-ray switch at APS
- Strong Field Molecular Alignment, at APS and SPPS
- Electro-optic measurements for timing synchronization at SLAC

II. RESULTS OF PRIOR RESEARCH

A. Laser at APS 7ID-D

B. Characterization of Ultrafast Strain Generation

The first experiment performed with the synchronized laser on sector 7 was a measurement of a coherent acoustic wavepacket (coherent strain) generated in impulsively laser-excited InSb. Coherent strain is one of the foremost responses to pulsed laser absorption when the pulse duration is short compared to the sound propagation time across the laser absorption depth [3, 4]. If the transverse size of the laser is large compared with the absorption length, then the resultant strain will be primarily uniaxial (longitudinal phonons). Strains on order of a percent, pressure of many Mbars, and frequencies up to tens of GHz are not uncommon ($\sim$ THz in superlattices).

False color images of the time-resolved diffraction pattern for laser excited InSb as a function of angle and time-delay are given in Fig **??** [5]. The large flux at the APS makes it possible to study the initial excitation and subsequent motion of the lattice in much greater detail than ever before, and we are able to make quantitative comparisons to the existing thermoelastic model [3]. X-ray diffraction resolves the transient strain into surface heating (thermal expansion) and coherent acoustic components. We find that the model calculations significantly underestimates the contribution of coherent acoustic phonons to the overall strain [5]. Similarly in the case of laser excited Ge we find that the thermoelastic model is not as important as carrier diffusion and electron-phonon coupling through the so-called deformation potential. Unlike Ge; however, diffusion is not important in InSb[6]. These two cases illustrate how detailed measurements of strain using x-ray diffraction can yield important information about the widely varying generation processes. Our technique has been featured in the National Academies Publication, *Frontiers in High Energy Density Physics*[7]

C. Coherent Control of Pulsed X-rays

A number of successful experiments on x-ray modulation and x-ray switching experiments were conducted during the just-finished grant period, in transmission geometries in crystalline Ge.

We were the first to propose the use of impulsive strain and the Borrmann effect to modulate x-ray pulses on an ultrafast time-scale. The excitation transfers energy between two spatially separated x-ray beams (the forward-diffracted and deflected-diffracted beams) initially in a time shorter than the synchrotron pulse duration. These two beams are linear combinations of two internal x-ray modes. The oscillations are the temporal analog of Pendellösung, and they result from interferences between these modes. The acoustic pulse is spatially thin and can be approximated as dividing the crystal into two unperturbed regions separated by a moving interface (one region increases in thickness at the speed of sound while the other decreases). It is the interface that acts to redistribute population in the internal x-ray modes, an unperturbed region is required as a phase-advance in which the interference effects build up. The time-scale of the oscillation corresponds to the Pendellösung length (the beat length between the modes) divided by the speed of sound. By simply adjusting the delay between the x-rays and the acoustic pulse one can coherently control the exit beams to preferentially switch energy from one beam to another, modulate the two beams together, and even enhance the anomalous transmission.

This work was published in *Nature* [10]. It has been the subject of a number of popular articles [11–13]in part because of its potential application as an ultrafast x-ray switch, for the results may be scaled to faster processes using optical phonon or other excitations.

D. Supersonic Strain Front Propagation

It is of interest to probe the mechanism responsible for the rapid switching of the x-ray intensities immediately following the laser-excitation. According to the results described above, greater than 75% of the energy is transferred between the two spatially coherent beams in a time shorter than the 100 ps resolution of the experiment (limited by the x-ray probe duration) [14]. If one scales this modulation with the Pendellösung length, this suggests that the energy transfer occurs over a depth that is many times greater than the laser penetration depth (in a time which is much shorter than the corresponding acoustic transit time). Subsequent measurements with an x-ray streak camera reveal this transient to occur in ~ 30 ps a seemingly unphysical suggestion that the strain pulse initially advances at about 8 times the speed of sound.

Detailed experiments were performed to reveal the true mechanism for the fast energy transfer. This work appeared in *Physical Review Letters* [14].

E. Optical phonon switches

Faster switching times could be achieved if we utilized high amplitude optical phonon distortions in x-ray scattering. We studied this during the grant period as well. We investigated whether high-energy ultrafast laser pulses might induce large amplitude coherent motion of crystalline lattices through impulsive stimulated Raman scattering. These large lattice distortions could then modulate x rays on an ultrafast time scale. We reported non-

linear excitation of high amplitude coherent optical phonon oscillations in Bi, measured by optical reflectivity changes larger than 1% Our calculations showed that this corresponds to lattice deformations of $0.1\mathring{A}$. As the amplitude of the optical phonon increases, a frequency shift is observed [15]. The lattice deformation of laser-excited Bismuth films has also been studied using laser-plasma x-rays as a structural probe, and the results make this look like a promising x-ray switch [16]

F. Single Shot Timing Measurements at SPPS

SPPS (the sub-picosecond pulse source) is an experiment at SLAC to produce and use sub-100 fs hard x-rays. The SLAC linac sends ultra-short electron bunches through an undulator to produce short-pulse, high-brightness X-rays. The 3 nC electron bunches are chirped in energy, and then sent to a bunch compressor chicane similar to the one designed for LCLS, and a final compression stage following acceleration to 28 GeV. Final electron pulse widths are on the order of 80 fs FWHM. A 5 m undulator produces 10^7 1.5 Angstrom X-rays at 10 Hz. SPPS tests many of the technical concepts needed for LCLS, in the production of the electrons, as well as the use of the x-rays.

Our Michigan group assumed the task of designing techniques to perform pump-probe experiments using the SPPS source. The principal problem is synchronization. Since these x-rays are produced far from the experimental area, and not naturally synchronized to the laser, sophisticated methods are required to deliver timing signals with sub-picosecond precision. We have considerable experience in locking a KLM laser to an external RF source, but this does not eliminate jitter of the electrons with respect to the RF, which can be on the order of a picosecond. To overcome this, we proposed to use electro-optic sampling of the coherent THz radiation produced by the relativistic electrons to establish the relative arrival time of the x-rays and the laser. We designed and implemented a vacuum chamber just upstream from the undulator, containing a 200 μm ZnTe crystal placed only 1cm from the electron beam. Part of the light from the laser system is split off *before amplification*, and sent to the EO apparatus through 150m of single-mode, polarization-preserving fiber. To make sure that short pulses arrived at the EO crystal, the light was pre-dispersed in a negative-dispersion grating expander and a liquid-crystal pulse shaper [17]. The pulse shape was optimized using a Genetic Algorithm, developed originally for coherent control problems. A report on this work is in preparation.

SPPS, and our part in it, has been very successful in our first year of operation. We have demonstrated short-term stability of the laser-x-ray synchronization of under 1 ps. We have measured the correlation between the x-rays and the laser, and we have shown that the timing uncertainty can be reduced to under 50 fsec by shot-by-shot EO sampling measurements to correct the time axis on pump-probe experiments.

---

[1] J. Liu, J. Wang, B. Shan, C. Wang, and Z. Chang, Applied Physics Letters **82**, 3553 (2003).

[2] A. Zholents, P. Heimann, M. Zolotorev, and J. Byrd, Nuclear Instruments and Methods A **425**, 385 (1999).

[3] C. Thomsen, H. Grahn, H. Maris, and J. Tauc, Phys. Rev. B **34**, 4129 (1986).

[4] S. Akhmanov and V. Gusev, Soviet Phys. Usp. **35**, 153 (1992).

[5] D. A. Reis, M. F. DeCamp, P. H. Bucksbaum, R. Clarke, E. Dufresne, M. Hertlein, R. Merlin, R. Falcone, H. Kapteyn, M. M. M. J. Larsson, et al., Phys. Rev. Lett. **86**, 3072 (2001).

[6] M. F. DeCamp, D. A. Reis, D. M. Fritz, P. H. Bucksbaum, E. M. Dufresne, and R. Clarke, submitted to J. Synch. Rad. (2004).

[7] Frontiers in High Energy Density Physics: The X-games of Contemporary Science, National Acadamies Press, 2003.

[8] B. Batterman and H. Cole, Rev. Mod. Phys. **36**, 681 (1964).

[9] W. Zachariasen, *Theory of X-ray diffraction in crystals* (John Wiley and Sons, Inc., 1945).

[10] M. F. DeCamp, D. A. Reis, P. H. Bucksbaum, B. Adams, J. M. Caraher, R. Clarke, C. W. Conover, E. M. Dufresne, R. Merlin, V. Stoica, et al., Nature **413**, 825 (2001).

[11] F. Krausz and C. Spielmann, Nature **213**, 784 (2001).

[12] FAST SWITCH X-RAY (C&EN: NEWS OF THE WEEK - FAST SWITCH X-RAY)", Chemical & Engineering News, 79 (44), October 29,2001
C&EN: CHEMISTRY HIGHLIGHTS 2001 - PHYSICAL CHEMISTRY", Chemical & Engineering News, 79 (50) 2001.

[13] R. Fitzgerald, Physics Today (2002).

[14] M. F. DeCamp, D. A. Reis, A. Cavalieri, P. H. Bucksbaum, R. Clarke, R. Merlin, E. M. Dufresne, D. A. Arms, A. M. Lindenberg, A. G. MacPhee, et al., Phys. Rev. Lett **91**, 165502 (2003).

[15] M. F. DeCamp, D. A. Reis, P. H. Bucksbaum, and R. Merlin, Phys. Rev. B **64**, 092301 (2001).

[16] K. Sokolowski-Tinten, C. Blome, J. Blums, A. Cavalleri, C. Dietrich, A. Tarasevitch, I. Uschmann, E. Förster, M. Kammler, M. Horn-von Hoegen, et al., NATURE **422**, 287 (2003).

[17] S. H. Lee, A. L. Cavalieri, D. M. Fritz, M. Myaing, and D. A. Reis, arXiv:physics/0406081 (submitted to Opt. Lett.) (2004).

K-Shell Photoionization of Singly Ionized Kr in a Synchrotron-Laser Pump-Probe Experiment

S. H. Southworth, R. W. Dunford, D. L. Ederer, E. P. Kanter, B. Krässig, and L. Young*
Argonne National Laboratory, Argonne, IL 60439

Various methods are being developed that use x-ray pulses to probe the time evolution of a dynamical process (electronic excitation; molecular alignment) initiated by a pulsed optical laser. At sector 7 at the Advanced Photon Source, a Ti:sapphire oscillator (800 nm, 88 MHz, 1 nJ, 50 fs) is phase locked to the storage-ring RF and hence is synchronized with the x-ray pulses produced by an undulator beamline with a double-crystal monochromator [1]. For the present experiment, a Ti:sapphire amplifier was used to produce optical pulses (800 nm, 887 Hz, 0.3 mJ, 60 fs) at low repetition rate but much higher energy. A rate of 887 Hz was chosen to match 1/3 of the x-ray pulses (2.66 kHz, 87 ps) transmitted by a mechanical chopper with the storage ring running in isolated-singlet mode. The laser beam was focused to 30 μm diameter over a Rayleigh range of ≈3 mm within an effusive jet of Kr atoms (≈10^{13} atoms/cm^3). The laser intensity within the focal volume (≈6×10^{14} W/cm^2) exceeded the intensity of 2×10^{14} W/cm^2 expected to saturate ionization of the Kr 4p electron (14 eV binding energy). Using Kirkpatrick-Baez mirrors, the x rays were focused to ≈10 μm × 16 μm with a flux ≈4×10^5/pulse and sampled the central portion of the laser focal volume after a delay of 12 ns. A Si(Li) detector viewing the interaction region recorded prompt x-ray fluorescence following K-shell excitation or ionization of either Kr or Kr^+. By scanning the beamline monochromator and recording the x-ray fluorescence yield, the near-edge x-ray absorption spectra were recorded concurrently for laser-on and laser-off conditions. We observed a distinct 1s → 4p pre-edge resonance at 14.313 keV in the laser-produced Kr^+ ions that is absent from the absorption spectrum of neutral Kr with its filled $4p^6$ subshell.

In follow up measurements with the laser only, an electrostatic analyzer and conventional ion time-of-flight methods were used to study the assembly of ≈10^7 ions produced by each laser pulse. The measurements suggest that the photoelectrons escape rapidly, leaving an assembly of ions that Coulomb explodes, as indicated by the Kr^+ kinetic energy distribution that extends to ≈80 eV. Higher charge states are also observed at energies up to ≈200 eV. The ion kinetic-energy distributions vary with gas density and laser-pulse energy. The focused x rays provide a penetrating probe of this ionized matter with spatial resolution ≈10 μm and temporal resolution ≈ 100 ps. In future experiments the dynamics of the ion assembly will be studied by varying the time delay between the laser and x-ray pulses. We will also record the entire pre-edge and continuum region for comparison with calculated x-ray absorption spectra of Kr ions. The laser system will be upgraded with a new amplifier and pump laser that will provide higher pulse energy and repetition rate and variable pulse width to enable dressed-atom experiments.

*Work done in collaboration with E. C. Landahl and J. Rudati (Advanced Photon Source).

[1] D. A. Reis *et al.*, Phys. Rev. Lett. **86**, 3072 (2001).

Theoretical Studies of Interactions of Atoms, Molecules and Surfaces

C. D. Lin
J. R. Macdonald Laboratory
Kansas State University
Manhattan, KS 66506
e-mail: cdlin@phys.ksu.edu

In this abstract I report recent progress and future plans in the theoretical studies involving atoms and molecules within my group. References to our published papers or preprints (full list given at the end of this report) are given in bold letters in the text.

1. **Interaction of intense laser fields with molecules and molecular clocks**

Recent Progress:

Following the initial idea of Corkum [Niikura et al., Nature 417, 917 (2002); 421, 826 (2003)], we have engaged in a detailed theoretical study of the ionization of D_2 (or H_2) molecules in an intense laser field resulting in their dissociation or ionization with the emission of D^+ ions. From the kinetic energy release it has been shown that physical processes leading to the ionization can be probed with subfemtosecond accuracy.

We first concentrate on the lower intensity region where the peak laser intensity is of the order of $2x10^{14}W/cm^2$ in the so-called nonsequential double ionization regime. Due to the lower ionization potential, the D_2 is first ionized at the initial phase of the laser pulse. This initial ionization embarks a correlated electron wave packet and a nuclear wave packet. The nuclear wave packet will propagate to larger internuclear separations and spreads as the time increases. In the meanwhile, the ionized electron is driven by the oscillating laser field and can return to the ion core at about 2/3 of an optical cycle later to excite or ionize the D_2^+ to an excited state. Once in the excited states, the D_2^+ can dissociate to form $D+D^+$, with the kinetic energy release reflecting the internuclear distance where the excitation occurs. The excited D_2^+ can also get ionized by the laser pulse when it reaches peak fields again at later cycles. The second ionization results in $D^+ + D^+$, again with kinetic energies reflecting where the ionization occurs.

The initial ionization, the rescattering by the returned electron, and the further ionization of D_2^+, all occur at characteristic times in terms of the optical cycles of the laser pulse. Each event occurs within subfemtoseconds. Thus if the ionization mechanisms are fully understood, then from the measured kinetic energy release of D^+, we can answer when the ionization or the excitation occurs, thus reading the molecular clock up to sub-fs accuracy.

This work has been completed. The whole theory is presented in details in paper **A1**. In **A2** we show how to read the molecular clocks accurately using lasers of different mean wavelengths. We have found that most of the D^+ comes from the double ionization instead of dissociation after the first ionization, and the results have been confirmed by experiments carried out by Lew Cocke's group (presented in the joint theory and experimental paper, **A3**). This work has attracted the attention of the editor of International Journal of Modern Physics, and we were invited to present a review paper for that journal (**A4**).

In the sequential double ionization region (peak intensity greater than 10^{15} W/cm^2) , the double ionization of D_2 can also be used to measure the time between the two ionizations as well, as demonstrated in the experiment of Legare et al [Phys. Rev. Lett. 91, 093002 (2003)]. We have formulated and performed calculations for such experiments and a paper has been submitted and accepted by Phys. Rev. A (**B2**).

In the intermediate intensity region, both mechanisms discussed above can contribute to the double ionization and distinct peaks can be observed. The experimental result from Cocke's group has been explained using our calculations, and a paper has been submitted to Phys. Rev. Lett. (see Cocke's report).

Future Plans.

Recently Cocke's group have studied the angular distributions of the breakup of N_2 and O_2 molecules and found distinctly different patterns for short pulses and long pulses. For laser pulses of durations of tens of femtoseconds it was generally believed that the molecules are not aligned by the laser fields. In view of the observations, we reexamined the dynamic alignment effect of molecules. Using the molecular ADK theory developed previously we show that molecules are aligned in a much shorter time scale, i.e., within tens of femtoseconds, much shorter than previously believed. This work is being investigated in more details.

2. **Attosecond Physics: Theory of laser-assisted autoionization by attosecond light pulses**

Recent Progress:

With the recently developed attosecond XUV (extreme ultraviolet) light pulses, it has been demonstrated that it is possible to obtain a time-resolved image of an Auger decay [Drescher et al, Nature 419, 803 (2003)], akin to the time-resolved spectroscopy for tracking atomic motion in molecules with femtosecond laser pulses. Limited by the pulse intensity, currently experimentalists employed XUV pump-IR(infrared) laser probe technique where electrons generated by the XUV pulses are steered in the few-cycle IR laser pulses by varying the pump-probe time delays. To extract the Auger lifetime, or in general, the properties of an autoionizing state, a quantum mechanical theory of the laser-assisted autoionization is needed. We have developed such a theory under the so-called strong field approximation (SFA). The SFA has been used for laser-assisted photoionization by attosecond light pulses. Our theory accounts for the interference effect and we have found a way to extract the lifetime or resonance width from such measurements. This work has been submitted to PRL for publications(**B3**).

Future plans:

We are developing computer codes that would allow us to do *ab initio* calculations involving two-electron atoms in a time-dependent laser + XUV attosecond pulses. Our goal is to go beyond the SFA. We expect that new effects stemming from the Stark field of the laser field will modify the motion of the two electrons significantly. We hope to study whether the normal modes of the joint motion (the rovibrational modes) of the two electrons that we learned from the energy domain analysis can be probed directly in the time-domain with the use of attosecond light pulses.

In collaboration with the experimental group (Chang) at KSU, we are also looking into the issue of how to characterize an attosecond light pulse.

3. Hyperspherical approach for low-energy rearrangement collisions

Recent Progress:

As first reported in the last DOE meeting we have developed a hyperspherical close coupling method (HSCC) for ion-atom collisions at low energies. The HSCC theory is free from the series difficulties of the standard close-coupling method based on the molecular orbitals where the difficulties are taken care *approximately* using electron translational factors or the reaction coordinates. In the past year, we have performed a number of calculations, mostly to resolve the outstanding discrepancies that are known to exist in the literature. We first calculated the charge transfer cross sections for Si^{4+} on H(D) and Be^{4+}+H collisions where good experimental data are available for comparison (**A5**). We then performed calculations for H^++Na where we concluded that the existing experimental data are not correct and that one of the earlier calculations based on the molecular orbital theory is also incorrect (**A6**). We also examined the excitation and charge transfer cross sections to n=2 states in H^++H collisions below 1 keV and concluded that the recent calculations based on the three-center atomic orbital expansion method is likely to be in errors (**A7**). Similarly, we revisited total charge transfer cross sections for C^{4+}+H collisions. We confirmed that the outstanding discrepancy with calculations lies mostly on the experimental side (**A8**).

For low-energy ion-atom collisions, one of the most elaborate theoretical methods is the use of reaction coordinates (instead of internuclear distance) within the molecular approach. This

method is computationally rather complicated but when properly done, it appears that the results are often in agreement with the HSCC method. We thus carried out a joint comparative study between the two methods for He^{++}+H collisions and check for the agreement within the partial wave cross sections. The agreement is quite good, thus making us to conclude that the reaction coordinate approach, despite of its ad hoc assumptions, does appear to be a practical method for obtaining reliable cross sections (**A9**).

In the meanwhile, in response to the recent experiment at KSU we have calculated the charge transfer cross sections for O^{8+} and Ar^{8+} on H, and the results are shown to be in good agreement with experiment (**A10**).

Future plans:

In connection with the HSCC method we have also developed a diabatization procedure which allows us to carry out the calculations using diabatic basis functions. This also offers the opportunity to eliminate channels which are considered unimportant for the processes of interest. We have applied this method to carry out charge transfer cross sections in O^{8+}+H to show that reliable cross sections can be obtained using a small number of channels (**A11**). We have also applied the method to study protonium formation in collisions between antiprotons with H, but assuming that the mass of (anti)proton to be 100. Again we showed that a truncated basis set is adequate (**A12**). In the coming months, we will extend the HSCC to a number of ion-atom, electron-atom and positron-atom collisions, especially systems involving highly excited states where channel elimination will be desirable, not only in simplifying the calculations but also in physical understanding of the calculations.

4. **Quadruply excited states of atoms**

(with T. Morishita, University of Electrocommunications, Tokyo, Japan)

Recent Progress:

In the past year we have succeeded in formulating and completing the calculations of adiabatic potential curves and analyzing the channel functions for Be within the so-called s^4 model where the orbital angular momentum of each electron is set to zero. This model allows us to analyze the nodal structures of singly, doubly, triply and quadruply excited states of an atom on equal footing (**B4**). Thus we have the tools to calculate quadruply excited states using the hyperspherical approach since it is straightforward to enlarge the basis set to remove the restriction of the s^4 model. However, there are no such experimental studies in sight and the work is rather complicated, we do not have a plan to extend this investigation in the coming year.

5. **Doubly excited states of atoms in a strong static electric field**

As a byproduct of our studies of two-electron atoms in an attosecond light pulse we have studied the 2l6l' and 2l7l' doubly excited states of He in a strong electric field in view of the recent experiment [Harries, PRL90, 133002, (2003)]. We have performed calculations in hyperspherical coordinates and found the propensity rule identifying what new doubly excited states are prominently populated due to the Stark effect. This work has been completed and published in PRL (**A13**). This study opens up many new opportunities. In the coming year we will examine the Stark effect by looking at the radiative decay channels where experiment is being carried out. We will examine doubly excited states of two-valence electron systems as well. This work provides guidance for analyzing the Stark effect of doubly excited states which can be studied using the present-generation synchrotron lights.

Publications (A1-13 new papers since last DOE meeting. Nine papers from 2002 not listed)

A1. X. M. Tong, Z. X. Zhao and C. D. Lin, "Correlation dynamics between electrons and ions in the fragmentation of D_2 molecules by short laser pulses", ***Phys. Rev. A68, 043412 (2003).***

A2. Z. X. Zhao, X. M. Tong and C. D. Lin, " Probing Molecular Dynamics at Attosecond Resolution with Femtosecond Laser Pulses", ***Phys. Rev. Lett. 91, 233203 (2003).***

A3. A. S. Alnaser, T. Osipov, E. P. Benis, A. Wech, C. L. Cocke, X. M. Tong and C. D. Lin, "Rescattering double ionization of D_2 and H_2 by intense laser pulses", ***Phys. Rev. Lett. 91, 163002 (2003)***

A4. X. M. Tong and C. D. Lin, "How to read a molecular clock with sub-femtosecond accuracy", ***International J. of Mod. Phys. B18, 1659-1678 (2004).***

A5. A. T. Le, M. Hesse, T. G. Lee and C. D. Lin, "Hyperspherical close coupling calculations for charge transfer cross sections in Si^{4+} +H(D) and Be^{4+} +H collisions at low energies, ***J. Phys. B36, 3281 (2003).***

A6. A. T. Le, C. N. Liu and C. D. Lin, "Charge transfer in slow collisions between H^+ with Na", ***Phys. Rev. A 68, 021705 (2003).***

A7. T. G. Lee, A. T. Le and C. D. Lin, "Charge transfer and excitation in slow 20 eV-2 keV H^+ +D(1s) collisions", ***J. Phys. B36, 4081 (2003)***

A8. C. N. Liu, A. T. Le and C. D. Lin, "Charge transfer in slow collisions of C^{4+} with H below 1 keV/amu", ***Phys. Rev. A 68, 062702 (2003)***

A9. A. T. Le, C. D. Lin, L. F. Errea, L. Mendez, A. Riera and B. Pons, "Comparison of hyperspherical vs Common Reaction Coordinates Close-Coupling Methods for Ion-atom Collisions at Low Energies", ***Phys. Rev. A 69, 062703 (2004)***

A10. E. Edgu-Fry, A. Wech, J. Stuhlman, T. G. Le, C. D. Lin and C. L. Cocke," Cold target recoil-ion momentum spectroscopy of capture from atomic and molecular hydrogen by O^{8+} and Ar^{8+}", ***Phys. Rev. A 69, 052714 (2004)***

A11. Teck G. Lee, Anh-Thu Le and C. D. Lin, "Charge transfer in slow collisions of O^{8+} and Ar^{8+} with H below 1 keV/amu", ***Phys. Rev. A 70, 012702 (2004)***

A12. M. Hesse, A. T. Le and C. D. Lin, "protonium formation in pbar-H collision at low energies by a new diabatic approach", ***Phys. Rev. A 69, 052712 (2004)***

A13. X. M. Tong and C. D. Lin, " Propensity rule for novel selective double photoexcitation of helium atoms in intense static electric fields", ***Phys. Rev. Lett. 92, 223003 (2004)***

A14. Z. X. Zhao, X. M. Tong and C. D. Lin, "Determination of the alignment dependent ionization probability of molecules in a double pulse laser experiment", ***Phys. Rev. A67, 043404 (2003).***

A15. X. M. Tong, Z. X. Zhao and C. D. Lin, "Abnormal pulse duration dependence of ionization probability of Na atoms in intense laser fields", ***J. Phys. B36, 1121 (2003).***

A16. C. N. Liu, A.T. Le, Toru Morishita, B. D. Esry and C. D. Lin, "Hyperspherical Close Coupling Calculations for Charge Transfer Cross Sections in He^{2+}+H(1s) Collisions at Low Energies," ***Phys. Rev. A67, 051801 (2003)***

A17. Toru Morishita and C. D. Lin, "Radial and Angular Correlations and the classification of intershell 2l2l'3l" triply excited states of atoms," ***Phys. Rev. A67, 022511 (2003).***

A18. M. Zamkov, E. P. Benis, C. D. Lin, T. Morishita, P. Richard, T. G. Lee and T. J. M. Zouros, "Experimental observation and theoretical calculations of triply excited $2s2p^2$ (S, P, D) and $2p^3$(P,D) states of fluorine," ***Phys. Rev. A67, 050703 (2003).***

Preprints (As of August 1, 2004)

B1. X. M. Tong, Z. X. Zhao and C. D. Lin, "Molecular Tunneling ionization and rescattering induced double ionization of H_2 and D_2 molecules", J. of Modern Optics (accepted)

B2. X. M. Tong and C. D. Lin, "Time-resolved sequential double ionization of D_2 molecules in an intense few-cycle laser pulse", Phys. Rev. A (accepted)

B3. Z. X. Zhao and C. D. Lin, "Theory of laser-assisted autoionization by attosecond light pulses", submitted to Phys. Rev. Lett.

B4. Toru Morishita and C. D. Lin, "Hyperspherical analysis of radial correlations in four-electron atoms", submitted to Phys. Rev. A.

Laser-Produced Coherent X-Ray Sources

Donald Umstadter
1006 Gerstaker Bldg., University of Michigan, Ann Arbor, MI 48109-2099
dpu@umich.edu

1 Program Scope:

We study the physics of generating x-rays by means of the interaction of ultraintense light pulses with free electrons from plasmas. The electron accelerator and the wiggler are both created by focusing laser light into a jet of gas, and are both less than one millimeter in length, many orders-of-magnitude shorter than in the case of a conventional synchrotron. Besides being compact in size, this all-optically-driven x-ray source delivers femtosecond duration pulses, which can be absolutely synchronized to a femtosecond optical light pulse. These features are advantageous for ultrafast pump-and-probe studies in relativistic nonlinear optics, ultrafast chemistry, biology, inner-shell electronic processes in atomic systems, and phase transitions in materials science.

2 Recent Progress:

We have investigated these sources both experimentally [1, 2, 3] as well as theoretically [4, 5, 6]. Two types of sources were demonstrated: one based on Thomson scattering [1, 2, 4, 5, 6], in which the laser light pulse acts directly as the wiggler, and another based on betatron oscillations [3], in which an ion channel—produced in the wake of the laser pulse—acts as the wiggler.

2.1 Experiment

The geometry used for the experiments involved a high intensity laser co-propagating with a laser-accelerated relativistic electron beam (see Fig. 1).

2.1.1 EUV generation by means of high-order harmonic generation

Using a long pulse laser (400-fs), a collimated beam of EUV-energy high-order harmonics was produced [1]. The characteristic signatures of this process were found to be the emission of even order harmonics, a linear dependence on the electron density, a significant amount of harmonics with circular polarization, and a small spatial extent of the source. The harmonics are emitted as a forward-directed beam with a divergence of $2 - 3^{\circ}$. The measured spatial profile of the harmonics was found to be in excellent agreement with calculations that assume that relativistic electrons play a significant part in the scattering process.

2.1.2 Beam of continuum x-rays

A collimated beam containing 5×10^9 x-ray photons/shot (integrating over all angles) was produced [2] by this same mechanism (see Figs. 2 and 3), but this time using a 30-fs, 30-TW laser located at the Laboratoire d'Optique Appliquee (LOA), in Palaiseau, France. The x-ray radiation had a broad continuous spectrum peaked at 0.15 keV, with a significant tail up to 2

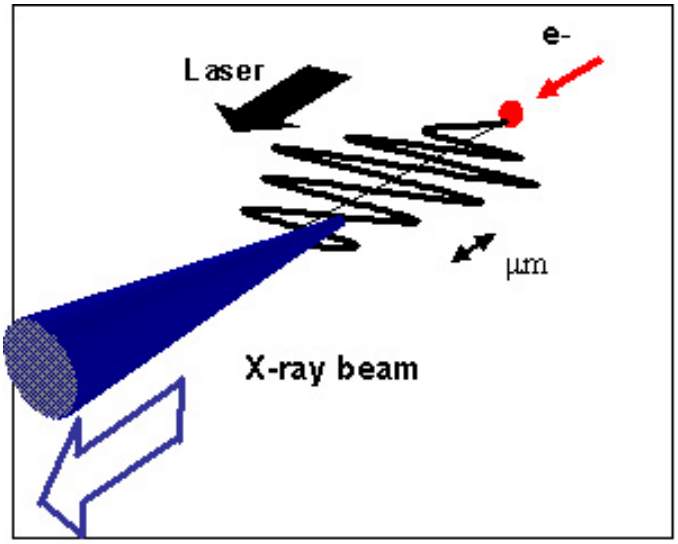

Figure 1: Schematic diagram of Thomson scattering from a co-propagating laser-driven electron beam.

keV. These characteristics were found to depend strongly on the laser strength parameter a_0. At high laser intensity, above $a_0 \sim 1$, the relativistic scattering of the laser light was found to originate from MeV-energy electrons inside the plasma.

In a separate experiment, in which x-ray generation from betatron oscillations was investigated [3], femtosecond duration pulses of broadband keV-energy radiation, lying within a narrow (50-mrad) cone angle, were produced.

2.2 Theory

We constructed simple scaling laws for the spectrum of the backscattered radiation of an electron by an intense laser, and found the optimal scattering conditions [5, 6]. These solutions suggest that an intense laser with $a_0 \sim \mathrm{O}(1)$, together with the most energetic counterpropagating electron beam, would produce the combined largest frequency up-shift and brightest backscatter power (see Fig. 4).

3 Future Plans:

Our ongoing research is focused on the following thrust areas: (1) Short-wavelength generation by the mechanism of betatron oscillations in a plasma channel will be studied by use of the ultrashort laser pulses ($\tau = 30$ fs) and higher laser intensities ($I \leq 5 \times 10^{20}$ W/cm^2). (2) Experimental studies will be conducted to verify theoretical predictions that more energetic photons can be produced by means of counter-propagating scattering, because of the relativistic Doppler upshift $\lambda = \lambda_L/4\gamma^2$. Theory shows that a 1-keV energy x-rays can be produced with only 10-MeV energy electrons. (3) Numerical simulations will be used to determine—for our laser-plasma conditions—the relative contribution to x-ray production from betatron oscillations and Thomson scattering. (4) Deflection of the electron beam in vacuum by a synchronized high-intensity laser pulse will be used to measure the electron bunch duration by means of cross-correlation.

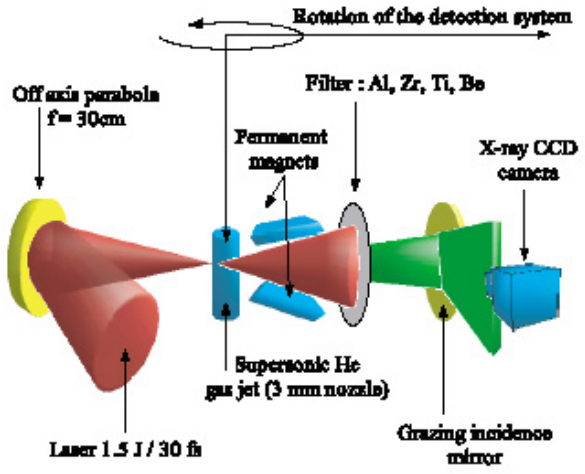

Figure 2: Schematic diagram of the experimental setup (from Ref. [2]).

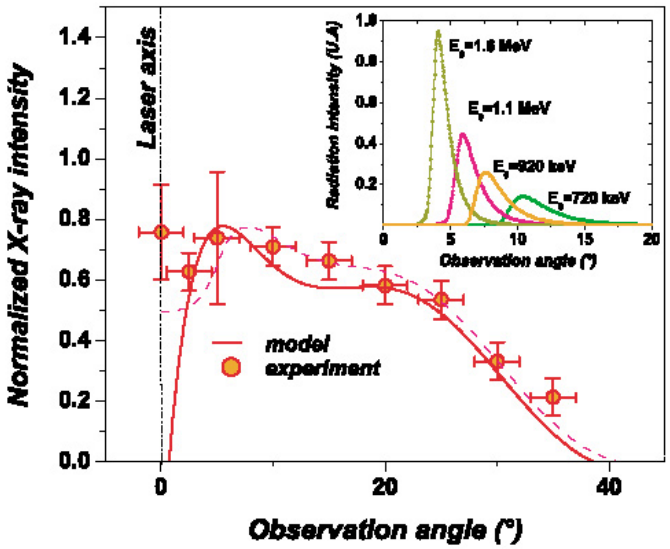

Figure 3: Spatial distribution of the observed x-ray emission for $a_0 = 5.6$ (from Ref. [2]). The solid line (dotted line) is the numerical result obtained for a Gaussian electron distribution with a temperature of 0.9 MeV and without (with) 5°-k spread. The inset shows the effect of the initial energy of monoenergetic electrons on the spatial distribution of the nonlinear Thomson scattering.

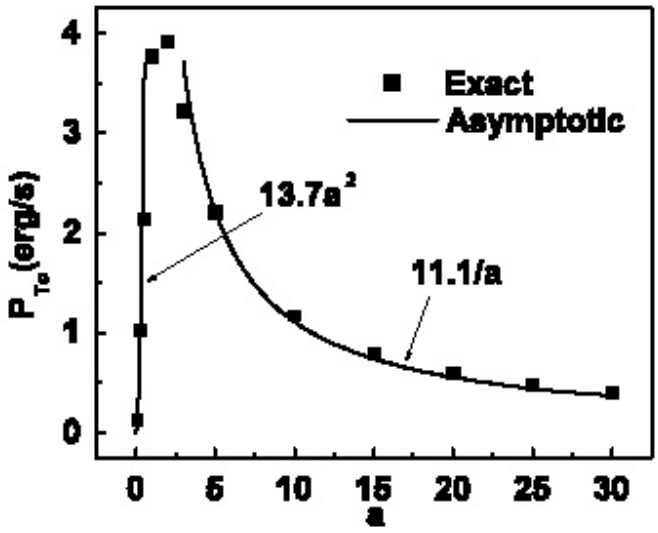

Figure 4: The total backscattered power, P_{T0}, per unit solid angle for the special case of the initial electron velocity is zero, and laser wavelength is 1 μm (from Ref. [5]).

References

[1] S. Banerjee, A. R. Valenzuela, R. C. Shah, A. Maksimchuk, and D. Umstadter, "High-harmonic generation in plasmas from relativistic laser-electron scattering," Journal of the Optical Society of America B (Optical Physics) **20**, 182-90 (2003).

[2] K. Ta Phuoc, A. Rousse, M. Pittman, J. P. Rousseau, V. Malka, S. Fritzler, D. Umstadter, and D. Hulin, "X-ray radiation from nonlinear Thomson scattering of an intense femtosecond laser on relativistic electrons in a helium plasma," Phys. Rev. Lett. **91**, 195001-1 (2003).

[3] A. Rousse, K. Ta Phuoc, R. Shah, A. Pukhov, E. Lefebvre, V. Malka, S. Kiselev, F. Burgy, J. P. Rousseau, D. Umstadter, and D. Hulin, "keV-energy Synchrotron X-ray Beams from Relativistic Laser-Plasma Interaction," Phys. Rev. Lett. accepted for publication (2004).

[4] D. Umstadter, "Relativistic laser-plasma interactions," Journal of Physics D (Applied Physics) **36**, 151-65 (2003).

[5] F. He Y. Y. Lau, D. Umstadter, and R. Kowalczyk., "Backscattering of an intense laser beam by an electron," Phys. Rev. Lett. **90**, 055002-1 (2003).

[6] Y.Y. Lau F. He, D. Umstadter, "Nonlinear Thomson scattering: a tutorial," Phys. Plasmas **10**, 2155-62 (2003).

[7] D. Umstadter, S. Banerjee, S. Chen, E. Dodd, K. Flippo, A. Maksimchuk, N. Saleh, A. Valenzuela, and P. Zhang, "Developments in relativistic nonlinear optics," *AIP Conf. Proc.* **611**, 95 (2002).

[8] D. Umstadter, "Laser-driven x-ray sources," *2003 Yearbook in Science and Technology* (McGraw-Hill, New York, 2003), p. 215.

[9] S. Banerjee, A. R. Valenzuela, R.C. Shah, A. Maksimchuk and D. Umstadter, "High Harmonic Generation in Relativistic Laser Plasma Interaction," *Phys. Plasmas* **9**, 2393 (2002).

Structure and Dynamics of Atoms, Ions, Molecules and Surfaces: Atomic Physics with Ion Beams, Lasers and Synchrotron Radiation

C.L.Cocke, Physics Department, J.R. Macdonald Laboratory, Kansas State University, Manhattan, KS 66506, cocke@phys.ksu.edu

The goals of this aspect of the JRML program are to explore mechanisms of ionization of atoms, ions and small molecules by intense laser pulses and ions and to investigate the dynamics of photoelectron emission from small molecules interacting with x rays from harmonic generation and synchrotron radiation.

Recent progress and future plans:

1) Double ionization of H_2 and D_2 by short intense laser pulses, *S.Voss, A. S. Alnaser, X.-M.Tong, C. Maharjan, P.Ranitovic, B.Ulrich, B.Shan, Z.Chang, C.D.Lin and C.L.Cocke*
The simplest molecule which can be doubly ionized is molecular hydrogen. For this reason, this molecule has, for more than a decade, served as the test molecule for revealing the fundamental ionization processes whereby short intense pulses of electromagnetic radiation excite and/or remove electrons from a molecule. Well known participatory processes established for this molecule include bond softening (leading to dissociation) and enhanced ionization (leading to double ionization). During the past two years we have used COLTRIMS techniques to study two additional processes for double ionization: rescattering ionization and sequential ionization with ultrashort pulses. Laser pulses from the Kansas Light Source (KLS) of pulse duration between 8 and 35 fs were focused onto a supersonic gas jet of hydrogen/deuterium gas to deliver a peak intensity between 1 and 12 x 10^{14} w/cm^2 . The resulting ions were propelled by an electric field onto the surface of a time- and position-sensitive detector. The time and position of hit of all ions produced for each laser pulse were recorded on an event-by-event basis and analyzed off-line to deduce the three-dimensional momentum vector for all ions from each pulse.

At the lowest intensities, around 1 x 10^{14} w/cm^2, the dominant process which produces proton pairs is a rescattering (RS) one. The electron released in the single ionization of the molecule returns to ionize/excite the molecular ion further, finally resulting in double ionization. With the help of theoretical modeling by X.-M. Tong *et al.* (1), this process has now been brought under good control. When 35 fs pulses are used, the returning electrons arrive 2/3 of an optical cycle after the initial pulse and additional full optical periods thereafter, providing a pulsed ionization source which can be used to follow the motion of the vibrational wave packet in the ground-state potential of the molecular

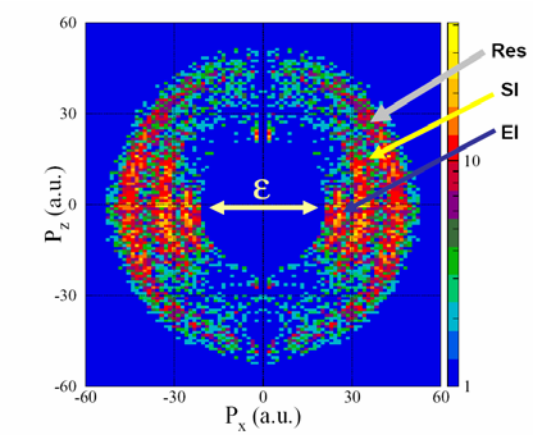

FIG. 1: Momentum image of the proton pairs produced in the double-ionization of H_2 by 12 fs, 3 x 10^{14} W/cm^2 laser pulses.

ion. If the pulse length is shortened to 8 fs, only the first return is effective, and this is observed in the data. If the laser intensity is now raised, using a 35 fs pulse, the well known enhanced ionization (EI) becomes the dominant process. However, if the 8 fs pulse is used, this process is suppressed and replaced by sequential ionization (SI) , whereby two successive tunneling removals of the two electrons occur. By adjusting the pulse length and peak intensity appropriately it is possible to see all three double ionization processes in a single spectrum, as is shown in the momentum display of the "explosion sphere" in fig. 1. These data are in nice agreement with a comprehensive model of Tong and Lin. Using this model, it is possible to follow the heavy particle motion on a fs time scale in a modified pump-probe picture, even though the laser pulse itself is 8 fs in duration (publication 1).

2) Double ionization of nitrogen and oxygen molecules by short intense laser pulses, *ibid.* It has been suggested that molecular dynamics might be followed in a pump-probe arrangement with intense photon pulses by initiating a heavy particle rearrangement in the molecule with a weak pump pulse and "Coulomb exploding" the molecule at a later time with a strong pulse. The momenta of the explosion fragments, measured for example in a COLTRIMS arrangement, could be inverted to find the arrangement of the heavy particles at the time of explosion. Is such an approach is to be brought under control the mechanisms which actually produce the explosion must be understood. With this in mind, we have used the approach discussed above for molecular hydrogen to examine the first step of the explosion process, the production of the doubly charged molecule, for oxygen and nitrogen. We have studied particularly the double ionization channel which produces singly charged ion pairs for which some understanding of the process can be reached. The choice of these particular molecules was also partially motivated by the fact that oxygen has "suppressed" ionization and displays an extended cutoff when used for harmonic generation, while nitrogen does not. This behavior has been suggested to be due to the difference in outer orbital structure of the two molecules. By using the COLTRIMS approach we are able to investigate this by measuring simultaneously high resolution KER spectra and angular distributions of the fragments over the range of pulse length and intensity discussed above. The major findings are (see publication 2):

1) For the lowest intensities and 8 fs pulse, the production of ion pairs is dominated by a rescattering process. The high-resolution KER spectra are very similar to those observed for electron bombardment and show that the process proceeds through well defined and identified states of the dication. The angular distributions are very marked and very different for oxygen and nitrogen, as shown in fig. 2. This behavior can be interpreted as due to the angular dependence of the first step of the tunneling ionization of the outer orbital of the parent molecule, which is predicted by the molecular ADK theory of Tong et al. (2) to reflect the orbital structure of the electron being removed. For oxygen the orbital is a π_g, which produces a distribution peaked roughly at 40 degrees to the polarization axis, while for the nitrogen it is a σ_g which peaks at zero degrees. It appears that modest intensity laser pulses can be thus used to probe the outer orbital structure of the molecule.

2) For higher intensities and 35 fs pulses the KER resolution on oxygen is lost, due to the advent of enhanced ionization. However, by using 8 fs pulses, the resolution is regained, due to the freezing of the internuclear distance by the short pulse.

3) Evidence for dynamic alignment of the molecules even with pulses as short as 8 fs is seen for higher intensity. This result is very unexpected from the literature but agrees with recent modeling of Tong *et al.* .

4) Coulomb explosion seems to be inhibited by 8 fs pulses, which deny the time necessary for enhanced ionization. This result may have serious unfavorable implications for the general use of Coulomb imaging.

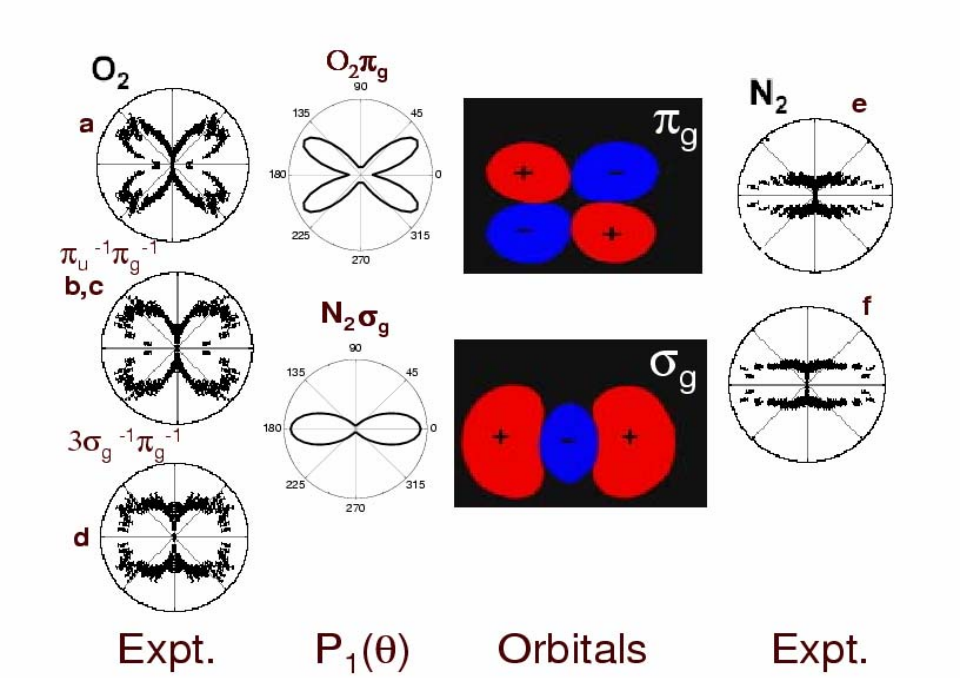

Fig. 2. Angular dependence of production rate of singly charged ions from oxygen and nitrogen by 8 fs pulses for several final states of the dication, compared to the shapes of the outer orbitals and to the predictions $P_1(\theta)$ of the molecular ADK (Tong *et al.* , ref. 2).

3) Picopulsing the Tandem, *Z.Chang, K.Carnes, V.Needham, C.L.Cocke*

We are implementing the production of (sub) ps pulses of fast heavy ions from our Tandem Van de Graaff accelerator. Intense laser pulses from the KLS will be focused into the source gas in the high-energy column of our 7MV EN Tandem to produce ions pulses with very small longitudinal and transverse emitance. Preliminary calculations indicate that, by choosing the appropriate ratio between acceleration and drift length, and by keeping the number of ions in each pulses sufficiently low, pulses of MeV ions with pulse lengths in the (sub) ps region can be delivered on target. We explore the possibility that these pulses can be used in a pump-probe arrangement to study physical processes on a (sub) ps time scale. When both pump and probe are energetic ions, even sub-ps time resolution may be possible. When the pump is the laser beam, the flight-time jitter associated with the small variations of the acceleration potential is expected to limit the time correlation to several ps. Experiments planned include time resolved heavy-particle diffraction for the probing of phase transitions in solids, laser assisted collisions and collisions with transiently modified targets. The transfer line from the KSL to the Tandem, the mechanism for mounting the mirror inside the terminal and the target chamber are under construction. First tests are expected in fall 2004.

4) Photoelectron diffraction from small molecules This project now encompasses two projects , one at the ALS (A) and one at KSU (B).

A. Synchrotron radiation: *T. Osipov, A.Alnaser, P.Ranitovic, C.Marhajan, B.Ulrich, C.L. Cocke (KSU), A. Landers (Auburn Univ.), R. Doerner, Th. Weber, L. Schmidt, A. Staudte, H. Schmidt-Boecking, et al. (U. Frankfurt), M.H. Prior (LBL).* At the Advanced Light Source, we have measured the correlated momentum-space distributions of photoelectrons and charged photofragments from energetic photons on small molecules using COLTRIMS. This work is carried out by a large multi-laboratory collaboration involving the University of Frankfurt, LLBL, Auburn Univ. and KSU. During the past year emphasis has been on molecular hydrogen, where both dissociative ionization and double ionization processes have been studied. See publication 4.

B. Harmonic generation source: *P.Ranitovic, A.Alnaser, C.L.Cocke, B.Shan, Z.Chang*. Using harmonics generated from a gas jet illuminated by pulses from the KLS at KSU, we have initiated a project to measure photoelectron angular distributions from "fixed in space" molecules. We use soft x-rays in the 10-80 eV range to ionize "inner" valence electrons from the target in a modified COLTRIMS geometry. The ultimate goal is to perform time-resolved photoelectron spectroscopy from small molecules, in a pump-probe arrangement, with the infrared KLS beam as the pump and the x rays as the probe. The COLTRIMS target chamber and jet are in place and the first yields of ions from the interaction of the harmonics with the COLTRIMS jet have been measured.

References:

1) X. M. Tong, Z. X. Zhao, and C. D. Lin, Phys. Rev. Lett. **91**, 233203 (2003); and Phys. Rev. A **68**, 043412 (2003).
2) X. M. Tong, Z. X. Zhao, and C. D. Lin, Phys.Rev.A, **66**, 033402 (2002).

Publications appearing in 2003-2004 not previously listed:

1. Rescattering Double Ionization of D_2 and H_2 by Intense Laser Pulses , A.S. Alnaser, T. Osipov, E.P. Benis, A. Wech, B. Shan, C.L. Cocke, X.M. Tong and C.D. Lin, Phys. Rev. Letters **91** 163002 (2003)
2. Effects of molecular structure on ion disintegration patterns in ionization of O_2 and N_2 by short laser pulses, A.S.Alnaser, S.Voss, X.-M.Tong, C.M.Maharjan,P.Ranotovic, B.Ulrich,T.Osipov,B.Shan, Z.Chang and C.L.Cocke, Phys. Rev. Lett. (accepted, 2004).
3. Momentum Imaging in Atomic Collisions , C. L. Cocke, Physica Scripta. Vol. **T110**, 9–21, (2004).
4. Fully Differential Cross Sections for Photo-Double-Ionization of D_2, Th.Weber, A. Czasch, O. Jagutzki, A. Müller, V. Mergel, A. Kheifets, J. Feagin, E. Rotenberg, G. Meigs, M. H. Prior, S. Daveau, A. L. Landers, C. L. Cocke, T. Osipov, H. Schmidt-Böcking, and R. Dörner1,, Phys. Rev. Lett. **92**, 163001, (2004).

PROBING DYNAMICS AND STRUCTURE IN ATOMS, MOLECULES AND NEGATIVE IONS USING THE ADVANCED LIGHT SOURCE

Nora Berrah
Physics Department, Western Michigan University, Kalamazoo, MI 49008
e-mail:Berrah@wmich.edu

Program Scope

The objective of the research program is to advance fundamental understanding of the interaction between vuv/soft x-ray photons and gas-phase targets as well as to achieve a better understanding of the dynamics and electronic structure of atoms, molecules, clusters and their negative ions. These studies allow an understanding, at the atomic and molecular level, of many processes important to the understanding of the properties of complex materials and of strongly correlated systems. We are in the process to design and build a movable ion beamline that will be used in the collinear and cross geometry with the Advanced Light Source photon beam. We present here results completed and underway this past year and plans for the immediate future.

Recent Progress

1) K-Shell Photodetachment Studies of Negative Ions

We have been focusing this past year on inner-shell photodetachment studies of negative ions to investigate the correlation and dynamics between a core and valence electrons in a situation where one valence electron is very loosely bound to the atoms, molecules or clusters. As such, negative ions targets constitute excellent systems for studying dynamics and for testing the ability of theoretical calculations to incorporate electron-correlation effects. Inner-shell photoionzation of negative ions leading to multi-photodetachment processes have so far revealed structure, differing substantially both qualitatively and quantitatively from the corresponding processes above the 1s ionization threshold in neutral atoms and positive ions. We report below on some of our recent efforts [1-5] in this part of our research program.

a) K-shell photodetachment of Li^-

In the case of the K-shell photodetachment experiment in Li^- [a], the comparison between measurements and theoretical [a, b] calculations have led to new developments in our interpretation and understanding of various discrepancies between theory and experiment. Specifically, theory predicted a 13 Mb shape resonance that was not observed. Recently [c] a new interpretation emerged that linked the suppression of the resonance to post-collision recapture of the slow photoelectron by the Li^+ ions, while the fast Auger electron gets ejected, producing neutral Li. We are presently in the process of testing a recently built neutral detector in order to measure the predicted neutral decay since our present apparatus is restricted to detecting the positive ion channel only. We have also carried out absolute cross section measurements in addition to better resolved data.

b) Double- photodetachment of He^-

Two years ago, our core-detachment study in He^- [1] stimulated new theories that disagreed with each other about the nature of the structure measured and showed discrepancies with the measurements, specially in the case of the first structure above the 1s threshold. Our early measurements [1], however, lacked the precision necessary to evaluate discrepancies among recent calculations. Thus, this year, we investigated accurate threshold positions, width and strength of predicted resonances in order to determine their nature since they represent sensitive parameters by which to evaluate *ab initio* calculations. Our resolution was increased by a factor of 3 over our previous work [1] allowing us to resolve the discrepancies among three theories [d]. In addition, we have measured the absolute double-detachment cross sections of thresholds structure and triply-excited quartet resonances in He^-.

We have also measured the $2s2p^2\ ^4P$ state of He^-, located just below the 1s threshold [d] and assumed to decay about 99% of the time to the neutral channel. In the case of this resonance, all *ab initio* calculations agree very well among themselves about its position, width and intensity. However, our observations show that this resonant state decays unexpectedly 13% of the time to the He^+ 1s ground state channel instead of the estimated 1% which would not have made it observable in the positive ion channel. This work represents the *first* evidence of a simultaneous 3-electron decay process in a core-excited negative ion. The absolute cross section measurement of this decay mechanism was also measured and a manuscript has been submitted to Physical Review Letters.

c) Inner-shell photodetachment of small clusters

We have investigated K-shell photodetachment of small negative ions clusters, B_2^- and B_3^-, as well as their monomer B^-. The molecular photodetachment mechanism produces both direct photoionization of the molecules as well as the dissociation of the molecules into fragments. We measured both processes and were able to make the following observations. The behavior of the core-photodetachment cross sections of B_2^- producing the B_2^+ channel is found to be surprisingly similar to the photodetachment of atomic B^- ion producing B^+. The photodissociation produces at some resonance energies a larger intensity of the fragment B^+ than the molecular B_2^+.
We have recently received theoretical calculations by the group of Robert Lucchese and discussions between the two groups are underway to understand these molecular systems. We have also carried out similar experiments in the 2p photodetachment in Si^-, Si_2^-, and Si_3^- This work will be completed this coming year.

2) New Low-Lying Mirroring Singly and Doubly Excited Resonances in Neon

Guided by the conclusions drawn from our work on Argon [e], the systematic search for mirroring behavior in a lighter atom such as the $Ne^+\ 2p^5\ ^2P_{1/2,3/2}$ partial photoionization cross sections, was undertaken. Mirroring behavior implies the observation of resonances

in the partial, but not the total photoionization cross sections to the spin orbit split states of atoms.
We have observed many new resonances in neon which have been discovered by virtue of their LS forbidden mirroring partial cross section profiles, as expected to occur in general systems [f]. In particular, all six of the previously undetected $2s^2 2p^4(^3P)3s(^{[2,4]}P)3p(^3[S, P, D]_1)$ resonances have been observed. These results confirm that mirroring triplet resonances can be observed in partial cross sections where continuum spin-orbit effects exist, and suggest that future experimental studies of other atoms or molecules will also reveal new resonances [6].

3) Probing the Molecular Environment using Spin-Resolved Photoelectron Spectroscopy.

Spin-resolved inner-shell photoionization and Auger decay have been investigated in detail for atoms [g,9] to determine the alignment and orientation parameters in order to provide more information to determine the transitions matrix elements as well as to determine the magnetic dipole moment and electric quadrupole moments. For molecules, only the outer shell spin-resolved photoionization of HI and HBr [h] have been reported previously.
Angle- and spin-resolved photoelectron spectroscopy with linearly and circularly synchrotron radiation polarized from beamline 4.0.1 was used to study the electronic structure of model triatomic molecules, hydrogen sulfide and carbonyl sulfide. The spin-polarization measurements of the molecular field split components of the S 2p photolines were different in the case of the two molecules, fingerprinting thus the different molecular environments. Simple atomic models were used successfully to explain the spectra [7, 8]

4) Inner-shell Photoionization of Laser-Excited Open-Shell Atoms.

We have this past year, in collaboration with the Orsay group, conducted inner-shell photoionization of laser-excited open-shell atoms. In this type of experiment, the laser excitation allows a selective population to be excited from the ground state to the first excited state. The resulting photoelectrons produced by synchrotron photoionization are detected by a high resolution electron spectrometer (Scienta SES-200).
We were able to observe, for the first time, clearly resolved strongly enhanced- or depressed-transitions lines. We have submitted a manuscript to Physical Review Letters.

Future Plans.

The principal areas of investigation planned for the coming year are to: (1) Continue our efforts in testing a neutral detector. 2) Finish up the analysis of the dissociation mechanism in small negative ions clusters. 3) Analyze high-resolution measurements of inner-shell photodissociation dynamics in diatomic neutral molecules (HCl, HBr and DBr). 4) Carry out new photoionization experiments in clusters systems (Ne, Ar, Xe).

Publications from DOE sponsored research.

[1] N. Berrah, J. D. Bozek, G. Turri, G. Akermann, B. Rude, H.-L. Zhou, and S. T. Manson, "K-Shell Photodetachment of He^-: Experiment and Theory", *Phys. Rev. Lett.* **88**, 093001 (2002).

[2] N. D. Gibson, C. W. Walter, O. Zatsarinny, T. W. Gorczyca, G. D. Ackerman, J. D. Bozek, M. Martins, B. M. McLaughlin, and N. Berrah, "K-shell photodetachment of C^-, Phys. Rev. A **67**, **R**030703 (2003).

[3] N. Berrah, J. D. Bozek, G. Ackerman, G. Turri, R. C. Bilodeau, S. Canton, and E. Kukk, "*From the Atomic to the Nano-Scale",* Proceeding of the International Workshop, ODU, Edited by C. T. Whelan and J. H. McGuire. (2003).

[4] N. Berrah, J. D. Bozek, R. C. Bilodeau and E. Kukk, "Studies of Complex Systems: From Atoms to Clusters", Radiat. Phys. Chem, **70**, Issue 1, 57 (2004).

[5] N. Berrah, R. C. Bilodeau, G. Ackermann, J. D. Bozek, G. Turri, E. Kukk, W. T. Cheng, and G. Snell " Probing atomic and Molecular Dynamics from Within" Radiat. Phys. Chem., **70**, 491 (2004)

[6] S. E. Canton, A. A. Wills, T. W. Gorczyca, E. Sokell, J. D. Bozek , G. Turri, M. Wiedenhoeft, X. Feng and N. Berrah "New Low-Lying Mirroring Singly and Doubly Excited Resonances in Neon", J. Phys. B. Lett. **36**, L181 (2003).

[7] G. Turri, G. Snell, B. Langer, M. Martins, E. Kukk, S. E. Canton, R. C. Bilodeau, N. Cherepkov, J. D. Bozek, and N. Berrah, " Probing the molecular environment using spin-resolved photoelectron spectroscopy", Phys. Rev. Lett. **92,** 013001 (2004).

[8] G. Turrri, G. Snell, B. Langer, M. Martins, E. Kukk, S. E. Canton, R. C. Bilodeau, N. Cherepkov, J. D. Bozek, and N. Berrah, "Probing the Molecular Environment using Spin-Resolved Photoelectron Spectroscopy", AIP (American Institute of Physics) conference proceedings **697,** ed: G.F. Hanne, L. Malegat, H. Schmidt-Boecking (2004).

[9] B. Lohmann, B. Langer, G. Snell, U. Kleiman, S. Canton, M. Martins, U. Becker and N. Berrah, "Angle and Spin Resolved Analysis of the Resonantly Excited Ar* $(2p^{-1}_{3/2}4s_{1/2})_{j=1}$ Auger Decay", AIP (American Institute of Physics) conference proceedings **697,** ed: G.F. Hanne, L. Malegat, H. Schmidt-Boecking (2004).

[10] J. D. Bozek, S. E. Canton, E. Kukk and N. Berrah, "Vibrationally resolved resonant Auger spectroscopy of formaldehyde at the C 1s-1* resonance", Chemical Physics, **289**, pages 149-161 (2003).

[11] James R. Harries, James P. Sullivan, James B. Sternberg, Satoshi Obara, Tadayuki Suzuki, Peter Hammond, John Bozek, Nora Berrah, Monica Halka, and Yoshiro Azuma, "Double Photoexcitation of Helium in a Strong dc Electric Field", Phys. Rev. Lett. **90,** 133002-1 (2003).

References:

[a] N. Berrah, et al., Phys. Rev. Lett. **87,** 253002-1 (2001); H. Kjeldsen et al., J. Phys. B 34, L353 (2001).

[b] H.-L Zhou et al., Phys. Rev. Lett. **87**, 023001 (2001)

[c] T. W. Gorczyca et al., Phys Rev. A. **68**, 050703(R) (2003) and references therein.

[d] J.L. Sanz-Vicario et al., *Phys. Rev. A* 66, 052713 (2002); O. Zatsarinny et al. *J. Phys. B* 35, 4161 (2002); H.-L. Zhou, et al., Phys Rev. A 64, 012714 ((2001).

[e] S. E. Canton-Rogan et al.Phys. Rev. Lett. **85,** 3113 (2000).

[f] C. N. Liu and A. F. Starace, Phys. Rev. A **59**, R1731 (1999).

[g] U. Heinzmann, Appl. Optics **19**, 4087 (1980) and references therein, G. Snell, et al., Phys. Rev. A **66**, 022701 (2002).

[h] N. Böwering et al., J. Phys. B **24**, 4793 (1991); M. Salzmann et al., J. Phys. B27, 1981 (1994).

Properties of Transition Metal Atoms and Ions

Donald R. Beck
Physics Department
Michigan Technological University
Houghton, MI 49931
e-mail: donald@mtu.edu

Program Scope

Transition metal atoms are technologically important in plasma physics (e.g., as impurities in fusion devices), Atomic Trap Trace Analysis (ATTA) (e.g., detection of minute quantities of radioactive species), astrophysical abundance (e.g., Fe II) and atmospheric studies, deep-level traps in semiconductors, hydrogen storage devices, etc. The more complicated rare earths which we are beginning to study are important in lasers, high temperature superconductivity, advanced lighting sources, magnets, etc.

Because of the near degeneracy of nd and $(n+1)s$ electrons in lightly ionized transition metal ions and the differing relativistic effects for d and s electrons [1], any computational methodology must simultaneously include the effects of correlation and relativity from the start. We do this by using a Dirac-Breit Hamiltonian and a Relativistic Configuration Interaction (RCI) formalism to treat correlation. Due to the presence of high-l (d) electrons, computational complications are considerably increased over those in systems with just s and/or p valence electrons. These include the following: (1) larger energy matrices (5-10 times larger) because the average configuration can generate many more levels [2]. Multi-root calculations with matrices of order 20-30 000 are becoming common, (2) increased importance of interactions with core electrons (d's tend to be more compact, and there can be more of them), (3) a significant variation of the d radial functions with level (J), which requires the presence of second order effects. Methodological improvements are most needed in the treatment of second order effects.

We desire to develop the methodology to a point where properties of $(d+s)^n$ states can be treated accurately and efficiently. To date, this is only possible for $n < 5$. A systematic knowledge of which basis functions are crucial to a physical property can allow us to limit basis set sizes, while retaining accuracy. To this end, contributions to properties are generated at all computational stages. These are particularly helpful in determining where the saturation of radial basis sets may need further exploration.

Recent Progress

[A] Mo V and Mo VI Energy Levels, Oscillator Strengths, Landé g-values

Previously, we had completed calculations for the isoelectronic Zr III and Nb IV $J = 0 \rightarrow J = 1^o$ E1 transitions [4]. Zr III is astrophysically important, semi-empirical f-values were only available for Zr III, and there was some doubt [5b] of the location of the Nb IV $5s^2\ J = 0$ state. Computationally, these species were of interest to us because of the near degeneracy

of the $4dnp$, $4dnf$ and $5s5p$ $J = 1$ levels, implying the need of carefully including correlation and relativistic effects.

For Mo V $J = 1$ states, these near degeneracies still persist, there are no f-values available, and even the energy level data is sparse and sometimes inconsistent [6,7]. Our completed calculations [8] have average energy errors of 229 cm^{-1} and 368 cm^{-1} ($J = 0, 1$) and the length and velocity f-values agree, on average, to 3.1%. Our energy levels agree better with the newer measurement [7], although the $5s5p$ ^1P level remains characteristically high ($\sim$1671 cm^{-1}).

An interesting aspect of the Mo V $J = 1$ results is the first appearance of "low-lying" $4p^5 4d^3$ levels (i.e. lying in the 30 lowest roots). These are somewhat difficult to place accurately ($<$ 2-3000 cm^{-1}),because of the changing $4p$ and $4d$ occupations which changes a "2" electron problem into an "8" electron problem (some core-core and more core-valence correlation is needed). At the suggestion of Joe Reader [5b], we extended our work to Mo VI, where these levels have been seen [9,10].

For Mo VI, we chose to look at the $J = 5/2^o$ levels, which involve the substantial interaction of the $4p^6nf$ series with the $4p^5 4d^3$ levels. The two measurements agree well for only one $4p^5 4d^3$ level, and the bottom five $4p^5 4d^2$ levels are "missing" from the newer tabulation. Our current results [11] have an average difference of 2178 cm^{-1} (10 levels) [9] and 3287 cm^{-1} [10]. When the $J = 5/2^o$ calculations are complete, we will obtain wavefunctions for the $4p^6nd$ $J = 3/2, 5/2$ levels and calculate the E1 f-values between the two sets of states.

[B] Fe III and Fe II Energy Levels and Oscillator Strengths

Last year, we completed a study of $(d + s)^7 \rightarrow (d + s)^6 p$ f-values in Tc I [2] to see if a transition could be identified which could be used in ATTA studies [12]. Due to the large number of open shell electrons, this lies at the frontier of *ab initio* relativistic-correlation calculations. Errors in energy differences for adjacent levels [13] can be doubled, and f-value gauge disagreements quintupled as compared to the much simpler "2" electron systems (e.g. Mo V).

A goal this year was to improve the accuracy for such complicated systems, and we chose as our focus the homologous, astrophysically important, Fe II ion. Many of the transitions of interest are of the "1" electron type, viz $3d^6 4s \rightarrow 3d^6 4p$, suggesting that the principle problem would be in getting the energy levels properly ordered, which in turn would depend properly correlating the $3d^6$ core.

For this reason, we first looked at the $3d^6$ $J = 4$ levels of Fe III, which is computationally simpler due to the absence of the $4s$ or $4p$ electron (particularly the latter). We carefully explored convergence of correlation effects as a function of l, number of virtuals, and included more excitations from the core than normal. With this, we were able to reduce the average error between adjacent energy levels to $\sim$450 cm^{-1}, about 100 cm^{-1} lower than in Tc I.

Using this knowledge (e.g. the significance of $3d^2 \rightarrow vfvh$), we are calculating the $J = 9/2, 9/2^o$ levels of Fe II. For $J = 9/2$, the average adjacent energy level error is 319 cm^{-1}, with 14 200 basis functions. For the $J = 9/2^o$, this error is 172 cm^{-1}, with 10 200 basis functions. Although the odd parity results seem more accurate, two levels are separated by only 75 cm^{-1}, and their identity is actually flipped, as can be determined by comparing the theoretical and experimental Landé g-values.

Both calculations include Breit effects, which seem modest, at least for energy differences and the larger f-values ($> .01$), but which increase computational costs considerably (10 times). On a Blade 2000, the odd parity Breit calculations took 53 hrs. F-values have been calculated for all 360 transitions, using our [3] "one shot" program which includes non-orthonormality effects. Gauge agreement is good, once the core excitations called for by FOTOS [14] are included; these improve the velocity result. Three of the transitions have been previously obtained [15-16] and our results are consistent with at least one of them.

[C] Polarizability of U VII

Better knowledge of properties of actinide atoms may be helpful to chemists and solid state physicists [17] working on matter containing actinide atoms. At the suggestion of Steve Lundeen [18] calculations were completed on the polarizability of U VII, a closed shell atom. For the isoelectronic Rn I, our results are in good agreement with a previous calculation [19].

[D] Kr II and Kr III Energy Levels and f-values

Experimental photoionization studies are underway at ANL [20], and some theoretical input is needed to obtain estimates for the $1s \rightarrow np$ excitations energies and f-values in Kr II and Kr III. Our calculations are well underway, and some results have already been conveyed to the ANL group.

[E] Hardware and Software Improvements

A second CPU has been added to the Blade 2000, and a large disk drive (146 GB). The RCI program [3] has been modified to create a substructure file, to be used during iteration. This should reduce iterating costs significantly, as only a small section of the total structure will need to be read in. The analysis program has been enhanced to check that all wavefunctions contain equivalent correlation effects (e.g. that $3p^2 \rightarrow 3d^2$ appears in all, if in one).

[F] DOE Publications 2002-2004

In addition to items 2, 4, and 8 in the reference list, we have also published f-values for K II [21], energy levels in Er IV (an important dopant for solid state lasers) [22], and Magnetic Quadrupole Lifetimes in the rare gases [23], for which there was previously a discrepancy between theory and experiment.

Future Plans

Near future applications include completion and publication of the Mo VI, Fe II, and Kr II (III) projects. RCI program development will continue to reduce the time needed to compute the Breit effects and make more effective use of the two CPUs, probably by making better use of the CPU caches.

References

[1] R. L. Martin and P. J. Hay, J. Chem. Phys. **75**, 4539 (1981).

[2] S. M. O'Malley and D. R. Beck, "Lifetimes of Tc I $(4d+5s)^6 5p$ and $4d^6 5s\ 6D$ States, Phys. Scr. **68**, 244 (2003).

[3] The RCI program suite consists of three unpublished programs written by D. R. Beck over a period of years. RCI calculates the bound state wavefunctions, hyperfine structure, and Landé g-values. RFE uses RCI wavefunctions and computes E1, E2, M1, and M2 f-values, including the effects of non-orthonormality. REDUCE minimizes the number of eigenvectors needed for a correlation manifold by rotating the original basis to maximize the number of zero matrix elements involving the reference functions; only rotated vectors having non-zero reference interactions are retained.

[4] D. R. Beck and L. Pan, "*Ab Initio* Energy Levels, Oscillator Strengths, and Landé g-values for $J = 0, 1$ states of Zr III and Nb IV", Phys. Scr. **69**, 91 (2004).

[5] J. Reader and N. Acquista, Phys. Scr. **55**, 310 (1997); (b) J. Reader, private communication.

[6] A. Tauheed, M. S. Z. Chaghtai, and K. Rhaimullah, Phys. Scr. **31**, 369 (1985).

[7] M. I. Cabeza, F. G. Meijer, and L. Iglesias, Phsy. Scr. **34**, 223 (1986).

[8] L. Pan and D. R. Beck, "Mo V $J = 0, 1$ Energy Levels, Oscillator Strengths, and Landé g-values", Phys. Scr. (in press).

[9] A. Tauheed, K. Rahimullah, and M. S. Z. Chaghtai, Phys. Rev. A **32**, 237 (1985).

[10] J. Sugar and A. Musgrove, J. Phys. Chem. Ref. Data **17**, 155 (1988).

[11] L. Pan and D. R. Beck, unpublished (Mo VI).

[12] C. Y. Chen, Y. M. Li, K. Bailey, T. P. O'Connor, L. Young, and Z.-T. Lu, Science **286**, 1139 (1999).

[13] This error is an important indicator of the correctness of the "mixing" of nearly degenerate basis functions (which may contribute very differently to various properties such as f-values and hfs) into the final wavefunction.

[14] C. A. Nicolaides and D. R. Beck, Chem. Phys. Letts. **36**, 79 (1975).

[15] S. N. Nahar and A. K. Pradhan, J. Phys. B **27**, 429 (1994).

[16] A. J. J. Raassen and P. H. M. Uylings, J. Phys. B **31**, 3137 (1998).

[17] E. S. Rittner, J. Chem. Phys. **19**, 1030 (1951).

[18] S. Lundeen, private communication.

[19] C. Hattig and B. A. Hess, J. Phys. Chem **100**, 6243 (1996).

[20] B. Dunford, E. Kantor, and S. Southworth, Argonne National Laboratory.

[21] D. R. Beck, "Oscillator Strengths for K II $3p^6$ to $3p^5(4s+3d)$ $J = 1$ Transitions", J. Phys. B **35**, 4155 (2002).

[22] D. R. Beck, "Important Correlation Effects for the Er IV $4f^{11}\ {}^4\mathrm{S}_{3/2} \rightarrow {}^4\mathrm{I}_{15/2}$ Laser Transition Energy", Int. J. Quant. Chem. **90**, 439 (2002).

[23] D. R. Beck, "Magnetic Quadrupole Lifetimes of $np^5(n+1)s$ $J = 2$ States of Rare Gases", Phys. Rev. A **66**, 034502 (2002).

Mode-specific polyatomic photoionization far from threshold: Molecular physics at third generation light sources*

Erwin D. Poliakoff, Chemistry Department, Louisiana State University, Baton Rouge, LA 70803, epoliak@lsu.edu

This research focuses on microscopic aspects of polyatomic molecular photoionization, and in particular, the ubiquitous electronic-vibrational coupling that accompanies this process. Photoionization phenomena frequently bring to light fundamental molecular scattering dynamics, and are theoretically tractable. In molecular ionization, the continuum electron can induce vibrational excitations as it traverses the anisotropic molecular field, and can do so with a remarkable degree of mode-specificity. For polyatomic systems, our understanding of such photoelectron scattering is relatively primitive, because only recently have the salient experiments been possible. Thus, there is an extensive unexplored area where studies are both feasible and desirable. They are enabled by the Advanced Light Source, in combination with the efforts of theorists using Schwinger variational scattering calculations that facilitate detailed interpretations of the experiments.

The strategy is to use vibrationally resolved photoelectron spectroscopy to probe the influence of mode-selected geometry changes on continuum resonances that result from the temporary trapping of the outgoing photoelectrons. The central idea is that an understanding of the photoelectron scattering emerges most clearly when molecular aspects of the scattering are probed, e.g., mode-specific vibrational excitations. As an example of how unanticipated arise from such vibrationally-resolved studies, the figure shows a comparison of vibrational branching ratio curves for two similar linear triatomic targets, CS_2 and N_2O. These curves display the relative rates of production of excited vibrational levels. For simplicity, we show results only for stretching vibrations: antisymmetric stretching data in the top frames, and symmetric stretching branching ratios in the bottom. The Franck-Condon expectation is that all of these curves would be constant as a function of energy. Not only is that not observed, it is significant that N_2O shows the symmetric stretch "lighting up" while CS_2 shows the opposite result: the antisymmetric stretch exhibits a large excursion. The peaks result from the temporary trapping of the photoelectron. However, the mechanism of photoelectron localization is qualitatively different for these two systems. The observed behavior can be understood in the independent-particle, Born-Oppenheimer framework. These results challenge many previous studies that have relied on qualitatively dissimilar nonadiabatic explanations to rationalize anomalous photoelectron intensities. These results demonstrate how new effects in molecular physics are generated by interrogating polyatomic photoionization in this detail. It is interesting to note that the theoretical framework used to explain these observations has been available for some time, but the effects were wholly unanticipated. In addition, because the mechanism responsible for such mode-specific phenomena is relatively simple, the lessons learned can be exploited in other types of UV and x-ray spectroscopies. As an illustration of how these experiments relate to spectroscopic applications, consider that most of the effects observed for valence-shell photoionization have corresponding phenomena in core-shell processes. Therefore, an understanding of these photoionization processes in relatively complex molecular targets can benefit x-ray spectroscopies more generally (e.g., XANES, XPS), including those applied to surface adsorbates, nanophase materials, and transient reactive species evolving in femtosecond pump-probe studies.

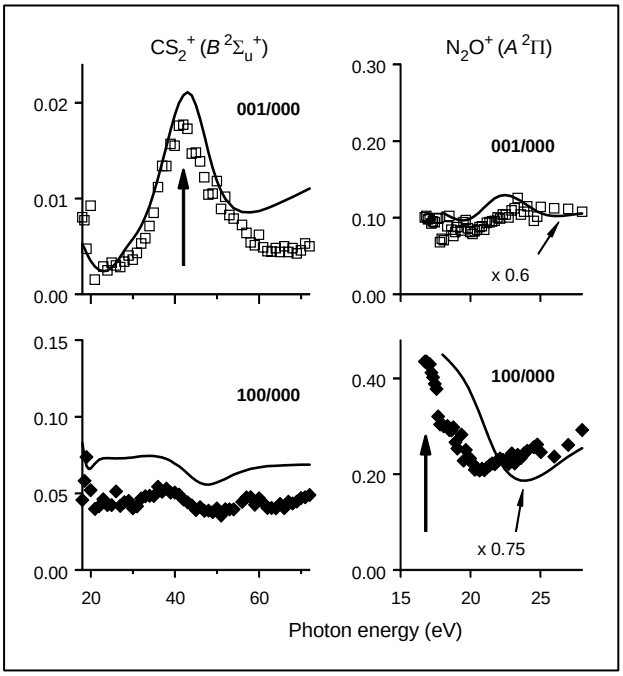

* This research is done in collaboration with John Bozek (LBL) and Robert Lucchese (Texas A&M)

Photoabsorption by Atoms and Ions

Steven T. Manson, Principal Investigator

Department of Physics and Astronomy, Georgia State University, Atlanta, Georgia 30303
(smanson@gsu.edu)

Project Scope

The goal of this research program is provide a theoretical adjunct to, and collaboration with, the various atomic and molecular experimental programs that employ third generation light sources, particularly ALS and APS. Calculations are performed employing cutting-edge methodologies with two major aims in mind: providing deeper insight into the physics of the experimental results; and providing guidance for future experimental investigations. At the outset, the general areas of programmatic focus are: manifestations of nondipole effects in atomic and molecular photoionization; photodetachment of inner and outer shells of negative ions; and photoionization of positive ions in ground and excited states.

Recent Progress

1. Nondipole Effects in the Photoionization of Xe 4*d*

Up until relatively recently, the conventional wisdom was that nondipole effects in photoionization were of importance only at photon energies of tens of keV or higher, despite indications to the contrary 35 years ago [1]. The last decade has seen an upsurge in experimental and theoretical results [2] showing that nondipole effects in photoelectron angular distributions could be important down to hundreds [3] and even tens [4] of eV. Furthermore, contrary to expectations, correlation in the form of interchannel coupling has been found to be significant in quadrupole channels [3]. Much of this understanding has been achieved as a result of experimental/theoretical collaboration. Our recent work has been involved in trying to understand the nondipole effects in the photoionization of Xe 4*d* in conjunction with the experimental group of Dennis Lindle working at the ALS. In a previous experimental/theoretical study on Xe 5*s*, it was found that experimental and theoretical relativistic-random-phase approximation (RRPA) nondipole parameters characterizing the photoelectron angular distribution were in quite good agreement [3]. Earlier work on the dipole parameters for Xe 4*d* were also in good agreement [5], indicating that RRPA treated the dipole channels well. For the nondipole parameters, which involve interferences between dipole and quadrupole channels, very significant disagreement was found [6]; we attribute this disagreement to the omission of quadrupole satellite channels in the calculation. As far as we know, this is the first indication of the importance of ionization plus excitation channels in the quadrupole manifold.

2. Photodetachment of the C^- Negative Ion

Negative ion photodetachment serves as a "laboratory" for the study of electron-electron correlation since many-electron interactions generally dominate both the structure and dynamics of negative ions. In connection with our recent studies of inner-shell photoabsorption by He^- [7,8] and Li^- [9,10], the R-Matrix code was enhanced to deal with photodetachment—particularly the final-state wave function which was beyond the then-extant R-Matrix code. Using this experience we have moved on to the C^- ion which is of interest for a number of reasons: there was significant theoretical disagreement for the photodetachment cross section of the ground state of C^-; C^- is one of the few negative ions to have a bound excited state; and there is experimental data on the cross section for K-shell photodetachment of C^-. As a first step, we have looked at the valence photodetachment of the ground ^4S state [11]. In this calculation, which agrees well with (limited) extant experiment, we have found the source of inaccuracy in the previous R-Matrix calculation and reconciled the disagreements. In addition, a new resonance was predicted and the cross section for each of the photoabsorption channels leading to the lowest seven states of neutral C has been presented and explained along with the photoelectron angular distribution asymmetry parameter β.

3. Photoionization of Positive Ions of Be Isoelectronic Sequence

Experimental studies of the photoionization of positive ions have seen a recent upsurge owing to the availability of facilities such as ALS and APS [12]. The Be isoelectronic sequence offers an attractive area of theoretical investigation for a number of reasons: the ions are four-electron systems so the possibility exists of treating them with high accuracy; the four-electron system is quite stable and, therefore, they are ubiquitous in many laboratory and astrophysical plasmas; and there have been recent experimental investigations of several members of the sequence. Employing the eigenchannel R-Matrix methodology [13] that we previously used to study the photoionization of neutral Be in it ground [14] and exited [15] states, a program to study the photoionization of the ions of Be sequence has been initiated. Our first results dealt with B^+ where the photoionization cross section of the ground state has been obtained including transitions to B^{2+} from the ground, 2*s* state up to 3*d* [16], i.e., up to a photon energy of about 50 eV. Of particular interest in this investigation is the energy region above the 2*p* threshold of B^{2+} where the resonances converging to the 3s, 3p and 3d states of B^{2+} all interfere with each other, leading to very strongly perturbed resonance series and almost chaotic-looking behavior. Despite the complexity, however, for each resonance we have been able to provide its identification, the resonance energy and the resonance width. Experimental cross sections have been measured in the region below the 2*p* threshold [17] and we find excellent agreement with the experimental results.

Future Plans

Fundamentally our future plans are to continue on the paths set out above. In the area of nondipole effects Xe 5*p* will be investigated to try to unravel the difficulties in two experimental results that disagree quantitatively. In addition, the search for cases

where nondipole effects are likely to be significant, as a guide for experiment, will continue. The study of the photodetachment of C^- shall move on to the excited bound ^2D state. Here the focus shall be upon how the slight excitation changes the photoabsorption. Following this, photoabsorption in the vicinity of the K-shell edge of both the ground ^4S and exited ^2D states shall be investigated to understand how the slight excitation of the outer shell affects the inner-shell photoabsorption. Finally, the study of the photoionization of the Be sequence shall continue with consideration of the first two excited states of B^+ and the ground and excited states of C^{2+}.

Publications Citing DOE Support Since September, 2003

"Photodetachment of the Outer Shell of C^- in the Ground State," H.-L. Zhou, S. T. Manson, A. Hibbert, L Vo Ky, N. Feautrier and J. C. Chang, Phys. Rev. A (in press).

"Nondipole Effects in the Photoionization of Xe $4d_{5/2}$ and $4d_{3/2}$: Evidence for Quadrupole Satellites," O. Hemmers, R. Guillemin, D. Rolles, A. Wolska, D. W. Lindle, K. T. Cheng, W. R. Johnson, H. L. Zhou and S. T. Manson, Phys. Rev. Letters (in press).

"Photoionization of the ground-state Be-like B^+ ion leading to the n=2 and n=3 states of B^{2+}," D.-S. Kim and S. T. Manson, J. Phys. B (submitted).

References

[1] M. O. Krause, *Phys. Rev.* **177**, 151 (1969).

[2] O. Hemmers, R. Guillemin and D. W. Lindle, *Radiation Phys. and Chem.* **70**, 123-148 (2004) and references therein.

[3] O. Hemmers, R. Guillemin, E. P. Kanter, B. Kraessig, D. W. Lindle, S. H. Southworth, R. Wehlitz, J. Baker, A. Hudson, M. Lotrakul, D. Rolles, W. C. Stolte, I. C. Tran, A. Wolska, S. W. Yu, M. Ya. Amusia, K. T. Cheng, L. V. Chernysheva, W. R. Johnson and S. T. Manson, *Phys. Rev. Letters* **91**, 053002 (2003).

[4] V. K. Dolmatov and S. T. Manson, *Phys. Rev. Letters* **83**, 939 (1999).

[5] H. Wang, G. Snell, O. Hemmers. M. M. Sant'Anna, I. Sellin, N. Berrah, D. W. Lindle, P. C. Deshmukh, N. Haque and S. T. Manson, *Phys. Rev. Letters* **87**, 123004 (2001).

[6] O. Hemmers, R. Guillemin, D. Rolles, A. Wolska, D. W. Lindle, K. T. Cheng, W. R. Johnson, H. L. Zhou and S. T. Manson, *Phys. Rev. Letters* (in press).

[7] H. L. Zhou, S. T. Manson, L. VoKy, A Hibbert and N. Feautrier, Phys. Rev. A **64**, 012714 (2001).

[8] N. Berrah, J. Bozek, G. Turri, G. Ackerman, B. Rude, H.-L. Zhou and S. T. Manson, *Phys. Rev. Letters* **88**, 093001 (2002).

[9] H. L. Zhou, S. T. Manson, L. VoKy, N. Feautrier and A. Hibbert, *Phys. Rev. Letters* **87**, 023001 (2001).

[10] N. Berrah, J. D. Bozek, A. A. Wills, H.-L. Zhou, S. T. Manson, G. Akerman, B. Rude, N. D. Gibson, C. W. Walter, L. VoKy, A. Hibbert and S. Fergusson, *Phys. Rev. Letters* **87**, 253002 (2001).

[11] H.-L. Zhou, S. T. Manson, A. Hibbert, L Vo Ky, N. Feautrier and J. C. Chang, *Phys. Rev. A* (in press).
[12] J. B. West, *J. Phys. B* **34**, R45 (2001) and references therein.
[13] F. Robicheaux and C. H. Greene, *Phys. Rev. A* **48** 4429-4440 (1993) and references therein.
[14] D.-S. Kim, S. S. Tayal, H.-L. Zhou and S. T. Manson, S. T., *Phys. Rev. A* **61**, 062701 (2000).
[15] D.-S. Kim, H.-L. Zhou, S. T. Manson and S. S. Tayal, *Phys. Rev. A* **64**, 042713 (2001).
[16] D.-S. Kim and S. T. Manson, *J. Phys. B*, submitted.
[17] S. Schippers, A. Müller, B. M McLaughlin, A. Aguilar, C. Cisneros, E. D. Emmons, M. F. Gharaibeh and R. A. Phaneuf, *J. Phys. B* **36**, 3371 (2003).

LOW ENERGY ELECTRON INTERACTIONS WITH CONDENSED ORGANIC AND BIOLOGICAL MOLECULES, INCLUDING DNA.

Léon Sanche, Groupe en Sciences des Radiations, Faculté de médecine, Université de Sherbrooke, Sherbrooke (Québec) Canada J1H 5N4

Electrons with energies in the range 0-45 eV can induce at interfaces and with condensed matter specific reactions which are of relevance to applied fields such as nanolithography, dielectric aging, radiation waste management, radiation processing, astrobiology, planetary and atmospheric chemistry, surface photochemistry, radiobiology, radiotherapy and ballistic electronics. Understanding these processes requires knowledge of the interaction of low energy electrons (LEEs) within condensed matter and/or at surfaces and interfaces. The results of investigations related to two of these applied fields, radiotherapy and dielectric aging, will be presented at this workshop. The action of LEEs in DNA is of relevance to the former, whereas that on polyethylene is of relevance to the latter application. The action of LEEs in polyethylene and dielectric aging of this material under high voltages is investigated with model systems consisting of thin films of doped saturated organic molecules. The action of LEEs on large biomolecules such as DNA is also investigated with model systems made of a basic subunit of the molecule, or a longer portion of it, immersed in different environments to mimic specific cellular conditions. The target molecules usually consist of a multilayer film deposited on a metal substrate bombarded by a LEE beam (0-45 eV) under ultra high vacuum (UHV) conditions. Depending on the experiment, it is possible to measure neutral fragments and ions emanating from these films. The products remaining in the films can be analyzed *in situ* by X-ray photoelectron and electron energy loss spectroscopies; they can also be removed from the UHV system and analyzed by HPLC and GC/MS. At the theoretical level, it is possible to treat electron attachment to and dissociation from such large molecules (e.g. DNA or polyethylene) with our newly developed framework or from segments using Density Fonctional Theory. In the case of DNA, comparing the results of the theory and different experiments, it is possible to determine fundamental mechanisms that are involved in the dissociation of basic DNA constituents and the production of single- and double-strand breaks. Such mechanisms involve (1) the formation of transient anions which play a dominant role in the fragmentation of all biomolecules investigated; (2) dipolar dissociation which produces an anion and a cation and (3) reactive scattering, which induces non-thermal reactions. The transient anions fragment the parent molecules by decaying into dissociative electronically excited states or by dissociating into a stable anion and a neutral radical. These fragments usually initiate other reactions with nearby molecules, causing further chemical damage. The damage caused by transient anions is dependent on the molecular environment. Thus, it appears that changes in the environment or topology of DNA may affect considerably the damage induced by LEEs and may therefore serve as a tool to modify DNA damage induced by high-energy radiation. The results of recent experiments performed on films of DNA and its basic subunits (i.e., H_2O, DNA bases and sugar analogs) will be presented at this conference. The major type of experiments will be briefly described and the results of theoretical studies summarized. Application of some of our results to radiotherapy will be discussed in the context multidisciplinary research. It will also be shown that electronic aging of electrical cables subjected to high field strengths is principally due to the action of LEEs. This research is financed by the CIHR, NSERC and the NCIC.

Theoretical Studies of Resonant Electron-Polyatomic Collisions

A. E. Orel
Department of Applied Science
University of California, Davis
Davis, CA 95616
aeorel@ucdavis.edu

Program Scope

This program is a broad first-principles attack on resonant electron-polyatomic collisions which removes the level of empiricism that characterizes most current theoretical efforts. Modern *ab initio* techniques, both for the electron scattering and the subsequent nuclear dynamics studies, are used to attack previously unreachable areas. Specifically, this work addresses vibrational excitation, dissociative attachment, and dissociative recombination problems in which a full multi-dimensional treatment of the nuclear dynamics is essential and where non-adiabatic effects are expected to be important.

Recent Progress

Ab Initio Study of Low-energy Electron Collisions with Tetrafluoroethene, C_2F_4

In collaboration with T. N. Rescigno, LBL, we have carried out a study of low-energy electron collisions with tetrafluoroethene using the complex Kohn variational method. Information regarding collisions of electrons with tetrafluoroethene, C_2F_4, is important in the plasma processing of semiconductors. C_2F_4 has attracted interest as a feed gas in plasma etching of the silicon oxide surface and has been proposed as a new plasma reactant due to its low carbon-carbon bond strength and low global warming potential, with a consequent relatively benign impact on the atmosphere. C_2F_4 is also formed within plasmas by dissociation of another common feed gas used for oxide etching, C_4F_8. There have been only very limited studies of the interaction of C_2F_4 with low-energy ($<$20 eV) electrons.

C_2F_4 is a closed-shell molecule which possesses a permanent quadrupole moment. C_2F_4 is isovalent with C_2H_4. Like C_2H_4, which we have recently studied, the low-energy electron scattering from C_2F4 shows a Ramsauer-Townsend minimum in ^2A_g symmetry and a narrow shape resonance in $^2B_{2g}$ symmetry caused by the temporary capture of the incident electron into an empty, antibonding valence orbital. The C_2F_4 cross sections are also found to display resonance features in the symmetries ^2A_g, $^2B_{1u}$ and $^2B_{2u}$.

We carried out variational calculations of elastic electron scattering by tetrafluoroethene, C_2F_4, with incident electron energies ranging from 0.5 to 20 eV, using the complex Kohn method and effective core potentials. Low-energy electron scattering by C_2F_4 was found to be sensitive to the inclusion of electronic correlation and target-distortion effects. It was therefore necessary to include dynamic polarization of the target by the incident electron. The results are in good agreement with recent experiment, in both integrated and differential electronically elastic cross sections, at energies above 4 eV. Below 4 eV, where the calculated results are extremely sensitive to polarization effects, there were larger differences, particularly in the differential cross sections at small scattering angles.

The results of the calculation are described in a paper published in Physical Review A.

Low-energy electron scattering by NO: *ab initio* analysis of the $^3\Sigma^-$, $^1\Delta$ and $^1\Sigma^+$ shape resonances in the local complex potential model

In collaboration with C. W. McCurdy and T. N. Rescigno, LBL we have carried out a study of low-energy electron scattering by NO. The diatomic molecule nitric oxide plays an important role in a number of physical, chemical and

Publications

1. *Ab Initio* study of low-energy electron collisions with ethylene C. S. Trevisan, A. E. Orel, and T. N. Rescigno Phys. Rev. A **68**, 062707 (2003)

2. Low-energy electron scattering of NO : *Ab Initio* analysis of the $^3\Sigma^-$,$^1\Delta$, and $^1\Sigma^+$ shape resonances in the local complex potential model, Z. Zhang, W. Vanroose, C. W. McCurdy, A. E. Orel, and T. N. Rescigno Phys. Rev. A **69**, 062711 (2004)

3. *Ab Initio* study of low-energy electron collisions with tetrafluoroethene C_2F_4, C. S. Trevisan, A. E. Orel, and T. N. Rescigno, Phys. Rev. A **70**, 012704 (2004)

Electron-Atom and Electron-Molecule Collision Processes

C. W. McCurdy and T. N. Rescigno
Chemical Sciences, Lawrence Berkeley National Laboratory, Berkeley, CA 94720
cwmccurdy@lbl.gov, tnrescigno@lbl.gov

Program Scope: This project seeks to develop theoretical and computational methods for treating electron collision processes that are currently beyond the grasp of first principles methods, either because of the complexity of the targets or the intrinsic complexity of the processes themselves. We are developing methods for treating low energy electron collisions with polyatomic molecules, complex molecular clusters and molecules bound to surfaces and interfaces, for studying electron-atom and electron-molecule collisions at energies above that required to ionize the target and for calculating detailed electron impact ionization and double photoionization probabilities for simple atoms and molecules.

Recent Progress and Future Plans: We report progress in three distinct areas covered under this project, namely electron-polyatomic molecule collisions, electron impact ionization and double photoionization.

1. Electron-Molecule Collisions

We have completed the first phase of a major study of dissociative electron attachment (DEA) to water. Low-energy dissociative attachment in water proceeds via Feshbach resonances corresponding to the formation of metastable negative ion states. Using the Complex Kohn Variational method, augmented with large-scale configuration-interaction studies, we constructed a complete, three-dimensional complex energy surface for the lowest ($^2B_1$) resonance and then carried out time-dependent wavepacket studies of the dissociation dynamics in full dimensionality using the Multi-Configuration Time-Dependent Hartree method in collaboration with H-D. Meyer (Heidelberg University). The results of this study, which represent the first ever fully *ab initio* calculation of dissociative electron attachment to a polyatomic target, were found to be in substantial agreement with experiment and were published in two papers in Physical Review A. We plan to extend these studies to the two higher ($^2A_1$ and $^2B_2$) resonance states, thereby providing a complete first-principles treatment of DEA in this important system, including cross sections and branching ratios between the H^- + OH and O^- + H_2 product arrangements .

The Complex Kohn method continues to serve as our principal tool for studying electron-molecule scattering. In collaboration with A. E. Orel (UC Davis), we have used this method to study low-energy electron scattering by ethylene and tetrafluoroethene , which are both important in low-temperature plasma technology. We also completed an initial study of the dynamics of resonant vibrational excitation of NO, using the complex Kohn method to characterize the resonance curves along with a local complex potential model for the nuclear dynamics. Our plans are to explore the importance of non-local

effects in the excitation dynamics of this molecule and to predict cross sections for dissociative electron attachment to NO. Experimental studies on dissociative attachment to NO are also underway at LBNL.

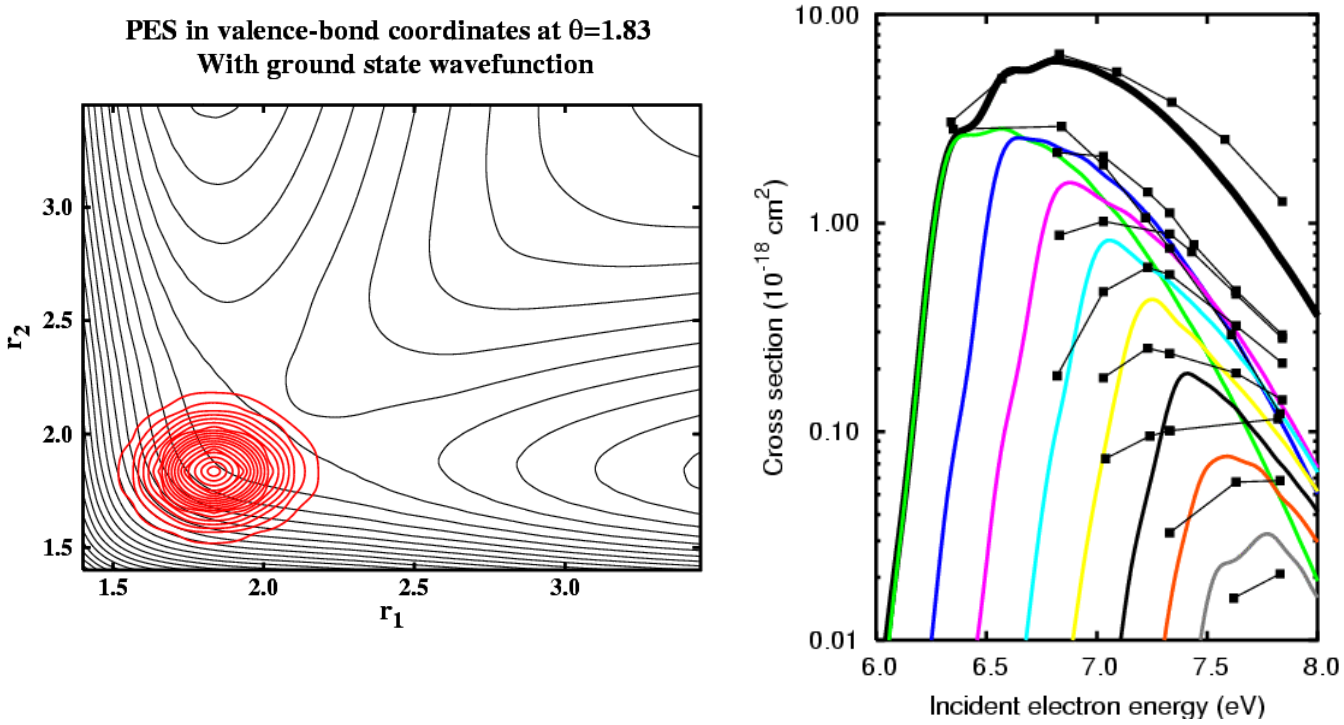

Left Panel: Initial wave packet shown on a cut of the 3D potential surface for the $^2B_1$ resonant state of H_2O. **Right Panel:** Comparison of calculated and measured (lines with squares) cross sections for production of OH in vibrational states v = 0 to v=7 in dissociative electron attachment to water. Thick line: total cross section.

2. Electron-Impact Ionization

Our studies of electron impact ionization are based on the e*xterior complex scaling* (ECS) method - an approach that has provided the only *complete* solution to the quantum mechanical three-body Coulomb problem at low collision energies to date. Using a time-dependent version of the basic ECS approach, we have successfully extended our studies to treat ionization of an atomic target with two active electrons. We have completed a study of electron-impact ionization of helium in the S-wave model, providing the first ever calculation of single differential ionization cross sections for a target with two active electrons. The results have been submitted to Physical Review A. We also plan to extend these studies to look at excitation-ionization and its signature on the differential ionization cross section.

3. Double Photoionization

We have continued with a theoretical effort, initiated in FY03, directed at studying double photoionization (one photon in, two electrons out) of atoms and molecules using the exterior complex scaling approach. The viability of the approach was successfully demonstrated this year with an extensive study of differential cross sections for double photoionization of helium which was published in Physical Review A along with a second paper on complex ionization amplitudes recently submitted for publication. We have also made substantial progress in extending these studies to a molecular target and have obtained preliminary results for double photoionization of H_2. All of this work has been carried out using an implementation of ECS with B-splines in collaboration with F. Martín (Autonomous University of Madrid). We are planning a further modification of our current approach that will replace the B-splines with a more efficient Discrete Variable Representation. We are also working on a hybrid approach that combines the use of molecular Gaussian basis sets with the Discrete Variable Representation and ECS. Such an approach avoids the use of single-center expansions, simplifies the computation of two-electron integrals and will pave the way for studies of double photoionization of more complex molecules.

Publications (2002-2004):

1. T. N. Rescigno, W. A. Isaacs, A. E. Orel, H.-D. Meyer and C. W. McCurdy, "Theoretical Studies of Excitation in Low-Energy Electron-Polyatomic Molecule Collisions", in *Photonic, Electronic and Atomic Collisions, Invited Papers*, *Proceedings of the XXII International Conference on Photonic, Electronic and Atomic Collisions,* Santa Fe, NM 2001 (Rinton Press, Princeton 2002).
2. C. W. McCurdy, M. Baertschy, W. A. Isaacs and T. N. Rescigno, "Reducing Collisional Breakup of a System of Charged Particles to Practical Computation: Electron-Impact Ionization of Hydrogen", in *Photonic, Electronic and Atomic Collisions, Invited Papers*, *Proceedings of the XXII International Conference on Photonic, Electronic and Atomic Collisions,* Santa Fe, NM 2001 (Rinton Press, Princeton 2002).
3. T. N. Rescigno, W. A. Isaacs, A. E. Orel, H.-D. Meyer and C. W. McCurdy, "Theoretical Study of Resonant Vibrational Excitation of CO_2 by Electron Impact", *Phys. Rev. A* **65**, 032716 (2002).
4. C. W. McCurdy, D. A. Horner and T. N. Rescigno, "Time-dependent approach to collisional ionization using exterior complex scaling", *Phys. Rev. A* **65**, 042714 (2002).
5. W. Vanroose, C. W. McCurdy and T. N. Rescigno, "On the Interpretation of Low Energy Electron-CO_2 Scattering", *Phys. Rev. A* **66**, 032720 (2002).
6. T. N. Rescigno and C. W. McCurdy, "Collisional Breakup in Coulomb Systems", in *Many-Particle Quantum Dynamics in Atoms and Molecules*, edited by V. Shevelko and J. Ullrich (Springer-Verlag, Heidelberg, 2003).

7. C. W. McCurdy, W. A. Isaacs, H.-D. Meyer and T. N. Rescigno, "Resonant Vibrational Excitation of CO_2 by Electron Impact: Nuclear Dynamics on the Coupled Components of the $^2\Pi_u$ resonance", *Phys. Rev. A* **67**, 042708 (2003).
8. T. N. Rescigno, M. Baertschy and C. W. McCurdy, "Resolution of phase ambiguities in electron-impact ionization amplitudes", *Phys. Rev. A* **68**, 020701 (R) (2003).
9. C. Trevisan, A. E. Orel and T. N. Rescigno , "Ab Initio Study of Low-Energy Electron Collisions with Ethylene", *Phys. Rev. A* **68**, 062707 (2003)
10. W. Vanroose , C. W. McCurdy and T. N. Rescigno, "Scattering of Slow Electrons by Polar Molecules: Application of Effective-Range Potential Theory to HCl", *Phys. Rev. A* **68**, 052713 (2003).
11. W. Vanroose, Z. Zhang , C. W. McCurdyand T. N. Rescigno, "Threshold Vibrational Excitation of CO_2 by Slow Electrons", *Phys. Rev. Letts*. **92**, 053201 (2004).
12. C. W. McCurdy and F. Martin, ""Implementation of Exterior Complex Scaling in B-Splines to Solve Atomic and Molecular Collision Problems", J. Phys. B **37**, 917 (2004).
13. C. W. McCurdy, D. A. Horner, T. N. Rescigno and F. Martin, "Theoretical Treatment of Double Photoionization of Helium Using a B-spline Implementation of Exterior Complex Scaling", *Phys. Rev. A* **69**, 032707 (2004).
14. Z. Zhang, W. Vanroose, C. W. McCurdy, A. E. Orel and T. N. Rescigno , "Low-energy Electron Scattering by NO: Ab Initio Analysis of the $^3\Sigma^-$, $^1\Delta$ and $^1\Sigma^+$ shape resonances in the local complex potential model", *Phys. Rev. A* **69**, 062711 (2004).
15. D. J. Haxton, Z. Zhang, C. W. McCurdy and T. N. Rescigno, "Complex Potential Surface for the $^2B_1$ Metastable State of the Water Anion", *Phys. Rev. A* **69**, 062713 (2004).
16. D. J. Haxton, Z. Zhang , H.-D. Meyer , T. N. Rescigno and C. W. McCurdy, "Dynamics of Dissociative Attachment of Electrons to Water Through the $^2B_1$ Metastable State of the Anion", *Phys. Rev. A* **69**, 062714 (2004).
17. C. S. Trevisan , A. E. Orel and T. N. Rescigno, "Ab initio study of Low-Energy Electron Collisions with tetrafluoroethene, C_2F_4" , *Phys. Rev. A* **70**, 012704 (2004).
18. C. W. McCurdy, M. Baertschy and T. N. Rescigno, "Solving the Three-Body Coulomb Breakup Problem Using Exterior Complex Scaling", *J. Phys. B* (topical review) (accepted).

"Low-Energy Electron Interactions with Complex Targets"

Thomas M. Orlando, *School of Chemistry and Biochemistry and School of Physics, Georgia Institute of Technology, Atlanta, GA 30332-0400*
Thomas.Orlando@chemistry.gatech.edu

Objectives: The primary objectives of this program are to investigate the fundamental physics and chemistry involved in low-energy (1-100 eV) electron scattering with molecular solids, surfaces and interfaces. The program is primarily experimental and concentrates on the important questions concerning how gas-phase concepts have to be modified when trying to understand electron collisions with complex condensed-phase targets.

Progress: This is the second year of the program which began in July 2002. We have focused on three main tasks that are being carried out in the Electron- and Photon-Induced Chemistry on Surfaces (EPICS) Laboratory at the Georgia Institute of Technology (GIT).

Task 1. ***The temperature dependence of low-energy (5 –250 eV) electron stimulated desorption of H^+, H_2^+, and $H^+(H_2O)_n$ and the uptake and autoionization of HCl on low-temperature water ice.*** We have used low-energy electron stimulated desorption (ESD) to study the production of H^+, H_2^+, and protonated water clusters ($H^+(H_2O)_n$) from pure non-porous amorphous solid water (ASW) and crystalline (CI) water ice films [1-4]. We observe a threshold energy of 22 ± 1 eV for the ESD of H^+ and H_2^+. H^+ ESD has a secondary threshold above ~ 40 eV and dominates the cation yields from both ASW and CI. A small yield of protonated clusters $H^+(H_2O)_n$, where n=1-8, is also observed for incident electron energies above ~ 40 eV, and the yield for $H^+(H_2O)_{n=1-8}$ increases significantly at ~ 70 eV. The $H^+(H_2O)_{n=1-8}$ yields are higher from ASW relative to CI and decrease with temperature, whereas the proton and H_2^+ yields show the opposite trend, increasing with temperature. All of these cation desorption channels involve localized two-hole states containing a_1 character. Since a_1 levels are involved in hydrogen bonding and are perturbed via nearest neighbor coupling, the ESD cation yields are very sensitive to the local potential and disorder in the terminal layer of the ice. The changes in the yields with phase and temperature are associated with structural and physical changes in the adsorbed water and longer lifetimes of excited state configurations containing a_1 character. This is shown below in Figure 1. Also shown is the thermal desorption data of 0.05 ML of HCl adsorbed on ASW.

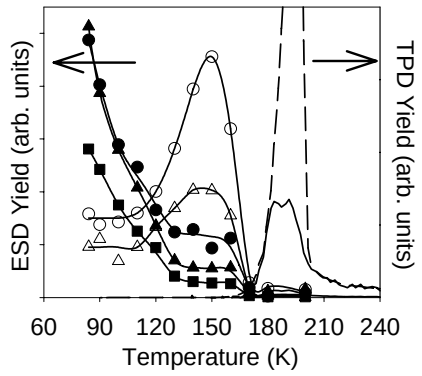

Figure 1. Temperature dependence of electron stimulated cation yields (left axis) compared to thermal desorption data (right axis). The H^+ (-○-) and H_2^+ (-Δ-) yields increase as a function of temperature, whereas the cluster ion yields (i.e. H_3O^+ (-•-), $H^+(H_2O)_2$ (-▲-) and $H^+(H_2O)_3$ (-■-) decrease. These changes occur prior to any appreciable thermal desorption of H_2O (dashed line) and molecular HCl (solid line). Note the HCl and H_2O desorption processes are correlated.

We have utilized the dependence of the ESD cation yields on the local potential to examine the details of HCl interactions on low-temperature (80- 140 K) water ice surfaces. This experiment relies upon the results of the previous task which examined the ESD of protons and protonated clusters $(H^+)(H_2O)_n$, where n=1-8. As discussed above, these cation desorption channels involve localized two-hole states and the yields are very sensitive to the local disorder in the terminal layer of the ice. We have observed an enormous reduction of the proton signal and a concomitant increase in the protonated cluster signals due to the presence of sub-monolayer quantities of HCl. This occurs at temperatures as low as 80 K and indicates rapid uptake and non-activated autoionization of HCl. This forms ion-pair states that lead to disorder, reduced numbers of dangling bonds and increased hole-localization. These results clearly demonstrate the utility of ESD to probe the interactions of acidic molecules with low-temperature ice surfaces.

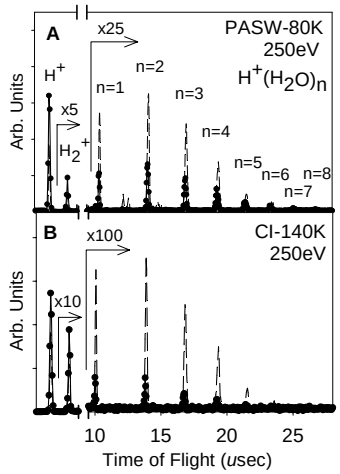

Figure 2. The time-of-flight distribution of cations produced and desorbed during pulsed 250 eV electron beam irradiation of PASW (A) and CI (B). The filled circles represent data obtained from pristine ice whereas the dashed line indicates the ion yield after the addition of 0.06 ML of HCl. The HCl ionizes causing a large reduction in H^+ and H_2^+ and an increase in $H^+(H_2O)_n$ yields.

Task 2. ***A theoretical description and experimental demonstration of diffraction in electron stimulated desorption (DESD).*** The role of diffraction in electron-stimulated desorption (DESD) is demonstrated and described theoretically [5,6]. Specifically, initial state effects in DESD of Cl^+ from Si(111)-(1×1):Cl is examined and the theory is expanded to encompass spherical-wave and multiple scattering effects of low-energy incident electrons by introducing a separable propagator method. The scattering amplitude is calculated and compared with a plane-wave approximation, which can be applied to reduce the calculation time of DESD. Qualitative analysis of Cl^+ desorption shows that the initial excitation occurring on the Si(111)-(1×1):Cl surface primarily involves the Si. Two desorption mechanisms are proposed, i) ionization of the Si(3s) level followed by Auger cascading from the σ-bonding surface state and shake-up of an electron in the non-bonding π-level and ii) direct ionization of the Si-Cl σ-bonding state. Temperature effects on DESD rates are also analyzed and modeled. The feasibility and potential utility of DESD for holographic imaging is also discussed.

Task 3. ***Low-energy electron-induced damage of DNA: Neutral fragments yields.*** We have utilized a VUV source using third-harmonic generation in rare gases to detect the neutral fragments produced during the low-energy electron beam induced damage of DNA plasmids physisorbed on graphite substrates. We are also monitoring the DNA damage using *in situ* Fourier transform infrared spectroscopy and post-irradiation gel-electrophoresis. The data indicates that negative ion-resonances of the interfacial water and substrate interactions contribute to the damage of DNA.

Future Plans:

Task 1. The role of co-adsorbates on ESD and DEA processes. We will continue our studies of low-energy electron stimulated desorption from low-temperature ice surfaces and interfaces containing co-adsorbed species. In particular, we will examine physisorbed O_2 and Cl_2 on multilayer ice. We will also examine interface structure, dynamics and electron scattering resonances associated with the presence of ions typically found in environmental and biological systems.

Task 2. Vacuum ultraviolet photo-induced processes in water films: The competition between ionization and dissociation. We plan to continue VUV based photo-ionization mass spectrometry techniques to examine the low-energy electron-induced damage of DNA plasmids and DNA strands. This work will involve very careful control (i.e. removal) of substrate effects. In addition, it will play close attention to the role intrinsic water plays in DNA damage initiated by low-energy electrons.

Task 3. Theoretical description of electron-molecule scattering with DNA and other complex organic molecules. We have used the theory developed to describe DESD from well-ordered Cl-terminated Si surfaces [5,6] to look at interference effects during the elastic and inelastic scattering of electrons with a model helical collision system constructed from of Ar scattering centers. The geometrical arrangement has been chosen to represent the B-DNA. We will continue this work by applying it to a collision system representative of the A form of DNA. We will also incorporate more realistic scattering potentials into the calculation.

References (Publications from this program)

1.) T. M. Orlando and M. T. Sieger, "The Role of Electron-stimluated production of O_2 from water ice and the radiation processing outer solar system surfaces" *Surf. Sci.* **528**, 1-7 (2003).

2.) J. Herring, A. Alexandrov, and T. M. Orlando**,** "The stimulated desorption of cations from pristine and acidic low-temperature ice surfaces" *Phys. Rev. Lett.* 92, 187602-1, (2004).

3.) J. Herring and A. Alexandrov,and T. M. Orlando "Electron-stimulated desorption of H^+, H_2^+ and $H^+(H_2O)_n$ from nanoscale water thin-films", *(accepted)*, *Phys. Rev. B.*. (2004).

4.) J. Herring, A. Alexandrov, and T. M. Orlando "Probing the interaction of hydrogen chloride on low-temperature water ice surfaces using electron stimulated desorption", (*submitted)*, *J. Chem. Phys.*

5.) T. M. Orlando**,** D. Oh, M. T. Sieger, and C. Lane, "Electron collisions with complex targets: diffraction effects in stimulated desorption", *Physica Scripta*, T110, 256, (2004).

6.) D. Oh, M. T. Sieger and T. M. Orlando, "A theoretical description of diffraction effects in electron-stimulated desorption"*(accepted), Phys. Rev. B.* (2004).

DYNAMICS OF FEW-BODY ATOMIC PROCESSES

Anthony F. Starace

The University of Nebraska
Department of Physics and Astronomy
116 Brace Laboratory
Lincoln, NE 68588-0111
Email: astarace1@unl.edu

PROGRAM SCOPE

The major goal of this project is to understand the physics underlying the interaction of real atomic systems with strong external fields. Most of the atomic systems considered for study are many-electron systems. We treat their interactions, i.e., electron correlations, as accurately as possible. The strong external fields considered are mainly intense laser fields. In some cases our studies are supportive of and/or have been stimulated by experimental work carried out by other investigators funded by the DOE AMO physics program.

RECENT PROGRESS

A. Elucidating the Mechanisms of Laser Double Ionization

We have investigated the interaction of a two-active electron system (Li^-) with linearly polarized, intense half-cycle, single-cycle, and double half-cycle pulses in order to elucidate the mechanisms leading to double ionization (see publication [7]). These numerical experiments were carried out by solving the time-dependent Schrödinger equation (including electron correlations) for the two active electrons of Li^- interacting with an intense laser pulse. The calculation employed the full dimensions of the problem, and the ionized electron angular distributions were analyzed. The "intensity" and "frequency" considered correspond to the multiphoton, above-barrier regime, which is only just beginning to be studied experimentally. For the single-cycle pulse (SCP), the electric field changes sign once, allowing electron wave packets created during the first half cycle to recollide with the parent atom or ion when driven back by the field. For the double half-cycle pulse (DHP), however, the electric field does not change sign, and electron wave packets created during the first half cycle are accelerated further away from the parent ion. We find that both single and double ionization are significantly larger for the SCP than for the DHP, thereby providing clear evidence for the role of the rescattering mechanism. On the other hand, doubly ionized electrons produced by a half-cycle pulse (HCP) and a DHP are found to have angular distributions in which one electron is ejected in the direction of the pulse field, and the other in the opposite direction. This clear signature of electron correlations suggests that "shake-off," "knockout," and, possibly, "multiphoton-sharing" processes are alternative contributing mechanisms for double ionization in this regime. Finally, our numerical experiments have also elucidated the mechanisms leading to angular distributions

in which both electrons are ejected *perpendicularly* to the laser polarization direction. We have found that these configurations occur with much higher probabilities for a SCP than for either a HCP or a DHP. These configurations thus appear to be clear signatures of the electron recollision mechanism of double ionization.

B. Circular Dichroism in Double Photoionization of He

We have extended our lowest order perturbative approach (LOPT) in electron-electron correlation (see publication [4]) to analyze the circular dichroism (CD) effect in double photoionization of He, i.e., the fact that the triply differential cross section (TDCS) is different for right- and left-circularly polarized light (see publication [8]). We find that our LOPT account of final state electron correlations combined with variational account of electron screening in the ground state provides predictions for the TDCSs that agree quite well with both experimental data and the most accurate ab initio theoretical results for excess energies up to 80 eV. Our predictions for CD are in excellent agreement with absolute experimental data for excess energies of 20 eV and 60 eV. Our theoretical analysis shows that the physical origin of the CD effect stems from the non-zero Coulomb phase shifts of the ionized electrons, i.e., the effect vanishes in the plane wave Born approximation.

C. Non-Dipole Effects in Double Photoionization of He

In recent years two major themes in both experimental and theoretical studies of atomic photoionization have been the analysis of nondipole (or retardation) effects in single-electron photoionization (both in the x-ray and the vuv regions) and the analysis of double photoionization (especially in the vuv energy region). Surprisingly, there have not been as yet any analyses of nondipole effects on double photoionization. In part this is because nearly all experimental measurements have been carried out with linear polarization in the orthogonal plane geometry (i.e., photoelectrons are detected in the plane perpendicular to the photon wave vector). For this case, non-dipole effects vanish. We have recently completed an analysis of nondipole effects in double photoionization of He (see publication [9]). Specifically, we have derived a general parameterization for the double photoionization amplitude of He taking into account both dipole (E1) and quadrupole (E2) components of the electron-photon interaction operator. Nondipole effects originate from the interference of the E1 and E2 amplitudes. Our numerical results show that these effects are significant in double photoionization of He even for excess energies as low as 80 eV and should be observable in experiments with current state-of-the-art capabilities.

For the case of linearly polarized light [9], we have analyzed our parameterized formulas for the TDCS and proposed two experimental geometries for which the nondipole effects are maximal, one for equal energy sharing and one for unequal energy sharing. Both are coplanar geometries, in which the momenta, $\mathbf{p}_1$ and $\mathbf{p}_2$, of the two ionized electrons lie in the plane defined by the photon wave vector, $\mathbf{k}$, and the linear polarization direction. In each case, the TDCS should be measured for two directions of the photon beam propagation: in the directions $\mathbf{k}$ and $-\mathbf{k}$ (with the direction of the linear polarization vector unchanged). Differences in the TDCSs of the order of 15%-20% of the maximum of the TDCS are predicted.

For the case of circularly polarized light, we have recently analyzed the influence of nondipole interactions on the circular dichroism (CD) effect in double photoionization of He [10]. It is well known that the CD effect vanishes ordinarily in the case that the two ionized electrons share the total available energy equally. We have shown analytically that there exists a nonzero CD effect for this case of equal energy sharing when one takes into account the interference of E1 and E2 transition amplitudes. We have also shown that this interference leads to unusual asymmetries of the TDCS for the case of elliptically polarized light. We have proposed two experimental arrangements for measuring each of these effects, which together provide a polarization sensitive means of measuring nondipole effects in double photoionization. Our numerical estimates indicate that CD effects are significant for electron energies as low as 40 eV.

D. GeV Electrons from Ultra Intense Laser Interactions with Highly Charged Ions

As described in Ref. [1], we have investigated laser interactions with highly charged hydrogenic ions using a three-dimensional relativistic Monte Carlo simulation. We first demonstrated that free electrons cannot be accelerated to GeV energies by the highest intensity lasers because they are quickly expelled from the laser pulse before it reaches peak intensity. We have shown that highly charged ions exist that (1) have deep enough potential wells that tunneling ionization is insignificant over the duration of an intense, short laser pulse, and (2) have potentials that are not too deep, so that the laser pulse is still able to ionize the bound electron when the laser field reaches its peak intensity. We have shown that when the ionized electron experiences the peak intensity of the laser field, then it is accelerated to relativistic velocity along the laser propagation direction (by the Lorentz force) within a tiny fraction of a laser cycle. Within its rest frame it then "rides" on the peak laser amplitude and is accelerated to GeV energies before being expelled from the laser pulse.

Recently, we have carried out an extensive set of calculations to examine the dependence of the ionized electron energy spectrum on the experimentally controllable parameters. These include the target ion and the laser intensity, frequency, duration, and, especially, the focal properties. A manuscript describing these calculations has recently been submitted for publication.

E. Control of Entanglement of Two Interacting Spin 1/2 (Heisenberg) Systems

In Ref. [2], we have shown that for the case of two interacting spin 1/2 qubits whose interaction is anisotropic (i.e., different in different directions), the critical temperature (above which entanglement no longer exists) is dependent on the magnitude of the magnetic field, which is chosen to be constant along the z axis. Recently, we have analyzed the entanglement of a two qubit XY chain in thermal equilibrium at temperature T in the presence of an external magnetic field B in arbitrary directions: $\mathrm{B} = \mathrm{B}_x\hat{\mathrm{x}} + \mathrm{B}_y\hat{\mathrm{y}} + \mathrm{B}_z\hat{\mathrm{z}}$. We find that for a B field confined to the x-y plane, ferromagnetic (FM) and antiferromagnetic (AFM) chains lead to different forms of entanglement, and that even for the isotropic XX chain the two qubits can be entangled at any finite T by adjusting the field strength. It is found that quantum phase transitions occur for AFM chains but not for FM chains. For the Heisenberg-Ising case, when the B-field is directed along the Ising axis, the entanglement is the same for AFM and FM chains. A manuscript on this work will soon be submitted for publication

FUTURE PLANS

Our group is currently carrying out research on the following projects: (1) Calculation of benchmark, two-photon ionization cross sections of He using a variationally-stable, coupled hyperspherical-channel approach; (2) Calculation of two-photon, double ionization cross sections for He using an LOPT approach; (3) Development of an effective range theory approach for laser-assisted electron-atom scattering; (4) Analysis of the polarization dependence of high energy plateau structures in laser-assisted, electron-atom scattering processes; (5) Analysis of the entanglement of interacting magnetic nanodots having large spins ($\sim 10^3 \hbar$).

2002-2004 PUBLICATIONS STEMMING FROM DOE-SPONSORED RESEARCH

[1] S.X. Hu and A.F. Starace, "GeV Electrons from Ultra-Intense Laser Interaction with Highly-Charged Ions," Phys. Rev. Lett. **88**, 245003 (2002).

[2] G. Lagmago Kamta and A.F. Starace, "Anisotropy and Magnetic Field Effects on the Entanglement of a Two Qubit Heisenberg XY Chain," Phys. Rev. Lett. **88**, 107901 (2002).

[3] G. Lagmago Kamta and A.F. Starace, "Multielectron System in an Ultrashort, Intense Laser Field: A Nonperturbative, Time-Dependent Two-Active Electron Approach," Phys. Rev. A **65**, 053418 (2002).

[4] A.Y. Istomin, N.L. Manakov, and A.F. Starace, "Perturbative Calculation of the Triply Differential Cross Section for Photo-Double-Ionization of He," J. Phys. B **35**, L543 (2002).

[5] G. Lagmago Kamta and A.F. Starace, "Two-Active Electron Approach to Multielectron Systems in Intense Ultrashort Laser Pulses: Application to Li^-," J. Mod. Optics **50**, 597 (2003).

[6] M. Masili and A.F. Starace, "Static and Dynamic Dipole Polarizability of the He Atom Using Wave Functions Involving Logarithmic Terms," Phys. Rev. A **68**, 012508 (2003).

[7] G. Lagmago Kamta and A.F. Starace, "Elucidating the Mechanisms of Double Ionization Using Intense Half-Cycle, Single-Cycle, and Double Half-Cycle Pulses," Phys. Rev. A **68**, 043413 (2003).

[8] A.Y. Istomin, N.L. Manakov, and A.F. Starace, "Perturbative Analysis of the Triply Differential Cross Section and Circular Dichroism in Photo Double Ionization of He," Phys. Rev. A **69**, 032713 (2004).

[9] A.Y. Istomin, N.L. Manakov, A.V. Meremianin, and A.F. Starace, "Non-Dipole Effects in Photo Double Ionization of He by a VUV Photon," Phys. Rev. Lett. **92**, 063002 (2004).

[10] A.Y. Istomin, N.L. Manakov, A.V. Meremianin, and A.F. Starace, "Circular Dichroism at Equal Energy Sharing in Photo Double Ionization of He," Phys. Rev. A **70**, 010702(R) (2004).

Structure and Dynamics of Atoms, Ions, Molecules, and Surfaces:
Molecular Dynamics with Ion and Laser Beams

Itzik Ben-Itzhak, J. R. Macdonald Laboratory, Kansas State University
Manhattan, Ks 66506; ibi@phys.ksu.edu

The goals of this part of the JRML program are to study the different mechanisms leading to molecular dissociation and charge exchange following fast collisions, slow collisions, or interactions with an intense short-pulse laser.

Dissociation and ionization of molecular ions by ultra-short intense laser pulses, *Itzik Ben-Itzhak, Pengqian Wang, Jiangfan Xia, A. Max Sayler, Mark A. Smith, Kevin D. Carnes, and Brett D. Esry,* – partly in collaboration with *Z. Chang's* group, *C. Fehrenbach*, and *C.L. Cocke*.

We have experimentally explored laser-induced dissociation and ionization of diatomic molecular ions, such as H_2^+, HD^+, N_2^+ and O_2^+, using coincidence 3D momentum imaging. Only a handful of experimental studies of intense ultrashort laser interaction with molecular ions have been conducted so far [1-3]. The vibrationally excited molecular ion beam (4-8 keV), in our case, is crossed by an ultrashort intense laser beam (28-150 fs, 10^{13}-10^{14} W/cm^2). The resulting fragments are recorded in coincidence by a position-sensitive detector. Complete angular distribution and kinetic energy release maps are reconstructed from the measured dissociation-momentum vectors as shown in figure 1. Dissociation of the vibrational states around v=9 is notable in the low intensity measurements. The dissociating H_2^+ exhibits stronger alignment with increasing energy difference from a KER of≅0.77 eV. However, lower KER values align along the laser polarization while the higher values are associated with alignment away from the polarization direction. Dissociative ionization was found to be smaller than dissociation in our measurements and increased with laser intensity and the alignment of the molecular axis with the laser polarization vector. The data is compared with recent calculations performed by *Esry*.

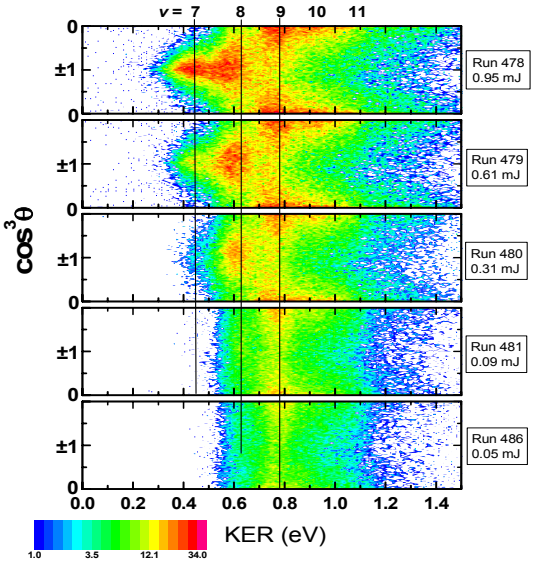

Figure 1. N(KER,cos$^3\theta$) density plots of H_2^+ exposed to 135 fs laser pulses with different pulse energies. The vertical lines are the approximate KER values expected from the vibrational states of the unperturbed H_2^+ if 1 net photon was absorbed.

Future plans: We plan to measure the dependence of ionization and dissociation of H_2^+, and other simple molecular ions, on the duration and intensity of the laser pulse.

1. I.D. Williams, P. McKenna, B. Srigengan, I.M.G. Johnston, W.A. Bryan, J.H. Sanderson, A. El-Zein,, T.R.J. Goodworth, W.R. Newell, P.F. Taday, and A.J. Langley, J. Phys. B **33**, 2743 (2000).
2. K. Sändig H. Figger, and T.W. Hänsch, Phys. Rev. Lett. **85**, 4876 (2000); C. Wunderlich, H. Figger, and T.W. Hänsch, Phys. Rev. A **62**, 023401-1 (2000). D. Pavićić et al., Eur. Phys. J. D **26**, 39 (2003).
3. A. Assion, T. Baumert, U. Weichmann, and G. Gerber, Phys. Rev. Lett. **86**, 5695 (2001).

Isotopic effects in bond-rearrangement of water ionized by fast proton impact. *Matt Leonard, A. Max Sayler, Pengqian Wang, Kevin D. Carnes, Brett D. Esry, and itzik. Ben-Itzhak.*

Studies of ionization and fragmentation of water molecules by fast protons and highly charged ions have revealed an interesting isotopic preference for H-H bond rearrangement. Specifically, the dissociation of $H_2O^+ \rightarrow H_2^+ + O$ is about twice as likely as $D_2O^+ \rightarrow D_2^+ + O$, with $HDO^+ \rightarrow HD^+ + O$ in between. Further investigations of this isotopic effect lead us to discover that bond rearrangement occurs also when the water molecule is multiply ionized, i.e. $H_2O^{2+} \rightarrow H_2^+ + O^+$, $H_2O^{3+} \rightarrow H_2^+ + O^{2+}$, etc. Calculations are underway to determine the relative production rates for the different isotopes from the overlap of the initial and final vibrational wave functions and the time evolution of the final wave function.

Future plans: The isotopic enhancement in the $H_2O^{2+} \rightarrow H_2^+ + O^+$ dissociative double ionization channel requires further investigation to determine if it is similar in magnitude to that found in single ionization.

Publications:

1. "Controlling HD^+ and H_2^+ dissociation with the carrier-envelope phase difference of an intense ultrashort laser pulse", Vladimir Roudnev, B.D. Esry, and I. Ben-Itzhak, Phys. Rev. Lett. (accepted) (2004).
2. "Ionization of atoms by the spatial gradient of the pondermotive potential in a focused laser beam", E. Wells, I. Ben-Itzhak, and R.R. Jones, Phys. Rev. Lett. **93**, 023001 (2004).
3. "Size dependent electron impact detachment of internally cold C_n^- and Al_n^- clusters", A. Diner, Y. Toker, D. Stasser, O. Heber, I. Ben-Itzhak, P.D. Witte, A. Wolf, D. Schwalm, M.L. Rappaport, K.G. Bhushan, and D. Zajfman, Phys. Rev. Lett. **93**, 063402 (2004).
4. "Electron impact detachment of small negative clusters", D. Zajfman, O. Heber, A. Diner, P.D. Witte, D. Stasser, Y. Toker, M.L. Rappaport, I. Ben-Itzhak, O. Guliamov, L. Kronik, D. Schwalm, and A. Wolf, proceedings of the International Conference on Electron and Photon Impact Ionization and Related Topics, Louvain-la-Neuve, Belgium, 1-3 July 2004 (accepted).
5. "Reexamining if long-lived N^- anions are produced in fast dissociative electron-capture collisions" I. Ben-Itzhak, O. Heber, I. Gertner, A. Bar-David, and B. Rosner, Phys. Rev. A **69**, 052701 (2004).
6. "Interference effects in double ionization of spatially aligned hydrogen molecules by fast highly charged ions", A.L. Landers, E. Wells, T. Osipov, K.D. Carnes, A.S. Alnasser, J.A. Tanis, J.H. McGuire, I. Ben-Itzhak, and C.L. Cocke, Phys. Rev. A (accepted) (2004).
7. "Probing very slow $H^+ + D(1s)$ collisions using the ground state dissociation of HD^+", E. Wells, K.D. Carnes, and I. Ben-Itzhak, Phys. Rev. **67**, 032708 (2003).
8. "Bond-Rearrangement in Water Ionized by Ion Impact", A.M. Sayler, J.W. Maseberg, D. Hathiramani, K.D. Carnes, and I. Ben-Itzhak, *Application of Accelerators in Research and Industry*, edited by J.L. Duggan and I.L. Morgan (AIP press, New York 2003), vol. **680**, p. 48.
9. "A comparative study of the ground state dissociation of H_2^+ and D_2^+ induced by ionizing and electron capture collisions with He^+ at velocities of 0.25 and 0.5 a.u.", W. Wolff, I. Ben-Itzhak, H.E. Wolf, C.L. Cocke, M.A. Abdallah, and M. Stöckli, Phys. Rev. A **65**, 042710 (2002).

Optical Trapping of Collisonally cooled molecules

David W. Chandler[1], James Valentini[2] and Mike Elioff[1]

[1]Sandia National Laboratories

Livermore, CA 94450, U.S.A.

[2]Chemistry Department, Columbia University

New York, New York

We recently reported our observations of a cooling process for molecules that relies upon a single collision between the molecule and an atom in a crossed molecular beam apparatus, producing molecules with a laboratory velocity that is nominally zero. The technique relies on a kinematic collapse of the laboratory velocity distribution of molecules that are scattered with a particular recoil velocity vector in the center-of-mass frame. The method depends on the fact that in binary collisions one of the collision partners can have a final center-of-mass-frame velocity that is essentially equal in magnitude and opposite in direction to the velocity of the center-of-mass, thus yielding a laboratory-frame velocity that is nearly zero. Cooling occurs because the center-of-mass velocity scales with initial NO velocity almost the same as the recoil velocity does.

Only collisions that result in NO molecules recoiling opposite to the direction of the motion of the center-of-mass experience the kinematic collapse. NO molecules recoiling in other directions have much larger laboratory velocities and quickly leave the scattering center. Therefore, only the NO molecules that have had their velocity distribution narrowed by collision remain in the region near the crossing point of the molecular beams.

This cooling process is very general, relying only on the experimentally selectable energy and momenta of the collision pair and not on any particular physical property of the colliding species. This technique can be used to prepare a single, selectable ro-vibronic quantum state for trapping. We demonstrated this technique using an existing crossed molecular beam experimental apparatus that is not specifically optimized for the production of cold molecules. Inelastic collisions were observed between NO molecules in one beam and Ar in the other, specifically $NO(^2\Pi_{1/2},j=0.5) + Ar \rightarrow NO(^2\Pi_{1/2},j'=6.5) + Ar$.

The crossed molecular beam experimental apparatus has been used to measure the differential cross section of the inelastically scattered NO molecules in NO + Ar collisions. A pair of doubly-skimmed pulsed free-jet expansions forms well collimated molecular beams that intersect at approximately 90^o. One of the beams is pure Ar, the other a mixture of 5% NO in Ar, with NO molecules predominantly in the ground rovibrational state. The Velocity Mapped Ion Imaging technique is used to characterize the scattering distribution and density of scattered NO molecules. In this method, the elastically and inelastically scattered NO products are observed by quantum-state-selective ionization using (1+1') resonance-enhanced multiphoton ionization (REMPI) through the NO ($A\,^2\Sigma \leftarrow X\,^2\Pi$) transition at 226.057 nm. The bandwidth of our excitation laser is sufficiently narrow to ensure that only those NO molecules in a selected J-state are excited to the $A^2\Sigma$ state and subsequently ionized by a 266-nm photon. The ions are formed in an electrostatic lens system that focuses and directs them onto a microchannel plate detector with a phosphorescent screen. Images created on the detector are captured with a CCD camera. Spatial positions in this image reveal the velocities of the scattered NO molecules being

detected, with the velocity given by the ratio of the displacement on the detector, measured from the beam crossing point, to the flight time of the ions from the laser/molecular beam intersection region to the detector, multiplied by an instrumental magnification factor.

A false-color image of $NO_{6.5}$ from $NO(^2\Pi_{1/2},j=0.5) + Ar \rightarrow NO(^2\Pi_{1/2},j'=6.5) + Ar$ is shown in Fig. 1. For this image the scattered $NO_{6.5}$ lies on a circle with a radius corresponding to its center-of-mass recoil velocity, about 410 m s^{-1}, associated with its share of the total relative collision energy of 5.73±0.20 kJ mol^{-1}. This circle of possible velocities appears in the Figure as a circle with varying intensity near its perimeter. The center of the scattering circle is the origin of the center-of-mass coordinate system. This origin is translated with respect to the origin of the laboratory-frame coordinate system, which is the intersection of the NO and Ar beams, by a distance that corresponds to the velocity of the center-of-mass of the NO + Ar system. The NO molecular beam contains a small amount of $NO_{6.5}$ not cooled in the expansion, which is seen as a small diagonal band of intensity intersecting the circle of scattered $NO_{6.5}$ on the left side of the image at $\theta=0^o$. On the circle of scattered $NO_{6.5}$ product, an intense and sharp peak is observed near the top of the circle ($\theta=85.6^o$ in the center-of-mass-frame coordinate system.) This peak is at the origin of the laboratory frame. This near-zero laboratory velocity arises from $NO_{6.5}$ produced by scattering of $NO_{0.5}$ from an argon atom.

Analysis of the near-zero velocity distribution of the NO left in the collision region reveals an upper limit root-mean-square velocity of 15 m s^{-1}. This distribution of NO velocities corresponds to a temperature of approximately 0.03 K. We find that scattering into the $NO_{6.5}$ state provides the highest density. The probability that an atom-molecule collision will result in an NO molecule that is cooled is small. From an analysis of our experimental data we estimate that the probability of a molecule having a collision resulting in a velocity less than 15 m s^{-1} is approximately 10^{-5}. In a typical crossed molecular beam experiment collision frequencies of approximately 10^{13} collisions per second can be achieved during a single molecular beam pulse lasting about 0.5 ms and contained in a crossed-beam volume of ~$10^{-4}$$cm^3$. We estimate that densities of 10^8-10^9 NO molecules cm^{-3} in this single ($^2\Pi_{1/2}$,v', j'=6.5) rovibrational quantum state have been achieved.

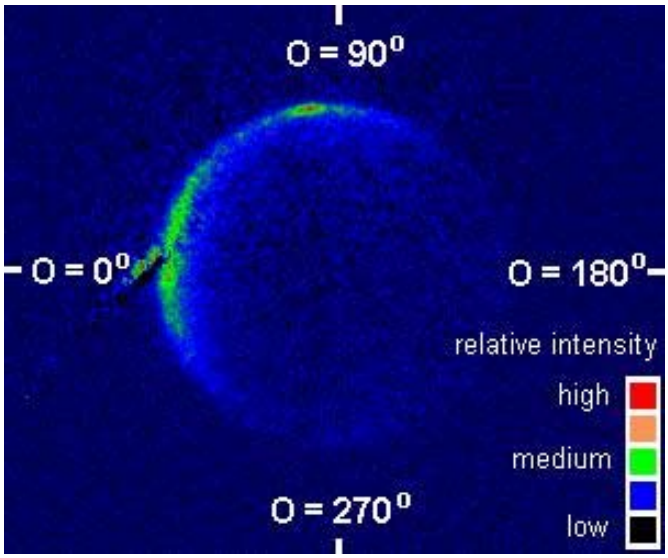

Figure 1. Velocity-mapped ion image for collisions between nitric oxide and argon, $NO(^2\Pi_{1/2},j=0.5) + Ar \rightarrow NO(^2\Pi_{1/2},j'=6.5) + Ar$ at a center-of-mass collision energy of 5.73±0.20 kJ mol^{-1}. The intense spot at the top of the scattering sphere is the result a collapse of the velocity spreads of the molecular beams for those molecules whose scattered velocity vector cancels the center-of-mass velocity of the collision pair.

Ultracold Molecules: Physics in the Quantum Regime

John Doyle
Harvard University
17 Oxford Street
Cambridge MA 02138
doyle@physics.harvard.edu

Our research encompasses a unified approach to the trapping of both atoms and molecules. Our goal is to extend our very successful work with CaH to NH and approach the ultracold regime. We plan to trap and cool more than 10^{11} NH molecules loaded directly from a molecular beam. We have switched to the NH molecule due to its higher magnetic moment, 2 Bohr magneton versus 1 Bohr magneton for CaH. Elastic and inelastic collisional cross sections will be measured and cooling to the ultracold regime will be attempted. To date, no collisional cross sections have been measured for ultracold heteronuclear molecules and theory offers no accurate predictions. We note that our work inherently contains the continued development of an important trapping technique, buffer-gas loading. This method was invented in our lab and has significant advantages over other approaches (large numbers of trapped atoms and molecules as well as general applicability). Following along these lines we have also embarked on the study of cold inelastic collisions in heteronuclear molecules. Our first measurement of such a cross section (in CaH) was followed by a theoretical prediction (by Krems and co-workers) of a scaling law that should be applicable to many heteronuclear diatomic molecules. We sought to test this model through the study of spin relaxation in CaF.

For the NH project we have achieved the following milestones:

x–spectroscopic detection of ground-state NH molecules via LIF
x–production of NH in a pulsed beam
x–spectroscopic detection of ground-state NH molecules via absorption
x–injection of NH beam into cryogenic buffer gas (including LIF and absorption detection)
x–realization of 4 T deep trap run in vacuum
x–injection of NH molecules into cryogenic trapping region

The project started 15 August 2002. In addition to our NH work, we completed measurements of CaF spin relaxation at low temperatures, a task not in our original proposal. There were several key questions about NH before us when this project began. Could we produce enough NH using a pulsed beam? Is it possible to introduce a large number of NH molecules into a buffer gas? Would the light collection efficiency be enough for us to adequately detect fluorescence from NH? Could we get absorption spectroscopy to work so that absolute number measurements could be performed? We have now answered these questions, all to the positive.

There are key questions left. Will the spin relaxation rates with helium be low enough for us to buffer-gas load a magnetic trap? Will the NH-NH collision rates be adequate for evaporative cooling or will another method (like sympathetic or laser cooling) be necessary to cool NH into the ultracold regime? Recent calculations by Krems indicate that the answer to the first question is "yes." The last question is still open and, indeed, answering this question is the key stated goal of this work. The recent work of Krems and co-workers predicted not only that NH inelastic rates should be low but also proposed scaling laws for inelastic cross-sections for both doublet and triplet sigma molecules. As such seminal theory is an important finding in the field, can be used as a guide for future experiments and deserves testing in its own right, we set out to test the scaling law with another molecule, CaF. We accomplished this by measuring directly the spin-relaxation rate for CaF and found our results to be consistent with the predicted scaling law.

Resonant Interactions in Quantum Degenerate Bose and Fermi Gases

Principal Investigator: Murray Holland

murray.holland@colorado.edu

440 UCB, JILA, University of Colorado, Boulder, CO 80309-0440

Program Scope

Our program of research is aimed at developing the effective quantum field theory which describes superfluidity in dilute atomic gases in the presence of resonant interactions. There are two distinct types of superfluidity. A first type occurs in fermionic systems in the presence of an effectively attractive fermion-fermion interaction (as in superconducting metals). The symmetry breaking there is associated with the development of mean-field pair-correlations with coherence length much larger than the interparticle spacing. A second type of superfluidity occurs in bosonic systems (such as atomic condensates) where the symmetry breaking is associated with the condensation of preformed bosons with spatial size much smaller than the interparticle spacing. For many years it has been conjectured that these two types of superfluidity are in fact alternative limits of a single universal phenomenon, and that one could continuously pass from fermionic to bosonic superfluidity by properly varying the fermion interaction parameters.

This conjecture has attracted a great deal of attention. It has been shown that the Bardeen-Cooper-Schrieffer (BCS) theory reduces to Bose-Einstein condensation (BEC) of bosonic dimers as the pair correlation length becomes small compared with the interparticle spacing. For a dilute Fermi gas, in which the mean interparticle spacing is large compared to the extension of the two-body potential, the simplest way to obtain the crossover is via a scattering resonance. This corresponds to bringing the highest-lying bound state from just above to just below threshold. In a dilute gas the atom-atom interaction can be parametrized by the only nonvanishing contribution to the two-body T-matrix at low energy, namely the fermionic s-wave scattering length a_F (with $T = 4\pi\hbar^2 a_F/m$ and m is the atomic mass). The crossover from fermionic to bosonic superfluidity thus appears through the tuning of a_F from negative values, through infinity, to positive values. A series of improvements to the basic theory to better account for the crossover region have been developed and extensively studied during the last decades.

The scientific goal of this program is to develop a detailed theoretical foundation of this problem as it relates to the crossover physics in dilute atomic gases induced by

a Feshbach resonance. This has been pursued on a number of fronts. We elaborate briefly on a few of them in what follows, and give a complete listing of recent papers at the end.

Effects of a pseudogap

By pseudogap effects, it is meant that a gap may open within the fermionic energy spectrum before the onset of superfluidity where one finds the traditional gap. This behavior, well documented within the high-Tc condensed-matter literature, was unfamiliar within the atomic physics community. Moreover the resonant interactions predicted to bring about pseudogap effects within ultracold atomic gases (well documented within the atomic community but now unfamiliar to the high-Tc community) had to be properly included. The resulting many-body theory was a model which extended beyond anything that had been done up until the present time.

This work showed two significant results. The first was that the critical temperature for achieving a superfluid transition retained a maximum near the resonance. This put the temperature range for observing the transition well into the experimentally accessible regime. Although predicted before, this was the first time a non-perturbative treatment of the resonant theory gave such a result, giving greater credence to its validity. The second result of this work was to show that care must be taken when looking for a signature for superfluidity. A pseudogaped superfluid does not show the same clear signatures of a phase transition as a superfluid governed by BCS theory. What's more, near resonance, signatures often identified with a superfluid phase transition may only signal the effect that a pseudogap has opened above Tc.

The role of atom-molecule correlations in the crossover

It was recently pointed out that although existing many-body theories model the passage from fermionic to bosonic superfluidity, they have one major flaw in that they fail to reproduce the correct equation of state of the system in the bosonic limit. This is due to the fact that they predict the wrong value for the boson-boson scattering length, $a_B = 2a_F$. A solution of the four-fermion Schrödinger equation for contact scattering in vacuum, which in principle can be determined exactly, has recently been found and provided the value $a_B \simeq 0.6a_F$. Progress in experiments with quantum atomic gases has lead to experimentally accessible systems which can directly address the crossover region using Feshbach scattering resonances. Bose-Einstein condensation of two-fermion dimers has been observed and the experimental study of the crossover is actively being pursued. The first data collected on the Bose-Einstein condensed cloud were consistent with the $0.6a_F$. A consequence is that crossover theories that predict

in the BEC limit the value $2a_F$ for the boson-boson scattering length will not yield the correct results for all observables dependent on interactions, e.g. the collective modes, the vortex core structure, the internal energy, and even the macroscopic spatial extent of a confined cloud.

We developed a theory of the crossover which correctly reproduces the Gross-Pitaevskii and Bogoliubov theory of the non-ideal Bose gas with the right boson-boson interaction. The theory recovered on the fermionic side the BCS theory including the Gorkov corrections due to density and spin fluctuations. We pointed out the essential ingredients which were missing in standard crossover theories and which had to be included to achieve this goal. Our approach was motivated by the few-body problem of four fermions interacting in vacuum. The essential property leading to the correct boson-boson T-matrix was identified within the contact scattering formalism as the three-particle correlation between a composite boson and a fermion pair. This followed from the observation that in the limit in which the distance $\boldsymbol{r}_1$ between any two of the fermions becomes small, the four-fermion wave function must factorize as

$$\Psi(\boldsymbol{r}_1, \boldsymbol{r}_2, \boldsymbol{R}) \to f(\boldsymbol{r}_2, \boldsymbol{R})(1/4\pi r_1 - 1/4\pi a_F),$$

where $\boldsymbol{r}_2$ is the distance between the two other fermions and $\boldsymbol{R}/\sqrt{2}$ the distance between the centers of mass of the pairs. The function $f(\boldsymbol{r}_2, \boldsymbol{R})$—an effective three-body wave function of a composite boson and two fermions—contains all information needed to determine the boson-boson scattering length. The reason why standard crossover theories fail to give the correct T-matrix in the BEC limit is then revealed, because they are typically based on the BCS assumption that only two-fermion correlations are important, and only those are withheld in the correlation hierarchy.

We showed that a self-consistent many-body theory of the crossover can be constructed which includes three-particle correlations, and correctly reduces to the known results in the appropriate limits. This modification not only brings about quantitative corrections, but also introduces a qualitative change in the crossover picture. A major consequence is that the superfluid order parameter in this crossover theory is not given by the simple integration of a BCS-type pairing field.

BCS/BEC crossover and mean-field theories

We have also written papers during this year on the thermodynamics of the BCS-BEC crossover including the atom and molecule degrees of freedom. In other work, the Gross-Pitaevskii theory has been applied to the study of topological mean-field solutions including vortices and solitons, and to periodic and step potentials.

Future work

The main future direction will be the application of the fundamental theory we have developed to observables which can be directly measured in experiment. This includes properties such as the release energy of a cloud, the excitation spectrum, vortex structure, and other properties arising from the equation of state.

Publications in peer-reviewed journals from 2003 on research supported by the grant

[1] M. Holland *Atomic Beads on Strings of Light* Nature **429**, 251 (2004).

[2] M.J. Holland, C.Menotti, L. Viverit, *The role of boson-fermion correlations in the resonance theory of superfluids*, submitted to Phys. Rev. Lett. (2004).

[3] Jelena Stajic, J. N. Milstein, Qijin Chen, M. L. Chiofalo, M. J. Holland, and K. Levin *Nature of superfluidity in ultracold Fermi gases near Feshbach resonances*, Phys. Rev. A **69** 063610 (2004).

[4] S. G. Bhongale, J. N. Milstein, M. J. Holland *Resonant formation of strongly correlated paired states in rotating Bose gases*, Phys. Rev. A **69**, 053603 (2004).

[5] J. N. Milstein, C. Menotti, M. J. Holland *Feshbach resonances and collapsing Bose-Einstein condensates*, New Journal of Physics, Focus Issue on Quantum Gases **5**, 52 (2003).

[6] B. Seaman, L. D. Carr, and M.J. Holland, *Effect of a potential step or impurity on the Bose-Einstein condensate mean field*, submitted to Phys. Rev. A (2004).

[7] L.D. Carr, R. Chiaramonte and M.J. Holland *Thermodynamics of an atom-molecule mixture*, accepted for Phys. Rev. A (2004).

[8] L.D. Carr and J. Brand *A Pulsed atomic solution laser*, accepted for Phys. Rev. A (2004).

[9] L.D. Carr and Charles W. Clark, *Vortices in attractive Bose-Einstein condensates in two dimensions*, submitted to Phys. Rev. Lett. (2004).

[10] L.D. Carr and Charles W. Clark *Vortices, Rings, and Spherical Shells in Bose-Einstein condensates. I. Case of Repulsive Nonlinearity*, submitted to Phys. Rev. A (2004).

July 2004

Theoretical Investigations of Atomic Collision Physics

A. Dalgarno

Harvard-Smithsonian Center for Astrophysics
Cambridge, MA 02138
adalgarno@cfa.harvard.edu

The research develops and applies theoretical methods for the interpretation of atomic, molecular and optical phenomena and for the quantitative prediction of the parameters that characterize them. The program is responsive to experimental advances and influences them. A particular emphasis has been the study of collisions in ultracold atomic and molecular gases.

A substantial effort has been given to ab initio calculations of the long-range interactions of complex atoms. The attractive van der Waals wells often exert a controlling influence on the dynamics of collisions at ultralow kinetic energies. Xi Chu is a postdoctoral fellow supported by DoE. She is an expert on density functional theory. We have developed time-dependent density functional theory (TDDFT) so that it can be used to determine dynamic polarizabilities and van der Waals coefficients, and we have obtained values of the leading scalar coefficient C_6 for a wide range of atomic systems. Table 1 lists results for pairs of first row transition metal atoms

Table 1

C6 of transition metal atom pairs in a.u.

Sc	Ti	V	Cr	Mn	Fe	Co	Ni	Cu	Zn
1383	1044	833	602	522	482	408	373	253	284

Fine-structure transitions may cause significant trap loss. Theoretical analyses shows that the efficiency of inelastic fine-structure transitions of atoms in states of non-zero orbital angular momentum depends directly on the separations between the potential energy curves corresponding to different values of the projection quantum number Λ. We have developed a procedure to use TDDFT to obtain the C_6 coefficients for the different molecular symmetries. Some preliminary results for Σ and Π states of *P*-state atoms interacting with helium and hydrogen are listed in Table 2.

Table 2

C6 for the interaction of P-state atoms with helium in a.u.

C_6 of X-He

X	C	Si	Ge	O	S	Se
Σ	6.90	15.9	16.7	4.97	13.7	16.9
Π	7.64	17.6	19.1	4.56	12.4	15.4

C_6 of X-H

X	C	Si	Ge	O	S	Se
Σ	15.3	38.6	39.5	10.3	30.6	39.0
Π	17.3	43.5	46.7	9.18	27.6	34.5

Few values of C_6 are available for excited atoms. We have extended the theory for their calculation and we have obtained results for the interactions of the excited ^2P states of the alkali metal atoms with helium. The results are reproduced in Table 3.

Table 3

C_6 for the $X^2\Pi$ $A^2\Pi$ and $B^2\Sigma$ states of the molecules NaHe, KHe and RbHe in a.u.

$X^2\Pi$	NaHe	KHe	RbHe
$A^2\Pi$	42.6	59.9	62.8
$B^2\Sigma$	78.3	111.0	112.7

We have continued our development of the theory of scattering of atoms and molecules in the presence and the absence of magnetic fields with R. V. Krems. Our analysis of spin-flip in collisions of structureless atoms with molecules in $^2\Sigma$ states in the lowest rotational level showed that the mechanism involved a coupling of the initial N = 0 state by the orientation-dependent interaction to the excited N = 2 rotational state in which spin-flip was driven by a spin-rotation interaction. We were able to predict which molecular characteristics would minimize the probability of spin-flip and the resulting trap loss. We have now extended the analysis to $^3\Sigma$ molecules where a different mechanism prevails. In $^3\Sigma$ molecules, the spin-spin interaction couples the N = 0 and N = 2 levels in the isolated molecule and the coupling is enhanced in the collision by the orientation-dependent interaction. Explicit rate coefficients for various magnetic fields have been determined for collisions of helium with the molecule NH.

We have further explored the phenomenon of the suppression of electronic anisotropy in transition metal atoms. In a collaboration with a quantum chemistry group (J. Kloo, M.F. Rode, M.M. Szczesnick and G. Chalasinski) and Roman Krems, the potential energy curves for Ti-He and Sc-H has been computed. The curves of Σ, Π, Δ and Φ symmetries lie remarkably close due to the shielding of the valence *d*-electrons by the outer filled *s*-shell.

Several studies were made of ultracold collisions of hydrogen and antihydrogen and the rate of direct positron-electron annihilation was compared to the rate of proton-antiproton annihilation. Lepton annihilation is much faster.

Renewed attention was given to the chemical reaction of F with H_2 and HD. The rate coefficient for F + HD $\rightarrow$ H F + D at ultralow temperatures is a factor of 5.2 larger than that for F + HD $\rightarrow$ D F + H, because of the more rapid tunneling of the lighter atom. The reaction F + H2 $\rightarrow$ FH + H is very much faster than the reaction F + D_2 $\rightarrow$ FD + D at zero temperature. To determine the reaction mechanisms we carried out scattering calculations for F reacting with a pseudo-hydrogen molecule of arbitrary mass. The calculations show that the enhanced rate for F-H_2 arises from a virtual state associated with the van der Waals well in the entrance channel. The calculations also show that rate coefficients at zero temperature can be as large as 10^{-9} cm^3 s^{-1} despite the presence of a barrier in the potential energy surface. The high value is achieved for cases where a zero energy resonance exists.

Publications

S. Jonsell, A. Saenz, P. Forelich, R.C. Forrey, R. C. Forrey, R. Côté and A. Dalgarno, Long-range Interactions between Two 2*S* Excited Hydrogen Atoms, Phys. Rev. A. 65, 042501, 2002.

A. Belyaev, A. Dalgarno and R. McCarroll, The Dependence of Nonadiabatic Couplings on the Origin of Electron Coordinates, J. Chem. Phys. 116, 5395, 2002.

E. Bodo, F. A. Gianturco and A. Dalgarno, Quenching of Vibrationally Excited CO(v=2) Molecules by Ultra-cold Collisions with ^{4}He Atoms, Chem Phys. Lett. 353, 127, 2002.

C. Zhu, A. Dalgarno and A. Derevianko, van der Waals Interactions between Molecular Hydrogen and Alkali-metal Atoms, Phys. Rev. A. 65, 034708, 2002.

E. Bodo, F. A. Gianturco and A. Dalgarno, The reaction of F + D_2 at Ultra-Cold Temperatures: The Effect of Rotational Excitation, J. Phys. B 35, 2391, 2002.

R. Krems and A. Dalgarno, Electronic and Rotational Energy Transfer in F($^2P_{1/2}$) + H_2 Collisions at Ultracold Temperatures J. Chem. Phys. 117, 118, 2002.

X. Chu and A. Dalgarno, Molecular Transition Moments at Large Internuclear Distances, Phys. Rev. A 66, 024701 (2002).

R.C. Forrey, V. Kharchenko and A. Dalgarno, On the Statistical Averaging Procedure for the Refractive Index of Matter Waves, J. Phys. B 35. L261, (2002).

A.M. Covington et al., Photoionization of Ne^+ Using Synchrotron Radiation, Phys. Rev. A. 66, 062710, 2002.

B. Zygelman, A. Dalgarno, M. J. Jamieson, and P.C. Stancil, Multichannel Study of Spin-Exchange and Hyperfine-Induced Frequency Shift and Line Broadening in Cold Collisions of Hydrogen Atoms, Phys. Rev. A 67,042715, 2003.

R.C. Forrey, S. Jonsell, P. Froelich and A. Dalgarno, Cold Collisions of Spin-Polarized Metastable Hydrogen Atoms, Phys. Rev. A 67 040701(R), 2003.

R. Krems and A. Dalgarno, Threshold Laws for Collisional Reorientation of Electronic Angular Momentum, Phys. Rev. A. 67, 050704-1, 2003.

N. Balakrishnan, G.C. Groenenboom, R.V. Krems and A. Dalgarno, The He-CaH($^2\Sigma^+$) Interaction: II. Collisions at Cold and Ultracold Temperatures, J. Chem. Phys. 118, 7386, 2003.

R. V. Krems, A. Dalgarno, N. Balakrishnan, and G. C. Groenenboom, Spin-flipping Transitions in $^2\Sigma$ Molecules Induced by Collisions with Structureless Atoms, Phys. Rev. A 67,060703 (R) (2003).

N. Balakrishnan and A. Dalgarno, On The Isotope Effect in F+HD Reaction at Ultracold Temperatures, J. Phys. Chem. 107, 7101, 2003.

R. V. Krems and A. Dalgarno, Disalignment Transitions in Cold Collisions of ^{3}P Atoms with Structureless Targets in a Magnetic Field, Phys. Rev. A 68, 013406, 2003.

R. V. Krems, H.R. Sadeghpour, A. Dalgarno, D. Zgid, and G. Chalasinski, Low-temperature Collisions of NH($X^3\Sigma^-$) Molecules with He Atoms in a Magnetic Field: an Ab initio Study, Phys. Rev. A 68 051401, 2003

P. Froelich, B. Zygelman, A. Saenz, S. Jonsell, S. Eriksson and A. Dalgarno, Hydrogen-antihydrogen Molecule and Its Properties, Few-Body Systems 0, 58, 2003.

S. Jonsel, A. Saenz, P. Froelich, and B. Zygelman and A. Dalgarno, Hydrogen-Antihydrogen Scattering in the Born-Oppenheimer Approximation, J. Phys. B. 37, 1195,2004

E. Bodo, F. A. Gianturco, N. Balakrishnan, and A. Dalgarno, Chemical Reactions in the Limit pf Zero Kinetic Energy: Virtual States And Ramsauer Minima in $F + H_2 \rightarrow HF+H$ in press

Zhu, C., Dalgarno, A., Porsey ,S. and Derevianko, A. Dipole Polarizabilities of Excited Alkali-Metal Atoms and Long Range Interactions with Helium Atoms, Phys. Rev. A in press.

Krems, R., Groenenboom, G. and Dalgarno, A., Electronic Interaction Anisotropy between Atoms in Arbitrary Angular Momentum States, J. Phys Chem A, in press.

Froelich, P. Jonsell, S. Saenz, A., Eriksson, S., Zygelman, B. and Dalgarno, A., Positron-Electron Annihilation in Hydrogen-antihydrogen Collisions, in press

Krems, R.V., Klos, J., Rode, M.F. Szczesniak, M.M., Chalasinski, G. and Dalgarno, A., Suppression of Electronic Anisotropy in Transition Metal Atoms, Phys. Rev. Lett. in press.

Optical Two-Dimensional Fourier Transform Spectroscopy of Disordered Semiconductor Quantum Wells and Quantum Dots

Steven T. Cundiff
JILA/University of Colorado and NIST
Boulder, CO 80309-0440
cundiffs@jila.colorado.edu

Program Scope: The goal of this program is to implement optical 2-dimensional Fourier transform spectroscopy and apply it to semiconductors. Specifically of interest are quantum wells that exhibit disorder due to well width fluctuations and quantum dots. In both cases, 2-D spectroscopy will provide information regarding coupling among excitonic localization sites.

Progress: During the last year, we have obtained the first experimental optical two-dimensional Fourier-transform spectra from semiconductors, see Figure 1. The sample in these measurements was a 10 period GaAs/AlGaAs multiple quantum well. The incident 100 fs laser pulses excite both the heavy-hole and light-hole excitons. In bulk GaAs, these excitons would be energetically degenerate, but quantum confinement lifts the degeneracy due to the differing masses.

The interferometer for generating the incident pulse sequence is actively stabilized with respect to the delay between the first two pulses. This is done by threading a HeNe laser through the same beam path that the femtosecond pulse follow. The resulting HeNe interference fringes are then detected and used as an error signal in a feedback loop that servos one of the mirrors. The servo loop is enable while spectra are taken. The loop is disabled and while a delay stage is driven by ½ or ¼ of the wavelength of the HeNe laser. The loop is then renabled. Both the error signal and the voltage applied to the piezoelectric transducer on the mirror are monitored to verify that the correct size steps are taken.

In addition, the delay between the reference pulse and the third pulse is actively locked by a second feedback loop. This is necessary to guarantee that the spectral interferometry of the signal pulse is done with a valid phase reference. Fortunately it only needs a fixed

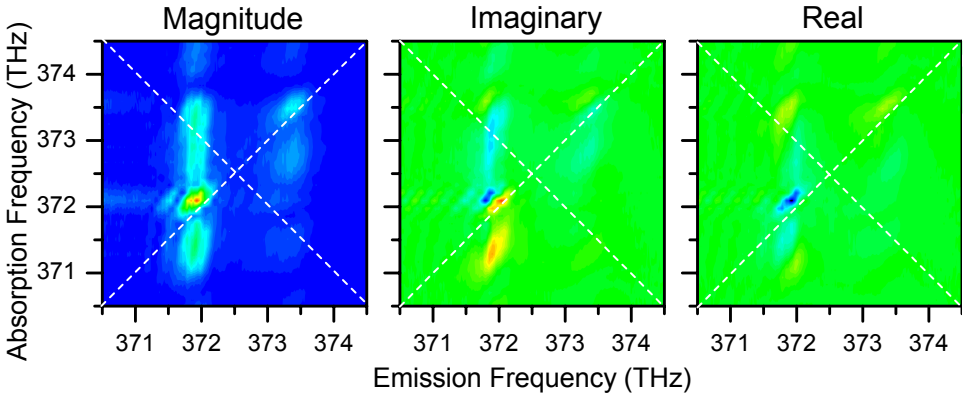

Fig. 1. Experimental optical 2D Fourier transform spectra of the heavy and light hole excitons in a GaAs/AlGaAs multiple quantum well.

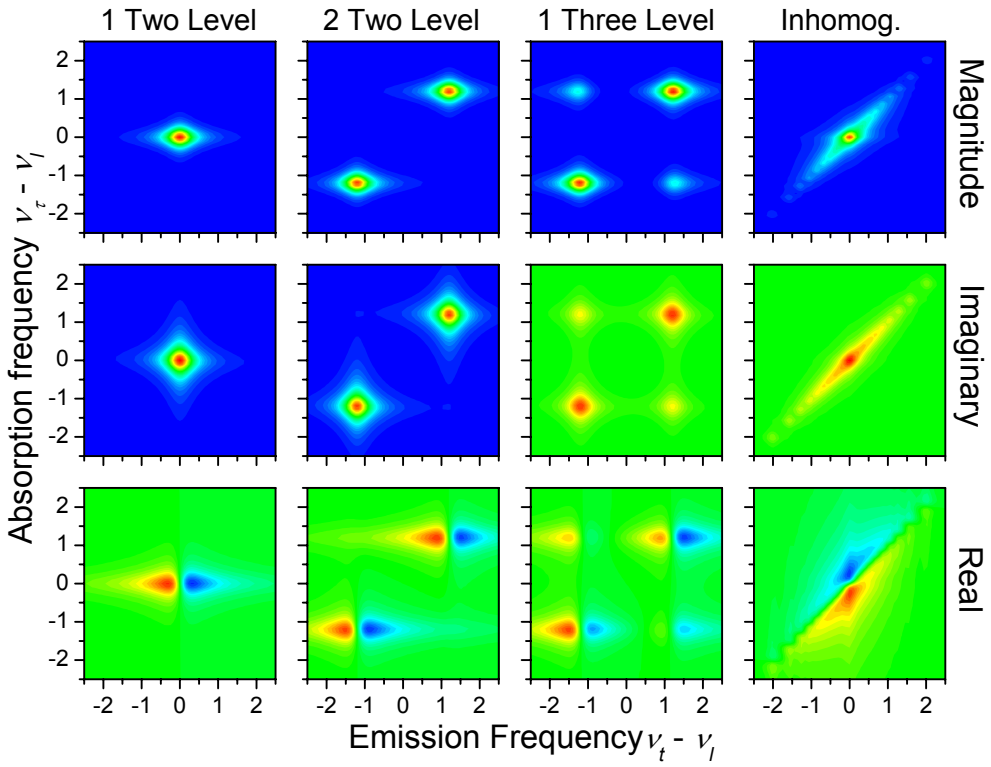

Figure 2. Theoretical 2D Fourier transform spectra for various level schemes, all without interactions.

delay.

Currently, there is some ambiguity in the phasing of the real and imaginary parts of the signal, i.e., there may be an arbitrary overall phase that mixes them together. We are working on developing techniques to address this.

The data show a number of interesting features, some expect, others that remain to be explained. We do see off-diagonal peaks, which are indicative of coupling between light- and heavy-hole excitons. This is expected for this data as we are using linearly polarized pulses and the true basis is circularly polarized. We see that the strongest signal is at the heavy-hole exciton, as expected due to it having 3 times the oscillator strength of the light-hole exciton. We also note that the heavy-hole exciton peak is slightly above the diagonal, even after double checking the calibrations. Currently we are ascribing this to Stokes shift due to relaxation within the inhomogeneous distribution. We also notice that features tend to lie along the diagonal, which we ascribe to the presence of inhomogeneous broadening by well-width fluctuations.

To begin developing an understanding of these results, we have also been performing theoretical calculations. We numerically solve the Optical Bloch equations (OBEs) to obtain the signal field and then generate two-dimensional spectra. Figure 2 shows the results for a various system without any many-body interactions. Note that we have chosen to use the real and imaginary parts, not the absorptive and dispersive parts often used in 2D NMR. These results are relatively straight forward, showing cross peaks for the 3-level system and diagonal features for inhomogeneously broadening.

The power of 2D Fourier transform spectroscopy becomes apparent when we turn on the many-body interactions that occur in semiconductors. For these simulations, this is a phenomenological treatment of them, a full theory would not use the OBEs but rather the semiconductor Bloch equations (SBEs) derived using dynamics controlled truncation and correlation terms. Nevertheless, we can see from the phenomenological calculations that 2D spectroscopy can help unraveling the various effects.

In Figure 3, the calculated 2D spectra are shown including the 3 most important many-body phenomena: excitation induced dephasing (EID), excitation induced shift (EIS) and the local field correction (LFC). In these simulations, there are two 2-level systems, but there is a cross-term in the many-body phenomena. For example, in the EID case, the dephasing rate of both resonances depends to the total population. Just from looking at these spectra, one can readily determine which many-body phenomena is at work, and distinguish coupling by many-body phenomena from a true 3 level system, which also shows cross peaks.

These results are very promising and show that 2D Fourier transform spectroscopy has significant potential to help understand coherent processes in semiconductors.

[1] C.N. Borca, T. Zhang and S.T. Cundiff, "Two-dimensional Fourier Transform Optical Spectroscopy of GaAs Quantum Wells," to appear in proceedings of SPIE (2004).

FEMTOSECOND AND ATTOSECOND LASER-PULSE ENERGY TRANSFORMATION AND CONCENTRATION IN NANOSTRUCTURED SYSTEMS

DOE Grant No. DE-FG02-01ER15213

Mark I. Stockman, Pi

Department of Physics and Astronomy, Georgia State University, Atlanta, GA 30303
E-mail: mstockman@gsu.edu, URL: http://www.phy-astr.gsu.edu/stockman

1 Program Scope

The program is aimed at theoretical investigations of a wide range of phenomena induced by ultrafast laser-light excitation of nanostructured or nanosize systems, in particular, metal/semiconductor/dielectric nanocomposites and nanoclusters. Among the primary phenomena are processes of energy transformation, generation, transfer, and localization on the nanoscale and coherent control of such phenomena.

2 Recent Progress

2.1 Nanofocusing of Optical Energy in Tapered Plasmonic Waveguides[1]

We have predicted theoretically that surface plasmon polaritons propagating toward the tip of a tapered plasmonic waveguide are slowed down and asymptotically stopped when they tend to the tip, never actually reaching it (the travel time to the tip is logarithmically divergent). This phenomenon causes accumulation of energy and giant local fields at the tip. There are various prospective applications of this proposed effect in nanooptics and nanotechnology.

2.2 SPASER: New Idea, Effect, and Prospective Devices[4,13,17]

The above-discussed and other known effects and applications in nanooptics are passive, i.e., based on the excitation of the nanosystem by external laser radiation. This mode of excitation has obvious drawbacks: most of the radiation is lost and only a small fraction of photons interact with the nanosystem; it is difficult or impossible to concentrate the excitation in space and time on nanometer-femtosecond scale; the exciting radiation creates a significant background to the relatively weak emissions by the nanosystem. We have introduced a principally different concept of SPASER (Surface Plasmon Amplification by Stimulated Emission of Radiation). The spaser radiation consists of surface plasmons that are bosons just like photons and undergo stimulated emission, but in contrast to photons can be localized on the nanoscale. Spaser as a system will incorporate an active medium formed by two-level emitters, excited in the same way as a laser active medium: optically, or electrically, or chemically, etc. One promising type of such emitters are quantum dots (QDs). These emitters transfer their excitation energy by radiationless transitions to a resonant nanosystem that plays the role of a laser cavity. These transitions are stimulated by the surface plasmons already in the nanosystem, causing buildup of a macroscopic number of the surface plasmons in a single mode. Spaser is predicted to generate ultrashort (10-100 fs) ultraintense (optical electric field ~10^8 V/cm or greater) pulses of local optical fields at nanoscale. When realized experimentally spaser may completely change the nanooptics.

2.3 Coherent Control of Ultrafast Energy Localization on Nanoscale[6,11,15,16,18-20]

Our research has significantly focused on problem of controlling localization of the energy of ultrafast (femtosecond) optical excitation on the nanoscale. This is a formidable problem since it is impossible to achieve such concentration by optical focusing due to the nanosize of the system, or by near-field excitation, because the energy of such excitation is transferred across the entire nanosystem during ultrashort periods on order of the light-wave oscillation. We have proposed and theoretically developed a distinct approach to solving this fundamental problem. This approach, based on the using the relative phase of the light pulse as a functional degree of freedom, allows one to control the spatial-temporal distribution of the excitation energy

on the nanometer-femtosecond scale. We have shown that using even the simplest phase modulation, the linear chirp, it is possible to shift in time and spatially concentrate the linear local optical fields, but the integral local energy does not depend on the phase modulation. In contrast, for nonlinear responses, the integral local energy efficiently can be coherently controlled. It is difficult to overestimate possible applications of this effect, including nano-chip computing, nanomodification (nanolithography), and ultrafast nano-sensing.

The effect of the coherent control of local fields on the nanoscale has recently been reported to be observed [*Imaging of localized silver plasmon dynamics with sub-fs time and nano-meter spatial resolution*, Atsushi Kubo, Ken Onda, Hrvoje Petek, Zhijun Sun, Yun S. Jung, Hong K. Kim; Univ. of Pittsburgh, USA. Conference on Ultrafast Phenomena, Talk FB1 (Invited), Niigata, Japan, July 2004].

2.4 Efficient Nanolens[3,10]

As an efficient nanolens, we have proposed a self-similar linear chain of several metal nanospheres with progressively decreasing sizes and separations. To describe such systems, we have developed the multipole spectral expansion method. Optically excited, such a nanolens develops the nanofocus ("hottest spot") in the gap between the smallest nanospheres, where the local fields are enhanced by orders of magnitude due to multiplicative, cascade effect of its geometry and high *Q*-factor of surface plasmon resonance. The spectral maximum of the enhancement is in the near ultraviolet, shifting toward the red as the separation between the spheres decreases. The proposed system can be used for nanooptical detection, Raman characterization, nonlinear spectroscopy, nano-manipulation of single molecules or nanoparticles, and other applications.

2.5 Depolarization, Dephasing and Correlations of Second Harmonic Generated on Rough Surfaces[8]

This research resulted from an international collaboration with the group of Prof. Joseph Zyss (France). Based on the spectral-expansion Green's function theory, we theoretically describe the topography, polarization, and spatial-coherence properties of the second-harmonic (SH) local fields at rough metal surfaces. The spatial distributions of the fundamental-frequency and SH local fields are very different, with highly enhanced hot spots of the SH. The spatial correlation functions of the amplitude, phase, and direction of the SH polarization all show spatial decay on the nanoscale in the wide range of the metal fill factors. This implies that SH radiation collected from even nanometer-scale areas is strongly depolarized and dephased, i.e., has the nature of hyper-Rayleigh scattering, in agreement with recent experiments. The present theory is applicable to nanometer-scale nonlinear-optical illumination, probing, and modification.

2.6 Strong Field Effects in Nanostructures: Forest Fire Mechanism of Dielectric Breakdown[9]

This research is a result of an extensive international collaboration (UK, Germany, Canada, and the USA). We have described the interaction of ultrashort infrared laser pulses with clusters and dielectrics. Rapid ionization occurs on a sub-laser wavelength scale below the conventional breakdown threshold. It starts with the formation of nanodroplets of plasma that grow like forest fires, without any need for heating of the electrons promoted to the conduction band. The dimensionality of the damaged area can be fractal and changes during the laser pulse. This mechanism is operative in both rare gas clusters and dielectrics interacting with ultrashort, moderately intense laser pulses that include only several periods of the driving field, so that the traditional avalanche mechanisms have no time to develop. This effect is very important for the physics of laser damage of semiconductors and dielectrics by a moderate-intensity radiation.

2.7 Theory of Coherent Near-Field Optical Microscopy[7,12]

We have developed theory of phase-sensitive near-field scanning optical microscopy (in collaboration with the group of Dr. Victor Klimov, LANL). Near-field spectroscopic studies of metal nanoparticles with broadband white-continuum femtosecond pulses have found that the near field extinction of metal nanoparticles in the blue region of the spectrum changes to the enhanced transmission in the red region. The developed theory shows that this effect is due to the interference of secondary electromagnetic waves emitted by the metal nanoparticles and the radiation of the near-field optical microscope (NSOM) tip. The latter radiation contains both magnetic-dipole and electric dipole parts. The interference of these radiations of the

tip and the metal nanosystem in the far zone depends on their relative phase that in turn is determined by the detuning from the surface plasmon resonance in the metal nanosystem. Owing to this interference, it is possible to determine the spectral phase of the surface plasmon resonances in metal nanoparticles. In turn, this allows us to determine the positions of these resonances with unprecedented resolution.

2.8 Enhanced Relaxation of Quantum Dot in Proximity of Metal Surface[5]

We have considered a nanoscale dipolar emitter (quantum dot, atom, fluorescent molecule, or rare earth ion) in a nanometer proximity to a flat metal surface. There is strong interaction of this emitter with unscreened metal electrons in the surface nanolayer that causes enhanced relaxation due to surface plasmon excitation and Landau damping. To describe these phenomena, we developed analytical theory based on local random-phase approximation. For the system considered, conventional theory based on metal as continuous dielectric fails both qualitatively and quantitatively. Applications of the present theory and related phenomena are discussed.

2.9 Microscopic Theory of Interacting Electrons in Semiconductor Nanosystems[14]

We have contributed to the microscopic, many-body theory of the electronic and optical properties of interacting electrons in semiconductor nanostructures based on the self-consistent Random Phase Approximation also known as *GW*-approximation. The technique used in this research is based on the non-equilibrium Green's function method by Baym and Kadanoff. This theory allows us to calculate the intersubband absorption, effective electron masses, and Fermi-edge discontinuity for electrons with Coulomb interaction in quantum wells without any adjustable parameters for finite temperatures.

3 Future Plans

We will develop both the theory in the directions specified above and the collaborations with the experimental and theoretical groups that we have developed. Among the future projects, we will consider effects of nonlocality of the dielectric response of nanosystems; this nonlocality is expected to dominate electromagnetic interaction in nanocomposites of metal nanoparticles and semiconductor quantum dots. Another project will be nanoplasmonic imaging, including the nanolenses. We will also consider different types of spasers. We will develop theory of the rapid adiabatic concentration of energy in nanoplasmonic waveguides with graded composition or geometry. Of course, the most exciting projects in the future may be those that we cannot foresee at this moment but which will appear by serendipitous ways.

Publications Resulting from the Grant (2002-2004)

Papers in Leading Journals

1. M. I. Stockman, *Nanofocusing of Optical Energy in Tapered Plasmonic Waveguides*, Phys. Rev. Lett. (2004) [Accepted for publication].
2. M. I. Stockman, *From Nano-Optics to Street Lights*, Nature Materials, **3**, 423-424 (2004).
3. P. Nordlander, C. Oubre, E. Prodan, K. Li, and M.I. Stockman, *Plasmon Hybridization in Nanoparticle Dimers*, Nano Letters **4**, 899-903 (2004).
4. D. J. Bergman and M. I. Stockman, *Can We Make a Nanoscopic Laser?,* Laser Phys. **14**, 409-411 (2004).
5. I. A. Larkin, M. I. Stockman, M. Achermann, and V. I. Klimov, *Dipolar Emitters at Nanoscale Proximity of Metal Surfaces: Giant Enhancement of Relaxation*, Phys. Rev. B (Rapid Communications) **69**, 121403(R)-1-4 (2004).
6. M. I. Stockman, D. J. Bergman, and T. Kobayashi, *Coherent Control of Nanoscale Localization of Ultrafast Optical Excitation in Nanosystems*, Phys. Rev. B. **69**, 054202-1-10 (2004).
7. A. A. Mikhailovsky, M. A. Petruska, Kuiru Li, M. I. Stockman, and V. I. Klimov, *Phase-Sensitive Spectroscopy of Surface Plasmons in Individual Metal Nanostructures*, Phys. Rev. B **69,** 085401-1-5 (2004).

8. M. I. Stockman, D. J. Bergman, C. Anceau, S. Brasselet, and J. Zyss, *Enhanced Second Harmonic Generation By Metal Surfaces with Nanoscale Roughness: Nanoscale Dephasing, Depolarization, and Correlations*, Phys. Rev. Lett. **92**, 057402-1-4 (2004).
9. L. N. Gaier, M. Lein, M. I. Stockman, P. L. Knight, P. B. Corkum, M. Yu. Ivanov and G. L. Yudin, *Ultrafast Multiphoton Forest Fires and Fractals in Clusters and Dielectrics,* J. Phys. B: At. Mol. Opt. Phys. **37**, L57-L67 (2004).
10. Kuiru Li, M. I. Stockman, and D. J. Bergman, *Self-Similar Chain of Metal Nanospheres as an Efficient Nanolens*, Phys. Rev. Lett. **91,** 227402-1-4 (2003).
11. M. I. Stockman, S. V. Faleev, and D. J. Bergman, *Femtosecond Energy Concentration in Nanosystems: Coherent Control*, Physica B: Physics of Condensed Matter **338**, 361–365 (2003).
12. A. A. Mikhailovsky, M. A. Petruska, M. I. Stockman, and V. I. Klimov, *Broadband Near-Field Interference Spectroscopy of Metal Nanoparticles Using a Femtosecond White-Light Continuum*, Optics Lett. **28**, 1686-1688 (2003).
13. D. J. Bergman and M. I. Stockman, *Surface Plasmon Amplification by Stimulated Emission of Radiation: Quantum Generation of Coherent Surface Plasmons in Nanosystems,* Phys. Rev. Lett. **90**, 027402-1-4 (2003).
14. S. V. Faleev, and M. I. Stockman, *Self-Consistent Random-Phase Approximation and Intersubband Absorption for Interacting Electrons in Quantum Well*, Phys. Rev. B **66**, 085318-1-11 (2002).
15. M. I. Stockman, S. V. Faleev, and D. J. Bergman, *Coherent Control of Femtosecond Energy Localization on Nanoscale*, Phys. Rev. Lett. **88,** 067402-1-4 (2002).
16. M. I. Stockman, S. V. Faleev, and D. J. Bergman, *Coherently-Controlled Femtosecond Energy Localization on Nanoscale*, Appl. Phys. B **74**(9), 63-67 (2002) [http://dx.doi.org/10.1007/s00340-002-0868-x].

Full Size Papers in Conference Proceedings

17. M. I. Stockman and D.J. Bergman), *Surface Plasmon Amplification through Stimulated Emission of Radiation (SPASER)*. In: Complex Mediums IV: Beyond Linear Isotropic Dielectrics (Martin W. McCall, Graeme Dewar; Eds.), *Proceedings of SPIE* Vol. **5218**, pp. 93-102 (2003).
18. M. I. Stockman, D. J. Bergman, and T. Kobayashi, *Coherent Control of Ultrafast Nanoscale Localization of Optical Excitation Energy*. In: Plasmonics: Metallic Nanostructures and Their Optical Properties (Naomi J. Halas, Ed.), *Proceedings of SPIE* Vol. **5221**, pp. 182-196 (2003) (Invited).
19. M. I. Stockman, *Ultrafast Processes in Metal-Insulator and Metal-Semiconductor Nanocomposites*, In: *Ultrafast Phenomena in Semiconductors VII*, Proceedings of SPIE Vol. **4992**, 60-74 (2003) (K. F. Tsen, J. Song, and H. Jiang, eds.) (Invited).
20. M. I. Stockman, S. V. Faleev, and D. J. Bergman, *Coherently-Controlled Femtosecond Energy Localization on Nanoscale*, In: Ultrafast Phenomena XIII (Springer Series in Chemical Physics), pp. 496-498 (Springer, Berlin, Heidelberg, New York, 2003).

Multiparticle Processes and Interfacial Interactions in Nanoscale Systems Built from Nanocrystal Quantum Dots

Victor Klimov
Chemistry Division, C-PCS, MS-J567, Los Alamos National Laboratory
Los Alamos, New Mexico 87545, klimov@lanl.gov, http://quantumdot.lanl.gov

Program Scope

Controlling functionalities of nanomaterials requires a detailed physical understanding from the level of the individual nanoscale building blocks to the complex interactions in the nanostructures built from them. This project concentrates on electronic properties of semiconductor quantum-confined nanocrystals (NCs) and the electronic and photonic interactions in NC nanoscale assemblies. Specifically, we study multiparticle processes in individual NCs and interfacial interactions in NC-based "homogeneous" and "hybrid" structures. Multiparticle states (e.g., quantum-confined biexcitons) and multiparticle interactions (e.g., Auger recombination) play an important role in both optical gain and band-edge optical nonlinearities in NCs. Interfacial interactions (e.g., electrostatic coupling) can enable communication between NCs (homogeneous systems) or between NCs and other inorganic or organic structures (hybrid systems), leading to such important functionality as energy transfer. The ability to understand and control both multiparticle processes and interfacial interactions developed in this project will lead to such new NC-based technologies as solid-state optical amplifiers and lasers, nonlinear optical switches, and electrically pumped tunable light emitters.

Recent Progress

1. Multiparticle interactions and optical gain in shape-controlled and heterostructured NCs

Because of size-controlled spectral tunability (achieved via the quantum confinement), high photoluminescence (PL) efficiencies, and chemical flexibility, semiconductor NCs are very attractive for applications in various optical technologies including optical amplification and lasing [1 - 4]. Optical gain in ultrasmall (sub-10 nm) NCs relies on emission from multi-exciton states [5, 6]. However, the decay of these states is dominated by nonradiative Auger processes rather than by radiative recombination [7], which makes them nominally non-emissive species. One approach to force these non-emissive multi-excitons to lase is by increasing the NC density in the sample until the rate of stimulated emission becomes greater than the rate of Auger decay [1 - 4]. Although this straightforward approach does work the suppression of Auger recombination remains an important current challenge in the field of NC lasing.

In our work, we explore the effect of NC "geometry" (e.g., NC shape) on the rates of the multi-particle decay. In particular, we study the influence of the zero- to one-dimensional (1D) transformation on multi-particle Auger recombination using a series of elongated semiconductor NCs (quantum rods). We observe an interesting new effect, namely, the transition from the three- to two-particle recombination process as the nanocrystal aspect ratio is increased [8]. This transition implies that in the 1D confinement limit, Auger decay is dominated by Coulomb interactions between 1D excitons that recombine in a bimolecular fashion. One consequence of this effect is strongly reduced decay rates of higher multi-particle states that lead to increased

optical gain lifetime and efficient light amplification due to transitions involving excited electronic states [9].

In another approach, we explore the use of NC core-shell heterostructures for suppressing Auger recombination [10, 11]. Specifically, we use inverted ZnSe(core)/CdSe(shell) nanoparticles to study the effect of type I vs. type II carrier localization on multiparticle Auger decay and optical gain performance of NCs. We observe that both Auger recombination rates and the amplified spontaneous emission thresholds are reduced in the case of type II localization. Furthermore, we use these hetero-NCs to demonstrate efficient amplified spontaneous emission that is tunable across a "difficult" range of green and blue colors.

Our findings suggest that shape control and heterostructuring may be key to developing practical lasing applications of NCs.

2. "Noncontact" pumping of NCs using energy transfer from a proximal quantum well

Understanding and ultimately controlling communication and coupling between NCs is of significant fundamental and technological interest. One mechanism for inter-NC coupling is via electrostatic Coulomb interactions. Such interactions can allow communication between nanoparticles via *incoherent* exciton transfer. To obtain direct information about time scales characteristic of the energy transfer in NC materials, we have recently performed spectrally selective time-resolved PL studies within the inhomogeneously broadened emission line of NC solids [12, 13]. We observe that inter-NC energy migration is dominated by direct energy transfer from "blue" to "red" sides of the emission band across an energy range on the order of tens of meV, which corresponds to the transition between NCs with a relatively large size difference. The high efficiency of this process is due to a strong coupling between the lowest "emitting" transition in a donor NC and a higher energy, strongly "absorbing" transition in an acceptor NC. We performed phenomenological modeling of exciton inter-NC dynamics that provides important insights into optimization of NC assemblies with respect to energy transfer efficiencies. Furthermore, we demonstrate a prototype energy-gradient structure (a NC bilayer), which is engineered in such a way as to boost the rate of the unidirectional (vertical) transfer. Studies of these gradient structures indicate that inter-NC transfer can approach ultrafast picosecond time scales in structurally optimized assemblies.

Furthermore, we demonstrate the feasibility of "energy-transfer" pumping of NC-based emitters and lasers using dipole-dipole interactions of NCs with excitations in a proximal quantum well (QW) [14]. Our direct experimental measurements indicate that this mechanism is fast enough to compete with exciton recombination in the QW and results in greater than 50% QW-to-NC transfer efficiencies. We also observe that the measured transfer rates are sufficiently large to provide NC pumping not only in the spontaneous but also in the stimulated-emission regime.

3. High efficiency exciton multiplication in semiconductor nanocrystals: Implications for solar energy conversion

Solar power holds significant potential as a clean source of renewable energy. Calculated thermodynamic conversion efficiency limits in solar cells (~31% for unconcentrated solar illumination) are based upon the assumption that absorption of an individual photon with energy above a semiconductor band gap (E_g) results in formation of a single exciton and that all photon energy in excess of E_g is lost as heat. However, this thermodynamic limit can be overcome once

methods of harnessing the excess energy of photo-generated carriers are developed. One such method involves carrier multiplication, which would provide increased power conversion efficiency in the form of increased solar cell photocurrent.

Carrier multiplication can occur via impact ionization, which is an Auger-type process whereby a high-energy exciton, created in a semiconductor by absorbtion of a photon of energy >2*Eg*, relaxes to the band edge via energy transfer of at least 1*Eg* to a valence band electron, which then is excited above the energy gap. The result of this energy transfer process is that *two excitons (i.e., a biexciton) are formed for one absorbed photon,* which doubles the photocurrent and improves the conversion of the high energy portion of the solar spectrum into usable energy. Because of the restrictions imposed by momentum and energy conservation, Auger ionization is not efficient in bulk materials. Even with band gap tuning via synthesis of bulk Si-Ge alloys, the optimized material only showed a <1% improvement in solar power conversion efficiency due to impact ionization. Carrier multiplication can be enhanced in quantum confined NCs due to relaxation in momentum conservation and enhanced Coulomb interactions. Recently, we have performed direct studies of impact ionization in PbSe NCs [15]. These studies demonstrate that *the exciton-to-biexciton conversion in these systems occurs with up to 100% probability*, indicating the feasibility of highly efficient impact-ionization-enhanced NC-based solar cells. Impact ionization, in addition to increasing solar cell power conversion efficiency, is also likely to provide other benefits such as reduced pump thresholds in NC-based optical amplifiers, lasers, and saturable absorbers as well as increased gain in avalanche photodiodes.

Future Plans

We are planning to continue our studies of carrier multiplication. While our initial results are very encouraging, there remain several critical issues to be addressed before impact ionization becomes a technologically usable phenomenon. One is the large energy threshold (~*3Eg*) resulting from the similar electron and hole masses in PbSe. To address this issue we will synthesize and investigate NCs of mercury-based compounds (e.g., HgSe and HgTe). In these materials electrons are much lighter than holes, and, therefore, they capture most of the photon excess energy, which should allow us to approach the theoretical $2E_g$ limit. Another issue is highly efficient Auger recombination that can lead to rapid recombination of biexitons created via impact ionization. In order to overcome this problem, we will engineer *Type-II* heterostructures, which will allow us to quickly separate electrons and holes spatially before Auger recombination occurs. We may pursue rod and branched (e.g., tetrapods) hetero-NCs, in addition to NCs with concentric geometries, in order to promote charge separation and improve charge extraction efficiencies and transport in photovoltaic devices.

In our optical-gain work, we will explore a novel concept for achieving NC lasing in the Auger-recombination-free regime using core-shell NCs that favor *electron-hole charge separation* (type II heterostructures) and promote *repulsive* exciton-exciton interactions. Such interactions provide the possibility for lasing in the *single-exciton* regime, where Auger recombination is inactive. As a result, optical gain lifetimes can be extended up to 100s of nanoseconds. Further, elimination of Auger decay should allow a dramatic reduction in the optical gain threshold (by at least 4-to-5 orders of magnitude), as well as the realization of NC lasing using cw excitation and, potentially, electrical injection. In addition to its conceptual novelty, this work will have a significant technological impact by bringing NC lasing from the laboratory stage to the arena of real optical technologies.

Publications

1. A. V. Malko, A. A. Mikhailovsky, M. A. Petruska, H. Htoon, J. A. Hollingsworth, M. G. Bawendi, and V. I. Klimov, From amplified spontaneous emission to microring lasing using nanocrystal quantum dot solids, *Appl. Phys. Lett.* **81**, 1303 – 1305 (2002).
2. H.-J. Eisler, V. C. Sundar, M. G. Bawendi, M. Walsh H. I. Smith and V. I. Klimov, Color-selective semiconductor nanocrystal laser, *Appl. Phys. Lett.* **80**, 4614 – 4616 (2002).
3. M. A. Petruska, A. V. Malko, P. M. Voyles, and V. I. Klimov, High-performance, quantum-dot nanocomposites for nonlinear-optical and optical-gain applications, *Advanced Materials* **15**, 610–613 (2003).
4. R. D. Schaller, M. A. Petruska, V. I. Klimov, Tunable Near-Infrared Optical Gain and Amplified Spontaneous Emission Using PbSe Nanocrystals, *J. Phys. Chem. B* **107**, 13765 (2003) (cover article).
5. A. A. Mikhailovsky, A. V. Malko, J. A. Hollingsworth, M. G. Bawendi, and V. I. Klimov, Multiparticle interactions and stimulated emission in chemically synthesized quantum dots, *Appl. Phys. Lett.* **80**, 2380 – 2382 (2002).
6. M. Achermann, J. A. Hollingsworth, and V. I. Klimov, Multiexcitons confined within a sub-excitonic volume: Spectroscopic and dynamical signatures of neutral and charged biexcitons ultrasmall semiconductor nanocrystals, *Phys. Rev. B* **68**, 245302 (2003).
7. S. A. Crooker, T. Barrick, J. A. Hollingsworth, and V. I. Klimov, Multiple temperature regimes of radiative decay in CdSe nanocrystal quantum dots: Intrinsic limits to the dark-exciton time, *Appl. Phys. Lett.* **82**, 2793 – 2795 (2003).
8. H. Htoon, J. A. Hollingsworth, R. Dickerson, and V. I. Klimov, Zero- to one-dimensional transition and Auger recombination in semiconductor quantum rods, *Phys. Rev. Lett.* **91**, 227401 (2003).
9. H. Htoon, J. A. Hollingsworth, A. V. Malko, R. Dickerson, and V. I. Klimov, Light amplification in semiconductor nanocrystals: Quantum rods vs. quantum dots, *Appl. Phys. Lett.* **82**, 4776 – 4778 (2003).
10. L. P. Balet, S. A. Ivanov, A. Piryatinski, M. Achermann, V. I. Klimov, Inverted core/shell nanocrystals continuously tunable between Type-I and Type-II localization regimes *Nanoletters* **4**, 1485 (2004).
11. S. A. Ivanov, J. Nanda, A. Piryatinski, M. Achermann, L. P. Balet, I. V. Bezel, P. O. Anikeeva, S. Tretiak, V. I. Klimov Light Amplification Using Inverted Core/Shell Nanocrystals: Towards Lasing in the Single-Exciton Regime, *J. Phys. Chem. B* **108**, 10625 (2004).
12. S. A. Crooker, J. A. Hollingsworth, S. Tretiak, and V. I. Klimov, Spectrally-resolved dynamics of energy transfer in quantum-dot solids: Towards engineered energy flows in quantum-dot assemblies, *Phys. Rev. Lett.* **89**, 186802-1(2002).
13. M. Achermann, M. A. Petruska, S. A. Crooker, and V. I. Klimov, Picosecond energy transfer in quantum dot Langmuir-Blodgett nanoassemblies, *J. Phys. Chem. B* **107**, 13782 (2003).
14. M. Achermann, M. A. Petruska, S. Kos, D. L. Smith, D. D. Koleske, V. I. Klimov, Energy-transfer pumping of semiconductor nanocrystals using an epitaxial quantum well, *Nature* **429**, 642 (2004).
15. R. D. Schaller and V. I. Klimov, High-efficiency carrier multiplication in PbSe nanocrystals: Implications for solar energy conversion, *Phys. Rev. Lett.*, **92,** 186601 (2004).

DE-FG02-98ER14877-Abs

Measurement of Electron Impact Excitation Cross Sections of Highly Ionized Ions

A. J. Smith

D. L. Robbins, Postdoctoral Associate

Morehouse College, 830 Westview Dr SW, Atlanta, GA 30314

email:asmith@morehouse.edu

Unfunded Liaison/Collaborator: P. Beiersdorfer

Lawrence Livermore National Laboratory, Livermore, California USA

Scope of work: During these project years, we have concentrated our efforts on the accurate measurement of cross sections for direct electron impact excitation of highly ionized ion species with low to intermediate values of Z. The ions were produced and excited in the high energy LLNL electron beam ion trap, EBIT-I. We excite the emission lines at energies from just above threshold to energies several kV above threshold for the level of interest. We have used several different types of spectrometers including a windowless Si(Li) detector for low resolution studies, an x-ray spectrometer and crystal spectrometers in flat and/or curved geometry for higher resolution studies. We observe x-rays emitted at 90° to the electron beam. The emitted photons are polarized, and we use polarization-sensitive spectrometers to observe the spectra. Polarization spectroscopy has become an important diagnostic tool for the determination of the presence of electron beams in high temperature plasmas. The degree of polarization of an x-ray emission line is a direct measure of the direct excitation cross section of the line. Our measurements therefore provide data which test atomic structure calculations of EIE cross sections at very fundamental levels. We give below summaries of some of the measurements we have carried out.

1 Direct electron Impact Excitation in heliumlike Ar^{16+}

We have measured cross sections for direct excitation of n = 3-1 resonance line, Kβ1 and intercombination line, Kβ2, in heliumlike argon at various excitation energies (4.9 kV - 20.0 kV). We use the LLNL electron beam ion trap, EBIT-I to produce and excite the ions, and record x-ray spectra at 90^o to the electron beam using a Bragg crystal spectrometer in von Hámos geometry. We have used a Si(220) crystal with a 2d spacing of 3.84 $\AA$ for these measurements. We have normalized our intensity measurements to radiative recombination measurements and theory, and we have compared our results with model predictions.

2 Polarization of Iron L-shell lines on EBIT-1

We have extended our polarization measurements to include polarization of neonlike and fluorinelike iron using the LLNL EBIT-1, and a two crystal technique. These results are important for the diagnostics of astrophysical as well as of laser-produced plasmas. The observed data is compared with calculations done using the flexible atomic code (FAC). The measurements are presented at the fourth US-Japan plasma spectroscopy coference. In earlier measurements we looked the polarization of heliumlike V^{21+}

3 Measurement of the Polarization of Heliumlike and Lithiumlike Sulphur

We have measured the polarization of the heliumlike sulfur resonance line 1s2p $^1P_1$ - $1s^2$ $^1S_0$, and of the blend of the lithiumlike sulfur resonance lines 1s2s2p $^2P_{3/2}$ - $1s^2$2s $^2S_{1/2}$ and 1s2s2p $^2P_{1/2}$ - $1s^2$2s $^2S_{1/2}$ as a function of electron beam energy from near threshold to 144 keV. These lines were excited with the LLNL high-energy electron beam ion trap and measured using a newly modified two-crystal technique. Our results test polarization predictions in an energy regime where few empirical results have been reported.

For these measurements, we have used a flat crystal spectrometer (FCS) with a PET crystal set at Bragg angle of $\theta_B = 35.2^o$, which corresponds to an integrating crystal reflectivity ratio of $R_{PET} \approx 0.28$. for the second crystal in this measurement, we have used a mica (002) crystal which was spherically bent into a Johann type spectrometer. This spectrometer was set at an initial Bragg angle close to 45^o, corresponding to a ratio of $R_{Mica} \approx 0.04$. For normalization we have used the the forbidden line (z) (1s2s $^3S_1$ - $1s^2$ $^1S_0$) in heliumlike sulfur. The line z is intrinsically unpolarized, but can be slightly polarized due to cascades. Our observations agree well with predictions made with the Flexible Atomic Code and the relativistic distorted-wave code.

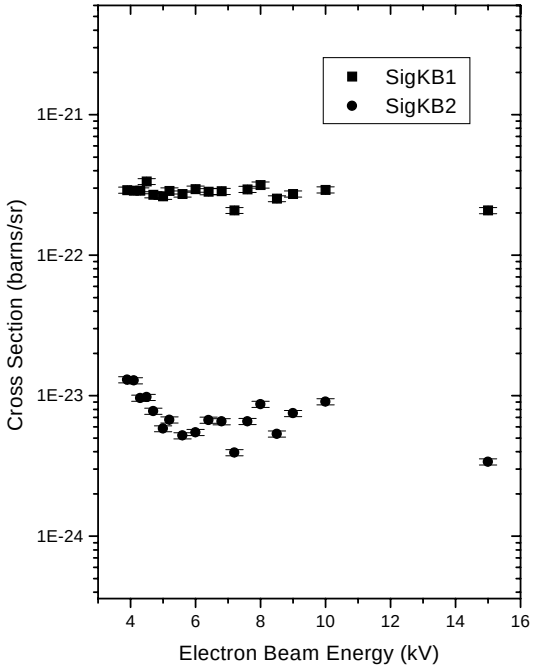

Figure 1. Cross section for electron impact excitation of Ar^{16+} ions, shown here as a function of electron beam energy.

4 A high-resolution compact Johann crystal spectrometer with the Livermore electron beam ion trap

A compact high-resolution $\lambda/\Delta\lambda = 10{,}000$ spherically bent crystal spectrometer in the Johann geometry was recently installed and tested on the Lawrence Livermore National Laboratory SuperEBIT electron beam ion trap. The curvature of the mica (002) crystal grating allows for higher collection efficiency compared to the flat and cylindrically bent crystal spectrometers commonly used on the Livermore EBIT. The spectrometers Johann configuration enables us to orient its dispersion plane parallel to the electron beam propagation. Used in concert with a flat crystal spectrometer, whose dispersion plane is perpendicular to the electron beam propagation, the polarization of x-ray emission lines can be measured (sulphur studies above).

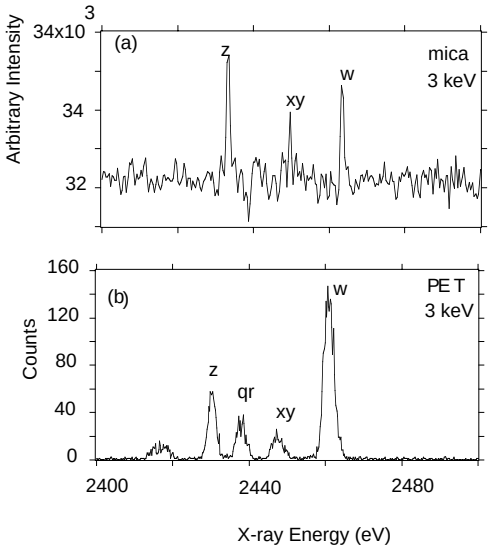

Figure 2. K-shell spectra of sulphur recorded with the spherically bent crystal (a) and with the flat crystal spectrometer (b) at 3 keV beam energy.

5 Level specific DR resonance strengths in He-like Ti^{20+} and Cr^{22+}

We have continued to analyze dielectronic satellite spectra for heliumlike Ti XXI and Cr XXIII, measured in separate earlier experiments using the LLNL EBIT-II and the EBIT high-resolution Bragg crystal spectrometers. We sweep the electron beam energy across individual DR resonances, and thus we have deduced level specific resonance strengths for the strongest DR resonances in doubly excited lithiumlike Ti XX and CrXXII. We have used the MCDF code to calculate the resonance strength, excitation energy, as well as the x-ray energies of these transition. We have wavelength-calibrated the observed spectra, and normalized the intensities to theoretical radiative recombination cross sections. See typical spectra in Fig. 3.

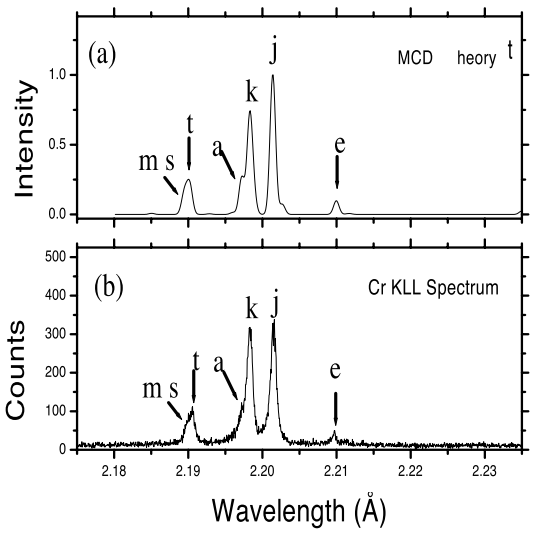

Figure 3. Dielectronic satellite spectra of heliumlike Cr^{22+}; theory (a), experiment (b).

6 Future Work

We plan to look more closely at the various discrepancies between theory and experiment with respect direct excitation cross sections. It should be possile to determine which models predict the best values for excitation cross sections.

7 Acknowledgments

We gratefully acknowledge support by the Office of Basic Energy Science, Chemical Sciences Division. This work was performed under the auspices of the Department of Energy by Lawrence Livermore National Laboratory under contract No. W-7405-ENG-48 and by Morehouse College under contract No. DE-FG02-98ER14877.

Publications List

[1] "Measurement of the Polarization of the Kβ2 line of V^{21+}", A. J. Smith, P. Beiersdorfer, K. L. Wong, and K. J. Reed, proceedings of 3rd US-Japan Plasma Polarization Spectroscopy workshop, June 18-21, 2000, LLNL, Livermore, ED P. Beiersdorfer and T Fujimoto, LLNL report no. UCRL-ID-146907, Livermore, CA 2002, p299-306.

2) " X-Ray Line Polarization of the K-shell Resonance Line Emission of Heliumlike and Lithiumlike Sulfur at Relativistic Electron Impact Energies," D.L. Robbins, H. Chen, P. Beiersdorfer, A. Ya. Faenov, T.A. Pikuz, M.J. May, J. Dunn, K.J. Reed, and A.J. Smith, Proceedings of 4th International Plasma Polarization Symposium, Kyoto, Japan February 3 - February 6 2004, LLNL Rep. UCRL-PROC-202750.

3) " Polarization measurement of Iron L-shell lines on EBIT-I," H. Chen, P. Beiersdorfer, D.L. Robbins, A.J. Smith, and M.F. Gu, Proceedings of 4th International Plasma Polarization Symposium, Kyoto, Japan February 3 - February 6 2004, LLNL Rep. UCRL-PROC-202745.

4) Measurement of the polarization of the K-shell resonance line emission of S^{13+} and S^{14+} a relativistic electron beam energies, D. L. Robbins, A. Ya Faenov, T. A. Pikuz, H. Chen, P. Beiersdorfer, M. J. May, J. Dunn, K. j. Reed, and A. J. Smith, PRA **70** 1(2004).

5) A high-resolution compact Johann crystal spectrometer with the Livermore EBIT, D. L. Robbins, H. Chen, P. Beiersdorfer, a. Ya Faenov, T. A. Pikuz, M. J. May, J. Dunn, A. J. Smith, RSI, 75 Oct(2004) 524410RSI 1.

ELECTRON/PHOTON INTERACTIONS WITH ATOMS/IONS

Alfred Z. Msezane (email: amsezane@ctsps.cau.edu)

Department of Physics and CTSPS, Atlanta, Georgia 30314

Program Scope:
We develop methodologies for calculating Regge poles trajectories and residues for both singular and nonsingular potentials, important in heavy particle collisions, chemical reactions and atom-diatom systems. Methods are developed for calculating the GOS, useful in probing the intricate nature of the valence- and open-shell as well as inner-shell electron transitions. Standard codes are used to generate sophisticated wave functions for investigating CI mixing and relativistic effects in atomic ions. The wave functions are utilized in exploring correlation effects in dipole and nondipole photoionization studies.

A. Regge Poles Trajectories for Nonsingular Potentials: Thomas-Fermi Type

A Dispersion Relations representation of the generalized oscillator strength (GOS) in the description of small-angle electron-atom differential cross sections (DCS's) through the GOS and understanding the role played by dynamic scattering resonances in chemical reactions, a key to laser control of reactions, require the investigation of Regge Poles Trajectories and associated residues for both regular and singular scattering potentials. In the complex angular momentum (CAM) techniques, the position of the Regge pole determines the angular velocity and the angular lifetime of the system, while the residue defines the magnitude of the resonance contribution in the DCS.

Developments in heavy-particle collisions, chemical reactions and atom-diatom systems [1], cluster physics, and small-angle electron DCS's using Dispersion Relations have inspired a recent upsurge in the theoretical investigations of Regge pole trajectories [2] and, most recently, residues [3] for singular scattering potentials, viz. potentials more singular than r^{-2} at the origin. Here we used the same anti-Stokes line (aSL) method as in the paper for singular potentials [4] to investigate Regge poles for nonsingular potentials (Thomas-Fermi type) [5]. In our investigation of Regge poles trajectories for the complicated nonsingular, such as the Thomas-Fermi type potentials we discovered a simple and powerful semiclassical method, based on the investigation of anti-Stokes line topology. We have found the interesting result that contrary to the case of singular potentials, the anti-Stokes lines topology for the Thomas-Fermi potentials is very complicated and requires a careful application of complex analysis. For large energies three of the five turning points are close to the poles of the effective potential. This permitted the introduction of the concept of small parameters for decomposing into a series the action integral (Bohr-Sommerfeld quantization condition).

Using Cauchy's theorem, we evaluated the resulting contour integrals to obtain an approximate expression for the Regge poles, which with the appropriate choice of the parameters of the effective potential reduces to the known result for the Coulomb potential. We discovered that the Bohr-Sommerfeld condition at low E can result in a triple connection, implying the failure of our assumption of connectivity. We have also applied a semiclassical CAM theory, used to analyze atom-diatom reactive angular distributions to several well-known potential (one-particle) problems [6]. Examples include resonance scattering, rainbow scattering, etc.

B. Generalized Oscillator Strengths for Inner-Shell Electron Transitions

The GOS, introduced by Bethe and further reviewed by Inokuti [7], is useful for probing the intricate nature of the valence- and inner-shell electronic excitations in atoms and molecules as well as for providing information about the nature of the electronic transitions and of the electron scattering process itself. Multiple minima, a manifestation of the properties of the radial parts of the wave functions, characterize the GOS's. Extrapolation of the GOS to the optical limit (momentum transfer q=0) allows for the determination of the dipole oscillator strengths.

A second-quantization formalism has been used to obtain a general expression for calculating the GOS for inner-shell electron transitions between two open-shells of any atom [8]. The general formula has been used together with the spin polarized technique of the Random Phase Approximation with Exchange (SPTRPAE) to investigate correlation effects in the GOS for the Na $2p^6 3s\ (^2S) \rightarrow 2p^5 3s^2\ (^2P)$ transition. The use of the SPTRPAE in the calculation is to insure that correlations among the p-s, p-d and s-p subshells are included. Hartree-Fock (HF) calculations were also performed. Generally, our SPTRPAE results agree better with the measurement [9] in comparison with those of the HF, demonstrating the importance of correlation effects for this Na transition. However, in the limit $q^2 \rightarrow 0$, the experimental data rise more rapidly in comparison with the calculated results and appear to behave contrary to the accepted behavior of the GOS in this limit. Unfortunately, the OOS for this Na transition is unavailable; there is a great need for an independent value of the OOS to check both the measurement and the theoretical calculations.

We have also used HF wave functions to calculate the GOS's for the C $2s^2 2p^2(^2P) \rightarrow 2s2p^3(^3P)$ and $2s^2 2p^2(^3P) \rightarrow 2s2p^4(^3D)$ transitions. Since in the limit $q^2 \rightarrow 0$, the GOS converges to the OOS, in the above cases the GOS should approach the multiplet OOS's. Indeed, for the carbon $2s^2 2p^2(^3P) \rightarrow 2s2p^4(^3P)$ transition, the multiplet OS is calculated to be 0.0659(L) and 0.0610(V), which agree excellently with the experimental result of 0.0634 [10]. However, for the transition carbon $2s^2 2p^2(^3P) \rightarrow 2s2p^4(^3D)$ the present multiplet OOS's are 0.0953(L) and 0.114(V), which agree reasonably well with the experimental value of 0.0718 [10].

C. Configuration Interaction (CI) Mixing and Relativistic Effects in Atomic Ions

Accurate and complete atomic data for all stages of ionization for elements at least up to Zn are needed for reliable extraction of the properties of the numerous cosmic plasmas and in fusion experiments with magnetically confined plasmas. However, despite recent improvement in data acquisition, the required data are often unavailable or are of insufficient quality [11] and, sometimes are riddled with errors. Therefore, their accuracy requires regular assessment.

C.1. Fine-Structure Levels of Cl V and their Lifetimes

A comprehensive R-matrix study of radiative data for neutral chlorine and its ions clearly demonstrated the importance and need for further studies of these ions [12]. Some of the radiative data on Cl ions contain inconsistencies. A recent extensive CI investigation [13] identified strong CI mixing among some levels of Cl II and resolved the controversy regarding the lowest $^1P^0$ level of Cl II.

Here we have used a large scale CI calculation, taking into account relativistic effects through the Breit-Pauli approximation to investigate in Cl V excitation energies of the lowest 49 fine-structure levels relative to the ground state $3s^2 3p\ (^1P^0_{1/2})$, oscillator strengths, line strengths and radiative rates for the optically allowed and intercombination transitions among these levels and the lifetimes for some relatively longer lived fine structure levels [14]. Our calculated fine structure energy levels agree very well with the NIST recommended data and confirm the interesting result that the lifetimes for the multiplets $3s3p^2\ (^4P)$ and $3s3p\ (^3P)\ 3d(^4F)$ are of the

order of microseconds [15]. The oscillator strengths and transition amplitudes compare reasonably well with available data, including that of Fischer [16]. Significant couplings are noted among the configurations belonging to the n=3 and n=4 complexes. We conclude that a reasonably extensive CI and relativistic effects are essential for a reliable calculation for Cl V.

C.2. Fine-Structure Energies in Al-Like and Mg-Like Ions

Recently, Safronova *et al*. [17] presented a "theoretical benchmark" relativistic many-body perturbation theory (MBPT) calculations of energies of the n=3 states of Al-like ions, with Z=14-100 and claimed excellent agreement with experimental data. A similar calculation was also for Mg-like ions [18]. We have negated the claim [19] by demonstrating, using Ar VI, Ti X, Fe XIV and Ni XVI as examples, disagreements between the Safronova *et al.* [17] data on the one hand and experimental data and other theoretical calculations, including the present results on the other hand, noting further that the calculations [17] clearly misidentify the ordering of the $^2D^0_{3/2,5/2}$ levels of the $3p^3$ and 3s3p ($^3P^0$) 3d configurations; there are others too which are interchanged by the MBPT calculation with respect to measurement.

To assess the reliability of the existing MBPT data for Al-like ions, we have performed [19] two sets of independent calculations using Program CIV3 and the GRASP code for the four Al-like ions Ar VI, Ti X, Fe XIV and Ni XVI. Extensive CI has been included in our CIV3 calculations, but relativistic effects are confined to the one-body operators only. The GRASP calculations are fully relativistic. The two sets of independent results are in near total agreement for the energies as well as level orderings and are also in agreement with other available theoretical and experimental results. The $^2D^0_{3/2,5/2}$ level energies of the $3p^3$ and the 3s3p ($^3P^0$) 3d configurations are distinctly separate in all the theoretical or experimental results for the four ions, but in the MBPT calculations they clearly disagree with all the other available data, including those of Ref. [20] for Ni XVI. The $^2D^0_{3/2,5/2}$ energies of the $3p^3$ and the 3s3p ($^3P^0$) 3d configurations exhibit fairly strong mixing, but are unambiguously identifiable. Therefore, the results [17] cannot be "benchmark calculations". Similar problems in Mg-like ions [18] are expected, where the $3p^2(^1D_2)$ couples strongly with the 3s3d ($^1D_2$) and $3p^2(^3P_2)$ [21].

For the transition $3s^2(^1S_0)\rightarrow 3s3p(^1P_1)$ in K VIII and Ti XI the results [18] agree the least with ours [22]. We conclude that the interactions among the configurations within the n=3 and n=4 complexes are of crucial importance for obtaining accurate data for K VIII and Ti XI. We note that the sophisticated wave functions for highly ionized systems are also utilized in our investigations of the applicability of Frame Transformation Methods in photoabsorption of open-shell systems such as Ni^{14+} [23] and the recent R-matrix calculation of photoionization of Ni^{15+} [24].

D. Correlation Structure in Nondipole Photoionization of Cs

Many-body effects are known to be important in atomic photoionization. Consequently, electron-electron correlations must be included in the theoretical description. Additional to correlation in the initial and final ionic discrete states, correlation in the final continuum state, often referred to as interchannel coupling [25] can be important.

The present investigation predicts an impressive manifestations of intradoublet interchannel interaction producing new structures in nondipole parameters of Cs [26], thereby demonstrating further situations where correlations affect nondipole parameters significantly. The calculation used the generalized Random Phase Approximation with Exchange (GRPAE), which takes into account the rearrangement of all atomic electrons due to the creation of a 3d vacancy, to investigate the nondipole parameters that characterize the angular distribution of photoelectrons from the 3d subshell of Cs. The inclusion of correlation in the form of

interchannel coupling between the $3d_{3/2}$ and $3d_{5/2}$ photoionization channels of Cs results in a prominent characteristic maximum only in the parameters for $3d_{5/2}$ photoionization. The effect upon the $3d_{3/2}$ channel is rather weak.

The basic origin of this structure can be understood essentially in the context of the recent demonstration [27] that the interaction between the photoionization channels belonging to different components of the spin-orbit doublets $3d_{3/2}$ and $3d_{5/2}$ in Xe, Cs and Ba dramatically affect the partial photoionization cross sections. There it was demonstrated that the $3d_{5/2}$ cross section acquired an additional prominent maximum.

References and Publications Acknowledging Program Support

1. D. Sokolovski, Chem. Phys. Lett. 370, 805(2003); S.C. Althorpe, F. Fernandez – Alonso, B.D. Bean, J.D. Ayers, A.E. Pomerantz, R.N. Zare and E. Wrede, Nature 416,67 (2002)
2. D. Vrinceanu, A.Z. Msezane, and D. Bessis, Phys. Rev. A**62**, 022719 (2000); _____ Chem Phys. Lett. 311, 395 (1999)
3. C.R. Handy, C.J. Tymczak and A.Z. Msezane, Phys. Rev. A**66**, 050701(R) (2002)
4. N.B. Avdonina, S. Belov, Z. Felfli, A.Z. Msezane and S.N. Naboko, Phys. Rev. A**66**, 022713 (2002)
5. S.M. Belov, N.B. Avdonina, Z. Felfli, M. Marletta, A.Z. Msezane, and S.N. Naboko, J. Phys. A**37**, 6943 (2004)
6. D. Sokolovski and A.Z. Msezane, Phys. Rev. A, In Press (2004)
7. H. Bethe, Ann. Phys. 5, 325 (1930); M. Inokuti, Rev. Mod. Phys. **43**, 297 (1971)
8. Zhifan Chen, and A.Z. Msezane, Phys. Rev. A, In Press (2004)
9. C.E. Bielschowsky, C.A. Lucas, G.G.B. de Souza, *et.al*., Phys. Rev. A**43**, 5975 (1991)
10. W.L. Wiese, J.R. Fuhr, and T.M. Deters, Atomic Transition Probabilities of Carbon, Nitrogen, and Oxygen, J. Chem. Phys. Ref. Data Monogram No. 7 (1996)
11. D.J. Hillier and T. Lanz, in Spectroscopic Challenges of Photoionized Plasmas, Ed. G. Ferland and D.W. Savin, ASP Conf. Ser. 247, p 343
12. K.A. Berrington and S. Nakazaki, At. Data Nucl. Data Tables 82, 1 (2002)
13. N.C. Deb, D.S.F. Crothers, Z. Felfli, and A.Z. Msezane, J. Phys. B**36**, L47 (2003)
14. K.B. Choudhurry, N.C. Deb, K. Roy, and A.Z. Msezane, Europ. Phys. Jour. 27, 103 (2003)
15. C. Jupen, and L.J. Curtis, Phys. Scripta 53, 312 (1996)
16. C. Froese Fischer, (http://www.vuse.vanderbilt.edu/cff/mchf-collection)
17. U.I. Safronova, C. Namba, J.R. Albritton, *et.al.,* Phys. Rev. A**65**, 022507 (2002)
18. U.I. Safronova, W.R. Johnson, and H.G. Berry, Phys. Rev. A**61**, 052503 (2000)
19. G.P. Gupta, K.M. Aggarwal and A.Z. Msezane, Phys. Rev. A, In Press (2004)
20. C. Froese Fischer (http://atoms.vuse.vanderbilt.edu/Elements/Ni/Al_28.14.mcdhf-lev.lt.db)
21. R. Das, N.C, Deb, K. Roy, and A.Z. Msezane, Physica Scripta 67, 401 (2003)
22. R. Das, N.C, Deb, K. Roy, and A.Z. Msezane, A & A 416,375 (2004)
23. Z. Felfli, T.W. Gorczyca, N.C. Deb, and A.Z. Msezane, Phys. Rev. A**66**, 042716 (2002)
24. Z. Felfli, T.W. Gorczyca, N.C. Deb, S.T. Manson and A.Z. Msezane, Bull. Am. Phys. Soc. 49, 37 (2004)
25. U. Fano, and J. Cooper, Rev. Mod. Phys. 81, 1199 (1968)
26. M. Ya. Amusia, A.S. Baltenkov, L.V. Chernysheva, Z. Felfli, S.T. Manson, and A.Z. Msezane, Phys. Rev. A67, 060702 (2003)
27. M. Ya. Amusia, L.V. Chernysheva, S.T. Manson, A.Z. Msezane, and V. Radojevic, Phys. Rev. Lett. **88**, 093002 (2002)

Two-Photon Decay

R. W. Dunford, E. P. Kanter, B. Krässig, S. H. Southworth, L. Young P. H. Mokler[1], and Th. Stöhlker[1]
Argonne National Laboratory, Argonne, IL 60439

The study of decays which proceed via the simultaneous emission of two photons provides a unique means of gaining insight on atomic structure. Typical measurements result in data on transition probabilities differential in the opening angle distribution and the energy of the individual photons. Together these characteristics provide a wealth of information on the atom. (See Ref. [1] for a recent review.) In this work, we are studying two-photon decay following photoionization of the K shell of heavy atoms. We also obtain information on vacancy cascades involving emission of successive photons or involving emission of two photons accompanied by a Coster-Kronig rearrangement in the intermediate state. The study of these cascades is part of a general effort by the group aimed at understanding the complex issue of vacancy cascades following photoionization. (For related work see Ref. [2].) In another effort we derived a generalization of one of the selection rules governing two-photon decay processes [3]. Our efforts to test the theory of two-photon decay also nicely complements our plans to study the time-reversed analog, namely multiphoton x-ray processes, with the next generation of x-ray photon sources such as the LCLS.

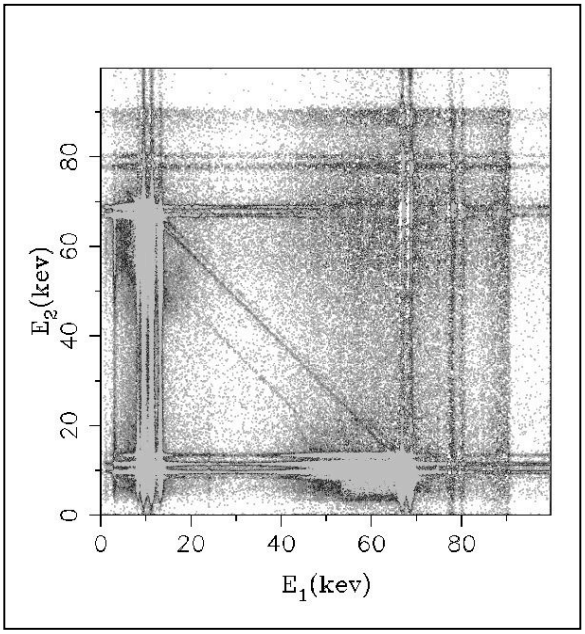

We recently measured two-photon decay of K-vacancies in gold atoms following photoionization with synchrotron radiation [4]. Two germanium detectors were arranged around a gold target which was irradiated with x-rays. The figure shows the correlation between energies from the two detectors for coincidence events. The diagonal features of constant sum energy arise from 2s → 1s, 3d → 1s and 4d → 1s two-photon decays. We will present our latest results and a comparison with theory.

[1] P. H. Mokler and R. W. Dunford, Physica Scripta **69**, C1-9 (2004).
[2] G. B. Armen, E. P. Kanter, B. Krässig, J. C. Levin, S. H. Southworth, and L. Young, Phys. Rev. A 69, 062710 (2004).
[3] R. W. Dunford, Phys Rev A **69**, 062502 (2004).
[4] R. W. Dunford, E. P. Kanter, B. Krässig, S. H. Southworth, L. Young, P. H. Mokler, and T. Stöhlker, Phys Rev A **67**, 054501 (2003).
[1]GSI, Planckstrasse 1, D64291 Darmstadt, Germany

Recent Progress and New Opportunities for Ion-Atom Merged Beams at MIRF

C. C. Havener and R. Rejoub
Physics Division, Oak Ridge National Laboratory, Oak Ridge, TN 37831-6372

At ORNL the Multicharged Ion Research Facility (MIRF) is currently undergoing a major upgrade which consists of installation of a new all-permanent-magnet ECR ion source on a new 250-kV platform and relocation of the present CAPRICE ECR ion source to a new floating beamline. The ion-atom merged-beams apparatus together with the intense ion beams available at MIRF provide a unique opportunity to study electron capture at low energies (meV/u – keV/u). Progress in the understanding of electron capture depends on the ability to perform benchmark measurements. Measurements for N^{2+} + H(D), Ne^{3+} + H(D)[1] and Ne^{4+} + H(D)[2] show a strong 1/v rise at meV/u energies, indicative of the strong ion-induced dipole attraction between reactants. Merged-beams measurements and theoretical predictions for N^{2+} + H(D) show significant structure in the total electron capture cross section throughout the energy range.

He^{2+} + H is one of the most-frequently theoretically studied collision processes and is viewed as a prototype one-electron heavy particle, asymmetric collision system. However, an exponentially decreasing cross section and the inherent difficulties in producing a ground-state atomic hydrogen target have made measurements difficult and scarce below 1 keV/u. Absolute total electron capture cross sections for He^{2+} + H have been measured[3] for collision energies from 380 eV/u to 2620 eV/u. Together with hidden-crossing coupled-channel calculations[3], an improved benchmark has been established for this system to which new methods, e.g., recent hyperspherical coupled channel calculations can be compared. Recent measurements[4] for Ne^{2+} + H(D), which also decrease toward lower energies, show a "change of slope" which, after careful analysis of all the potential curves, is associated with rotational coupling to quartet states.

Modifications to the merged-beams apparatus to take advantage of the ECR upgrade project are well underway. The upgrade will provide higher energy and less divergent ion beams which significantly enhance the capabilities of the ion-atom merged-beams apparatus. The Cs sputter source allows merged-beams measurements to be performed with a variety of neutral beams other than H and D, such as Li, B, Na, Cr, Fe, etc., and molecular beams such as O_2, CH_2,…

1. R. Rejoub, M. E. Bannister, C. C. Havener, D. W. Savin, C. J. Verzani, J. G. Wang, and P. C. Stancil, PRA **69** 052704 (2004)
2. C. C. Havener, R. Rejoub, C. R. Vane, H. F. Krause, D. W. Savin, J. G. Wang, and P. C. Stancil, to be published in Phys. Rev. A (2004).
3. C. C. Havener, R. Rejoub, P. S. Krstic, and A. C. H. Smith, submitted to Phys. Rev. A (2004).
4. T. Mroczkowski, D. W. Savin, R. Rejoub, P. S. Krstic, and C. C. Havener, Phys. Rev. A **68,** 032721 (2003).

Research Summaries

(multi-PI programs by institution)

AMO Physics at Argonne National Laboratory

R. W. Dunford, E. P. Kanter, B. Krässig, S. H. Southworth, L. Young
Argonne National Laboratory, Argonne, IL 60439

dunford@anl.gov, kanter@anl.gov, kraessig@anl.gov, southworth@anl.gov, young@anl.gov

Our central goal has been to establish a quantitative understanding of x-ray interactions with free atoms and molecules with attention to both structural and dynamical aspects. As ultrafast, ultraintense x-ray light sources become available, new classes of experiments are emerging, namely, nonlinear and strong-field processes in the hard x-ray range and probing of sub-picosecond phenomena with hard x-rays. These inspire new types of experiments at Argonne's Advanced Photon Source, such as the coupling of strong-field optical lasers to modify standard, weak-field x-ray processes. Foundational to these new experiments is the detailed understanding of x-ray photoionization and decay processes which we have gained over many years using coincidence and multichannel detection techniques. We have explored a broad energy range where the dominant interaction evolves from photoabsorption to scattering, with careful attention to regions near resonances and thresholds. We have focused on understanding the limitations of *ab initio* theory, in particular the validity of the independent particle approximation and the role of multipole effects in the weak-field regime. Finally, we are able to address unique problems in few-body physics with the specialized target technology that we are developing, ultracold Li combined with ion momentum imaging capabilities and metastable Kr. These targets have additional applications of wide-ranging interest as well. Recent progress is described below.

X-ray processes in the presence of strong-optical fields

R.W. Dunford, D.L. Ederer, E.P. Kanter, B. Krässig, E.C. Landahl[1], S.H. Southworth, L. Young

Many proposed experiments for the next generation x-ray sources involve laser/x-ray pump–probe techniques on the ≈100 fs timescale. At the compressed timescale, the laser intensity used to initiate a dynamical process can easily approach 10^{14} W/cm^2, i.e. a field strength of ≈ 3 Volts/Ångstrom which is comparable to the field binding an electron to the nucleus. Therefore, it is important to understand how the x-ray physics of an atom is perturbed due to the presence of a high-power laser. We are investigating how the field from an ultrafast laser modifies the x-ray photoionization and vacancy decay of an isolated atom. Theoretically, the problem simplifies to the behavior of an atom under the influence of a strong, low-frequency dressing beam (laser) as probed by a weak, high-frequency beam (x-ray). Two major effects have been theoretically predicted and observed for valence electrons where the weak probe beam is in the vacuum-ultraviolet region: 1) the ponderomotive shift of the ionization threshold, and, 2) the appearance of sidebands in photoelectron and Auger spectra. Here, we investigate inner-shell threshold structure for the first time.

Despite the "long" pulse length at the APS, ≈87 ps FWHM, we can already address these issues at intensities relevant to the next generation sources. A combination of microfocusing of the x-ray beam to ≈ 1 x 1 μm^2 and tight focusing of the dressing laser to $10\tilde{x}1\mu m^2$ is required. Clearly, shortening of the x-ray pulselength and tightening of the x-ray focus will extend the accessible parameter space. An early goal is to observe the evolution of the near-edge x-ray absorption spectrum as a function of applied laser intensity. At high intensities, the atom is ionized and a dramatic edge shift and strong pre-edge resonance will be apparent. At

intermediate intensities, the atom is "dressed" and the ponderomotive threshold shift combined with AC Stark shifts of optically-accessible Rydberg levels will modify the near-edge x-ray absorption spectrum. These modifications influence the interpretation of near-edge spectra that are widely used in x-ray diagnostics.

This past year we have succeeded in measuring the laser-induced modification of the near-edge spectrum of krypton in the high intensity (ionizing) regime. This followed a considerable effort to develop alignment and overlap tools for the x-ray and laser beams. A striking pre-edge feature is observed, as predicted by multiconfiguration Dirac-Fock calculations, with a S/N of 10 for an integration time of 4 hours. Optimization in time overlap can yield a ten-fold increase in S/N. We have strong evidence for Coulomb explosion of the laser-produced ions and indeed the x-rays can be used to monitor those dynamics. Highly energetic krypton ions (~100 eV) created by repulsion from the central core of charge produced by the laser are observed. The densities correspond to the "underdense" plasma regime. In addition, our initial results indicate that the laser pump/x-ray probe method is a viable tool for x-ray ion spectroscopy. Incipient ion densities are $\approx 10^{12}$ /cm^3 with an interaction length of 0.1 cm, compared to the typical collinear ion beam methods with densities of 10^7 /cm^3 and interaction length of 100 cm. A laser system upgrade is underway which will yield a ten-fold increase in laser pulse energy over that typically obtained and a five-fold increase in repetition rate. This will permit access to the dressed atom regime and facilitate other experiments with, e.g., aligned molecular targets.

Double K-photoionization of heavy atoms

E. P. Kanter, R. W. Dunford, D. S. Gemmell, B. Krässig, S. H. Southworth, and L. Young

The double K-photoionization of heavy atoms is a rare process that produces a *hollow* atom. The process itself is of fundamental interest as a measure of electron-electron correlations in high-Z systems, but this work has several practical applications as well. For example, planning for future work with the LCLS requires a more complete understanding of the decay paths of such multiply-ionized atoms. We have recently reported on a comprehensive study of double K-photoionization of Ag (Z=47) [submitted Phys. Rev. A]. Measurements were carried out at several photon energies from just below the double K-ionization threshold (51.782 keV) to the region of the expected maximum in the cross-section (~90 keV). The energy-dependence of these data has been fitted with a model in which the shakeoff and scattering contributions are calculated independently. Because of extensive previous studies of this atomic system using the electron capture (EC) decay of ^{109}Cd, the shakeoff contribution is well known experimentally for the single-electron final state produced in EC. Thus, our photoionization measurements served to isolate the effects of the dynamic electron-electron scattering term. Analysis of these results demonstrates a significantly larger scattering contribution than in lighter atoms. The measured ratio (double/single ionization) in the peak region is found to agree well with the Z-dependence we had found from fitting previous measurements and much slower than the characteristic $1/Z^2$ dependence of shakeoff, further confirming the large scattering contribution in the peak region.
We have developed a model, based on the scaling properties of electron impact ionization cross sections, which quantitatively describes these observations. An important goal for the immediate future is to complete this work in Ag with additional measurements beyond the peak region to verify this proposed new model.

Inner-shell vacancy cascades

G.B. Armen[2], E.P. Kanter, B. Krässig, J. Levin[2], S.H. Southworth, L. Young

Atomic x-ray absorption typically excites or ejects a deep inner-shell electron, producing a vacancy state which relaxes by a series of radiative (x-ray fluorescence) and radiationless (Auger-electron emission) processes. A range of final ion charge states is observed due to alternative decay pathways. If the initial vacancy is produced in an atomic constituent of a molecule, a similar vacancy cascade occurs, but removal of delocalized valence electrons produces positive charge on two or more atomic centers and results in ion fragmentation (Coulomb explosion). Coincidence techniques, in which two or more ejected photons, ions, or electrons are detected simultaneously, allow specific decay pathways to be selected from a complex vacancy-cascade process. K-shell vacancies in high-Z atoms decay preferentially by K-L x-ray fluorescence in which the vacancy is transferred to the L-shell. By using this fluorescent x-ray as an event marker in a coincidence circuit, the ion charge-state distributions of Kr were measured as the absorbed x-ray energy was tuned across the K edges at 14.3 keV. Our earlier work [6] studied decays coincident with Kα or Kβ x-rays, i.e. those proceeding via either 2p or 3p hole states. Our latest studies [20] distinguish the 2p vs the 3p cascade by using a high-resolution Si(Li) detector to resolve the decay fluorescence. For x-ray excitation much above the K-edge, cascade decay occurs with the excited electron in the continuum. These observations are reasonably well explained by Hartree-Fock calculations [Kochur *et al* J. Phys. B (1995), El Shemi *et al* J. Phys. B (1997)]. However, for x-ray excitation near the K-edge, the excited electron can be parked in a Rydberg state and may act as a spectator to the decay, resulting in a lower charge state and deviations from the Hartree-Fock predictions. A "spectator cascade decay" model was developed to describe the sticking probability for the Rydberg electron as a function of the hole and final charge state.

Two-photon decay

R. W. Dunford, E. P. Kanter, B. Krässig, S. H. Southworth, L. Young, P. H. Mokler[3], and Th. Stöhlker[3]

The study of decays that proceed via the simultaneous emission of two photons provides a unique means of testing atomic theory. Typical measurements result in data on transition probabilities differential in the opening angle distribution and the energy of the individual photons. Together these characteristics provide a wealth of information to test the details of the calculations. (See [18] for a recent review.) In this work, we are studying two-photon decay following photoionization of the K shell of heavy atoms. We also obtain information on vacancy cascades involving emission of successive photons or involving emission of two photons accompanied by a Coster-Kronig rearrangement in the intermediate state. The study of cascades is part of a general effort by the group aimed at understanding the complex issue of vacancy cascades following photoionization. (For related work see [6,20].) In another effort we derived a generalization of one of the selection rules governing two-photon decay processes [21]. The group's efforts to test the theory of two-photon decay also nicely complements our plans to study multiphoton x-ray processes with the next generation of x-ray photon sources such as the LCLS [1].

Recently, we studied two-photon decay of single K-vacancies in gold atoms following photoionization with synchrotron radiation [7]. A pair of germanium detectors was arranged around a gold target that was irradiated with x-rays from the Advanced Photon Source APS. Some of the K-holes produced in the gold target decayed by emission of two photons. This process was studied by looking for coincidences between the two detectors that had a total energy corresponding to a level separation in the system. The results determined the differential transition probabilities for the 2s $\rightarrow$ 1s, 3d $\rightarrow$ 1s and 4d $\rightarrow$ 1s two-photon decays for events in which the two photons share the transition energy equally and have opening angles near $\theta = \pi/2$. Although no calculations have been done for gold our results give a lower transition probability than would be expected by extrapolating results from calculations that were done for lighter atoms. To resolve this issue and provide more information to test the calculations, we recently completed an improved experiment designed to measure the spectral shape of the two-photon continuum from gold atoms. Longer integration times were used in order to gain sufficient statistical accuracy for the differential measurements. Analysis of these data is currently in progress.

Near threshold double ionization of lithium by electron impact: four-body continuum

M.-T. Huang[4], S. Hasegawa[5], E. P. Kanter, S. H. Southworth, L. Young

The dependence on excess energy of a multiple-ionization cross section near threshold is a many-body process whose theoretical description and experimental measurement remains of current interest. The well-known Wannier threshold law, $\sigma(E) \propto E^{\alpha}$, where E is the excess energy and $\alpha = 1.127$, describes a three-body-continuum cross section with two electrons and a positive ion. The four-body continuum with three slow electrons and a positive ion is less well studied, but a Wannier-type power law is also expected with an exponent $\alpha \approx 2$. Experimentally, the challenge is to measure α and determine the energy range of validity of the power law while the cross section vanishes as threshold is approached. Double ionization of Li near threshold is particularly interesting because the target electons have very different binding energies, 5.4 and 64.4 eV for the 2s and 1s electrons, respectively. A classical trajectory Monte Carlo calculation [F. Sattin and K. Katsonis, J. Phys. B **36**, L63 (2003)] for the electron-impact double-ionization of Ar found that the power-law exponent $\alpha = 2.03$ when the two target electrons are given equal binding energies but $\alpha = 1.27$ when they are given different binding energies. This suggests that an exponent much less than 2 might be expected for double-ionization of Li. The ionization mechanism in this case might be roughly described as knockout of the 1s electron accompanied by shakeoff of the 2s electron.

We have previously used a magneto-optical trap (MOT) of Li atoms as a target for measurements of single-, double-, and triple-ionization by electron impact at high excess energies [3,13]. The Li MOT has certain advantages in such studies compared with diffuse atomic beams, such as the elimination of dimers and other impurities in the target and the production of ions in a small ($\approx$ 1 mm dia.) localized spot that is well-suited for ion-imaging detection. We employ a timing and gating procedure in which the optical and magnetic trapping fields are cycled off to avoid their effects on the ion yields. The Li^{2+}/Li^{+} ion-yield ratio was measured from near the Li^{2+} threshold (81 eV) to 160 eV excess energy. The Li^{2+} cross section was determined by scaling this ratio to the measured Li^{+} cross section. As a check on our

measurement and data analysis methods, we used identical procedures to measure the threshold cross section for double ionization of Ne for comparison with other reported measurements. We also determined the peak energy and energy spread of our electron beam through measurements of elastically-scattered electrons and low-energy Auger electrons. Data analysis is in progress and, at this time, we can only report a preliminary result that we observe an exponent less than the value $\alpha \approx 2$ expected from Wannier theory. We plan to complete our analysis and report our results in the coming year.

Nondipole asymmetries of valence-shell photoelectrons of molecular nitrogen

E. P. Kanter, B. Krässig, S. H. Southworth

New aspects of the photoionization of atoms, molecules, and materials have been studied in recent years through measurements and theoretical calculations of the nondipole asymmetries of photoelectron angular distributions. Nondipole asymmetries arise from cross terms of electric-dipole with electric-quadrupole and magnetic-dipole photoionization amplitudes. While treatment of nondipole interactions in atoms, including many-electron effects, is a relatively straight-forward extension of atomic photoionization theory, the corresponding treatments for diatomic molecules is more challenging [P. W. Langhoff *et al.*, J. Electron Spectosc. **114–116**, 23 (2001)]. The experimental observation of nondipole asymmetries for K-shell photoelectrons of N_2 that greatly exceed atomic N 1s asymmetries demonstrated that uniquely molecular effects can play a significant role [O. Hemmers *et al.*, Phys. Rev. Lett. **87**, 273003 (2001)]. Motivated by that result, we have measured the nondipole asymmetries of the $3\sigma_g$, $1\pi_u$, and $2\sigma_u$ valence-shell photoelectrons of N_2. Measurements were made over the 26–100 eV photon-energy range at Wisconsin's Synchrotron Radiation Center using four rotatable electron spectrometers as described in [5]. Our results were combined with measurements over 80–200 eV made by our collaborators at Berkeley's Advanced Light Source [O. Hemmers *et al.*, unpublished]. While the magnitudes of the measured asymmetries are comparable to those for corresponding atomic orbitals, the $2\sigma_u$ asymmetry shows a distinctly different energy variation than those for $3\sigma_g$ and $1\pi_u$. Concurrent theoretical developments have produced calculated asymmetries within the frozen-core Hartree-Fock approximation [B. Zimmermann, V. McKoy and P.W. Langhoff, unpublished]. Preliminary comparisons of theory and experiment are encouraging and lead to identification of observed features with dipole and nondipole molecular-symmetry channels. When completed, this experimental and theoretical study will provide an initial benchmark for understanding nondipole interactions in valence-shell photoionization of molecules.

Optical production of metastable rare gases

R.W. Dunford and L. Young

Metastable rare gas atoms have numerous applications in fields such as optical lattices, cold collisions physics, atom lithography, medical imaging, tests of fundamental symmetries and rare isotope detection. The importance of metastable rare gas atoms arises because it is very difficult to manipulate and control rare gas atoms when they are in the ground state but it is typically easy to control such atoms once they are excited to a relatively long-lived metastable state. Metastable rare gas atoms are normally produced by direct extraction from a DC or rf discharge and produce beams with a metastable fraction of less than 0.1%. We recently

developed a new optical metastable production scheme [4]. In this scheme, an ultraviolet lamp is used to create a population of Kr atoms in the 5s[3/2]J=1 state. These short-lived excited atoms are immediately pumped to the 5p[3/2]J=2 level, using 819-nm light from a Ti-Sapphire laser. This state decays to the metastable state with a branching ratio of 77%. Our initial experiments to test the concept were done in a gas of krypton atoms in a cell. We achieved a metastable production rate of 10^{14} metastable atoms/s. This corresponded to a UV-photon-to-metastable conversion efficiency of about 5% and the metastable fraction in the interaction region was estimated to be about 2%.

Recently we completed a new apparatus which was designed to produce a metastable Kr beam and initial experiments are in progress. The goal is to obtain a metastable flux of better than $2x10^{14}$ metastable atoms per second and an angular flux of 0.8 - $4x10^{17}$ metastables/s/sr. Such a beam could be used for electron scattering or photoionization experiments or to feed an atom trap as part of a new trace analysis technique that has been developed at Argonne [C.Y. Chen *et al.*, Science (1999)].

[1]Advanced Photon Source, Argonne National Laboratory
[2]University of Tennessee, Knoxville
[3]GSI, Planckstrasse 1, D64291 Darmstadt, Germany
[4]Saginaw Valley State University, Saginaw, MI
[5]University of Tokyo, Tokyo, Japan

Future Plans

We plan to emphasize those aspects of our program related to the ultrafast and ultraintense x-ray sources of the future. This includes the studies of strong-field effects on x-ray photoionization and vacancy decay. Future areas of interest include ultrafast x-ray probes of strong-field-controlled molecular processes, where Argonne, with its high-brilliance x-ray source coupled with the high-power ultrafast laser facility at the APS Sector 7, is uniquely positioned to play a leading role. Our traditional program studying higher-order x-ray induced photoprocesses serves as a basis for these studies. As resources allow, we will continue to develop/use the ultracold Li target for studies of the three- and four-body Coulomb continuum. Similarly, we will continue development of the metastable krypton source for a variety of applications.

Selected Publications 2002 – 2004

[1] Interaction of atomic systems with x-ray free-electron lasers,
M. A. Kornberg, A. L. Godunov, S. Itza-Ortiz, D. L. Ederer, J. H. McGuire, and L. Young.,
J. Synchrotron Rad. 9, 298-303 (2002).

[2] Photoexcitation of a Dipole-Forbidden Resonance in Helium,
B. Krässig, E. P. Kanter, S. H. Southworth, R. Guillemin, O. Hemmers, D. W. Lindle, R. Wehlitz, and N. L. S. Martin., Phys. Rev. Lett. **88**, 203002 (2002).

[3] Measurements of the electron-impact double-to-single ionization ratio using trapped lithium
M.-T. Huang, L. Zhang, S. Hasegawa, S. H. Southworth, L. Young
Phys. Rev. A **66**, 012715:1-7 (2002).

[4] Optical production of metastable krypton
L. Young, D. Yang, R.W. Dunford
J. Phys. B **35**, 1-8 (2002).

[5] Nondipole asymmetries of Kr 1s photoelectrons,
B. Krässig, J.-C. Bilheux, R. W. Dunford, D. S. Gemmell, S. Hasegawa, E. P. Kanter, S. H. Southworth, L. Young, L. A. LaJohn and R. H. Pratt., Phys. Rev. A **67**, 022707 (2003).

[6] Threshold krypton charge-state distributions coincident with K-shell fluorescence,
G. B. Armen, E. P. Kanter, B. Krässig, J. C. Levin, S. H. Southworth, and L. Young,
Phys. Rev. A **67**, 054501 (2003).

[7] Two-photon decay in gold atoms following photoionization with synchrotron radiation,
R.W. Dunford, E.P. Kanter, B. Krässig, S.H. Southworth, L. Young, P.H. Mokler, and Th. Stöhlker., Phys. Rev. A **67**, 054501 (2003).

[8] Applications of position sensitive germanium detectors for X-ray spectroscopy of highly charged heavy ions, T. Stöhlker, D. Banas, H.F. Beyer, A. Gumberidze, C. Kozhuharov, E. Kanter, T. Krings, W. Lewoczko, X. Ma, D. Protic, D. Sierpowski, U. Spillmann, S. Tachenov, and A. Warczak., Nucl. Instrum. Meth. B **205**, 210-214 (2003).

[9] Double K-shell photoionization of neon,
S. H. Southworth, E. P. Kanter, B. Krässig, L. Young, G. B. Armen, J. C. Levin, D. L. Ederer, and M. H. Chen., Phys. Rev. A **67**, 062712 (2003).

[10] E1-E2 interference in the VUV photoionization of He,
E. P. Kanter, B. Krässig, S. H. Southworth, R. Guillemin, O. Hemmers, D. W. Lindle, R. Wehlitz, M. Ya. Amusia, L. V. Chernysheva, and N. L. S. Martin., Phys. Rev. A **68**, 012714 (2003).

[11] Dramatic nondipole effects in low-energy photoionization: experimental and theoretical study of Xe 5s, O. Hemmers, R. Guillemin, E. P. Kanter, B. Krässig, D. W. Lindle, S. H. Southworth, R. Wehlitz and J. Baker, A. Hudson, M. Lotrakul, D. Rolles, W. C. Stolte, I. C. Tran, A. Wolska, S. W. Yu, M. Ya. Amusia, K. T. Cheng, L. V. Chernysheva, W. R. Johnson, and S. T. Manson., Phys. Rev. Lett. **91**, 053002 (2003).

[12] Towards ultrahigh sensitivity analysis of ^{41}Ca
I.D. Moore, K. Bailey, Z.-T. Lu, P. Müller, T.P.O'Connor and L. Young,
Nucl. Instr. Meth. B **204**, 701-704 (2003).

[13] Triple Ionization of Lithium by Electron Impact
M.-T. Huang, W.W. Wong, M. Inokuti, S.H. Southworth, L. Young
Phys. Rev. Lett. **90**, 163201:1-4 (2003).

[14] From the atomic to the femtoscale
L. Young, in From the Atomic to the Nano-Scale (AIP Press NY, C.T. Whelan & J.H. McGuire, Ed., 2003) p204

[15] Higher-order processes in X-ray photoionization and decay
R.W. Dunford, E.P. Kanter, B. Krässig, S.H. Southworth, and L. Young
Radiation Physics and Chemistry **70,** 149 (2004).

[16] Inner-shell photoionization in weak and strong radiation fields
S.H. Southworth, R.W. Dunford, D.L. Ederer, E.P. Kanter, B. Krässig, and L. Young
Radiation Physics and Chemistry **70**, 655 (2004).

[17] Lifetime of the 2^3P_0 state of He-like ^{197}Au
S. Toleikis, B. Manil, E. Berdermann, H. F. Beyer, F. Bosch, M. Czanta, R. W. Dunford, A. Gumberidze, P. Indelicato, C. Kozhuharov, D. Liesen, X. Ma, R. Marrus, P. H. Mokler, D. Schneider, A. Simionovici, Z. Stachura, T. Stöhlker, A. Warczak, and Y. Zou
Phys. Rev. A **69,** 022507 (2004).

[18] Two-Photon Decay in Heavy Atoms and Ions
P. H. Mokler and R. W. Dunford
Physica Scripta **69**, C1 (2004).

[19] Counting Individual Ca Atoms with a Magneto-Optical Trap
I. D. Moore, K. Bailey, J. Greene, Z.-T. Lu, P. Muller, T. P. O'Connor, Ch. Geppert, K. D. A. Wendt, and L. Young
Phys. Rev. Lett. **92**, 153002 (2004).

[20] Spectator electron behavior during cascade decay in krypton
G.B. Armen, E.P. Kanter, B. Krässig, J.C. Levin, S.H. Southworth, and L. Young
Phys. Rev. A **69,** 062710 (2004).

[21] Nonvanishing $J=1 \leftrightarrow 0$ two-photon decay: E1M2 decay of the He-like 2^3S_1 state
R. W. Dunford
Phys. Rev. A **69**, 062502 (2004).

Structure and Dynamics of Atoms, Ions, Molecules, and Surfaces:
Electronic Excitation of Highly Charged Ions and Nanotubes

P. Richard
J. R. Macdonald Laboratory [JRML], Kansas State University Manhattan, KS 66506
[richard@phys.ksu.edu]

The scope of this part of the JRML program is to search for the electronic excitation of image-potential states formed above the surface of nanotubes, which has recently been predicted by theory but not previously observed in the laboratory. The states are studied by electron time-of-flight measurements following a pump-probe excitation-ionization process using the JRML fs laser facility. We have observed the formation of these states in multiwalled carbon nanotubes.

The scope of the second part of this JRML program is to study electronic excitation of highly charged ions with the use of the high velocity ion beams from the JRML accelerators. The study is directed toward a determination of triply excited states in the neutral Li-like isoelectronic sequence from Z= 6 to 9 formed in collisions of bare ions with Ar and Kr targets. The states are formed by triple electron capture in this series of experiments. The states are also produced by dielectronic excitation in electron - He-like metastable ion collisions. In both series of experiments the states are observed in high-resolution zero-degree projectile Auger electron spectroscopy. This subject was discussed in last year's abstract and will not be discussed here.

Time–resolved photoexcitation of image–potential states in carbon nanotubes: Experimental
(M. Zamkov, N. Woody, S. Bing, H.S. Chakraborty, Z. Chang, U. Thumm, and P. Richard)

This is a new project in which we use the new capabilities of the JRML ultra-high intensity, fs laser facility. In this effort we have obtained the first experimental evidence for the existence of image-potential states in carbon nanotubes. The observed features constitute a new class of surface image states due to their quantized centrifugal motion. These types of states were recently predicted in a Phys. Rev. Letters article by B.E. Granger, P. Kral, H.R. Sadeghpour, and M. Shapiro[1]. Measurements of binding energies and the temporal evolution of image electron wave–packets were performed using the femtosecond time–resolved photoemission. The associated image electron lifetimes are found to be one order of magnitude longer than those of image states above metal surfaces, indicating a strong localization of an image–potential state in front of the nanotube's surface.

Quantized states are known to form in front of surfaces due to the polarizing image–interaction of an external electron. For years the investigation of these states above metal surfaces has served as a powerful tool for probing a variety of physical and chemical phenomena on the nanometer scale[2,3]. The unique properties of image states are determined by the extreme sensitivity of "image" electrons to any changes in the dielectric susceptibility at the surface. Therefore, through measurements of their binding energies and lifetimes it is possible to elucidate many complex processes that ultimately promote our knowledge of surface structure, optical properties at interfaces, electronic structure at heterojunctions, layer growth morphology, and surface reactivity [4].

The experimental setup consisted of a Ti:sapphire laser system generating 35 femtosecond pulses at 2 kHz. Frequency–tripled UV photons were produced through non–linear

effects during the photoionization of N_2 molecules. The fluence of the resulting 100 fs UV pump–pulse used for promoting an electron population into unoccupied image states was estimated to be $40\mu J/cm^2$. Binding energies and temporal dynamics of photoexcited electrons were subsequently probed with a delayed IR probe–pulse having a fluence of $30\mu J/cm^2$. The single–photon ionization regime, critical for the correct interpretation of the photoelectron energy distribution, was established by requiring that the photoemission signal is independent of the polarization of the IR probe–beam. In order to increase the count rate to pulse fluence ratio, the laser spot size on the sample for both UV and IR beams was maintained relatively large ($\sim 400\mu m$). Following the photoionization by IR pulses, electrons drifted into the magnetically and electrically shielded 30-cm long spectrometer tube and were detected with a strip–and– wedge position sensitive detector. The overall energy resolution of the system in the case of 1 eV electrons was 20 meV. In the present study, the energy of the UV photon exceeded the sample work function of 4.24 ± 0.10 eV by 0.47 eV, resulting in a pump–only photoemission of low–energy electrons. In order to isolate the photoemission originating from image–potential states, we recorded the change in the photoelectron signal induced by the IR probe–pulse. This approach is illustrated in Fig. 2(c) showing the two photoelectron spectra, resulting from "pump only" and "pump and probe" photoemission. The corresponding "excitation" difference is shown in Fig. 2(b). For a negative pump–probe delay, the IR pulse is incident first, promoting the electron population from below the Fermi level into the conduction band. The resulting perturbation, consisting of e^-–h pairs, is then probed with a UV pulse, giving rise to a characteristic feature [5] in the photoelectron spectrum (the bipolar peak in 2(b)). This signal fades for a positive pump–probe delay of approximately 150 fs (the convoluted duration of UV and IR pulses), since the number of UV photons following the IR pulse probing excited carriers at the Fermi level, is now negligibly small. For delays exceeding 200 fs, most of the photoelectrons are created with a single IR probe–photon. The corresponding window of accessible electronic states for this configuration is located within 1.57 eV below the vacuum level (see Fig. 3(a)), which is degenerate with the expected positions of image–potential states as well as the continuum of states at the top of the conduction band. The excited electron population in the latter has a characteristic lifetime of just a few femtoseconds. Meanwhile, the photoelectron signal is still observed for pump–probe delays of up to 0.5 ps (not shown here). Therefore, the observed photoemission, shown in Fig. 2(b), is attributed to the photoionization of image–potential states in MWNTs. An article on this work has been submitted to Physical Review Letters.

1) B.E. Granger, P. Kral, H.R. Sadeghpour, and M. Shapiro, Phys. Rev. Lett. **89**, 135506 (2002).
2) U. Hofer, I.L. Shumay, C. Rruß, U. Thomann, W. Wallauer, and T. Fauster, Science **277**, 1480 (1997).
3) T. Hertel, E. Knoesel, M. Wolf, and G. Ertl, Phys. Rev. Lett. **76**, 535 (1996).
4) N. Memmel and E. Bertel, Phys. Rev. Lett. **75**, 485 (1995).
5) T. Hertel and G. Moos, Phys. Rev. Lett. **84**, 5002 (2000).

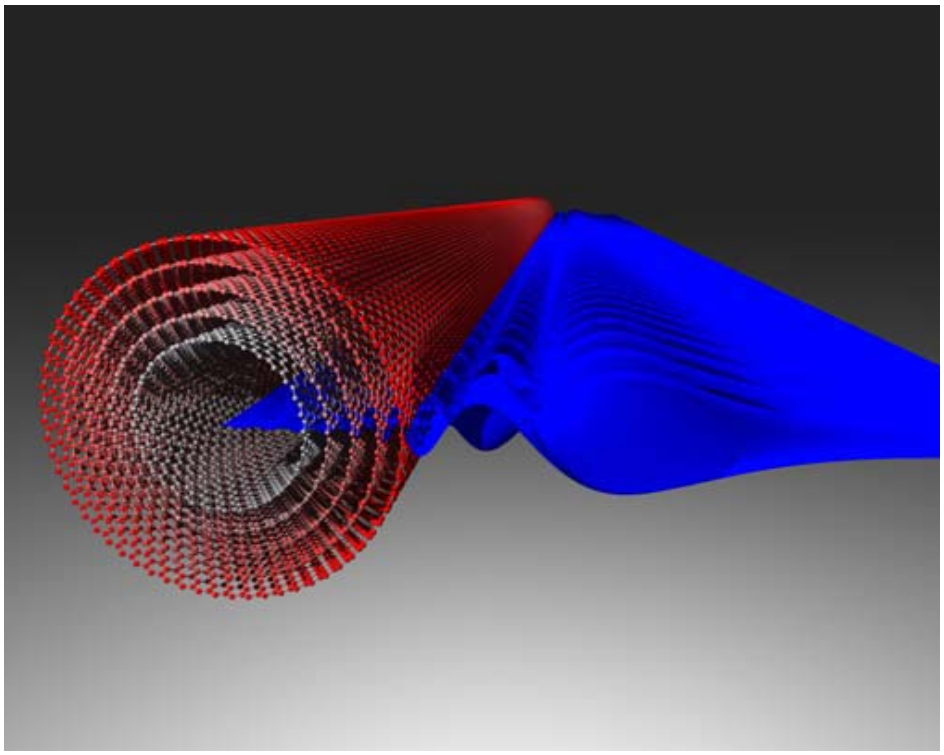

FIG. 1: "Image" electron wave function, $\psi_{n=3,l=1}(\rho)e^{ikz}$ calculated for a 5 nm MWNT. See Theory next section.

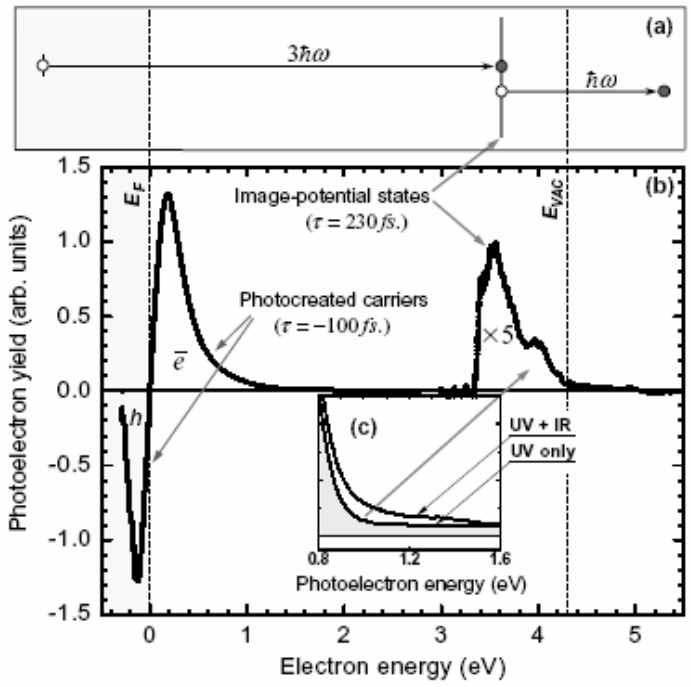

FIG. 2: (a). The energy diagram of a two–photon photoexcitation technique. In the first step, a 100 fs UV pulse (photon energy = 4.71 eV) promotes the electron population into image–potential states. A second IR pulse (photon energy =1.57eV) photoionizes these electrons and their resulting kinetic energy is measured. (b). The experimental photoelectron signal is plotted verses the electron energy relative to the Fermi level. If the IR pulse precedes the UV pulse (e.g. $\tau = -100fs$), e^--h pairs (excitons) are created in the vicinity of E_F (taken as zero of the energy scale). Image–potential states are observed just below the vacuum level for a positive delay , (e. g. $\tau =$ 230 fs). (c). The insert shows the change in the UV photoelectron signal induced by the IR probe–pulse.

Time–resolved photoexcitation of image–potential states in carbon nanotubes: Theory
(M. Zamkov, H.S. Chakraborty, A. Habib, N. Woody, U. Thumm, and P. Richard)

In support of the research reported above on the experimental observation of image potential states, we have undertaken a program to calculate the wave functions and energy spectra of image potential states for both single and multi walled carbon nanotubes. This first result of this work has been accepted for publication in Phys. Rev. and will be published in the September issue.

The existence of low angular momentum image–potential states is predicted both for single and multi walled nanotubes. The states are confined between the self–induced potential on the vacuum side and the surface barrier, created by the central ascent in the transverse nanotube potential. Effective interactions near the surface of the nanotube are modelled with a cylindrical jelliumlike surface barrier, parameterized to ensure the correct transition into the long–range image potential. Binding energies and wave functions are calculated for (12,0), (10,10), (9,0) single walled and (d = 9.48 nm) multi walled nanotubes for different values of electron angular momenta. In addition, the expected relative lifetimes were calculated for the case of zero–angular momentum states of a (10,10) SWNT. The possible formation of image–potential states in nanotube bundles is briefly discussed.

Publications:

Elastic resonant and nonresonant differential scattering of quasifree electrons from $B^{4+}(1s)$ and $B^{3+}(1s^2)$ ions E. P. Benis, T. J. M. Zouros, T. W. Gorczyca, A. D. González, and P. Richard, Phys. Rev. A **69**, 052718 (2004) *(20 pages)*

Experimental observation and theoretical calculations of triply excited $2s2p^2\ ^2S^e$, $^2,\ ^4P^e$, $^2D^e$ and $2p^3\ ^2P^o$, $^2D^o$ states of fluorine M. Zamkov, E. P. Benis, C. D. Lin, T. G. Lee, T. Morishita, P. Richard, and T. J. M. Zouros, Phys. Rev. A **67**, 050703(R) (2003). *(4 pages)*.

Isoelectronic study of triply excited Li-like states E. P. Benis, T. J. M. Zouros, T. W. Gorczyca, M. Zamkov, and P. Richard, J. Pys.B:At. Mol. Opt. Phys. **36**, L341 (2003) *(6 pages).* Letter to the Editor.

Absolute measurements and calculation of triple electron capture cross sections in fast 0.1-1.1 MeV/u C^{6+} on Ar collisions M. Zankov, E. P. Benis, P. Richard, T. G. Lee, T. J. M. Zouros, NIM in Physics Research B 205 522 (2003) *(6 pages).*

Attosecond pulses and femtosecond x-ray streak camera

Zenghu Chang
J. R. Macdonald Laboratory, Department of Physics,
Kansas State University, Manhattan, KS 66506, chang@phys.ksu.edu

The goals of this aspect of the JRML program are (1) to study attosecond x-ray sources based on high-order harmonic generation, (2) to develop a femtosecond x-ray detector for time-resolved x-ray spectroscopy at the 3rd and 4th generation x-ray sources facilities.

1. Generation of the attosoecond XUV supercontinuum by a polarization gating, *Bing Shan, Ghimire Shambhu, and Zenghu Chang*

The shortest optical pulse generated so far is around 250 attosecond pulses, which was produced by high-order harmonic generation with 5 fs linearly polarized laser pulses. For studying electron motion in atoms with high precision, it is beneficial to have even shorter single attosecond pulses. The generation of single attosecond pulse by the polarization gating of the high-order harmonic generation process has been proposed a decade ago. Recently, it has been demonstrated by the PI's group both experimentally and theoretically that a supercontinuum covering the plateau and cutoff region is generated when the driving laser pulse with a time-dependent elliptically is composed by a few cycle pulses [1, 2]. The broad spectral should support much shorter pulses than that produced with the linearly polarized laser.

High harmonic generation efficiency decreases rapidly with the ellipticity of the driving laser field [3]. The polarization gating takes the advantage of this fact. A pulse with a time-dependent ellipticity can be constructed by a left circularly polarized pulse and a delayed right circularized pulse. In the composed pulse, the polarization varies from circular to linear and then back to circular. When such a pulse is used, the oscillating electron will be driven away from the parent ion at both the head and tail parts by the transverse component of the field. This will eliminate the possibility of re-collision and recombination of the electron with the parent ion. Thus, harmonics can only be produced by the center portion of the laser pulse that is nearly linearly polarized. This portion can be made shorter than one optical cycle by using a very short input pulse so that only one reclusion occurs to emit a single isolated attosecond pulse.

Figure 1 shows the experimental setup for high-order harmonic generation using the pulse with a time-dependent ellipticity. The output beam from *Kansas Light Source* laser system was focused into a hollow-core fiber. The pulse passed through two pairs of chirp mirrors and became negatively chirped with a center wavelength at 750 nm. This chirp was compensated by a fused silica plate so that the pulse duration became tunable by adjusting the plate thickness. The pulse with a time-dependent ellipticity was then produced with a delay of 15 fs induced by a 0.5 mm quartz plate. Finally the pulse was focused by a parabolic mirror (f = 250 mm) into an argon gas jet. The pulse energy was ~

260 μJ which yielded an intensity of ~1.5×10^{14} W/cm^2 on the target for the linear portion of the pulse.

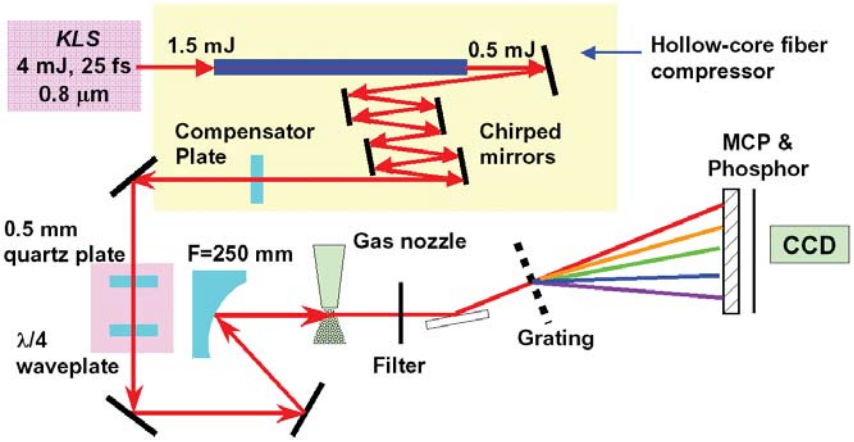

Figure 1. Production of the pulse with a time-dependent ellpticity and its application to the generation of XUV supercontinuum.

When the thickness of the fused silica fully compensated the frequency chirp, resulting in an 8 fs input pulse. The high harmonic spectrum showed a supercontinuum from 25 nm to 40 nm, corresponding to the harmonic order of 19 to 31. The spectrum is shown in Fig. 2(c). The supercontinuum yielded a single attosecond pulse with the transform limited pulse duration of 190 attoseconds as shown in Fig. 2(d). The Fourier transforms assuming flat phases. The harmonic spectrum generated by 9 fs laser pulse is shown in Fig. 2(a), The discrete spectrum resulted in three attosecond pulses with a time interval of half cycle of the driving field shown in Fig. 2(b). Fig. 2 (e)-(h) are from numerical simulations that qualitatively agree with the experiments.

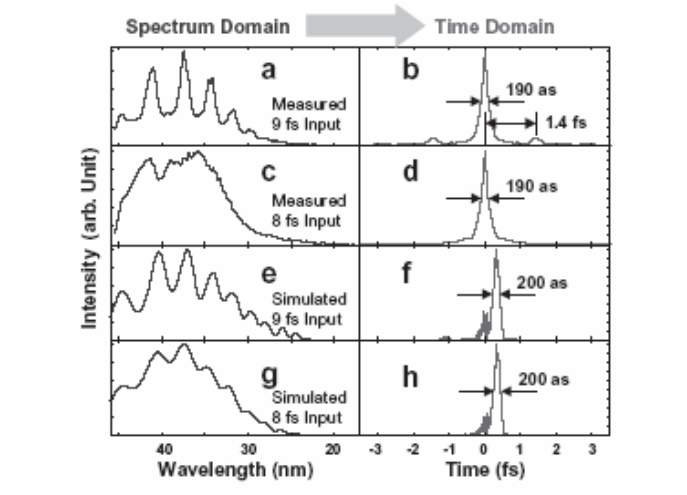

Fig. 2. The XUV supercontinuum generated by a polarization gating.

To the best of our knowledge, this is the first time that a supercontinuum was obtained by using a polarization gating. The ultrafast pulse with a time-dependent ellipticity can be used for other research that involves the re-collision process, such as the ionization of atoms and molecules in intense laser fields [4, 5].

2. An accumulative x-ray streak camera with 280 fs resolution, *Mahendra Shakya and Zenghu Chang*

The x-ray streak cameras developed by the PI's group and our collaborators [6] have been used at the *Advanced Light Source* and the *Advanced Photon Source* synchrotron facility for ultrafast time-resolved x-ray scattering and spectroscopy studies [7-9]. Since the x-ray photon number in a single pulse from the third generation x-ray sources is low, the x-ray streak camera must be operated in an accumulation mode. Recently, we improved of the camera resolution by confining the electron beam size with a variable slit in the streak tube. The new streak camera design is shown schematically in Figure 3. There is a 25 μm slit on the anode that defines the field of view of the camera. A second slit in front of the electrostatic lens is for reducing the electron beam size in the lens and in the deflection plates. We study the effect of the electron beam size in the deflection plates on the temporal resolution of the camera.

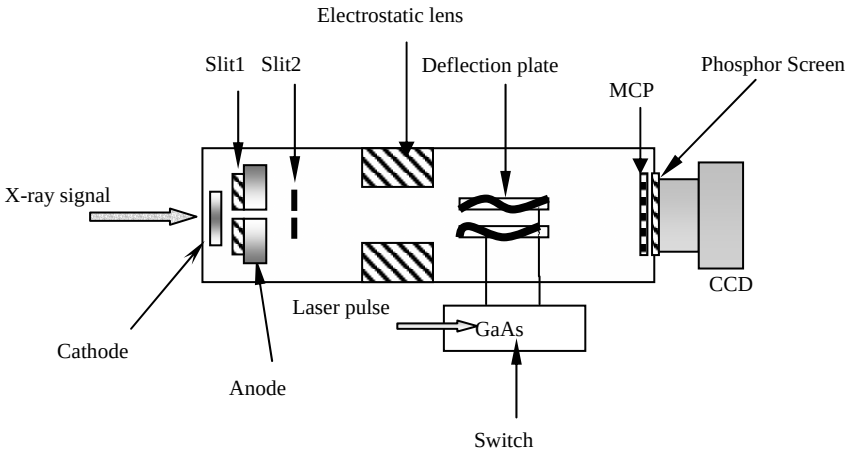

Figure 3 Schematic of the x-ray streak camera with a second slit.

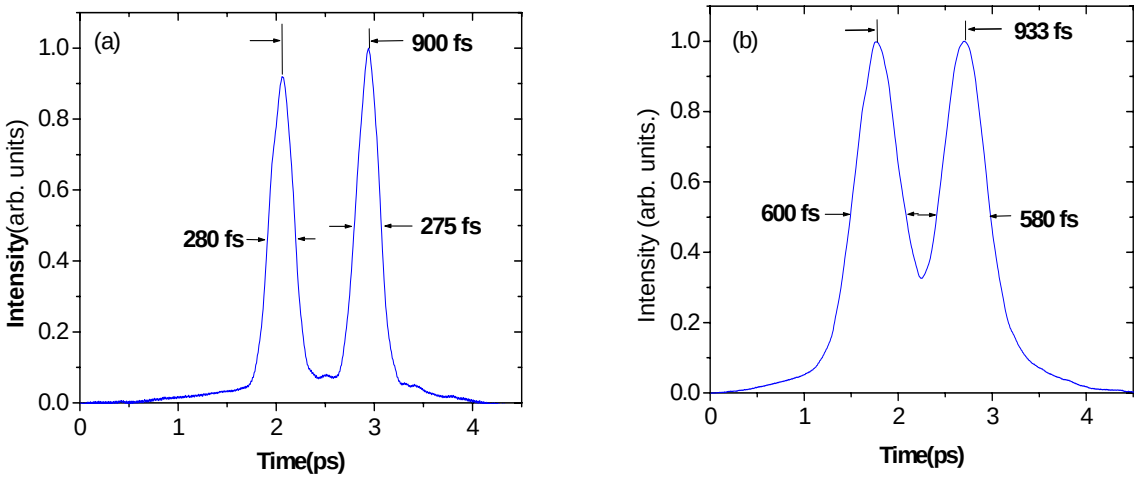

Figure 4. Measured temporal resolution: (a) with the 2nd slit, (b) without the 2nd slit.

Theoretically the temporal resolution can be improved by reducing the size of the electron beam in the defection plates. The effect of the beam size, *d*, on the temporal resolution can be estimated by,

$$\Delta t_d = d\alpha / v_a \quad (1)$$

where α is the maximum deflection angle in radian and v_a is the average electron axial velocity. The measured temporal resolution is 280 fs as shown in Figure 4(a) when a 5 μm second slit was used. The result without the slit is shown in Figure 4(b). It is clear that reducing the electron beam size is effective way to obtain high-temporal resolution.

To the best of our knowledge, the 280 fs is the best resolution ever achieved with a camera operating at the accumulation mode. X-ray cameras with such a high resolution will not only push the research at the third generation facility to a femtosecond level, but will also impact the development and applications of the fourth generation x-ray sources.

PUBLICATIONS

1. Bing Shan, Shambhu Ghimire, and Zenghu Chang, *"Generation of attosoecond XUV supercontinuum by polarization gating,"* Journal of Modern Optics, accepted (2004).
2. Zenghu Chang, *"Single attosecond pulse and xuv supercontinuum in the high-order harmonic plateau,"* Phys. Rev. A, accepted (2004).
3. Bing Shan, Shambhu Ghimire, and Zenghu Chang, *"The effect of orbital symmetry on high-order harmonic generation from molecules,"* Phys. Rev. A. **69**, 021404(R) (2004).
4. E. P. Benis, J. F. Xia, X. M. Tong, M. Faheem, M. Zamkov, B. Shan, P. Richard, and Z. Chang, *"Ionization suppression of Cl_2 molecules in intense laser fields,"* Phys. Rev. A, accepted (2004).
5. A.S. Alnaser, S. Voss, X.-M. Tong, C.M. Maharjan, P. Ranitovic, B. Ulrich, T.Osipov, B. Shan, Z. Chang and C. L. Cocke, *"Effects of molecular structure on ion disintegration patterns in ionization of O_2 and N_2 by short laser pulses,"* Phys. Rev. Lett., accepted (2004).
6. Jinyuan Liu, Jin Wang, Bing Shan, Chun Wang, Zenghu Chang, *"An accumulative x-ray streak camera with sub-600 fs temporal resolution and 50 fs timing jitter,"* Appl. Phys. Lett., **82**, 3553 (2003).
7. M. F. DeCamp, D. A. Reis, A. Cavalieri, P. H. Bucksbaum, R. Clarke, R. Merlin, E.M. Dufresne, and D. A. Arms, A. Lindenberg and A. Macphee, Z. Chang, J. S. Wark and B. Lings**,** *"Transient Strain Driven by a Dense Electron-Hole Plasma,"* Phys. Rev. Lett. **91**, 165502 (2003).
8. S. L. Johnson, P. A. Heimann, A. M. Lindenberg, H. O. Jeschke, M. E. Garcia, Z. Chang, R.W. Lee, J. J. Rehr, and R. W. Falcone, *"Properties of liquid silicon observed by time-resolved x-ray absorption spectroscopy,"* Phys. Rev. Lett. **91**, 157403 (2003).
9. A. M. Lindenberg, I. Kang, S. L. Johnson, R. W. Falcone, P. A. Heimann, Z. Chang, R. W. Lee, J. S. Wark, *"Coherent control of phonons probed by time-resolved x-ray diffraction,"* Optics Letters **27**, 869 (2002).

MOTRIMS Experiments at Kansas State University

B. D. DePaola, 116 Cardwell Hall, Kansas State University; Manhattan, KS 66506; depaola@phys.ksu.edu

A novel methodology for the study of a variety of AMO processes has been developed over the past few years. Combining two mature technologies, magneto optical traps (MOT) and recoil ion momentum spectroscopy (RIMS), MOTRIMS was implemented to improve upon the well-established COLTRIMS technique, both in resolution by decreasing target temperature, and in extending the target species by using targets that are readily laser-excited. In the initial experiments charge transfer cross sections, involving keV-range singly charged projectile ions were measured. It was soon realized, however, that unforeseen benefits of the MOTRIMS methodology included the capability of measuring relative excited state fractions in the target species, here, Rb. Experiments carried out in the past year include charge transfer cross section measurements; extensive studies of coherent excitation of the 5s-5p-4d ladder system in Rb using the so-called STIRAP (stimulated Raman adiabatic passage) protocol; and measurement of relative cross sections for ion formation in MOTs due to Penning and associative ionization. A side benefit of the basic TRIMS apparatus was that, if operated in position-imaging (rather than the usual momentum-imaging) mode, detailed measurements of above-threshold ionization could be made. In the remainder of this abstract, each of these projects will be described, with particular emphasis on the STIRAP studies.

Charge transfer cross section measurements

Single electron transfer in ion-atom collisions is an old field in AMO physics. Particularly in the case of singly charged projectile ions, the process seems to be well understood. Nevertheless, only in a very few systems have measurements been made that are differential in projectile scattering angle, initial state (n and l) and final state (n' and l') for a range of initial states, and with great precision in scattering angle. MOTRIMS has shown itself to be an ideal vehicle for this type of collision study. As in all TRIMS variants, the momentum vector of the recoiling target ion is measured event by event. Through conservation of energy and momentum, this directly yields the relative cross section as a function of scattering angle for each charge transfer channel. In general, the number of counts in a particular transfer channel is proportional to the product of the cross section for that channel's process and the relative number of atoms or molecules in the initial state of that channel. One can show that by switching on and off the production of the initial state, that this product can be separated into its constituent multiplicands. Thus, both the relative cross sections of the different entrance (and exit) channels *and* the relative populations of the initial states can be measured.

In the case of the KSU MOTRIMS experiments, scattering angle is measured with a resolution of about 25 microradians, and the target was in a mixture of ground Rb($5s_{1/2}$) state, first excited Rb($5p_{3/2}$) state, and Rb($4d_{5/2}$) state. Relative cross sections were measured for a variety of singly charged projectiles over a range of collision energies. Through a variety of innovative experimental and analytical manipulations, differential cross sections were measured even for channels having energy degenerate Q-values.

Penning and associative ionization cross sections in magneto optical traps

It has been established that the having excited atoms a MOT can result in trap loss due to ionization, though the actual ionization mechanism was never established. In experiments carried out at KSU, atoms in a ^{87}Rb MOT were stepwise excited from Rb($5s_{1/2}$) to Rb($5p_{3/2}$) using a cw laser designated as "L1", and then to Rb($4d_{5/2}$) using a pulsed laser designated as "L2". Note that in this case, a single photon from either L1 or L2 is energetically insufficient to photoionize Rb($4d_{5/2}$). Using the electric field of the recoil spectrometer, ions produced in the MOT were extracted and detected on the position sensitive detector of the spectrometer. When measured as a function of time with respect to the pulse of light from L2, the ions were separated into two mass peaks corresponding to Rb^+ and Rb_2^+. Neglecting higher order photon excitation processes, the only collision mechanisms by which these product ions could be produced are:

Penning ionization: $Rb(4d) + Rb(4d) \rightarrow Rb^+ + e^- + Rb(5s)$

Assoc. Ionization: $Rb(4d) + Rb(4d) \rightarrow Rb_2^+ + e^-$
$Rb(4d) + Rb(4p) \rightarrow Rb_2^+ + e^-$

Note that Penning ionization for Rb(5p) + Rb(4d) in not energetically possible. The "rate equations" corresponding to these reactions are:

$$C_M \propto \sigma_{dd}^M n_d^2$$

$$C_D \propto \sigma_{dd}^D n_d^2 + \sigma_{pd}^D n_p n_d ,$$

where the constant of proportionality is the same for these two equations. The superscripts *M* and *D* refer to collisions resulting in monomer and dimer ions, respectively; the *C*'s are the count rates in the monomer and dimer ion peaks; the subscripts *dd* and *pd* refer to 4d-4d and 5p-4d collisions, respectively; the *n*'s are the populations of the Rb(4d) and Rb(5p) states; and the σ's are the cross sections indicated by their super- and subscripts. Taking the ratio of these rate equations gives

$$\frac{C_D}{C_M} = \frac{\sigma_{dd}^D}{\sigma_{dd}^M} + \frac{\sigma_{pd}^D}{\sigma_{dd}^M}\frac{n_p}{n_d} .$$

Then, by plotting the ratio of dimer to monomer ion yields as a function of n_p/n_d, which is measured using charge transfer to Na^+ ions, one should obtain a straight line. The y-intercept of this line is $\sigma_{dd}^D / \sigma_{dd}^M$, while the slope is $\sigma_{pd}^D / \sigma_{dd}^M$. The ratio n_p/n_d is varied by changing the detuning of L2, while keeping its intensity a constant. These experiments are in progress at the time of this writing.

Above-threshold ionization measurements

A persistent problem in the measurement of above-threshold ionization rates is that the finite target size implies that the rates have been integrated over some range of laser intensity. Because the ionization rate is, in general, a non-linear function of intensity, some systematic error could be associated with such measurements. Some groups have tried to reduce this effect by making measurements which were differential in 1 or 2

dimensions. Using the basic TRIMS apparatus, we have demonstrated proof-of-principle for measurements of above-threshold ionization rates as a function of position in 3 dimensions, and therefore, as a function of laser intensity. This was accomplished by changing the potentials on the recoil spectrometer such that position, instead of momentum was imaged. In effect, the spectrometer was converted into an electrostatic lens having a measured magnification of approximately 5×. The third dimension was given by the flight time of the recoil ions. Results of proof-of-principle experiments indicated that for best spatial resolution, the target must be cold. This could be done in a magneto-optical trap, but could, perhaps, be better accomplished through the use of a conventional supersonic expansion.

Charge Transfer as a Probe of Population Dynamics during Coherent Excitation

Coherent excitation techniques are of ever increasing importance in a variety of sub-fields in physics. Two diverse examples include studies in quantum degenerate gasses, and implementations of excitation schemes of potential importance in quantum information and computation. An example of one particular coherent excitation process is STIRAP (stimulated Raman adiabatic passage). Through the use of STIRAP on an idealized 3-level ladder system in which spontaneous emission is neglected, for example, it is theoretically possible to move 100% of the system's population, initially in the ground state, into the highest excited state, with no population at any time appearing in the intermediate state. In realistic implementations, in which spontaneous emission is not neglected, it is still theoretically possible to place a very large fraction of the population into the highest excited state. In the system under study here, the lowest level is $^{87}Rb(5s_{1/2}, F = 2)$; the intermediate state is $^{87}Rb(5p_{3/2}, F = 3)$; and the highest excited state is $^{87}Rb(4d_{5/2}, F =4)$. For this system theory predicts that under proper conditions more than 80% of the population can be placed in the 4d state. Unlike n-photon pi-pulses, STIRAP is relatively insensitive to laser intensity (or, more correctly, Rabi frequency). Thus, unlike other efficient excitation protocols, STIRAP shows great promise for a great variety of applications.

By now, quite a few groups have studied STIRAP. However in none of those studies was it possible to simultaneously measure the populations of all the relevant states as they developed in time. Furthermore, the time resolution in the evolution of the state under measurement has been limited by either the lifetime of that state and/or the lifetime of the state which that state decayed to. By contrast, in the work presented here the populations of all three levels are measured on the few nanosecond time scale. This new capability allows one to compare theory with experiment, differentially in time. In the work discussed here, studies are focused on the population dynamics of coherent excitation under adiabatic conditions (essential for STIRAP). These are contrasted with the measured population dynamics for the same system undergoing coherent excitation under non-adiabatic conditions.

In the STIRAP studies carried out at KSU, MOTRIMS is used as the tool by which the population dynamics are measured. In this application, a beam of 7 keV Na^+ ions is directed onto a target of cold ^{87}Rb while the Rb is being coherently excited using the

STIRAP protocol. Charge transfer is thus continuously taking place in the interaction region. One is thus able to obtain a spectrum of the Q-value, or energy defect, of the collision. Because relative capture cross sections from the various initial states in Rb to various final states in Na have been measured, the Q-value spectrum gives a direct measurement of the relative populations of all the Rb levels. By plotting the Q-value spectrum as a function of time, with respect to the pulsed coherent excitation sequence, one can directly measure the development of these relative populations as a function of time.

The present temporal resolution of the technique is about 2 nsec, and is limited by the energy spread of the ion beam ($\Delta E/E$ = 1 eV/ 7 keV). The focus of these studies was on the time evolution of coherent excitation through STIRAP, but the methodology is far more general in application. Future studies will include measurement of population dynamics in coherent 3-photon excitation to Rydberg states of Rb, that is, the excitation sequence Rb(5s) → Rb(5p) → Rb(4d) → Rb(nf). This system is of current interest due to possible applications in quantum information and cold plasma formation. Other applications could include the study of 3-body collisions in BECs. Using MOTRIMS as a diagnostic could prove invaluable in efforts to measure these and other processes.

Recent Publications

"Recoil ion momentum spectroscopy using magneto-optically trapped atoms", H. Nguyen, X. Fléchard, R. Brédy, H. A. Camp, and B. D. DePaola, Rev. Sci. Instrum. **75,** 2638 (2004).

"Measurement of the interaction strength in a Bose-Fermi mixture ^{87}Rb and ^{40}K", J. Goldwin, S. Inouye, M. L. Olsen, B. D. DePaola, and D. S. Jin, Phys. Rev. A **70**, 021601 (2004).

"State selective charge transfer cross sections for Na^+ with excited rubidium: A unique diagnostic of the population dynamics of a magneto-optical trap", X. Fléchard, H. Nguyen, R. Brédy, S. R. Lundeen, M. Stauffer, H. A. Camp, C. W. Fehrenbach, and B. D. DePaola **91**, Phys. Rev. Lett. 243005 (2003).

"MOTRIMS as a generalized probe of AMO processes", R. Brédy, H. Nguyen, H. Camp, X. Fléchard, and B. D. DePaola, Nucl. Instrum. Meth. B **205**, 191 (2003).

"Differential charge transfer cross sections for systems with energetically degenerate channels", H. Nguyen, R. Brédy, H. A. Camp, T. Awata, and B. D. DePaola, Phys. Rev. A (accepted).

"Three-dimensional spatial imaging in above-threshold ionization rate measurements", R. Bredy, H. A. Camp, H. Nguyen, T. Awata, B. Shan, Z. Chang, and B. D. DePaola, J. Opt. Soc. Am. B (accepted).

Abstract submitted by Igor Litvinyuk
J.R. Macdonald Laboratory, Kansas State University

1. Laser Coulomb explosion imaging of small molecules[1]

Intense, few-cycle laser pulses can ionize a molecule so rapidly that atomic motion is approximately frozen by inertia until ionization is complete. If many electrons have been stripped from the molecule, it will Coulomb-explode. We measure the correlated momenta of exploded fragments to reconstruct the original molecular structure of D_2O and SO_2. In both cases we show that the measured structure approaches the ground state structure of the neutral molecule. We simulate the Coulomb explosion of D_2O by using an atomic tunnelling model to describe ionization, and classical mechanics to describe the motion of the fragments. When used in combination with a pump pulse, Coulomb explosion imaging will permit the 3-D structural dynamics of any small molecule to be traced.

2. Laser-Induced Interference, Focusing, and Diffraction of Rescattering Molecular Photoelectrons[2]

We solve the time-dependent Schrödinger equation in three dimensions for H_2^+ in a one-cycle laser pulse of moderate intensity. We consider fixed nuclear positions and Coulomb electron-nuclear interaction potentials. We analyze the field-induced electron interference and diffraction patterns. To extract the ionization dynamics we subtract the excitations to all significant low-lying bound states explicitly. In the simulation we follow the time evolution of well-defined wavepacket, that is formed near the first peak of the laser field. We observe the subsequent fragmentation of the wavepacket due to molecular focusing. We show how to retrieve diffraction molecular image by taking the ratio of the momentum distributions in the two perpendicular directions. Even at moderate laser intensities, the position of the diffraction peaks is well described by the classical slit diffraction rule.

3. Shake-up excitation during intense field tunnel ionization[3]

"Shake-off" and "shake-up" play an important role in the X-ray double ionization of atoms. The first electron is ionized by absorbing an X-ray photon and shakes up a second electron on its way out. We investigate shake-up in the opposite, low frequency, strong field limit, both theoretically and experimentally. Theoretically, a complete analytical theory of shake-up in intense laser fields is developed. We predict that shake-up produces one excited σ_u D_2^+ state in 10^5 ionization events. Shake-up is measured experimentally by using the molecular clock provided by the internuclear motion. The number of measured events is found to be in excellent agreement with theory.

4. Imaging ultra-fast molecular dynamics using laser Coulomb explosion[4]

We demonstrate a novel technique for direct imaging of ultrafast molecular dynamics. The technique is based on pump-probe approach employing few-cycle (8 fs) laser pulses. The technique is applied to directly map nuclear motion in vibrating D_2^+ and dissociating SO_2^{2+}/SO_2^{3+} molecules. In each case, the dynamics is launched by ionizing a neutral molecule with the pump pulse. The time-dependent molecular structure is then interrogated with a delayed probe pulse by analysing the momenta of the Coulomb explosion fragments. The method traces atomic motion with 5 fs time resolution.

References

1. F. Légaré, Kevin F. Lee, I.V. Litvinyuk, P.W. Dooley, S.S. Wesolowski, P.R. Bunker, P. Dombi, F. Krausz, A.D. Bandrauk, D.M. Villeneuve, P.B. Corkum, *Submitted to PRL*

2. S. N. Yurchenko, S. Patchkovskii, I. V. Litvinyuk, P. B. Corkum, and G. L.Yudin, *Submitted to PRL*

3. I. Litvinyuk, F. Legare, P. W. Dooley, D. M. Villeneuve, P. B.Corkum, J. Zanghellini, A. Pegarkov, C. Fabian, and T. Brabec, *Submitted to PRL*

4. F. Légaré, K.F. Lee, I.V. Litvinyuk, P.W. Dooley, A.D. Bandrauk, D.M. Villeneuve, P.B. Corkum, *Manuscript in preparation*

Time-dependent Treatment of Three-body Systems in Intense Laser Fields

B.D. Esry
J. R. Macdonald Laboratory, Kansas State University, Manhattan, KS 66506
esry@phys.ksu.edu
http://www.phys.ksu.edu/ esry

Program Scope

The primary goal of this program is to understand the behavior of H_2^+ in an intense laser field. Because the system is so complex, past theoretical descriptions have artificially reduced the dimensionality of the problem or excluded one — or more — important physical processes such as electronic excitation, ionization, vibration, or rotation. One component of this work is thus to systematically include these processes in three-dimensions and gauge their importance based on actual calculations. Further, as laser pulses get shorter and more intense, approaches that have proven useful in the past may become less so. A second component of this program is thus to develop novel analytical and numerical tools to describe H_2^+. The ultimate goal is to understand the dynamics of these strongly coupled systems in quantum mechanical terms.

Carrier-envelope phase difference dependence of HD^+ and H_2^+ dissociation

V. Roudnev, I. Ben-Itzhak, B.D. Esry

Recent progress

Our first effort to calculate the response of H_2^+ to an intense laser field actually involved the isotope HD^+. For this molecule, the dissociation channels are easily distinguished, making the final state analysis simpler. We first solve the time-dependent Schrödinger equation with a two-dimensional model (both nuclear and electronic motion restricted to be along the direction of laser polarization) with soft-core Coulomb potentials, but soon found that the amount of ionization predicted was in complete disagreement with experiment no matter how we softened the Coulomb singularity. In particular, the two-dimensional model predicted nearly 100% ionization where experiment only saw a few percent. We thus began a series of calculations using a three-dimensional model that required no softening of the Coulomb potential. This model still restricted the nuclei to move only along the direction of laser polarization, but allowed the electron two degrees of freedom (the azimuthal angle about the molecular axis can be eliminated by symmetry).

We solved the time-dependent Schrödinger equation by discretizing the spatial degrees of freedom with finite differences. Our implementation allowed us, however, to treat non-Cartesian coordinates with nonuniform grids while maintaining the symmetry of the Hamiltonian. The time evolution was accomplished through a combination of split operator techniques and Crank-Nicolson propagation. We also took advantage of the mass difference between the nuclei and electron by using larger time steps for the nuclear propagation than for the electronic propagation. This trick let us shave about 25% off the CPU time.

While we set out to do calculations for laser parameters comparable to those used by I. Ben-Itzhak's experimental group, the three-dimensional calculations proved too time-consuming, forcing us to consider shorter — but still achievable — laser pulses of 10 fs duration. At 10 fs, however, the phase difference between the carrier wave and the modulating pulse envelope becomes important. Other groups have identified the impact of this difference on atomic and molecular ionization, but no one had yet seen an effect for the neutral dissociation channels of H_2^+ or its isotopes.

Figure 1 shows the results of our three-dimensional model calculations for four different peak intensities. They show a rather strong dependence of the dissociation probabilities on the carrier-envelope phase difference (CEPD) ϕ, growing to more than a factor of two for each of the three highest intensities. Moreover, the phase dependence is similar enough for each of the intensities to give some hope that it will survive averaging the intensity over the focal volume of the laser.

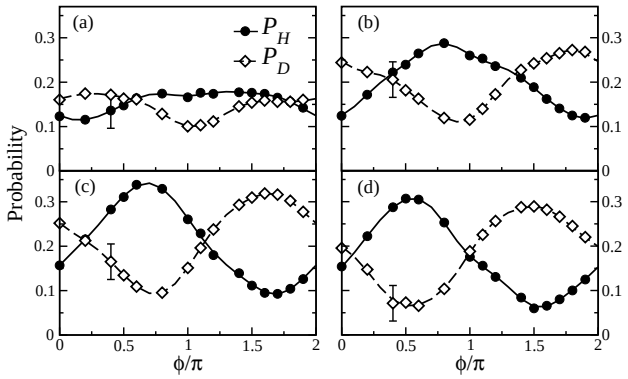

Figure 1: Phase dependence of the HD^+ dissociation probabilities to H+d (solid lines) and to p+D (dashed lines) for different intensities: I= (a) 6.0, (b) 7.0, (c) 8.0, and (d) 9.0 in units of 10^{14} W/cm^2. The error bars indicate our estimated numerical error and are the same for each point in each plot. (Adapted from Ref. [6].)

To show that the CEPD dependence of the dissociation probability is not a product of the permanent dipole of HD^+ or of the mass difference, we also carried out the calculation for H_2^+. The results are shown in Fig. 2. The two channels are not distinguished by their mass now, but rather by their direction in space. The probability to observe a neutral at 0° or 180° relative to the laser polarization does indeed show a CEPD dependence, although not as strong as for HD^+.

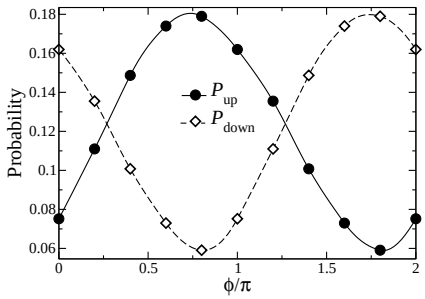

Figure 2: Phase dependence of the H_2^+ dissociation probabilities to H at 0° (solid lines) and to H at 180° (dashed lines) for I=9 10^{14} W/cm^2. (Adapted from Ref. [6].)

Future plans

Our calculations to date have used a simple method to solve the time-dependent Schrödinger equation and was relatively inefficient. We are in the process of applying coordinate scaling methods which make the calculation much more numerically stable and accurate. We will also look for better spatial representations to reduce the computational burden. With a more efficient code, we can more easily explore the CEPD effects by initial vibrational state, eventually combining the results according to the Franck-Condon factors from the H_2 ground state. Several intensities can

also be calculated so that an intensity average can be performed to give a realistic comparison with experiment. More differential information, such as the kinetic energy distribution, will also be calculated.

H_2^+ in an intense laser field via coupled Born-Oppenheimer channels

in collaboration with I. Ben-Itzhak's group

Recent progress

I have begun solving the time-dependent Schrödinger equation for H_2^+ using the Born-Oppenheimer representation. This approach amounts to propagating the nuclear motion on one-dimensional potentials coupled by the electronic dipole matrix elements. For intensities below roughly 5 10^{13} W/cm^2, the lowest two channels, $1s\sigma_g$ and $2p\sigma_u$, are sufficient to obtain converged results. For higher intensities, more channels are rapidly required for convergence. I have calculated all of the relevant potentials and dipole matrix elements up to and including the n=3 manifold of H, yielding acceptable accuracies for intensities up to a little above 10^{14} W/cm^2. At greater intensities, ionization — which is beyond this model — becomes an important channel.

Motivated by the recent experimental results from I. Ben-Itzhak's group and by discussions with them, I performed the calculations over a range of intensities from 8 10^9 W/cm^2 to 1 10^{14} W/cm^2 for each of the 20 vibrational states of H_2^+. The laser pulse length was 50 fs full-width at the $1/e$ point with a wavelength of 790 nm. While the experiments used H_2^+ as a target rather than H_2, the ion source produced a Franck-Condon distribution of vibrational states. To compare with experiment, then, the results from individual vibrational states had to be combined with Franck-Condon weights. The kinetic energy release (KER) of the total dissociation probabilities thus obtained are shown in lefthand pair of plots in Fig. 3 as a function of intensity.

Notice that the onset of dissociation is linear in $\sqrt{I}$ for low KER (the intensity scale is a square root scale). This behavior is thus consistent with dissociation proceeding by going over a barrier whose height is determined by the field. At low intensities, there are distinct peaks that can be almost perfectly connected to individual vibrational states. As the intensity increases, however, the labeling of peaks in the KER spectrum with vibrational quantum numbers becomes increasingly difficult. Instead, one sees rather broad distributions localized near zero KER and near the two-photon energy.

The righthand side of Fig. 3 shows the result of averaging over intensity at the laser focus. It is clear that intensity averaging has a huge effect on the KER. The low intensity peaks dominate even to high intensity with a low-energy shoulder developing at the highest intensities. The two-photon peaks, so clear in the lefthand plots, are difficult to distinguish.

Future plans

This work is just beginning and there remains considerable analysis of the results to extract the physics. Longer pulses will be investigated along with the dependence on the angle between the laser polarization and molecular axis. At each point, comparison with the results from I. Ben-Itzhak's group will be sought.

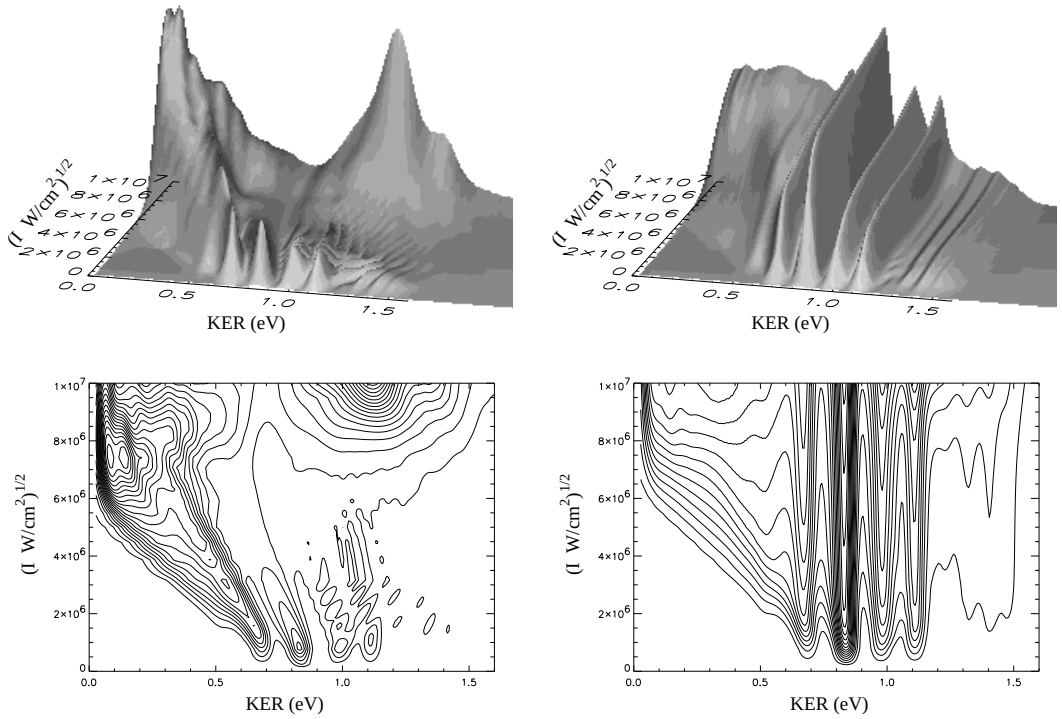

Figure 3: Total dissociation probabilities kinetic energy release starting from a Franck-Condon distribution of vibrational states of H_2^+. The lefthand pair show the results *without* intensity averaging while the righthand pair show the intensity averaged results.

Publications

6. "Controlling HD^+ and H_2^+ dissociation with the carrier-envelope phase difference of an intense ultrashort laser pulse," V. Roudnev, B.D. Esry, and I. Ben-Itzhak, Phys. Rev. Lett. (accepted) (2004).

5. "Localized component method: application to scattering in a system of three atoms," V. Roudnev, Proceedings of the Seventeenth International IUPAP Conference on Few-Body Problems in Physics, Elsevier (2004), p. S292.

4. "Split diabatic representation," B.D. Esry and H.R. Sadeghpour, Phys. Rev. A **68**, 042706 (2003).

3. "Hyperspherical close coupling calculations for charge transfer cross sections in He^{2+}+H($1s$) collisions at low energies," C.N. Liu, A.T. Le, T. Morishita, B.D. Esry and C.D. Lin, Phys. Rev. A **67**, 052705 (2003).

2. "Ultraslow $\bar{p}$-H collisions in hyperspherical coordinates: Hydrogen and protonium channels," B.D. Esry and H.R. Sadeghpour, Phys. Rev. A **67**, 012704 (2003).

1. "Boundary-free scaling calculation of the time-dependent Schrödinger equation for laser-atom interactions," Z.X. Zhao, B.D. Esry and C.D. Lin, Phys. Rev. A **65**, 023402 (2002).

Interactions of Ions and Photons with Surfaces, and Molecules

Uwe Thumm
J.R. Macdonald Laboratory, Kansas State University, Manhattan, KS 66506
thumm@phys.ksu.edu

1. Laser-assisted collisions (with Thomas Niederhausen)

Project scope: This project seeks to develop numerical and analytical tools to efficiently predict the effects of a strong laser field on the dynamics of electron capture and emission in ion-atom collisions. In particular, we are interested in calculating and understanding the probabilities for electron transfer, emission, and loss in the elementary three-body laser-assisted collision system of slow protons colliding with atomic hydrogen as a function of both, collision and laser parameters. These investigations may motivate and assist in the planing of future challenging experiments with crossed laser and particle beams. In the long run, our studies may contribute to the improved control of chemical reactions with intense laser light.

Recent progress: We investigated the effects of a strong 1064nm laser field on electron capture and emission in slow (keV) proton-hydrogen collisions within a reduced dimensionality model of the scattering system in which both, the motion of the active electron and the laser electric field vector are confined to the scattering plane (Fig.1).

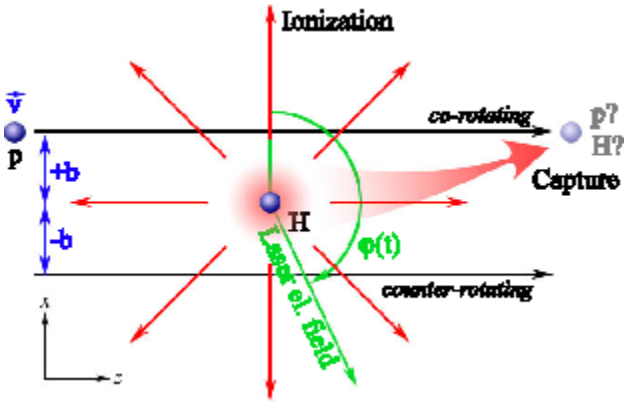

Fig.1. *Collision scenario for a proton on a straight-line trajectory with impact parameter b and velocity v colliding with an atomic hydrogen target. The rotating laser electric field breaks the azimuthal symmetry: For positive impact parameters, the projectile follows the rotating laser field ("co-rotating" case); for negative impact parameters, the projectile moves against the rotating electric field ("counter-rotating" case).*

By solving the time-dependent Schrödinger equation on a two-dimensional numerical grid, we examined the probabilities for electron capture and ionization as a function of the laser intensity, the projectile impact parameter b, and the laser phase Φ that determines the orientation of the laser electric field with respect to the internuclear axis at the time of closest approach between target and projectile. Our results for the b-dependent ionization and capture probabilities show a strong dependence on both Φ and the helicity of the circularly polarized laser light. For intensities above 2×10^{12} W/cm^2 our model predicts a noticeable circular dichroism in the capture probability for slow proton-

hydrogen collisions. Interestingly, this dichroism persists after averaging over Φ. Capture and electron emission probabilities defer significantly from results for laser-unassisted collisions. Furthermore, we find evidence for a charge resonance enhanced ionization mechanism that may enable the measurement of the absolute laser phase Φ [1].

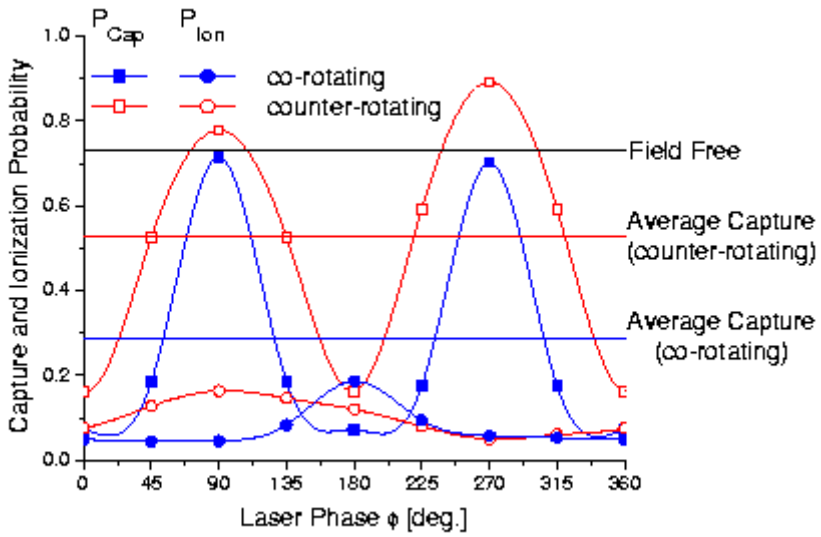

Fig.2. *Capture and ionization probability as a function of the laser phase for 1 keV p-H collisions at b=±4 a.u. The laser intensity is 5x10^{13} W/cm^2. Phase-averaged results for the capture probability differ significantly for co- and counter-rotating collisions.*

The presence of the laser radiation during the collision process results in an additional dependence of the electronic dynamics on the laser phase Φ at the time of closest approach. For a fixed impact parameter, b=±4, and a laser intensity of *5x10^{13} W/cm^2,* the capture probability as a function of Φ shows large amplitude oscillations and differs from the field-free results most strikingly at Φ = 0° and 180° (Fig.2). It displays a strong dichroism effect, i.e., a substantial difference in the electron capture probability for positive and negative impact parameters, or, equivalently, for co-rotating as compared to counter-rotating collisions. Ionization probabilities depend less sensitively on Φ, and their phase averages differ much less for co- and counter-rotating collisions than the phase-averaged capture probabilities. The difference in the capture cross sections for co- and counter rotating collisions, σ_{cap}^{+} and σ_{cap}^{-}, amounts to up to 40 % at a laser intensity of 5x10^{13} W/cm^2 (Fig.3). We consider these differences as upper limits for the dichroism effect and expect them to decrease slightly in full three-dimensional calculations.

Future plans: (i) Laser pulses with lengths of a few nano-seconds and intensities of about 10^{12} W/cm^2 and higher should allow for the experimental verification of the predicted dichroism in the capture probability. We intend to improve the accuracy of our calculation in full (3D) calculations. **(ii)** We found evidence for a charge resonant enhanced ionization (CREI) mechanism in laser-assisted ionization [1]. In conjunction with phase-locked lasers, this effect may be used in angle-differential laser-assisted collision experiments to select a specific orientation of the laser electric field at the time of closest approach between projectile and target. We plan to investigate this effect for various collision systems and parameters.

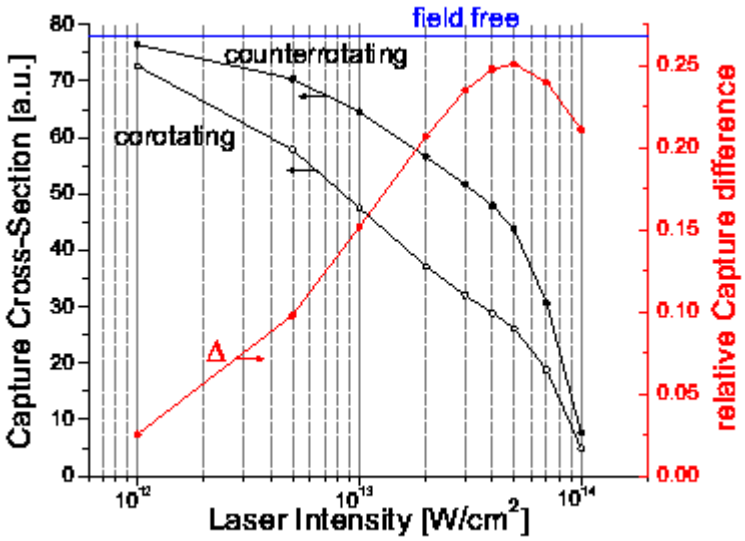

Fig.3. *Total electron capture cross-sections as a function of the laser intensity for co- and counter-rotating collisions. The relative difference* $\Delta = | \sigma_{cap}^{+} - \sigma_{cap}^{-} | / (\sigma_{cap}^{+} + \sigma_{cap}^{-})$ *is largest at a laser intensity of* 5×10^{13} W/cm^2 .

2. Surface-morphology effects in the neutralization of negative hydrogen ions near silver surfaces (with Himadri Chakraborty)

Project scope: The goal of this project is to study in detail the resonant transfer of a single electron, initially bound to the projectile, during the reflection of a slow incoming ion or atom on a metal surface. Apart from contributing to the qualitative understanding of the interaction mechanisms through computer animations, this project contributes to the quantitative assessment of charge transfer and wave function hybridization in terms of level shifts, decay widths, and ion-neutralization probabilities. In the long run, it may improve our understanding of surface chemical reactions, catalysis, and diagnostics.

Recent progress: We compared the resonant neutralization of hydrogen anions in front of plane Ag surfaces of symmetries (100) and (111) using the Crank-Nicholson wave-packet propagation method [2]. The Ag(100) surface binds a the surface state that is degenerate with the valence band and rapidly decays while being populated by the ion. For Ag(111), in contrast, the population of a quasi-local Shockley surface state inside the projected L-band gap impedes the electron decay into the bulk along the direction normal to the surface. This difference in the decay pattern strongly affects the survival of 1 keV ions scattered from these surfaces (Fig.4), and scattering off the Ag(111) surface results in about an order of magnitude higher ion-survival probabilities as compared to that off Ag(100). Our results for Ag(111) show good agreement with the measurements by Guillemot and Esaulov [Phys.Rev.Letts. **82**, 4552 (1999)].

The anion-survival for the (111) surface is much higher since, on the time scale of the ion-surface interaction, the surface state retains electrons and enables their recapture by the ion. Except for grazing incidences, at $\theta > 10^{0}$, our calculations agree with measured reflected ion fractions.

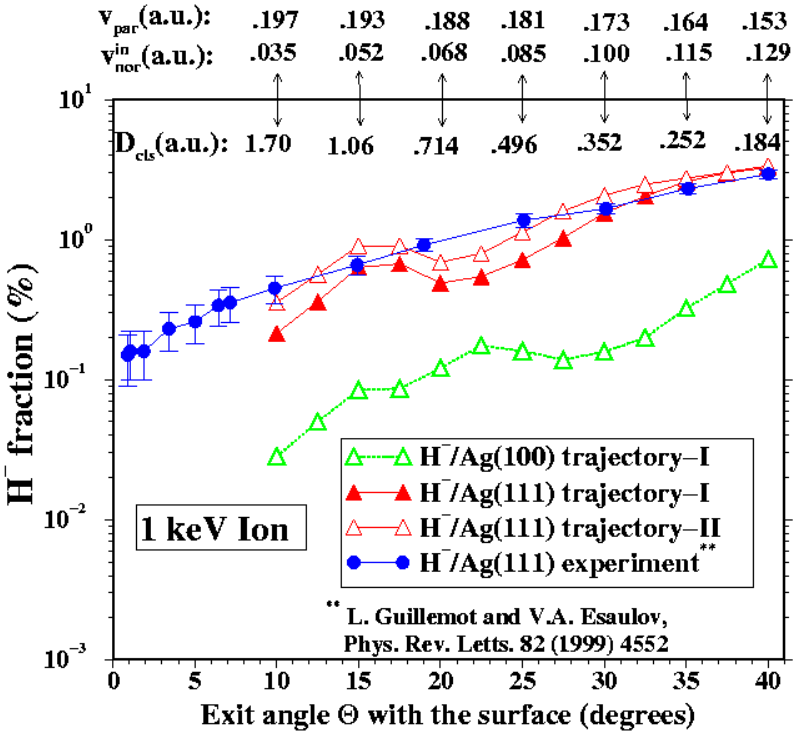

Fig.4: *Survival probability of H^- scattered from Ag(100) and Ag(111) surfaces as a function of the exit angle with respect to the surface plane. Initial normal velocities v_{nor}^{in}, parallel velocities v_{par}, and distances of closest approach D_{cls} are given along the upper x-axis. For details of the model projectile trajectories I and II, see [2].*

Future plans: We plan to extend our Ag(111/100) calculations to three dimensions. We will try to quantify to what degree the inclusion of the active electron's motion in the surface plane affects resonance widths, and shifts. Furthermore, we intend to investigate the neutralization dynamics of H^- near the (111) and (100) surfaces of Al and Pt. Taking advantage of the flexibility of the wave-packet-propagation scheme with regard to the choice of an effective surface potential, we have begun to investigate resonance formation and charge exchange near near vicinal and nano-structured surfaces.

[1] T. Niederhausen, B. Feuerstein, and U. Thumm, "Circular Dichroism in Laser-Assisted Proton - Hydrogen Collisions", Phys. Rev. A, accepted for publication (2004).

[2] H.S. Chakraborty, T. Niederhausen, and U. Thumm, "Effects of the Surface Miller Index on the Resonant Neutralization of Hydrogen Anions near Ag surfaces", Phys. Rev. A., **69**, 052901 (2004).

[3] M. Zamkov, H.S. Chakraborty, A. Habib, N. Woody, U. Thumm, and P. Richard, "Image-Potential States of Single- and Multi-Walled Carbon Nanotubes", Phys. Rev. B, accepted for publication (2004).

[4] A.A. Khuskivadze, I.I. Fabrikant, and U. Thumm, "Static Electric Field Effects in the Photodetachment of Cs-", Phys. Rev. A., **68**, 063405 (2003).

[5] B. Feuerstein and U. Thumm, "Mapping of Coherent and Decohering Nuclear Wave Packet Dynamics in D_2+ with Ultrashort Laser Pulses", Phys. Rev. A., **67**, 063408 (2003).

[6] B. Feuerstein and U. Thumm, "Fragmentation of H_2+ in strong 800nm Laser Pulses: Initial Vibrational State Dependence", Phys. Rev. A. 67, 043405 (2003).

[7] B. Feuerstein and U. Thumm, "On the Computation of Momentum Distributions in Wave Packet Propagation Calculations", J. Phys. B**36**, 707-716(2003).

[8] B. Bahrim and U. Thumm, "Electron Transfer and Orbital Hybridization in Slow Collisions between Excited Hydrogen Atoms and Aluminum Surfaces", Surface Science B **521**, 84-94 (2002).

[9] C. Bahrim, U. Thumm, A.A. Khuskivadze, and I.I. Fabrikant, "Near-Threshold Photodetachment of Heavy Alkali-Metal Anions", Phys. Rev. A. **66**, 052712 (2002).

[10} U. Thumm, "Interactions of Highly Charged Ions with C_{60} and Surfaces", in: The Physics of Multiply and Highly Charged Ions, ed. F. Currel (Kluwer Academic, 2002).

[11] U. Thumm, "Ion--Surface Interactions", Book of invited papers, XXII International Conference on Physics of Electronic and Atomic Collisions, Santa Fe, New Mexico (Rinton Press, Princeton, NJ, 2002).

Inner-Shell Photoionization of Atoms and Small Molecules at the Advanced Light Source

A. Belkacem, M. Prior and M. Hertlein

Chemical Sciences Division, Lawrence Berkeley National Laboratory, Berkeley, CA 94720

Email: abelkacem@lbl.gov, mphertlein@lbl.gov, mhprior@lbl.gov

Objective and Scope

The goal of this part of the LBNL AMOS program is to understand the structure and dynamics of atoms and molecules using photons as probes. The current research carried at the Advanced Light Source is focused on studies of inner-shell photoionization and photo-excitation of atoms and molecules, as well as breaking new ground in the interaction of x-rays with atoms and molecules dressed with femto-second laser fields. The low-field photoionization work seeks new insight into atomic and molecular processes and tests advanced theoretical treatments by achieving new levels of completeness in the description of the distribution of momenta and/or internal states of the products and their correlations. The intense-field two-color research is designed to provide new knowledge of the evolution on a femto-second time scale (ultimately atto-second) of atomic and molecular processes as well as the relaxation of atomic systems in intense transient fields.

Electron correlation during photoionization and relaxation of potassium and argon after K-shell photoexcitation.

The dynamics of inner-shell photoionization and the resulting relaxation of the excited atom are complicated by the collective response of all the electrons of the atomic target. Furthermore this correlated response of the electrons in the atom couples the photoionization and the relaxation processes.

In this work we compare the different ion yields and charge states distributions for potassium and argon after K-shell ionization with photon energies from about 100 eV below to about 100 eV above their respective K-shell edge. Though loosely bound, the potassium valence electron plays a major role in the ionization dynamics. Striking differences and surprising similarities are observed between the charge state distributions, which can be traced to the interplay between the various processes (shake-up, correlation between the valence electron and the photoelectron, post-collision interaction effects, pre-edge K-shell ionization, and double-excitation).

We find that the valence electron is rarely a spectator during core relaxation, and its presence enhances loss of the photoelectron excited into Rydberg levels or strongly suppress recapture of slow photoelectrons through post-collision interaction.

The influence of the valence electron is distinctly observable in the fractional ion yield of K+, which is strongly suppressed at the 1s-4p resonance energy, in stark contrast to the Ar+ yield. This indicates that the valence electrons have a high ionization probability and K-shell excitation rarely leads to K+. At the 4p resonance, most potassium charge states

reach a fractional yield close to their high-energy limit and any post collision interaction effect is minimal.

Vibrationally resolved K-shell photoionization of CO.

Diffraction of a low energy (< 4 eV) carbon-K-photoelectron wave, created inside a CO molecule by absorption of a circularly polarized photon, has been studied using the COLTRIMS technique at the LBNL ALS Beam Line 4.0 (Phys. Rev. Lett. to be published). The measurements resolve the vibrational states of the K-shell ionized CO^+ molecule and display the photoelectron diffraction patterns in the molecular frame. These show significant variation for the different vibrational states. This effect is stronger than predicted by state-of-the-art theory. This study is performed close to C-K-threshold and therefore far below the molecule's σ-shape resonance, thus this surprisingly strong effect is not related to that resonance phenomenon.

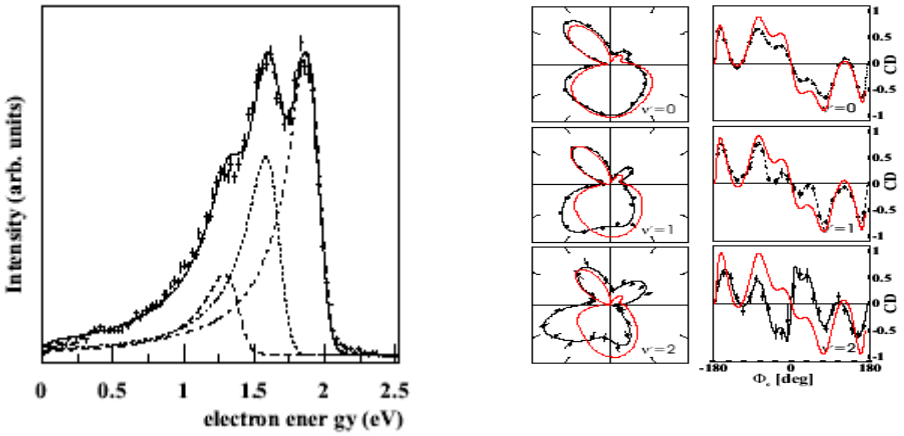

Left panel: C-K-photoelectron energy distribution created by photons of 298.3 eV energy. The solid line is a sum of the photo lines of the contributing vibrational (v'=0,1,2) $C(1s^{-1})O^+$ states (dotted lines), represented by distorted Lorentz shapes. The middle panel shows the molecular frame photoelectron distributions, while the right panel shows the circular dichroism (CD, the normalized difference between the angular distribution obtained for left and right circularly polarized light). The molecule is oriented horizontally within the plane of the middle figure with the O atom to the left. The figure plane corresponds to the polarization plane of the left hand circularly polarized photons (propagating into the plane). Grey line: relaxed core HF calculations normalized to the maximum of the experimental distribution. The black line is a fit of spherical harmonics up to l = 5.

Single photon, double ionization of the Deuterium molecule.

We have reported (Phys. Rev. Lett. 92, 163001 (2004) the first kinematically complete study of the four-body fragmentation of the D_2 molecule following absorption of a single photon. For equal energy sharing of the two electrons and a photon energy of 75.5 eV, we observed the relaxation of one of the selection rules valid for He photo double ionization and a strong dependence of the electron angular distribution on the orientation

of the molecular axis. This effect is reproduced by a model in which a pair of photo ionization amplitudes is introduced for the light polarization parallel and perpendicular to the molecular axis. We also have observed a strong dependence of the electron angular distribution on the inter-nuclear separation of the D nuclei at the instant of photo ionization (Nature to be published). This observation is the first of its kind and is not reproduced by readily applied theoretical approaches.

X-ray ionization atoms and molecules excited with femtosecond laser pulses (pump-probe).

An atom is a multielectron system that responds as a whole when perturbed by a strong laser field. The modifications to the atomic structure by the femto-second laser (acting on the outer electrons only) can indirectly extend to inner-shells through electron correlation. In particular the presence of the laser during relaxation of an atom with an inner-shell hole will modify the autoionization of the upper states as well as the post-collision interactions (e.g. between photo- and Auger electrons) changing the end products.

We used a 1.5 mJ, 800 nm, femtosecond laser pulse as a pump and synchrotron radiation x-rays at the ALS as a probe. The laser is used to remove or excite the 4s-electron of potassium and while the x-rays are tuned around the K-shell ionization threshold to probe the shifts of the transition energies and the continuum.

We observe a laser induced three electron-volt shift of the 1s-4p transition from 3608 eV to 3611 eV. We also observe a two electron-volt shift the ionization threshold from 3613 eV to 3615 eV. This shows that changes to the valence electrons using a femtosecond laser result in major changes in the x-ray absorption edges.

We tuned the x-ray energy to 3611 eV and varied the time delay between the laser pulse and x-ray pulse. We measured a cross correlation between the x-ray beam and the laser pulse that reflect the 50 ps time width of the ALS pulse.

The experimental technique is based on the detection of Auger electrons using a high efficiency magnetic spectrometer and time-of-flight. This technique is well suited for studies involving femtosecond x-ray and will be used with the sliced x-ray beam next year on beamline 6 at the ALS and at LCLS when available.

Future Plans

We plan to continue the pump-probe experiments at the ALS. We will continue our studies with potassium and extend the measurements to molecules such as H-Cl and I-Br. Time-resolved XANES has the capability to observe the degree of charge transfer by making use of the intensity of bound-bound transitions to monitor the whereabouts of the photoexcited electron. Interhalogens like I-Br are suitable for this because we can monitor the intensity of the 2s-4p absorption intensity.

We plan to continue application of the COLTRIMS approach to achieve complete descriptions of the single photon double ionization of H_2 and its analogs. New measurements will be made close to the double ionization threshold and approaching the regime where the outgoing electrons and the ions have more nearly the same velocities. We also will conduct new studies of K-shell ionization or excitation in suitable small molecular systems. Our earlier observations of the isomerization of acetylene to the vinylidene configuration forms a basis for possible further studies of this phenomena

perhaps using deuterated acetylene to alter the relative time scales of molecular rotation and the dissociation dynamics.

Recent Publications

"Vibrationally resolved K_-shell photoionization of CO with circularly polarized light", T. Jahnke, L. Foucar, J. Titze, R. Wallauer, T. Osipov, E. P. Benis, A. Alnaser, O. Jagutzki, W. Arnold, S. K. Semenov, N. A. Cherepkov, L. Ph. H. Schmidt, A. Czasch, A. Staudte, M. Schöffler, C. L. Cocke, M. H. Prior, H. Schmidt-Böcking, and R. Dörner, *Phys. Rev. Lett. accepted for publication.*

"Complete photo-fragmentation of the deuterium molecule" T. Weber, A. O. Czasch, O. Jagutzki, A. K. Mueller, V. Mergel, A. Kheifets, E. Rotenberg, G. Meigs, M. H. Prior, S. Daveau, A. Landers, C. L. Cocke, T. Osipov, R. Diez Muiño, H. Schmidt-Bőcking and R. Dőrner, *Nature, accepted for publication*

"Fully Differential Cross Sections for Photo-Double-Ionization of D_2", Th. Weber, A. Czasch, O. Jagutzki, A. Müller, V. Mergel, A.Kheifets, J. Feagin, E. Rotenberg, G. Meigs, M.H. Prior, S. Daveau, A.L. Landers, C.L. Cocke, T. Osipov, H. Schmidt-Böcking and R. Dörner, *Phys. Rev. Lett,* ***92****, 163001 (2004).*

‘'Metal-insulator transitions in an expanding metallic fluid: particle formation kinetics", T.E. Glover, G. D. Ackerman, A. Belkacem, P. A. Heimann, Z. Hussain, R. W. Lee, H. A. Padmore, C. Ray, R. W. Schoenlein, W. F. Steele, and D. A. Young, *Phys. Rev. Lett,* ***90****, 23102-1 (2003)*

"Measurement of vacuum-assisted photoionization at 1 GeV for Au and Ag targets", D. Dauvergne, A. Belkacem, F. Barrue, J. P. Bocquet, M. Chevallier, B. Feinberg, R. Kirsch, J. C. Poizat, C. Ray, and D. Rebreyent, *Phys. Rev. Lett.* ***90****, 153002 (2003)*

"Auger electron emission from fixed-in-space CO", T. Weber, M. Weckenbrock, M. Balser, L. Schmidt, O. Jagutzki, W. Arnold, O. Hohn, M. Schoffler, E. Arenholz, T. Young, T. Osipov, L. Foucar, A. de Fanis, R. D. Muino, H. Schmidt-Bocking, C.L> Cocke, M.H. Prior, and R. Dorner, *Phys. Rev. Lett.* ***90****, 153003 (2003)*

"Photoelectron-photoion momentum spectroscopy as a clock for chemical rearrangements: isomerization of the Di-cation of acetylene to vinylidene configuration", T. Osipov, C.L. Cocke, M. Prior, A. Landers, T. Weber, O. Jagutzki, L. Schmidt, H. Schmidt-Bocking and R. Dorner, *Phys. Rev. Lett.* ***90****, 233002 (2003)*

"Dynamics of ionization mechanisms in relativistic collisions involving heavy and highly charged ions", D. C. Ionescu and A. Belkacem, *Eur. Phys. J.* ***D18****, 301-307 (2002)*

"Observation of a nearly isotropic, high energy Coulomb explosion group in the fragmentation of D2 by short laser pulses", A. Staudte, C.L. Cocke, M.H. Prior, A. Belkacem, C. Ray, H.H.W Chong, T.E. Glover, R.W. Schoenlein, *Phys. Rev A* ***65****, 020703(R) (2002)*

"Energy sharing and asymmetry parameters for photo double ionization of helium 100 eV above threshold in single-particle and Jacobi coordinates", A. Knapp, M. Walter, T. Weber, A.L. Landers, S. Schossler, T. Jahnke, J. Nickles, S. Krammer, O. Jagutzki, L. Schmidt, T. Osipov, J. Rosch, M. Prior, H. Schmidt-Bocking, C.L. Cocke and R. Dorner, *Journal of Physics B-Atomic Molecular & Optical Physics,* ***35****, L521 (2002)*

"Mechanisms of photo double ionization of helium by 530 eV photons", A. Knapp, A. Kheifets, I. Bray, A. Landers, S. Schossler, T. Jahnke, J. Nickles, S. Kammer, O. Jagutzki, L. Schmidt, T. Osipov, R. Rosch, M. Prior, H. Schmidt-Bocking, C.L. Cocke, and R. Dorner, *Phys. Rev. Lett.* ***89****, 033004 (2002)*

S L O W M O L E C U L E S

Harvey Gould

Mail Stop: 71-259, Lawrence Berkeley National Laboratory, Berkeley, CA 94720
e-mail:gould@lbl.gov • tel (510) 486-7777

I. Introduction

Slow collisions are different: because the collision energies are small enough, compared to the well depth in the intermolecular potential, to form resonant quasi-bound states. The large numbers of low-lying rotational states results large numbers of resonances, causing dramatic variations in cross sections - unique to slow molecules. These predicted effects have not yet been observed.

Low energy molecule- molecule scattering cross sections are expected to be as large as 10^{-11} to 10^{-16} cm^2/molecule - possibly larger. The well depths of molecules that readily form dimers (H_2O for example) can be very large compared to the slow collision energies, leading to the expectation of exotic scattering behavior.

Chemical reactions are fundamentally different for slow molecules because in the presence of a barrier, insurmountable by their kinetic energy, the reaction proceeds by tunneling, enhanced by the van der Waals attraction and by the long duration of the collision. Again, these effects have not yet been observed.

Cold molecules in nature: The expanding gas in the Boomerang Nebula (Fig. 1) has been measured [R. Sahai, and L.-Å. Nyman, "The Boomerang Nebula: The Coldest region of the Universe?" Astrphy. J. **487**, L155 (1997)] to be *at or below 1K*. Molecules of O, N, C, and H are present.

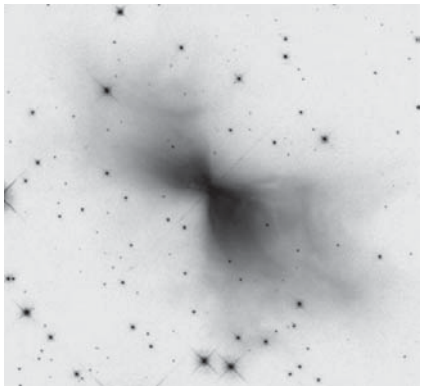

Fig. 1. Reverse image grey scale rendition of a Hubble Space Telescope photograph of the Boomerang Nebula [Photo credit: R. Sahai and J. Trauger taken with the Hubble Space Telescope. http://antwrp.gsfc.nasa.gov/apod/ap030220.html]. This is the fate of most stars in our galexy.

II. Work at LBNL

Experimental Approach - To observe the effects described above, a sufficient number of cold molecules must be available and they must be made to interact with each other or with another sample of cold molecules or cold atoms. Below 10 K this is likely to require not just cold molecules but slow molecules.

Our approach is to use molecular beam(s) of cold molecules produced by a seeded pulsed jet source (a form of buffer gas cooling) and slowed by a time-varying electric-field-gradient linear decelerator. Our decelerator has been designed to work with polar molecules in strong-field-seeking states which will allow it to decelerate any polar molecule with mass < 100 amu and moderate electric dipole moment and rotational constant. Molecules in strong-field-seeking states are much more difficult to focus and deflect than those in weak-field-seeking states because they can only be focused in one transverse direction while necessarily defocusing in the other (see recent progress).

Molecular beam transport, focusing, slowing, and storage in a ring for molecules in strong-field-seeking states have been extensively analyzed as part of an LBNL-directed study by Juris Kalnins, Glen Lambertson, and Hiroshi Nishimura, from LBNL's Accelerator and Fusion Research Division, who have also designed our proposed molecular decelerator, and myself. Papers describing some of our results are in the publications list. Others have been submitted or are being prepared.

The molecular decelerator is a pulsed apparatus and can be adjusted between pulses of molecules. For our initial molecule-molecule scattering experiments we plan to have a bunch of slow molecules overtake and collide with a previous bunch of slower molecules in a rear-end collision. This will be done by turning off the last few slowing elements before the second of two bunches of molecules reached the end of the decelerator. For chemical reactions the beam can be scattered from ultracold atoms in a magneto optic trap.

III. Recent Progress

Focusing tests - Slow molecules are more difficult to focus than are fast molecules because as the molecules is slowed the transverse velocity becomes relatively larger and fringe fields and nonlinearities have a greater effect. To test our designs we (J. Amini and H. Gould) constructed a focusing triplet and used it to focus a fountain of slow cesium atoms. The atoms have a similar Stark potential to molecules in strong-field-seeking states and are easier to detect and image. (The fountain is the same apparatus that we recently used to make the world's most precise measurement of an alkali atom polarizability - see publications)

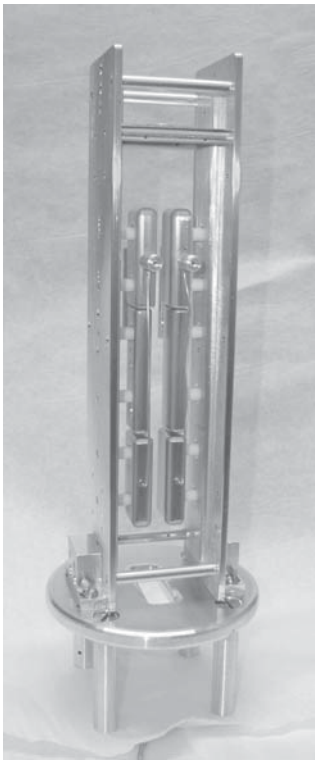

Three-lens focusing triplet

Starting with the electrode shape, and adding the effects of end fields, and nonlinearities, George Kalnins successfully pre-

dicted the voltages needed to: a) bring the beam to a focus in both transverse directions; b) produce a nearly parallel beam in both transverse directions; and c) bring the beam to a focus in one transverse direction while it remains nearly parallel in the other. These results will be written up for publication.

IV. Immediate Plans:

Slow molecule filter source - We are assembling five focusing elements and a three-degree bend element into a velocity spectrometer. It will produce beams of state selected moderately slow molecules (kinetic energy of about 5 K) from the low velocity tail from a thermal beam of molecules. The spectrometer passes the least rigid molecules which in mostly cases are slow molecules in the lowest rotational state. The intensity decreases rapidly with kinetic energy but a modeling calculation for D_2O predicts an intensity, at 5 K, of 1×10^6 molecules/s (with a ±3.5% band pass and a few mm diameter focus). While this is probably too weak for measuring molecule-molecule scattering cross sections, it may find application in experiments with solid targets.

V. Recent Publications of BES Supported Research

1. J. A. Amini and H. Gould, "High Precision Measurement of the Static Dipole Polarizability of Cesium," Phys. Rev. Lett. **91**, 153001 (2004).

2. H. Nishimura, G. Lambertson, J. G. Kalnins, and H. Gould, "Feasibility of a synchrotron storage ring for neutral polar molecules," Rev. Sci. Instr. **74**, 3271 (2003).

3. J. G. Kalnins, G. Lambertson, and H. Gould, "Improved alternating gradient transport and focusing of neutral molecules," Rev. Sci. Instr. **73**, 2557 (2002).

VI. Acknowledgments

This work is supported by the Office of Basic Energy Sciences, of the U.S. Department of Energy under Contract DE-AC03-76SF00098. J.G. Kalnins is supported by the Office of High Energy and Nuclear Physics of the U.S. Department of Energy, and J. Amini is supported by NASA and NIST.

Femtosecond X-ray Beamline for Studies of Structural Dynamics

Robert W. Schoenlein

Materials Sciences Division
Lawrence Berkeley National Laboratory
1 Cyclotron Rd. MS:2-300
Berkeley, CA 94720
email: rwschoenlein@lbl.gov

Background and Program Scope

Modern synchrotrons providing high-brightness, tunable x-ray beams, have driven rapid advances in our understanding of the atomic and electronic structure of condensed-matter via x-ray diffraction and spectroscopy techniques such as EXAFS and XANES. The fundamental time scale on which atomic structural changes can occur is the time scale of a vibrational period, ~100 fs. This is the limiting time scale for atomic motion that determines the course of phase transitions in solids, the kinetic pathways of chemical reactions, and even the function and efficiency of biological processes. The direct study of structural dynamics is a frontier research area in physics, chemistry, materials science and biology. However, the development of this research area has been limited by the lack of suitable tools for probing structural dynamics on the femtosecond time scale. A significant limitation of synchrotron sources is the pulse duration (~100 ps) as determined by the duration of the stored electron bunch. In contrast, advanced femtosecond laser technology now enables the measurement of dynamic processes on time scales shorter than 10 fs. However, femtosecond lasers probe the extended electronic states of condensed matter (using low-energy visible photons) and such states are only indirect indicators of atomic structure.

Our research group has pioneered the development of a novel technique for generating femtosecond x-ray pulses from a synchrotron storage ring by using femtosecond optical pulses to modulate the energy (and time structure) of a stored electron bunch. A simple bend-magnet beamline, incorporating this technique, has been constructed at the Advanced Light Source. The beamline provides ~100 fs x-ray pulses over an energy range of 0.1-12 keV with a flux of ~10^3 ph/sec/0.1% BW.

The scope of this research program includes the development and characterization the synchrotron bend-magnet beamline generating 100 fs x-ray pulses. In addition to providing for the development of femtosecond x-rays, this beamline will be a proving ground for time-resolved x-ray science incorporating femtosecond laser systems and end stations suitable for time-resolved x-ray diffraction, EXAFS, XANES, and photoionization measurements. Finally, this research program seeks to develop scientific applications and associated measurement techniques including pump-probe with femtosecond visible and x-ray pulses, ultrafast x-ray streak camera detectors, and dispersive measurement schemes. Initial research will focus on ultrafast solid-solid phase transitions in crystalline solids, light-induced structural changes in molecular crystals, and x-ray interactions with atoms in the presence of strong laser fields.

Recent Progress

During this year, beamline development has focused on improving the capability for generating femtosecond x-rays. We have made the first observation of coherent synchrotron radiation in the infrared region (~100 μm) which is a direct result of the ultrafast time structure created in the long electron bunch by the femtosecond optical pulse. Bolometer-based

measurement techniques of the coherent synchrotron radiation in the far infrared have been developed as a diagnostic of the laser/electron-beam interaction efficiency. This has enhanced the reliability of the femtosecond x-ray generation. Another important area of beamline development has been the improvement in the efficiency and resolution of the soft-x-ray spectrometer. Specifically, a high-efficiency varied-line-spacing holographic grating has been incorporated which improves both the spectral resolution and the spectrometer throughput. In addition, a high-efficiency soft x-ray detector (consisting of a grazing incidence photocathode and electron multiplier) has been incorporated in the spectrometer. In the past few months, a new interaction wiggler has been installed and commissioned. This allows for more efficient interaction between the femtosecond laser pulses and the stored electron beam, and will simultaneously provide x-rays for the existing protein-crystallography beamlines at the ALS.

Progress has been made in the development of an ultrafast x-ray streak camera with a target resolution approaching 100 fs. This device provides enhanced electron detection efficiency and spatial resolution, and incorporates improved electron imaging optics and photoconductive switch design. A single-shot temporal resolution of ~500 fs has been demonstrated by illuminating the streak camera with 60 fs pulses at 266 nm. In accumulating mode, a resolution of ~1 ps has been obse rved integrating at 1 kHz for 1 sec.

Scientific applications have focused on time-resolved XANES measurements in the model correlated electron system VO_2. The objective is to elucidate the relationship between electronic changes and atomic structural changes associated with the photo-induced metal-insulator transition. Previous measurements at the V L-edge near 516 eV (probing the correlated d-bands from the V-$2p_{3/2}$ state) revealed a distinct shift associated with the collapse of the insulator bandgap within the 70 ps duration of the full ALS x-ray pulse followed by nucleated thermal growth of the metallic phase at a speed of 40 m/sec [Cavalleri et al., PRB, 153106, 2004]. Recent measurements using femtosecond x-ray pulses at 516 eV reveal a prompt sub-picosecond transient increase in x-ray absorption which partially recovers within a few picoseconds. Complementary measurements at 530 eV (probing unoccupied valence states from the O-1s state) exhibit a simultaneous sub-picosecond transient bleach in the x-ray absorption which also recovers within a few picoseconds. These preliminary results reflect the ultrafast electronic dynamics associated with the photo-doping process that initiates the insulator-metal transition in this correlated compound. A more complete analysis of these new results is in progress.

In addition, initial measurements have been made of structural changes in liquid water following photoexcitation of solvated molecules. Preliminary analysis of x-ray diffraction rings from a liquid jet indicate distinct changes in the pair-correlation of the water molecules on the 100 ps time scale.

Our current achievements make efficient use of only ~10^4 x-ray photons per pulse (at 80 ps duration) provided by the 5.3.l bend magnet. The average flux is a significant limitation for nearly all experiments, and this underscores the scientific need for the additional flux provided by a femtosecond undulator beamline. This new beamline is now under development, and is a fundamental component of the future plans for this research program.

Future Plans

The primary objectives of this research program are: (a) to develop a unique femtosecond undulator beamline and associated instrumentation for time-resolved x-ray research, and (b) to develop measurement techniques, scientific applications and experiments in time-resolved x-ray

science. As the new undulator beamline is completed, we will begin commissioning and characterization of this new source. We will develop advanced diagnostics and instrumentation for femtosecond operation of the beamline including a gated x-ray 2D area detector and 1D photodetectors for isolating single synchrotron pulses. This development will build on the techniques currently being employed for the x-ray streak camera.

Time-resolved NEXAFS measurements in VO_2 will investigate changes in short-range order and bonding following laser excitation. Measurements using femtosecond x-rays from the ALS bendmagnet beamline will be optimized with the goal of eventually utilizing the higher flux provided by the undulator beamline for time-resolved EXAFS measurements. VO_2. is a correlated electron system which is an insulator at room temperature (rutile structure), and undergoes an insulator-metal transition at ~340 K (monoclinic structure). Previous time-resolved optical and x-ray (Bragg) measurements indicate that the phase transition can be induced electronically on a sub-picosecond time scale. Time-resolved XANES measurements on the V L-edge will provide new information about the electronic dynamics, while EXAFS measurements will simultaneously provide information on the short-range structural dynamics, and may elucidate the role of the V-O bonding on the phase transition.

New experiments on structural dynamics of solvated molecules will focus on metal carbonyls such as $Cr(CO)_6$ in alcohol. Photoexcitation of these molecules results in photodetachment of a carbonyl ligand. The subsequent molecular intermediates are thought to involve solute attachment to the $Cr(CO)_5$ in two different conformations. Initial experiments will focus on XANES measurements to provide information on the electronic changes associated with the photodetachment process. Future EXAFS measurements will provide direct information about transient changes in ligand coordination, geometry, and bond distances.

AMO research on BL5.3.1 will investigate the bound-state structure of a laser-dressed atom and the resulting perturbations to the x-ray scattering with such dressed atoms. Experiments will focus on the modification of the absorption of x-rays resulting from the laser excitation of the outer electron of Na and K atoms.

In order to meet the stringent flux requirements for future x-ray spectroscopy on the femtosecond time scale, we are developing an undulator beamline (the Ultrafast X-ray Science Beamline) at the ALS, which will be dedicated for time-resolved x-ray research. The development, commissioning, operation, and scientific support of this beamline are important components of the future plans for this research program. The beamline will consist of a 1.5 T undulator/wiggler providing femtosecond x-rays for two branchlines: a soft x-ray branchline operating in the 0.3-2 keV range, and a hard x-ray branchline operating in the 2-10 keV range. The soft x-ray branchline will include a spectrograph providing <1 eV resolution for single-wavelength experiments, and ~100 eV bandwidth for dispersive spectroscopic measurements. The hard x-ray branchline will include a double-crystal monochromator providing ~2 eV resolution. The beamlines will include a high repetition rate (40 kHz) femtosecond laser system with an average power approaching 100 W. The average flux from this beamline is expected to be 10^7 –10^8 ph/sec/0.1% BW (with roughly 100x increase in flux from the insertion device relative to the current bend-magnet, and another 10x increase over the present laser repetition rate). The beamline will provide ~200 fs duration x-ray pulses for a wide range of experiments in ultrafast x-ray science.

Publications from DOE Sponsored Research (since 2002)

C. Bressler, M. Saes, M. Chergui, D. Grolimund, R. Abela, in: Femtochemistry and Femtobiology: Ultrafast Dynamics in Molecular Science, A. Douhal, J. Santamaria, Eds., World Scientific Publishing Co., Singapore, 449-458 (2002).

C. Bressler, M. Saes, M. Chergui, D. Grolimund, R. Abela, and P. Pattison, "Towards Structural Dynamics in Condensed Chemical Systems Exploiting Ultrafast Time-Resolved X-Ray Absorption Spectroscopy," J. Chem. Phys., **116**, 2954 (2002).

M. Saes, C. Bressler, R. Abela, D. Grolimund, S. Johnson, P.A. Heimann, and M. Chergui, "Observing Photochemical Transients by Ultrafast X-Ray Absorption Spectroscopy," *Phys. Rev. Lett.*, **90**, 047403, (2003).

A. Staudte, C.L. Cocke, M.H. Prior, A. Belkacem, C. Ray, H.H.W. Chong, T.E. Glover, R.W. Schoenlein, and U. Saalmann, "Observation of a nearly isotropic, high-energy Coulomb explosion group in the fragmentation of D_2 by short laser pulses," *Phys. Rev. A*, **65**, 2002.

T.E. Glover, G.D. Ackermann, A. Belkacem, P.A. Heimann, Z. Hussain, H.A. Padmore, C. Ray, R.W. Schoenlein, and W.F. Steele, "Kinetics of cluster formation during femtosecond laser ablation," **Ultrafast Phenomena XIII**, R.D. Miller, M.M. Murnane, N.F. Scherer, A.M. Weiner, Eds., Springer-Verlag, p 42, (2002).

T.E. Glover, G.D. Ackerman, A. Belkacem, P.A. Heimann, Z. Hussain, R.W. Lee, H.A. Padmore, C. Ray, R.W. Schoenlein, W.F. Steele, and D.A. Young, "Metal-insulator transitions in an expanding metallic fluid: particle formation kinetics," *Phys. Rev. Lett.*, **90**, pp.236102/1-4, (2003).

A.Cavalleri and R.W. Schoenlein, "Femtosecond x-ray studies of lattice dynamics in solids," in **Ultrafast Dynamical Processes in Semiconductors**, ed. by K.T. Tsen, *Topics in Applied Physics* Series No. 92, Springer Verlag, (2004).

M. Saes, C. Bressler, F. van Mourik, W. Gawelda, M. Kaiser, M. Chergui, D. Grolimund, R. Abela, T.E. Glover, P.A. Heimann, R.W. Schoenlein, S.L. Johnson, A.M. Lindenberg, and R.W. Falcone, "A setup for ultrafast time-resolved x-ray absorption spectroscopy", *Rev. Sci. Inst.*, **75**, pp. 24-30, (2004).

P. A. Heimann, H. A. Padmore, and R. W. Schoenlein, "ALS Beamline 6.0 For Ultrafast X-ray Absorption Spectroscopy", in **Synchrotron Radiation Instrumentation**, T. Warwick, J. Author, H.A. Padmore, and J. Stohr Eds., AIP Conf. Proc. 705, 1407 (2004).

R. W. Schoenlein, A. Cavalleri, H. H. W. Chong, T. E. Glover, P. A. Heimann, A. A. Zholents, and M. S. Zolotorev, "Generation of Femtosecond Synchrotron Pulses: Performance and Characterization", in **Synchrotron Radiation Instrumentation**, T. Warwick, J. Author, H.A. Padmore, and J. Stohr Eds., AIP Conf. Proc. 705, 1403 (2004).

A. Cavalleri, H.H.W. Chong, S. Fourmaux, T.E. Glover, P.A. Heimannn, J.C. Kieffer, B.S. Mun, H.A. Padmore, and R.W. Schoenlein, "Picosecond soft x-ray absorption measurement of the photo-induced insulator-to-metal transition in VO_2," *Phys. Rev. B*, **69**, 153106 (2004).

ATOMIC AND MOLECULAR PHYSICS RESEARCH AT OAK RIDGE NATIONAL LABORATORY

David R. Schultz, Group Leader, Atomic Physics
ORNL, Physics Division, P.O. Box 2008
Oak Ridge, TN 37831-6372

Principal Investigators

E. Bahati [bahatie@ornl.gov], postdoctoral fellow
M. E. Bannister [bannisterme@ornl.gov]
C. C. Havener [havenercc@ornl.gov]
H. F. Krause [krausehf@ornl.gov]
J. H. Macek [macek@utk.edu]
F. W. Meyer [meyerfw@ornl.gov]
C. Reinhold [reinhold@ornl.gov]
D. R. Schultz [schultzd@ornl.gov]
C. R. Vane [vanecr@ornl.gov]
L. I. Vergara [vergarali@ornl.gov], postdoctoral fellow

The ORNL atomic physics program has as its overarching goal the understanding and control of interactions and states of atomic-scale matter. The scientific objective is to enhance progress toward development of detailed understanding of the interactions of multicharged ions, charged and neutral molecules, and atoms with electrons, atoms, ions, surfaces, and solids. Towards this end, a robust experimental program is carried out by our group centered at the ORNL Multicharged Ion Research Facility (MIRF) and as needed at other world-class facilities such as the ORNL Holifield Radioactive Ion Beam Facility (HRIBF) and the CRYRING heavy-ion storage ring in Stockholm. Closely coordinated theoretical activities support this work as well as lead investigations in complementary research. Specific focus areas for the program are broadly classified as particle-surface interactions, atomic processes in plasmas, and manipulation and control of atoms, molecules, and clusters, the latter focus area cross cutting the first two.

The MIRF Upgrade Project – *F. W. Meyer, M. E. Bannister, C. C. Havener, H. F. Krause, and C. R. Vane*

In order to expand the range of energies of intense beams of multicharged ions for atomic collision experiments at MIRF, the first of a two-part upgrade project is nearing completion. The first part consists of installation of a 250-kV high-voltage platform with an all-permanent magnet Electron Cyclotron Resonance (ECR) ion source. The ECR ion source, designed and fabricated by CEA, Grenoble, will operate in the frequency range 12.75 – 14.5 GHz. The higher-energy multicharged ion beams will significantly enhance the capabilities of present online experiments, and make possible investigations at previously inaccessible energies. For example, the higher energy center-of-mass energies available for the merged electron-ion beams energy loss (MEIBEL) experiment studying electron-impact excitation cross sections will enable measurements of very low threshold excitation cross sections as well as extension of cross-section measurements to higher energies above threshold. In addition, the higher beam energies will make possible new lines of investigation with this apparatus, such as measurements of dissociative recombination of molecular ions with mass >30, which are sometimes difficult with the present generation of storage rings.

For the ion-atom merged beams experiment, the higher energy beams will make possible achievement of velocity matching conditions for heavier multicharged projectiles, and, after suitable increase of the neutral beam energies, measurements at higher center-of-mass energies with a correspondingly higher resolution and larger collection solid angle in the laboratory frame.

The second part of the MIRF upgrade project entails fabrication of a floating beamline for the existing CAPRICE ECR ion source, to permit deceleration of extracted ion beams to energies as low as a few eV/q

during injection into experimental chambers at ground potential. This scheme simplifies the present approach of studying low-energy ion-surface interactions, which employs a floating scattering chamber. The new approach will also expand the range of ion-surface investigations in the very low-energy-impact regime, to include, e.g., X-ray spectroscopy studies, and it will permit low-energy ion-atom collision studies with complex, state-selective techniques such as COLTRIMS.

With exception of the ECR ion source, whose delivery (initially expected late 2003) has been delayed until late August 2004, fabrication and installation of the first phase of the upgrade project is essentially complete. First delivered beam from the platform is now anticipated in September 2004. Implementation of the floating beamline for the CAPRICE ECR source will occur in the first half of 2005.

Low-Energy Ion-Surface Interactions – *F. W. Meyer, H. F. Krause, and L. Vergara*

The principal aim of the ORNL MIRF investigations is to study the interactions of slow, singly and multicharged, atomic and molecular ions with metal, semiconductor, and insulator surfaces. Our specific goal is to improve fundamental understanding of neutralization, energy dissipation, physical and chemical sputtering processes occurring in such interactions, and subsequently to apply the knowledge gained to probe and modify surfaces of amorphous materials, single crystals, thin films, and nanostructures. This year our focus has been on the development of a new experiment studying ion-surface interactions that are relevant to controlled fusion devices.

One of the critical problems in the development of commercially viable fusion technology is identification of materials for use in plasma facing components (PFC's). Because of their high-thermal conductivities, excellent shock resistance, absence of melting, low activation, and low atomic number, carbon-based materials are very attractive candidates for such environments. Different types of graphite or carbon fiber composites (CFC's) are already used in present tokamaks, and CFC tiles (together with some tungsten) are being considered for use in the ITER divertor.

The use of carbon-based materials, however, brings its own set of problems. Oxygen etches carbon very efficiently, forming CO and CO_2 only loosely bound to the carbon surface. At the low-plasma temperatures characterizing the divertor environment, chemical erosion of the carbon surface by low-energy hydrogen-ion impact, leading to the ejection of light hydrocarbon molecules, is significant, and determines in large part the carbon-based-material lifetime. Considering the additional proposed use of Be in PFC's outside the divertor, the potential exists for a complex mixture of materials at the divertor strike points (due to CFC erosion and CFC/W/Be redeposition) that may significantly alter chemical sputtering yields (and thus core impurities and target plate lifetimes). The issue of how these material mixtures affect the chemical sputtering yield from graphite surfaces that have been exposed to high-power tokamak operating conditions has remained largely unexplored. Such effects are difficult to measure, at best, in tokamak environments. Laboratory experiments providing fundamental chemical sputtering data in conjunction with theoretical simulations of re- and co-deposition may provide an alternative approach to understanding and assessing the importance of such effects.

For this reason, measurements were started at ORNL MIRF to investigate chemical sputtering of graphite surfaces in the limit of very low impact energies. Our initial investigation was focused on virgin ATJ graphite. Subsequent measurements will be extended to ATJ graphite tile samples recently removed from the DIII-D tokamak at General Atomics in San Diego after exposure to eight years of tokamak discharges, as well as to virgin HOPG single crystal samples, in order to determine the effects of extensive plasma exposure (i.e., including redeposition and boronization effects) and target structure (i.e., amorphous vs. crystalline, and extent of hydrogen saturation) on chemical sputtering by low-energy hydrogen (deuterium) beams.

In our initial measurements, mass selected, decelerated beams of D_2^+ impacted the sample at normal incidence. The spatial profiles of the incident ion beams were approximately Gaussian in profile with FWHM's in the range 1-2 mm, as determined by a wire scanner that could be inserted in the plane of the target sample. From the beam currents intercepted by the sample and the beam-profile measurements, typical beam fluxes of $2 - 8 \times 10^{15}$ D/cm^2 s were deduced for the present energy range of 30 – 130 eV/u. Fluxes in excess of 1×10^{15} D/cm^2 s were obtained down to energies as low as a few eV/u.

The experimental approach used a sensitive quadrupole mass spectrometer which monitored the partial pressures of selected mass species in the range 1 – 60 u present in the scattering chamber. A Macintosh-based data acquisition system was used to measure mass distributions at fixed intervals in time, or alternatively, to follow the intensities of selected mass peaks as function of beam exposure times. The

evolution of the detected intensities of hydrocarbon species such as CD, CD_2, CD_3, CD_4, C_2D_2, C_2D_4, and C_2D_6 was followed as a function of accumulated beam dose until saturation in their intensities occurred.

To date we have made measurements[1-2] in the energy range of 30 – 130 eV/u. Some interpretation of the acquired mass spectra was attempted using known cracking patterns of CD_4, C_2D_2, C_2D_4, and C_2D_6, which were verified by *in-situ* measurements using calibrated leaks. At the lowest investigated impact energies, CD_4 appears to be the dominant light-stable hydrocarbon produced at room temperature. With increasing sample temperature, its contribution was found to decrease, while the contribution of C_2D_2 increased. At the higher impact energies, however, the CD_4 yield increased strongly in comparison to C_2D_2, and appears to become the dominant product even at 800 K.

1. F. W. Meyer, H. F. Krause, and L. I. Vergara, "Measurements of Chemical Erosion of ATJ Graphite by Low Energy D_2^+ Impact," 16th International Conference on Plasma Surface Interactions, Portland, ME, May 24-28, 2004 , to be published in J. Nucl. Mater. (2004).
2. L. I. Vergara, F. W. Meyer, and H. F. Krause, "Chemical Sputtering of ATJ Graphite Induced by Low-Energy D_2^+ Bombardment," ICACS-21, July 4-9, 2004, Genoa, Italy, to be published in Nucl. Instrum. Methods Phys. Res. (2004).

Angular Distribution Studies of Ions Guided Through a Nanocapillary Array – *H. F. Krause, C. R. Vane, and F. W. Meyer*

This section deals with investigations of the transport, angular scattering, charge exchange, and energy loss of low-energy (10–20 keV/q) multicharged ions in a mesoscopic structure. This work is part of the larger beam-surface effort at the ORNL MIRF that seeks to develop a fundamental understanding of neutralization, energy dissipation, and sputtering processes that occur when slow, highly charged ions interact with metal, semiconductor, and insulator surfaces.

The consequences of incident 10–20 keV/q ions of Ar^+, Ar^{3+}, Ne^{3+}, and Ne^{7+} scattered in an Al_2O_3 nanocapillary array have been studied. The array consists of a dense distribution of nanopores typically 100-nm diam. and 60 micron length. These nanochannels are six times longer than those used to guide much lower energy ions in insulating PET films.[1] Heretofore, experimental high-resolution angular scattering studies have not been reported for any nanocapillary target.

To minimize charging of the sample, entrance ions passed through a high-transmission grounded grid before entering the array (insulator). The target array was mounted in a precision goniometer to allow alignment with the incident beam and to study changes in angular distributions when the alignment of capillaries and the beam was varied in a controlled manner. Ions emerging from the array were electrostatically deflected out of plane so that final charge-state-selected angular distributions (including emerging neutrals) could be obtained. Resultant two-dimensional angular distributions were measured using a rotatable high-resolution 2D position-sensitive detector that sampled ~± 0.9°.

The principal transmitted charge state observed was the incident charge state in all cases. The transmitted fraction (~2 x 10^{-8}) is many orders of magnitude smaller than the array's surface porosity (~30%). No evidence of significant energy loss was observed for the transmitted ions. Yields in lower charge states and neutrals formed by electron capture were typically below 1% of the entrance charge-state yield. Observed angular distributions consist of well-resolved two-dimensional structures sitting on a continuum distribution.

The angular distribution and sharp angular structures are easily steered in the direction of the nanochannels within ~±1° by rotating the sample with respect to the incident beam. Structures observed match the effective collimation of individual nanopores (~1.6 mrad). The intensity of periodic structure decreases as the angle between the nanochannel direction and the beam is increased. All data suggest that the structure in the scattered ions arises when they bounce at ultra-low grazing angles in very large impact parameter Coulomb collisions with electrically charged nanopore walls. When the goniometer is rotated, the transmitted ion intensity initially decreases about 50% immediately before slowly building up to its former intensity in a transient lasting about 500 sec for a 6 nA incident beam (i.e., presumably during the redeposition of charge within the nanopores).

Results for these rare projectile charge-conserving ultra-low grazing angle collisions with an insulator surface contrast sharply with previously obtained results for low-energy grazing collisions on ordered insulator surfaces such as LiF, where charge capture and neutralization processes dominate in much larger

angle scattering events. The nanocapillary experiments have potential implications for the production and steering of low-intensity micro-beams.

1. N. Stolterfoht et al., "Transmission of 3 keV Ne^{7+} Ions through Nanocapillaries Etched in Polymer Foils: Evidence for Capillary Guiding," Phys. Rev. Lett. **88**, 133201 (2002); N. Stolterfoht et al., "Guided Transmission of 3-keV Ne^{7+} Ions through Nanocapillaries Etched in a PET Polymer," Instrum. Methods Phys. Res. B**203**, 246 (2003).

Electron-Molecular Ion Interactions – *M. E. Bannister, C. R. Vane, E. Bahati, and M. Fogle*

Electron-molecular ion recombination, dissociation, and excitation and ionization processes are important from a fundamental point of view, especially in that they provide a testable platform for investigating and fully developing our understanding of the mechanisms involved in electronic energy redistribution in fragmenting many-body quantum mechanical systems. These processes are also important practically in that electron-ion collisions are in general ubiquitous in plasmas and molecular ions can represent significant populations in low to moderate temperature plasmas. Neutral and charged radicals formed in dissociation of molecules in these plasmas represent some of the most highly reactive components in initiating and driving further chemical reaction pathways. Thus electron-molecular ion collisions are important in determining populations of some of the most reactive species in a wide variety of environments, such as the diverter edge regions in fusion reactors, plasma enhanced chemical vapor deposition reactors, environments where chemistries are driven by secondary electron cascades, for example in mixed radioactive waste, the upper atmospheres of planets, and cooler regions of the solar or other stellar atmospheres. To correctly model these environments it is absolutely essential to know the strengths (cross sections and rates), branching fractions, and other kinematical parameters of the various possible relevant collision processes.

Dissociative Excitation and Ionization: Measurements of cross sections for electron-impact dissociative excitation (DE) and dissociative ionization (DI) of molecular ions have continued using the MIRF crossed-beams apparatus.[1] The CH^+ and C^+ ion fragment channels have been studied for the CH_3^+ target ion, and cross sections for both channels exhibited a smooth energy dependence over the 3–100 eV range of the measurements with no apparent resonance features. The dissociation of DCO^+ ions producing CO^+ ions has also been investigated. Unlike the data for the CH_3^+ dissociation, the experimental results exhibited a strong resonance feature near 15 eV similar to that observed for the production of CH^+ from the dissociation of CH_2^+. [2]

The dissociation experiments discussed above used molecular ions produced by the ORNL MIRF Caprice ECR ion source,[3] but other cooler sources will also be used in order to understand the role of electronic and ro-vibrational excited states. A second ion source, a hot-filament Colutron ion source, is presently online and expected to produce fewer excited molecular ions. An even colder pulsed ion source, very similar to the one used for measurements[4] on the dissociative recombination of rotationally cold H_3^+ ions at CRYRING, is under development for use at the ORNL MIRF. Additionally, work continues on a supersonically-expanded surface-wave-plasma that serves as a CW source of cold molecular ions. With this range of ion sources, one can study dissociation with both well-characterized cold sources and with hotter sources that better approximate the excited state populations in plasma environments found in applications such as fusion, plasma processing, and aeronomy.

1. M. E. Bannister, H. F. Krause, C. R. Vane, N. Djuric, D. B. Popovic, M. Stepanovic, G. H. Dunn, Y.-S. Chung, A. C. H. Smith, and B. Wallbank, "Electron-Impact Dissociation of CH^+ Ions: Measurement of C^+ Fragment Ions," Phys. Rev. A **68**, 042714 (2003).
2. C. R. Vane, M. E. Bannister, and R. Thomas, "Electron-Impact Dissociation of CH_2^+ Producing CH^+ Fragments," XXIII ICPEAC Abstracts, Stockholm, Sweden (2003).
3. F. W. Meyer, "ECR-Based Atomic Collision Research at the ORNL MIRF," in *Trapping Highly Charged Ions: Fundamentals and Applications*, edited by J. Gillaspy (Nova Science, Huntington, NY, 1997), p. 117.
4. B. J. McCall et al., "An Enhanced Cosmic-Ray Flux towards Zeta-Persei Inferred from a Laboratory Study of the H_3^+-e^- Recombination Rate," Nature **422**, 500 (2003).

Dissociative Recombination: Studies of the process of dissociative recombination (DR) of relatively simple three-body molecular ions are being continued in our ongoing collaboration with Prof. Mats Larsson and colleagues at the Manne Siegbahn Laboratory (MSL), Stockholm University. Absolute cross sections, branching fractions, and measurements of the dissociation kinematics, especially of the three-body breakup channel, are being investigated at zero relative energy for a variety of light and heavy vibrationally cold triatomic di-hydrides. This research is carried out using the MSL CRYRING heavy ion storage ring facility, which is now expected to continue to be available for our electron-molecular ion measurements at least into calendar year 2007. We have now completed analysis of CH_2^+, and NH_2^+ three-body DR measurements and the results compared with H_2O^+ are being reported in Physical Review A.[1]

In the last year, we have initiated studies of three new systems PD_2^+, SH_2^+, and LiH_2^+. These experiments are a continuation of previous measurements concerning the DR of similar molecules, such as H_2O^+, NH_2^+, and CH_2^+ that have all revealed three-body break-up as the dominant reaction channel.[2-4] In order to study the three body break-up dynamics in detail, a high-resolution imaging technique is used to measure the displacement of the fragments from the center of mass of the molecule.[5] The displacement is related to the kinetic energy of the fragments and therefore information about the dynamics involved in the process can be obtained, i.e., the internal state distribution of the fragments. These event-by-event measurements yield information about how the kinetic energy is distributed between the two light fragments and the angular distribution of the dissociating molecules. In all of the triatomic dy-hidride systems previously studied, the branching fractions showed very roughly (7:2:1) ratios for (X + H + H; XH + H: X + H_2), while the observed energy sharing and angular distributions of the three-body breakup product channel could depend heavily on the structure, bonding and charge centre of the parent molecular ion. For $^{34}SH_2^+$ and PD_2^+, we have measured energy-dependent DR cross sections and thermal-rate coefficients along with branching fractions and dynamics of the three-body breakup channel products. For PD_2^+ ions, the branching fractions measured are (0.75; 0.16; 0.09) for (P + D + D: PD + D; P + D_2). In three-body dissociation, formation of excited P(^{2}D) is highly favored. For SH_2^+, the branching fractions are not yet determined. However, three-body DR dominates with the majority leading to formation of ground-state S(^{3}P) + H(1s) + H(1s). We are exploring these observations further by investigating the DR of one of the simplest such systems, LiH_2^+ (Li^+, H_2). This system, a Van der Waals' cluster with the charge centre located on the lithium atom, provides an excellent opportunity for investigating the role played by the type of bonds and charge center in the DR process. For LiH_2^+, we have made preliminary measurements of DR cross sections, branching fractions, and dynamics for the dominant two-body channel Li + H_2. We find, unlike all other systems studied, that the LiH_2^+ ion dissociates predominantly through the two-body channel to Li + H_2, with preliminary results for branching fractions being (0.17; 0.06; 0.77) for (Li + H + H; LiH + H; Li + H_2). Initial analysis and results for these systems have been reported at the 6th International Conference on Dissociative Recombination, Mosbach, Germany, July 12-16, 2004. All the above results are preliminary and analysis is still in progress.

1. R. Thomas et al., "Three-Body Fragmentation Dynamics of Amidogen and Methylene Radicals via Dissociative Recombination," accepted for publication in Phys. Rev. A (2004).
2. L. Vikor et al., "Branching Fractions in the Dissociative Recombination of NH^+ and NH_2^+ Molecular Ions," Astron. Astrophys. **344**, 1027 (1999).
3. Å. Larson et al., "Branching Fractions in Dissociative Recombination of CH_2^+," Astrophys. J. **505**, 459 (1998).
4. S. Rosén et al., "Recombination of Simple Molecular Ions Studied in a Storage Ring: Dissociative Recombination of H_2O^+," Faraday Discussions **115**, 295 (2000).
5. R. Thomas et al., "Investigating the Three-Body Fragmentation Dynamics of Water via Dissociative Recombination and Theoretical Modeling Calculations," Phys. Rev. A **66**, 032715 (2002).

Near-Thermal Collisions of Multicharged Ions with H and Multi-Electron Targets – *C. C. Havener, R. Rejoub, C. R. Vane, P. S. Krstic, and D. R. Schultz*

The merged-beams technique[1] is being used to explore near-thermal collisions (meV/u – keV/u) of multicharged ions with neutral atoms and molecules, providing benchmark measurements for comparison with state-of-the-art theories. Electron capture by multicharged ions from neutrals is important in many technical plasmas including those used in materials processing, lighting, ion-source development, and for

spectroscopic diagnostics and modeling of core, edge, and diverter regions of magnetically confined fusion plasmas.

Due to the relatively small number of atomic states effectively involved in the electron-capture process at low energies, He^{2+} + H is one of the most-frequently theoretically studied collision process and is viewed as a prototype one-electron heavy-particle, asymmetric collision system. An exponentially decreasing cross section and the inherent difficulties in producing a ground-state atomic hydrogen target have made measurements difficult and scarce below 1 keV/u. Independently, absolute total electron-capture cross sections for He^{2+} + H have been measured[2] using merged beams for collision energies from 380 eV/u to 2620 eV/u. Together with hidden-crossing coupled-channel calculations performed at ORNL,[2] an improved benchmark has been established for this system to which new methods, e.g., the recent hyperspherical coupled channel calculations of Le et al.[3] can be compared.

Preliminary measurements for another fundamental system N^{2+} + H suggest the electron capture cross section sharply increases below 10 eV/u and continues to rise below 100 meV/u in contrast to several theoretical calculations. Such a sharp increase is indicative of trajectory effects due to the ion-induced dipole attraction and has been seen in recent Ne^{4+} + H(D) measurements.[4] The observation of possible structure in the total cross section below 1 eV/u is being investigated. Structure at similar collision energies is being theoretically investigated for H^+ + H.

Modifications to the merged-beams apparatus to take advantage of the ECR upgrade project are well underway. The upgrade will provide higher energy and less divergent ion beams, which enhance the capabilities of the merged-beams apparatus. Enhancements include the ability to perform measurements with both H and D for direct observation of isotope effects, improvements in the energy resolution in order to investigate structure in the cross section below an eV/u, improvements in the angular collection, thereby eliminating concerns over incomplete collection, and the ability to perform measurements for the first time with heavy multicharged ions at eV/u energies and below. The new Cs sputter source allows merged-beams measurements to be performed with a variety of neutral beams other than H and D, such as Li, B, Na, Cr, Fe, etc., and molecular beams such as O_2, CH_2,… Our goal is to measure He^{2+} + Li, where strong shape resonances are predicted due to the strong ion-induced dipole attraction between reactants.

We have also continued the development of new theoretical tools to study processes such as charge transfer over a broad range of energies. In particular, we recently implemented a method to describe charge transfer in ion-atom collisions that hybridizes the lattice, time-dependent Schrödinger equation (LTDSE) approach with the atomic-orbital, coupled-channel technique. This method takes advantage of the completeness of the treatment of the collision problem through the LTDSE approach within a relatively small space around the distance of closest approach during the collision. It then extends the solution into the asymptotic regime through the less computationally intensive continuation of the time evolution of the electronic states under consideration utilizing a small, external coupled-channels expansion. This method is employed to calculate coherence parameters of an electron captured into the n=2 shell of hydrogen in H^+ + He collisions to illustrate its effectiveness. The results show excellent agreement with experimental measurements and constitute improvements over various existing theoretical treatments. We have also applied this approach to treat swift collisions of Ar^{18+} with carbon in support of transport modeling (described below) and for Be^{4+} + H collisions as a new benchmark for certain fusion energy relevant cross sections.

1. C. C. Havener, "Low-Energy Electron Capture Measurements Using Merged Beams," in *The Physics of Multiply Charged Ions*, Vol. 2, Kluwer Academic Publishers, The Netherlands, 2003, pp. 193-218.
2. C. C. Havener, R. Rejoub, P. S. Krstic, and A. C. H. Smith, "Charge Transfer in Low Energy Collisions of He^{2+} with Atomic Hydrogen," submitted to Phys. Rev. A (2004).
3. Anh-Thu Le et al., "Comparison of Hyperspherical Versus Common-Coordinate Close-Coupling Methods for Ion-Atom Collisions at Low Energies," Phys. Rev. A **69,** 062703 (2004).
4. C. C. Havener, R. Rejoub, C. R. Vane, H. F. Krause, D. W. Savin, J. G. Wang, and P. C. Stancil, "Electron Capture by Ne^{4+} Ions from Atomic Hydrogen," to be published in Phys. Rev. A (2004).

Transport of Ions in and above Solids – C. O. *Reinhold*

Open quantum systems are usually described by their reduced density matrices. Their dynamics is governed by a Lindblad master equation that can be solved in terms of quantum trajectory Monte Carlo (QTMC) sampling. For systems involving a high-dimensional Hilbert space, QTMC methods are

advantageous in terms of computer storage compared to a direct solution of the Lindblad equation. One key feature of the standard Lindblad equation is that it describes strictly unitary time transformations of the reduced density matrix. This property is of limited value in simulations of atomic systems when only finite subspaces can be represented within any realistic finite basis size and the coupling to the complement cannot be neglected. We have derived a generalized Lindblad form (and its QTMC implementation) that accounts for the outgoing flux of probability out of the finite Hilbert subspace while neglecting the back flow. For the case of multi-level radiative decay of an ion, where the exact solution can be obtained, our approach yields the correct result. We are implementing the new approach to describe multiple collisions with particles in a solid and the line emission intensities arising from the transmission of fast Ar^{18+} ions through amorphous carbon foils in an attempt to explain recent experimental data.[1]

The production of selected Stark states at high n ($n > 100$) remains a challenge because the oscillator strengths associated with their excitation are small, and because the Stark energy levels are closely spaced requiring the use of narrow line-width frequency-stabilized lasers and the minimization of Doppler effects. We have demonstrated that strongly polarized quasi-one-dimensional very-high-n (potassium) Rydberg atoms can be produced by photo-excitation of an ensemble of Stark states in the presence of a weak dc field. Calculations and experiment show that states located near the Stark-shifted d-level have sizable polarizations. We plan to study the non-linear dynamics of these polarized states under the influence of a train of unipolar pulses. Depending on the orientation of the Rydberg states, the dynamics is expected to be regular or chaotic and should yield clear differences in the survival probability of Rydberg atoms. When the dynamics becomes globally chaotic, the resulting system provides a low-dimensional laboratory to study quantum localization.

We have developed a Liouville master equation approach to describe the interaction of highly charged ions with insulator surfaces including the close-collision regime above the surface. Our approach employs a Monte-Carlo solution of the master equation for the joint probability density of the ionic motion and the electronic population of the projectile and the target surface. It includes single as well as double particle-hole de-excitation processes and incorporates electron correlation effects through the conditional dynamics of population strings. The input in terms of elementary one- and two-electron transfer rates is determined from CTMC calculations as well as quantum mechanical Auger calculations. For slow projectiles and normal incidence, the ionic motion depends sensitively on the interplay between image acceleration towards the surface and repulsion by an ensemble of positive hole charges in the surface ("trampoline effect"). For Ne^{10+} ions we find that image acceleration dominates and no collective backscattering high above the surface takes place. For grazing incidence, our simulation delineates the pathways to complete neutralization, in accordance with recent experimental observations.[3]

1. E. Lamour et al., "Ar^{17+} Excited State Populations through Solid and Gaseous Targets," Book of Abstracts, Intl. Conf. on the Physics of Highly Charged Ions, Sept. 1-6, 2002, Caen, France, p. 172.

Analysis of Structure in Low-Energy Ion-Atom Collisions – *J. H. Macek and S. Yu. Ovchinnikov*

For low-energy ion-atom collisions the interactions between three charged particles, namely an electron and two positively charged nuclei, are non-negligible even at nuclear separations of thousands of atomic units. It is impractical to treat this "distant" region by numerical methods that give exact solutions in small volumes. Rather, such solutions must be joined to analytic solutions at larger distances. Such analytic solutions are not known in complete generality, but we have obtained an expression that reliably represents motion in the top-of-barrier region, i.e., the region where the force on the electron due to the charged particles nearly vanishes.[1] When this analytic representation is used with numerical calculations of Schultz and coworkers,[2] we obtain results that are in qualitative agreement with measured energy and angular distributions.

A key quantity for applications of ionization of atomic hydrogen by ion impact is the total detachment cross section. Different *ab initio* calculations of this quantity give results that disagree with experiment and among themselves by about twenty percent at the cross section maxima. There is some indication that this may be due to differing treatments of Rydberg states. We will investigate this discrepancy by using our Sturmian based method to compute the Rydberg state contribution for comparison with the Lattice Time Dependent Schrödinger Equation (LTDSE) results of Schultz and coworkers.

We will also investigate sources of oscillatory structure in low-energy ion-impact capture cross sections. In particular we will investigate whether some recently discovered, purely quantal structures in proton-hydrogen collisions are present in collisions of other species.[3]

1. J. H. Macek and S. Yu. Ovchinnikov, "Energy and Angular Distributions of Electrons Ejected from Atomic Hydrogen by Low Energy Proton Impact," accepted for publication in Phys. Rev. A (2004).
2. D. R. Schultz, C. O. Reinhold, P. S. Krstic, and M. R. Strayer, "Ejected Electron Spectra in Low-Energy Proton-Hydrogen Collisions," Phys. Rev. A **65**, 052722 (2002).
3. P. Krstic, J. H. Macek, and S. Yu. Ovchinnikov, "Computations of Elastic Scattering and Spin Exchange in H^+ + H Collisions for Impact Energies between 10^{-4} and 10 eV," accepted for publication in Phys. Rev. A (2004).

References to Publications of DOE Sponsored Research from 2002-2004 (decending order)

Year 2004 publications

"Multi-Electron Dynamics for Neutralization of Highly Charged Ions Near Surfaces," J. Burgdorfer, L. Wirtz, C. O. Reinhold, and C. Lemell, Vacuum **73**, 3 (2004).

"Classical and Quantum Scaling for Localization of Half-Cycle Pulse-Driven Rydberg Wavepackets," D. G. Arbo, C. O. Reinhold, and J. Burgdorfer, Phys. Rev. A **69**, 023409 (2004).

"Characterization of Quasi One-Dimensional Rydberg Atoms Using Half-Cycle Pulse Applied Perpendicular to the Atomic Axis," W. Zhao, J. C. Lancaster, F. B, Bunning, C. O. Reinhold, J. Burgdorfer, Phys. Rev A **69**, 041301 (2004).

"High-Energy Ion Generation by Short Laser Pulses," A. Maksimchuk, K. Klippo, H. Krause, G. Mourou, K. Nemoto, D. Schultz, D. Umstadter, R. Vane, V. Yu. Bychenkov, G. I. Dudnikova, V. F. Kovalev, K. Mima, V. N. Novikov, Y. Sentoku, and S. V. Tolokonnikov, Plasma Phys. Rep. **30**, 473 (2004).

"Dynamics of Ionization in Atomic Collisions," S. Yu. Ovchinnikov, G. N. Ogurtsov, J. H. Macek, and Yu. S. Gordeev, Phys. Rep. **389**, 119 (2004).

"Tailoring and Controlling Wave Packets In Multi-Photon Atom Collisions," Yoshida, S., E. Persson, C. O. Reinhold, J. Burgdörfer, B. E. Tannian, C. L. Stokely, and F. B. Dunning, [Invited Presentation], Proceedings of XXIII International Conference on Photonic, Electronic, and Atomic Collisions (ICPEAC), Stockholm, Sweden, July 23-29, 2003, Physica Scripta **T110**, 424 (2004).

"Electron Capture by Ne^{3+} Ions from Atomic Hydrogen," Rejoub, R., M. E. Bannister, C. C. Havener, D. W. Savin, C. J. Verzani, J. G.Wang, and P. C. Stancil, Phys. Rev. A **69**, 052704 (2004).

"Charge Changing Interactions of Ultrarelativistic Pb Nuclei," C. Scheidenberger, I. A. Pshenichnov, K. Summerer, A. Ventura, J. P. Bondorf, A. S. Botvina, I. N. Mishustin, D. Boutin, S. Datz, H. Geissel, P. Grafstrom, H. Knudsen, H. F. Krause, B. Lommel, S. P. Moller, G. Munzenberg, R. H. Schuch, E. Uggerhøj, U. Uggerhøj, C. R. Vane, Z. Z. Vilakazi, and H. Weick, Phys. Rev. C **70**, 014902 (2004).

"Site-Specific Neutralization of Slow Multicharged Ions Incident on Solid Surfaces," F. W. Meyer, H. F. Krause, V. A. Morozov, C. R. Vane, and L. I. Vergara, Physica Scripta **T110**, 403 (2004).

"Low Energy Charge Transfer with Multi-Charged Ions Using Merged Beams," C. C. Havener, Proceedings, American Physical Society Spring Meeting on Atomic Processes in Plasmas, Santa Fe, New Mex., April 19-22, 2004, AIP Conference Proceedings, American Institute of Physics, Woodbury, N.Y., 2004.

"Charge Transfer in Low Energy Collisions of He^{2+} with Atomic Hydrogen," C. C. Havener, R. Rejoub, P. S. Krstic, and A. C. H. Smith, submitted to Phys. Rev. A (2004).

"Computations of Elastic Scattering and Spin Exchange in H^+ + H Collisions for Impact energies between 10^{-4} and 10 eV," P. Krstic, J. H. Macek, and S. Yu. Ovchinnikov, accepted for publication in Phys. Rev. A (2004).

"Analysis of Structures in the Cross Sections for Elastic Scattering and Spin Exchange in Low Energy H^+ + H Collisions," P. S. Krstic, J. H. Macek, S. Yu. Ovchinnikov, and D. R. Schultz, submitted to Phys. Rev. A (2004).

"Regg Oscillations in Integral Cross Sections for Proton Impact on Atomic Hydrogen," J. H. Macek, P. S. Krstic, and S. Yu. Ovchinnikov, submitted to Phys. Rev. Lett. (2004).

"Electron Capture by Ne^{4+} Ions from Atomic Hydrogen," C. C. Havener, R. Rejoub, C. R. Vane, H. F. Krause, D. W. Savin, J. G. Wang, and P. C. Stancil, submitted to Phys. Rev. A (2004).

"Energy and Angular Distributions of Electrons Ejected from Atomic Hydrogen by Low Energy Proton Impact," J. H. Macek and S. Yu. Ovchinnikov, accepted for publication in Phys. Rev. A (2004).

"Measurements of Chemical Erosion of ATJ Graphite by Low Energy D_2^+ Impact," F. W. Meyer, H. F. Krause, and L. I. Vergara, Proceedings, International Conference on Plasma Surface Interactions, Portland, Maine, May 24-28, 2004, submitted to J. Nucl. Mater. (2004).

"Energy and Angular Distributions of Electrons Ejected from Atomic Hydrogen by Low Energy Proton Impact," J. H. Macek and S. Yu. Ovchinnikov, submitted to Phys. Rev. A (2004).

"Chemical Sputtering of ATJ Graphite Induced by Low-Energy D_2^+ Bombardment," L. I. Vergara, F. W. Meyer, and H. F. Krause, submitted to Nucl. Instrum. Methods Phys. Res. B (2004).

"Response of Highly Polarized Rydberg States to Trains of Half-Cycle Pulses," C. O. Reinhold, W. Zhao, J. C. Landcaster, F. B. Dunning, E. Persson, D. G. Arbo, S. Yoshida, and J. Burgdorfer, submitted to Phys. Rev. A (2004).

"Non-Unitary Master Equation for the Internal State of Ions Transversing Solids," M. Seliger, C. O. Reinhold, T. Minami, and J. Burgdorfer, submitted to Nucl. Instrum. Methods Phys. Res. B (2004).

"Steering Rydberg Wave Packets Using a Chirped Train of Half-Cycle Pulses," S. Yoshida, C. O. Reinhold, E. Persson, J. Burgdorfer, and F. B. Dunning, submitted to J. Phys. B. (2004).

"Coherence Parameters for Charge Transfer in Collisions of Protons with Helium Calculated Using a Hybrid Numerical Approach," T. Minami, C. O. Reinhold, D. R. Schultz, and M. S. Pindzola, submitted to J. Phys. B (2004).

Year 2003 publications

"Absolute Measurements of Cross Sections for Near-Threshold Electron-Impact Excitation of Na-like and Mg-like Multiply Charged Ions," A.C.H. Smith, M. E. Bannister, Y.-S. Chung, A M. Derkatch, N. Djuric, H. F. Krause, D. B. Popovic, B. Wallbank, and G. H. Dunn, Nucl. Instrum. Methods Phys. Res. B **205**, 421 (2003).

"Electron-Impact Dissociation of CH^+ Ions: Measurements of C^+ Fragment Ions," M. E. Bannister, H. F. Krause, C. R. Vane, N. Djuric, D. B. Popovic, M. Stepanovic, G. H. Dunn, Y.-S. Chung, A.C.H. Smith, and B. Wallbank, Phys. Rev. A **68**, 042714 (2003).

"Observation of Trielectronic Recombination in Be-like Cl Ions," M. Schnell, G. Gwinner, N. R. Badnell, M. E. Bannister, S. Böhm, J. Colgan, S. Kieslich, S. D. Loch, D. Mitnik, A. Müller, M. S. Pindzola, S. Schippers, D. Schwalm, W. Shi, A. Wolf, and S.-G. Zhou, Phys. Rev. Lett. **91**, 043001 (2003).

"Production of Quasi-One-Dimensional Very-High-n Rydberg Atoms," C. L. Stokely, J. C. Lancaster, F. B. Dunning, D. G. Arbo, C. O. Reinhold, and J. Burgdörfer, Phys. Rev. A **67**, 013403 (2003).

"Liouville Master Equation for Multi-Electron Dynamics: Neutralization of Highly Charged Ions Near an LiF Surface," K. Wirtz, C. O. Reinhold, C. Lemell, and J. Burgdörfer, Phys. Rev. A **67**, 012903 (2003).

"Three-body Reaction Dynamics in Dissociative Recombination," R. Thomas, F. Hellberg, M. Larsson, C. R. Vane, P. Andersson, J. Pattersson, A. Petrignani, and W. J. van der Zande, AIP Conference Proceedings **680**, 187-190 (2003).

"Recent Studies of Three-Body Fragmentation Dynamics via Dissociative Recombination in CRYRING," R. Thomas, S. Datz, M. Larsson, W. J. van der Zande, F. Hellberg, A. Petrignani, S. Rosén, A. M. Derkatch, A. Neau, and C. R. Vane, in *Dissociative Recombination of Molecular Ions with Electrons*, ed., S. Guberman, Kluwer Academic Publication (2003) pp. 95-100.

"Quantum Trajectory Monte Carlo Method for Internal State Evolution of Fast Ions Traversing Amorphous Solids," T. Minami, C. O. Reinhold, J. Burgdörfer, Phys. Rev. A **67**, 022902 (2003).

"Quantum Trajectory Monte Carlo Method Describing the Coherent Dynamics of Highly Charged Ion," T. Minami, C. O. Reinhold, and J. Burgdörfer, Nucl. Instrum. Methods Phys. Res. B **205**, 818 (2003).

"Low-Energy Electron Capture Measurements Using Merged Beams," C. C. Havener, in *The Physics of Multiply and Highly Charged Ions*, Vol. 2 of *Interactions with Matter*, ed. Fred J. Currell, Kluwer Academic Publishers, The Netherlands (2003), pp. 193-218.

"Ionization of Helium by Antiprotons: Fully Correlated, Four-Dimensional Lattice Approach," D. R. Schultz, and P. S. Krstic, Phys. Rev. A **67**, 022712 (2003).

"Elastic and Transport Cross Sections for Argon in Hydrogen Plasmas," P. S. Krstic, D. R. Schultz, and T. Chung, Phys. Plasmas **10**, 869 (2003).

"Site-Resolved Neutralization of Slow Singly and Multiply Charged Ions during Large-Angle Backscattering Collisions with RbI(100)," F. W. Meyer, H. F. Krause, and C. R. Vane, Nucl. Instrum. Methods Phys. Res. B **203**, 231 (2003).

"Laser-Modified Charge Transfer Processes in Proton Collisions with Lithium Atoms," M. S. Pindzola, T. Minami, and D. R. Schultz, Phys. Rev. A **68**, 013404 (2003).

"Excited-State Evolution Probed by Convoy-Electron Emission in Relativistic Heavy-Ion Collisions," Takabayashi, Y., T. Ito, T. Azuma, K. Komaki, Y. Yamazaki, H. Tawara, E. Takada, T. Murakami, M. Seliger, K. Tökesi, C. O. Reinhold, and J. Burgdörfer, Phys. Rev. A **68**, 042703 (2003).

"Electron Capture by Ne^{2+} Ions from Atomic Hydrogen," T. Mroczkowski, D. W. Savin, R. Rejoub, P. S. Krstic, and C. C. Havener, Phys. Rev. A **68**, 032721 (2003).

"Quantum Localization in the Three-Dimensional Kicked Rydberg Atom," E. Persson, S. Yoshida, X.-M. Tong, C. O. Reinhold, and J. Burgdörfer, Phys. Rev. A **68**, 063406 (2003).

"Projectile Neutralization in Large-Angle Back-Scattering of Slow F^{q+}, Ne^{q+}, and Ar^{q+} Incident on RbI(100)," F. W. Meyer, H. F. Krause, and C. R. Vane, Nucl. Instrum. Methods Phys. Res. B **205**, 700 (2003).

"Highly Transverse Velocity Distribution of Convoy Electrons Emitted by Highly Charged Ions," M. Seliger, K. Tokesi, C. O. Reinhold, and J. Burgdörfer, Nucl. Instrum. Methods Phys. Res. B **205**, 830 (2003).

"Pulse-Induced Focusing of Rydberg Wavepackets," D. G. Arbo, C. O. Reinhold, J. Burgdörfer, A. K. Pattanayak, C. L. Stokely, W. Zhao, J. C. Lancaster, and F. B. Denning, Phys. Rev. A **67,** 063401 (2003).

"Annihilation of Low Energy Antiprotons in Hydrogen," S. Yu. Ovchinnikov and J. H. Macek, *CAARI 2002*, AIP Conference Proceedings **680** (2003).

"Quantum Trajectory Monte Carlo Method Describing the Coherent Dynamics of Highly Charged Ions," T. Minami, C. O. Reinhold, and J. Burgdörfer, Nucl. Instrum. Methods Phys. Res. B **205**, 818 (2003).

"Liouville Master Equation for Multi-electron Dynamics: Neutralization of Highly Charged Ions near a LiF Surface," L. Wirtz, C. O. Reinhold, C. Lemell, and J. Burgdorfer, Phys. Rev. A **67**, 012903 (2003).

"Interaction of Highly Charged Ions with Insulator Surfaces at Low Velocities: Estimates for Auger Rates," J. Burgdorfer, C. O. Reinhold, and F. Meyer, Nucl. Instrum. Methods Phys. Res. B **205**, 690 (2003).

"The Kicked Rydberg Atom: A New Laboratory for Study of Non-Linear Dynamics," F. B. Dunning, C. O. Reinhold, and J. Burgdörfer, Physica Scripta **68**, C44 (2003).

"Correlated Electron Detachment in H^- - He Collisions," G. N. Ogurtsov, V. M. Mikoushkin, S. Yu. Ovchinnikov, and J. H. Macek, submitted to Phys. Rev. Lett. (2003).

"Target Orientation Dependence of the Charge Fractions Observed for Low-Energy Multicharged Ions Ne^{q+} and F^{q+} Backscattered from RbI(100)," L. I. Vergara, F. W. Meyer, and H. F. Krause, [Invited Presentation], Proceedings, 13th International Conference on Surface Modification of Materials by Ion Beams (SMMIB), San Antonio, TX, Sept. 21-26, 2003, Surface and Coating Technology (2003).

Year 2002 publications

"Lassettre's Theorem for Excitation of Ions by Charged Particle Impact," J. H. Macek and N. Avdonina, J. Phys. B **35**, 1775 (2002).

"Electron Capture in Collisions of S^{4+} with Helium," J. G. Wang, A. R. Turner, D. L. Cooper, D. R. Schultz, M. J. Rakovic, W. Fritsch, P. C. Stancil, and B. Zygelman, J. Phys. B **35**, 3137 (2002).

"Merged-Beams Measurements of Electron-Impact Excitation of $Al^{2+}(3s^2S \rightarrow 3p^2P)$," M. E. Bannister, H. F. Krause, N. Djuric, D. B. Popovic, G. H. Dunn, Y.-S. Chung, and A.C.H. Smith, Phys. Rev. A **66**, 032707 (2002).

"Ion-Implantation-Related Atomic Collision Studies at the ORNL MIRF," F. W. Meyer, M. E. Bannister, C. C. Havener, H. F. Krause, P. Krstic, D. R. Schultz, A. Aggarwal, D. Swensen, and F. Yan, pp. 125-134 in Proceedings, 13th APS Topical Conference on Atomic Processes in Plasmas, Gatlinburg, Tenn., April 22-25, 2002, AIP Conference Proceedings **635**, American Institute of Physics, Melville, N.Y., 2002.

Proceedings of Third International Conference on Atomic and Molecular Data and Their Applications (ICAMDATA), Gatlinburg, Tenn., April 24-27, 2002, ed. D. R. Schultz, P. S. Krstic, and F. Ownby, AIP Conference Proceedings **636**, American Institute of Physics, Woodbury, N.Y., 2002.

Proceedings of 13th APS Topical Conference on Atomic Processes in Plasmas, *Gatlinburg, TN, April 22-25, 2002*, ed. D. R. Schultz, F. W. Meyer, and F. Ownby, AIP Conference Proceedings **635**, American Institute of Physics, Woodbury, N.Y., 2002.

"Quantum Localization in the High Frequency Limit," E. Persson, S. Yoshida, X.-M. Tong, C. O. Reinhold, and J. Burgdörfer, Phys. Rev. A **66**, 043407 (2002).

"Electromagnetically Induced Nuclear-Charge Pickup Observed in Ultrarelativistic Pb Collisions," C. Scheidenberger, I. A. Pshenichnov, T. Aumann, S. Datz, K. Sümmerer, J. P. Bondorf, D. Boutin, H. Geissel, P. Grafström, H. Knudsen, H. F. Krause, B. Lommel, S. P. Møller, G. Münzenberg, R. H.

Schuch, E. Uggerhøj, U. Uggerhøj, C. R. Vane, Ventura, Z. Z. Vilakazi, and H. Weick, Phys. Rev. Lett. **88**, 042301 (2002).

Photonic, Electronic, and Atomic Collisions, Proceedings of the Invited Talks, XXII ICPEAC, ed. J. Burgdörfer, J. S. Cohen, S. Datz, and C. R. Vane (Rinton Press, Princeton, NJ, 2002).

"Laboratory Measurements of Charge Transfer on Atomic Hydrogen at Thermal Energies," C. C. Havener, C. R. Vane, H. F. Krause, P. C. Stancil, T. Mrodzkowski, and D. Savin, *Proceedings, NASA Laboratory Astrophysics Workshop*, NASA-Ames Research Center, CA, May 2002.

"Ejected-Electron Spectrum in Low-Energy Proton-Hydrogen Collisions," D. R. Schultz, C. O. Reinhold, P. S. Krstic, and M. R. Strayer, Phys. Rev. A **65**, 052722 (2002).

"Exact Electron Spectra in Collisions of Two Zero-Range Potentials with Non-Zero Impact Parameters," S. Yu. Ovchinnikov, D. B. Khrebtukov, and J. H. Macek, Phys. Rev. A **65**, 032722 (2002).

"Evidence of Collisional Coherences in the Transport of Hydrogenic Krypton Through Amorphous Carbon Foils," T. Minami, C. O. Reinhold, M. Seliger, J. Burgdörfer, C. Fourment, B. Gervais, E. Lamour, J. P. Rozet, and D. Vernhet, Nucl. Instrum. Methods Phys. Res. B **193**, 79 (2002).

"Time Dependent Dynamics of Atomic Systems," M. S. Pindzola, F. J. Robicheaux, J. Colgan, D. M. Mitnik, D. C. Griffin, and D. R. Schultz, in *Photonic, Electronic & Atomic Collisions, Proceedings of the XXII ICPEAC,* J. Burgdörfer, J. S. Cohen, S. Datz, and C. R. Vane, eds. (Rinton Press, Princeton, 2002), p. 483.

"Recent Advances and Applications of Lattice, Time-Dependent Approaches: Fundamental One- and Two-Electron Collision Systems," D. R. Schultz, P. S. Krstic, C. O. Reinhold, M. R. Strayer, M. S. Pindzola, and J. C. Wells, in *Photonic, Electronic & Atomic Collisions, Proceedings of the XXII ICPEAC*, J. Burgdörfer, J. S. Cohen, S. Datz, and C. R. Vane, eds. (Rinton Press, Princeton, 2002), p. 536.

"Comparative Study of Surface-Lattice-Site Resolved Neutralization of Slow Multicharged Ions During Large-Angle Quasi-Binary collisions with Au(110): Simulation and Experiment," F. W. Meyer and V. A. Morozov, Nucl. Instrum. Methods Phys. Res. B **193**, 530 (2002).

"Large-Angle Backscattering of Ar^{q+} (q = 1 – 13) During Quasi-Binary Collisions with CsI(100) in the Energy Range 10 eV/q – 2.8 keV/q: Energy Loss Analysis and Scattered Charge-State Distributions," F. W. Meyer, V. A. Morozov, J. Mrogenda, C. R. Vane, and S. Datz, Nucl. Instrum. Methods Phys. Res. B **193**, 508 (2002).

Quantum Localization in the High Frequency Limit," E. Persson, S. Yoshida, X. Tong, C. O. Reinhold, and J. Burgdörfer," Phys. Rev. A **66**, 043407 (2002).

"Quantum Transport of Kr^{35+} Ions through Amorphous Carbon Foils," T. Minami, C. O. Reinhold, M. Seliger, J. Burgdörfer, C. Fourment, B. Gervais, E. Lamour, J.-P. Rozet, and D. Vernhet, Phys. Rev. A **65**, 032901 (2002).

"Transient Phase Space Localization," C. L. Stokely, F. B. Dunning, C. O. Reinhold, and A. K. Pattanayak, Phys. Rev. A **65,** 021405 (2002).

"Absolute Cross Sections for Electron-Impact Excitation of the $3d^2\ ^3F \rightarrow 3d4p\ ^3D,\ ^3F$ Transitions in Ti^{2+}," D. B. Popovic, M. E. Bannister, R.E.H. Clark, Y.-S. Chung, N. Djuric, F. W. Meyer, A. Müller, A. Neau, M. S. Pindzola, A.C.H. Smith, B. Wallbank, and G. H. Dunn, Phys. Rev. A **65**, 034704 (2002).

"Three-Body Recombination of Ultracold Atoms Near a Feshbach Resonance," O. J. Kartavtsev and J. H. Macek, Few-Body Systems **31**, 249 (2002).

Research Summaries

(single-PI grants by PI)

Molecular Structure and Electron-Driven Dissociation and Ionization

Kurt H. Becker and Vladimir Tarnovsky
Department of Physics and Engineering Physics and Center for Environmental Systems,
Stevens Institute of Technology, Hoboken, NJ 07030
phone: (201) 216-5671; fax: (201) 216-5638; kbecker@stevens.edu

Program Scope:

This program is aimed at investigating the molecular structure and the collisional dissociation and ionization of selected molecules and free radicals. The focus areas are (1) ionization studies of selected molecules and free radicals and (2) the study of electron-impact induced neutral molecular dissociation processes. Targets of choice for ionization studies include WF_6, $SiCl_4$ and BCl_3 and their radicals, the molecular halogens Cl_2, Br_2, and F_2 and the radicals SF, SF_2, and SF_4. Targets of choice for the neutral molecular dissociation studies include $SiCl_4$, BCl_3, NO_2, and N_2O. The fragments to be probed include Si(^{1}S), Si(^{1}D), Si(^{3}P), BCl($X\ ^1\Sigma$), B($^2P^o$), and NO ($X\ ^2\Pi$). This choice is motivated on one hand by the relevance of these species in specific technological applications involving low-temperature processing plasmas and, on the other hand, by basic collision physics aspects (WF_6 is similar in its structure to SF_6, $SiCl_x$ and BCl_x are similar to $TiCl_x$ and SiF_x).

The scientific objectives of the research program can be summarized as follows:

(1) to provide the atomic and molecular data that are required in efforts to understand the properties of low-temperature processing plasmas on a microscopic scale

(2) to identify the key species that determine the dominant plasma chemical reaction pathways

(3) to measure cross sections and reaction rates for the formation of these key species and to attempt to deduce predictive scaling laws

(4) to establish a broad collisional and spectroscopic data base which serves as input to modeling codes and CAD tools for the description and modeling of existing processes and reactors and for the development and design of novel processes and reactors

(5) to provide data that are necessary to develop novel plasma diagnostics tools and to analyze more quantitatively the data provided by existing diagnostics techniques

Specific Recent Progress:

Ionization of SF_3 and SF_5 Radicals:

Absolute Ionization Cross Section Measurements and Calculations: When the measured total single ionization cross sections for SF_3 and SF_5 were compared to BEB and DM calculations, it was found that much like in the case of the CF_x and NF_x radicals there was a serious discrepancy between experimentally determined and calculated cross section. The recent work of Dr. Huo in conjunction with a thorough re-analysis of our earlier data has demonstrated that the use of a modified and improved siBEB method has resolved this issue (as in the case of the CF_x and NF_x species). We now have excellent agreement between measured and calculated ionization cross sections for both radicals.

SF_3^+ Ionization Cross Section Shape: While most partial ionization cross sections for the formation of positive fragment ions from SF_6 exhibit the smooth energy dependence, which is typical for ionization cross section curves, the SF_3^+ partial ionization cross section function displays a pronounced structure around 40 eV. This structure might indicate that several processes with different threshold energies contribute to the measured SF_3^+ partial ionization

cross section. We carried out a detailed study of the formation of SF_3^+ fragment ions produced by electron impact on SF_6 using the mass-analyzed ion kinetic energy (MIKE) scan technique. The use of this technique allowed us to identify a contribution to the measured SF_3^+ signal arising from the Coloumb explosion of doubly positively charged SF_4^{2+} ions into two singly charged ions, SF_3^+ and F^+, with a threshold energy of about 43 eV. The direct dissociative ionization of SF_6 leading to the formation of SF_3^+ fragment ions has a threshold of about 22 eV.

Ionization of WF_6: We measured absolute partial cross sections for the formation of positive ions followed by electron impact on WF_6 from threshold to 900 eV using a time-of-flight mass spectrometer. Dissociative ionization processes resulting in seven different singly charged ions (F^+, W^+, WF_x^+, x = 1–5) and five doubly charged ions (W^{2+}, WF_x^{2+}, x = 1-4) are the dominant ionization channels. The ion spectrum at all impact energies is dominated by WF_5^+ ions. At 120 eV, the partial WF_5^+ ionization cross section has a maximum value of 3.92×10^{-16} cm^2 (43% of the total ion yield). The cross section values of all the other singly charged fragment ions at 120 eV range from $0.39 - 0.73 \times 10^{-16}$ cm^2. The ionization cross sections of the doubly charged ions are more than one order of magnitude lower than the cross section of WF_5^+. Double ionization processes account for 21% of the total ion yield at 120 eV. The absolute total ionization cross section of WF_6 was obtained as the sum of all measured partial ionization cross sections and is compared with available calculated cross sections.

Ionization of Cl_2: We measured absolute partial cross sections for the formation of Cl_2^+, Cl_2^{++}, Cl^+, and Cl^{++} ions following electron impact on molecular chlorine (Cl_2) from threshold to 900 eV using a time-of-flight mass spectrometer. The ion spectrum at all impact energies is dominated by the singly charged fragment ions with maximum cross section values of 4.6×10^{-16} cm^2 for Cl_2^+ at 32 eV and 4.0×10^{-16} cm^2 for Cl^+ at 70 eV. The cross sections for the formation of the doubly charged ions are more than one order of magnitude lower. Double ionization processes account for about 6% of the total ion yield at 70 eV. The absolute total ionization cross section of Cl_2 was obtained as the sum of all measured partial ionization cross sections.

Ionization of Uracil: Even though we did not propose to study any biologically important molecules in our original proposal, we seized the opportunity to carry out a measurement of partial cross sections for the formation of selected positive and negative ions resulting from electron interactions with the RNA base uracil ($C_4H_4N_2O_2$) and put them on an absolute scale. Absolute calibration of the measured partial cross sections for the formation of the three most intense positive ions, the parent $C_4H_4N_2O_2^+$ ion and the $C_3H_3NO^+$ and OCN^+ fragment ions, was achieved by normalization of the total single uracil ionization cross section (obtained as the sum of all measured partial single ionization cross sections) to a calculated cross section based on the semi-classical Deutsch-Märk (DM) formalism at 100 eV. Subsequently, we used the OCN^+ cross section in conjunction with the known sensitivity ratio for positive and negative ion detection in our apparatus (obtained from the well-known cross sections for SF_4^+ and SF_4^- formation from SF_6) to determine the dissociative attachment cross section for OCN^- formation from uracil. This cross section was found to be roughly an order of magnitude smaller, about 5×10^{-22} m^2 at 6.5 eV, compared to previously reported preliminary value. We attribute this discrepancy to the difficult determination of the uracil target density in the earlier work. Using a reliably calculated cross section for normalization purposes avoids this complication.

Ionization Cross Section Calculations. All experimental ionization studies were also supported by our continuing effort to extend and refine our semi-classical approach to the calculation of total single ionisation cross sections for molecules and free radicals. In general, we now have a

achieved a level of agreement between calculation and experiment of better than 20% (and in many cases of better than 10%). This level of agreement gives us confidence as to the predictive capabilities of our approach for molecules for which no experimental data are available.

Neutral Molecular Dissociation Studies. We completed the first stage of a cross-comparison of neutral dissociation cross sections for SiH_4, SiF_4, and several Si-organic compounds (TMS, HMDSO, TEOS) with particular emphasis on the determination of final-state specific cross sections for the formation of $Si(^1S)$ and $Si(^1D)$ atoms. As a first result, in the case of the formation of $Si(^1S)$ atoms from SiH_4 and SiF_4 we found cross sections of about 5 x 10^{-17} cm^2 (SiH_4) and 2.8 x 10^{-17} cm^2 (SiF_4) at 60 eV. We note that the cross sections for $Si(^1S)$ formation from SiH_4 and SiF_4 have distinctly different energy dependences.

Ongoing studies and future work - Ionization

$SiCl_4$ and the $SiCl_x$ radicals: $SiCl_4$ has a similar structure to fluorinated and hydrogenated targets that we studied in the past (SiF_4, SiH_4). No ionization cross section data are available for the molecule. Perhaps most importantly, the $SiCl_4$ molecule is a candidate for electron-impact ionization studies on thin deposited $SiCl_4$ films (T. Orlando, private communication, 2002). This affords a unique opportunity to explore how the ionization properties of a molecule change from the gas phase to the condensed phase. Absolute cross sections for $SiCl_4$ have now been obtained and we are in the process of carrying out a comprehensive series of absolute partial ionization cross section measurements for the $SiCl_x$ (x=1-3) radicals using our fast-beam apparatus. The experimental results will be complemented by semi-classical calculations of the total single ionization cross sections.

SF, SF_2, and SF_4 Free Radicals: The recent work of Dr. Huo has demonstrated that the use of a modified and improved siBEB method has resolved this earlier discrepancy between measured and calculated ionization cross sections for and SF_5. We now re-visit the experimental determination of the ionization properties of the remaining 3 radicals SF, SF_2, and SF_4 and determine a comprehensive set of cross sections for the ionization and dissociative ionization.

Br_2 and F_2: The status of the collisional and spectroscopic data bases for F_2 and Br_2 are in general much more fragmentary than those for Cl_2. After our work on Cl_2 we will carry out similar studies for the Br_2 and F_2 molecules in an attempt to establish common trends and similarities (or a lack thereof) in the data for the 3 molecular halogens F_2, Cl_2, and Br_2.

BCl_3 and the BCl_x radicals: There is some information in the literature on the formation of positive and negative ions formed by electron impact on BCl_3 and on the spectroscopy of BCl_3 and the BCl free radical, which is widely used in optical diagnostics studies of BCl_3-containig plasmas. There have also been some recent calculations of electron collisions with BCl_3. Earlier ionization studies used Fourier transform mass spectrometry (FTMS) to obtain absolute partial ionization cross sections. Results obtained by this technique can be plagued by serious systematic errors. We are in the process of measuring a complete set of absolute partial ionization cross sections for BCl_3 and for the BCl radical with special emphasis on the low-energy, near-threshold region using the fast-beam technique. Based on some preliminary studies we will be using pure BCl_3 or a defined mixture of BCl_3 and Ar to produce the primary ions.

Ongoing studies and future work – Neutral Dissociation

$SiCl_4$: This molecule is a natural choice as a target for the neutral dissociation studies leading to final-state specific Si cross sections as it extends the sequence of SiH_4 and SiF_4 to the chlorine-containing compound. Moreover, similar to SiH_4 and SiF_4, we also measure ionization and

dissociative ionization cross sections for $SiCl_4$, so that this becomes another molecule for which we will have a broad data base of collisional data on ionization and dissociation.

***BCl_3*:** The significance and importance of the BCl_3 molecule in various applications has already been discussed in the previous section. We will investigate the two neutral dissociation channels which have most likely the largest partial dissociation cross sections, (i) the break-up of the parent molecule into a ground-state BCl fragment in the ($X\ ^1\Sigma$) state which will be detected by pumping and probing the strong $X\ ^1\Sigma \rightarrow A\ ^1\Pi^+$ transition near 272 nm and (ii) the boron atom in its ($^2P^o$) ground-state which will be probed via the (2p) $^2P^o \rightarrow$ (3s) ^2S transition at 250 nm. Both measurements will require the use of the frequency doubler.

NO_2 and N_2O: The studies of the neutral molecular dissociation of NO_2 and N_2O into NO complement the (dissociative) ionization studies for these compounds that were carried out recently. The formation of NO from these molecules is an important reaction pathway in combustion processes and in atmospheres.

Publications Acknowledging DOE Support (since 2002)

1. "Calculated Absolute Cross Section for the Electron-Impact Ionization of CO_2^+ and N_2^+", J. Phys. B 35, L65, (2002), with H. Deutsch, P. Defrance, U. Onthong, R. Parajuli, M. Probst, S. Matt, and T. Märk
2. "Calculated Cross Sections for the K-Shell Ionization of Fe, Co, Mn, Ti, Zn, Nb, and Mo Using the DM Formalism", Int. J. Mass Spectrom. 213, 5 (2002), with H. Deutsch, B. Gstir, and T.D. Märk
3. "Calculated Absolute Electron Impact Ionization Cross Sections for the Molecules CF_3X (X=H,Br,I)", Int. J. Mass Spectrom. 214, 53 (2002), with U. Onthong, H. Deutsch, S. Matt, M. Probst, and T. Märk
44. "Total Electron Impact Ionization Cross Sections of CF_x and NF_x (x=1-3)", Chem. Phys. Lett. 358, 328 (2002), with W.M. Huo and V. Tarnovsky
5. "Absolute Total and Partial Electron-Impact Ionization Cross Sections for C_2F_6", Int. J. Mass Spectrom. 214, 365 (2002), with R. Basner, M. Schmidt, E. Denisov, P. Lopata, and H. Deutsch
6. "Electron Impact Ionization of NO, N_2O, and NO_2", Int. J. Mass Spectrom. 225, 25 (2003), with J. Lopez and V. Tarnovsky
7. "Calculated Absolute Cross Sections for the Electron-Impact Ionization of Simple Molecular Ions", Int. J. Mass Spectrom. 223/224, 639 (2003), with H. Deutsch, P. Defrance, U. Onthong, M. Probst, S. Matt, P. Scheier, and T.D. Märk
8. "Absolute Total and Partial Electron-Impact Ionization Cross Sections for B_2H_6", J. Chem. Phys. 118, 2153 (2003), with R. Basner and M. Schmidt
9. "Revised High-Energy Behavior of the DM Formula for the Calculation of Electron Impact Ionization Cross Sections of Atoms", Int. J. Mass Spectrom. 233, 13-7 (2004), with H. Deutsch, P. Scheier, and T.D. Märk
10. "Calculated Cross Sections for the Electron-Impact Detachment from Negative Ions Using the DM Formalism", Chem. Phys. Lett. 382, 26-31 (2003), with H. Deutsch, P. Scheier, and T.D. Märk
11. "Measurement of Absolute Partial and Total Electron Ionization Cross Sections of Tungsten Hexafluoride", Int. J. Mass Spectrom. 233, 25-31 (2004), with R. Basner and M. Schmidt
12. "Electron Impact Ionization Cross Sections of SF_5 and SF_3", Int. J. Mass Spectrom. 233, 111-6 (2004), with W.Huo and V. Tarnovsky
13. "The Anomalous Shape of the Cross Section for the Formation of SF_3^+ Fragment Ions Produced by Electron Impact on SF_6 Revisited", J. Chem. Phys. 120, 11465-8 (2004), with S. Feil, K. Gluch, P. Scheier, and T.D. Märk
14. "Calculated Cross Sections for the Electron Impact Ionization of Excited Ar Atoms Using the DM Formalism, Int. J. Mass Spectrom. 233, 39-43 (2004), with H. Deutsch, A.N. Grum-Grzhimailo, K. Bartschat, H. Summers, M. Probst, S. Matt-Leubner, and T.D. Märk

Bose and Fermi Gases With Strong Anisotropic Interactions

John L. Bohn
JILA, UCB 440
University of Colorado
Boulder, C 80309
bohn@murphy.clolrado.edu

Quantum degenerate Bose and Fermi gases have produced an incredible wealth of many-body phenomena in a carefully controlled experimental environment. Remarkably, the vast majority of phenomena can be described theoretically within a mean-field approach, and assuming that particle interactions take the form of isotropic contact potentials. This reflects the fact that the internal structure of the atoms is *almost* irrelevant, although on the microscopic scale it is ultimately this structure that gives rise to atomic scattering lengths and their manipulation via magnetic-field Feshbach resonances.

This mean-field description is not longer adequate for strongly interacting systems. Notable among these are "resonant superfluids" in the vicinity of Feshbach resonances, and quantum degenerate gases composed of dipolar molecules. The work supported by this DOE grant, which will begin September 2004, will focus on strongly interacting degenerate gases with built-in anisotropies.

The first of these will be a resonant superfluid interacting via Feshbach resonances of p-wave character. Ordinarily, p-wave interactions in a single-component Fermi gas would generate a negligible interaction, owing to the Wigner threshold law. The situation is of course quite different in the presence of a resonance, which opens the exciting prospect of p-wave superfluidity in this dilute system. In addition, careful parametrization of the p-wave Feshbach resonance in $\left| fm_f \right\rangle = \left| 9/2, -7/2 \right\rangle$ states of optically trapped ^{40}K indicates that the next-order term in the expansion of scattering phase shift versus energy must also be included [1]. These interactions can be incorporated in the many-body theory via a generalized anisotropic contact potential that was derived in Refs. [2-4] for the non-resonant case. High-partial-wave resonances will moreover generally exhibit a multiplet structure [1], guaranteeing that each such resonance will generate its own anisotropy.

The second class of anisotropic gases will consist of atoms or molecules with large dipole moments. Preliminary theoretical work by several groups has discovered unusual features of quantum gases interacting via dipole forces. For example, the stability of a Bose gas against collapse turns out to be a function of the trapping geometery [5-9]. This is because the trap can either force the dipoles to lie predominantly side-by-side in a repulsive (hence stable) configuration, or else predominantly head-to-tail in an attractive (unstable) configuration. The stability is also strongly dependent on the counterplay between the long-range, anisotropic dipolar interaction, with the isotropic, short-range atomic potential [5]. This link is also

important for defining the character and stability of collective excitations [10-13], as well as ballistic expansion of the gas [14,15].

To date, all such theoretical studies have assumed that the dipoles are in the presence of a strong external field that aligns them along the field axis. Thus the interaction potential takes the simple form for polarized species:

$$V_p(r,\theta) = \frac{\mu^2}{r^3}\left(1-3\cos^2\theta\right), \tag{1}$$

where μ is the dipole moment, r is the distance between the molecules, and θ is the angle that the interparticle axis makes with respect to the field. For *finite* values of the external field, however, the dipoles can begin to point in other directions and can exert torques on one another. Thus the interaction has nontrivial angle and field dependencies, which should lead to a richer internal physics of the gas.

The interaction between real molecules, however, is strongly influenced by details of the molecules' internal structure. We have demonstrated this dramatically in the case of OH molecules, where the effective potential between the two molecules can have an *inner* classical turning point at dozens of Bohr radii [16,17]. This effective potential is moreover extremely sensitive to the influence of an external electric field, meaning that the macroscopic properties of the gas are likely to be highly variable and subject to experimental control. We will study the explicit field dependence of the gas. Because of the changing anisotropy with field, passing from the low-field to high-field limit is *not* equivalent to merely increasing the size of the dipole moment, as has been the case in previous treatments. Thus new phenomena are expected, for example, field-dependent phase transitions between different classes of condensates, distinguished by their shapes. One such example, cited by Giovanazzi *et al*, is the transition in a cigar-shaped trap to a gas that is self-trapping along the long axis, due to a spatially varying electric field in an intense laser [18,19]. Reducing the field applied to an already polarized gas may result in hysteresis phenomena in the polarization, leading to a kind of gaseous ferroelectric phase.

Many-body calculations will be performed largely at the Hartree-Fock level of approximation, essentially generalizing the familiar Gross-Pitaevskii equation to nonlocal interactions. Approximate variational solutions, using Gaussian or parabolic trial wave functions, are also extremely useful, and will provide us with qualitative guidance. Equally importantly, we will be sensitive to the fact that a mean-field approach may prove inadequate for such a strongly interacting system, which may manifest itself in the behavior of the collective excitation spectrum.

References:

[1] C. Ticknor, C. A. Regal, D. S. Jin, and J. L. Bohn, *Multiplet Structure of Feshbach Resonances in Nonzero Partial Waves*, Phys. Rev. A **69**, 042712 (2004).

[2] R. Roth and H. Feldmeier, *Stability of trapped ultracold Fermi gases using effective s- and p-wave contact interactions*, J. Phys. B **33**, L787 (2000).

[3] R. Roth and H. Feldmeier, *Effective s- and p-wave contact interactions in trapped degenerate Fermi gases*, Phys. Rev. A **64**, 043603/1 (2001).

[4] R. Roth and H. Feldmeier, *Phase diagram of trapped degenerate Fermi gases including effective s- and p-wave interactions*, J. Phys. B **34**, 4629 (2001).

[5] K. Goral, K. Rzazewski, and T. Pfau, *Bose-Einstein condensation with magnetic dipole-dipole forces*, Phys. Rev. A **61**, 051601/1 (2000).
[6] L. Santos, G. V. Shlyapnikov, P. Zoller, and M. Lewenstein, *Bose-Einstein condensation in trapped dipolar gases*, Phys. Rev. Lett. **85**, 1791 (2000).
[7] S. Yi and L. You, *Trapped atomic condensates with anisotropic interactions*, Phys. Rev. A **61**, 041604/1 (2000).
[8] S. Yi and L. You, *Trapped condensates of atoms with dipole interactions*, Phys. Rev. A **63**, 053607/1 (2001).
[9] P. M. Lushnikov, *Collapse of Bose-Einstein condensates with dipole-dipole interactions*, Phys. Rev. A **66**, 051601/1 (2002).
[10] K. Goral and L. Santos, *Ground state and elementary excitations of single and binary Bose-Einstein condensates of trapped dipolar gases*, Phys. Rev. A **66**, 023613/1 (2002).
[11] S. Yi and L. You, *Probing dipolar effects with condensate shape oscillation*, Phys. Rev. A **66**, 013607/1 (2002).
[12] L. Santos, G. V. Shlyapnikov, and M. Lewenstein, *Roton-maxon spectrum and stability of trapped dipolar Bose- Einstein condensates*, Phys. Rev. Lett. **90**, 250403/1 (2003).
[13] D. H. J. O'Dell, S. Giovanazzi, and G. Kurizki, *Rotons in gaseous Bose-Einstein condensates irradiated by a laser*, Phys. Rev. Lett. **90**, 110402/1 (2003).
[14] S. Yi and L. You, *Expansion of a dipolar condensate*, Phys. Rev. A **67**, 045601/1 (2003).
[15] S. Giovanazzi, A. Gorlitz, and T. Pfau, *Ballistic expansion of a dipolar condensate*, J. Opt. B-Quantum Semicl. Opt. **5**, S208 (2003).
[16] A. V. Avdeenkov and J. L. Bohn, *Linking ultracold polar molecules*, Phys. Rev. Lett. **90**, 043006/1 (2003).
[17] A. V. Avdeenkov, D. C. E. Bortolotti, and J. L. Bohn, *Field-Linked States of Ultracold Polar Molecules*, Phys. Rev. A **69**, 012710 (2004).
[18] S. Giovanazzi, D. O'Dell, and G. Kurizki, *One-dimensional compression of Bose-Einstein condensates by laser-induced dipole-dipole interactions*, J. Phys. B **34**, 4757 (2001).
[19] S. Giovanazzi, D. O'Dell, and G. Kurizki, *Density modulations of Bose-Einstein condensates via laser-induced interactions*, Phys. Rev. Lett. **88**, 130402/1 (2002).

Atomic and Molecular Physics in Strong Fields

Shih-I Chu
Department of Chemistry, University of Kansas
Lawrence, Kansas 66045
E-mail: sichu@ku.edu

Program Scope

In this research program, we address the fundamental physics of the interaction of atoms and molecules with intense ultrashort laser fields. The main objectives are to develop new theoretical formalisms and accurate computational methods for *ab initio* nonperturbative investigations of multiphoton quantum dynamics and very high-order nonlinear optical processes of one-, two-, and many-electron quantum systems in intense laser fields, taking into account detailed electronic structure information and many-body electron-correlated effects. Particular attention will be paid to the exploration of novel new physical mechanisms, time-frequency spectrum, and coherent control of high-harmonic generation (HHG) processes for the development of table-top x-ray laser light sources. Also to be explored is the ionization mechanisms of molecules in intense laser fields and attosecond physics.

Recent Progress

1. Development of *Self-Interaction-Free* Time-Dependent Density Functional Theory (TDDFT) for Nonperturbative Treatment of Multiphoton and HHG Processes of Many-Electron Atomic and Molecular Systems in Intense *Pulsed* Laser Fields

To study multiphoton and very-high-order nonlinear optical processes of many-electron quantum systems in strong fields using the *ab initio* wave function approach, it is necessary to solve the time-dependent Schrödinger equation of 3N spatial dimensions in space and time (N = the number of electrons). But this is beyond the capability of current supercomputer technology. The *single-active-electron* (SAE) model with *frozen core* is commonly used and has been successful for some strong-field processes where only one valence electron plays the dominant role. However, within the SAE model, important physical phenomena such as excited state resonances, dynamical response from individual valence electron spin-orbitals, inner core excitation, and dynamical electron correlations, etc., cannot be treated. Clearly, a more complete formalism beyond the SAE and other phenomenological models is very desirable for making further progress in the exploration of the atomic and molecular physics in strong fields. Recently we have initiated a series of new developments of *self-interaction-free* time-dependent density functional theory (TDDFT) for probing strong-field processes of many-electron atomic and molecular systems, taking into account electron correlations and detailed electronic structure [1-5]. Given below is a brief summary of the progress in 2002-2004.

a) High-Order Harmonic Generation of Ar Atoms and Ar+ Ions in Super Intense Pulsed Laser Fields

Recently it has been demonstrated experimentally [6] that the generation of very high-order harmonics (HHG), up to 250 eV, can be obtained by using the Ar gas. Using the ADK model, they inferred that the high harmonic photons arise from the ionized Ar atoms. However there is no full quantum treatment of this process yet. The experimental advance is made possible by using a waveguide geometry to limit plasma-induced laser beam defocusing, allowing the generation of high harmonics from Ar ions. This work also shows that HHG from ions may be able to extend laser-based coherent up-conversion into the soft x-ray region of the spectrum.

To explore the underlying quantum dynamics responsible for the production of the high-energy HHG, we have recently performed a detailed *all-electron* study of multiphoton ionization (MPI) and HHG processes of Ar atoms [8] by means of the *self-interaction-free* TDDFT recently developed in our group [1-5]. The time-dependent exchange-correlation (xc) energy functional with proper short- and long-range potentials are constructed by means of the *time-dependent optimized effective potential* (TD/OEP) method and the incorporation of an explicit *self-interaction-correction* (SIC) term. The TD/OEP-SIC equations can be solved accurately and efficiently by the use of the *time-dependent generalized pseudospectral* technique [1-5,7]. In our study, all the valence electrons are treated explicitly and nonperturbatively and their partial contributions to the ionization and HHG are analyzed. By comparing the HHG power spectrum from Ar and Ar+ in superintense laser fields, we found that the high-energy photons are dominantly contributed by the Ar+ ions. Our calculated HHG cut-off positions are also in good agreement with the experimental data. This study demonstrates that the TD/OEP-SIC formalism can provide detailed *ab initio* quantum description of the whole process, namely, the creation of Ar+ from Ar and the HHG from Ar+ and Ar in a single calculation [8]. Extension of the method to the study of other rare gas atoms (He and Ne) and their ions is under way. From these studies, one can predict whether it is possible to achieve harmonic energies of one keV or more by using stronger laser intensities and different laser parameters.

b) Ionization Behavior of Diatomic Molecules in Intense Laser Fields

The ionization and multiphoton ionization (MPI) of atoms, one of the fundamental processes initiated during the exposure of an atom to an intense laser field, has been extensively studied both experimentally and theoretically in the past decade. Recently, there is also considerable interest in the study of the ionization mechanism of diatomic molecules in intense laser fields. At lower intensities, dissociation may compete with ionization, fragmentation may play an important role, ionization may be sensitive to the alignment of the molecule with the laser field, and multicharged ions formed at higher intensities may be unstable due to Coulomb explosion. The ionization behavior of molecules is thus considerably more complicated than that of the atoms with comparable ionization potentials. The exploration of strong-field molecular ionization is only at the beginning stage.

Most theoretical studies of strong-field molecular ionization in the recent past are based on approximate models such as the KFR (Keldysh-Faisal-Reiss) or ADK (Ammosov-Delone-Krainov) tunneling models. To lowest order, these models predict ionization rates that depend upon only on laser wavelength and intensity, and the ionization potential of the species of interest. Although these models have some partial success but they fail to provide an overall consistent picture of the ionization behavior of different molecules (such as N_2, O_2, and F_2, etc), particularly for the case of F_2. We note that all the theoretical models and mechanisms proposed so far considered only the response of the outermost valence molecular orbital (MO).

Recently we have started to extend the self-interaction-free TDDFT for the investigation of the effect of electronic structure and multi-electron response to the ionization mechanisms of diatomic molecules in intense short-pulsed lasers [9]. Our initial results indicated that it is not adequate to use only the outermost valance electron for describing the molecular ionization behavior. Moreover, the ionization potential (IP) is not the only factor determining the total ionization rates. Further study will be continued along this direction.

c) Quantum Fluid Dynamics Approach to Strong-Field Processes

We have recently explored the feasibility of extending the quantum fluid dynamics (QFD) approach for nonperturbative investigation of many-electron quantum systems in strong fields [10]. Through the amalgamation of the QFD and density functional theory (DFT), a single time-dependent hydrodynamic equation can be derived. This equation has the form of a generalized nonlinear Schrödinger equation

(GNLSE) but include the many-body effects through a local time-dependent exchange-correlation potential. A time-dependent generalized pseudospectral method is developed for the solution of the GNLSE in spherical coordinates, allowing *nonuniform* and optimal spatial discretization and accurate solution of the hydrodynamic wave function and density in space and time. The procedure is applied to the study of MPI and HHG of He and Ne atoms in intense laser fields [10]. Excellent agreement with the *ab initio* TDDFT/OEP-SIC calculations [3] is obtained for He, and for Ne, good agreement is achieved. The QFD/DFT method offers a conceptually appealing and computational practical approach for nonperturbative treatment of complex many-electron systems well beyond the time-dependent Hartree-Fock level. More exploration of this formalism is in progress.

2. Recent Development of Generalized Floquet Formalisms & Complex Quasienergy Methods for Nonperturbative Treatment of Multiphoton Processes in Intense One-Color or Multi-Color Laser Fields

a) In the last several years, we have developed various generalized Floquet formalisms and complex quasienergy methods for nonperturbative treatment of a broad range of multiphoton and high order nonlinear optical processes in intense monochromatic (periodic) or polychromatic (quasi-periodic) laser fields. An extensive review article on these developments and their applications has been recently published [11]**.**

b) For the treatment of more complex quantum systems, we have recently also initiated the development of the Floquet formulations of time-dependent density functional theory (TDDFT) and time-dependent current density functional theory (TDCDFT) [12,13,14]. Further we have determined exact relations of the quasienergy functional and the exchange-correlation potential [13]. The Floquet-TDDFT approach allows exact transformation of the *periodically* (one-color) or *quasi-periodically* (multi-color) time-dependent Kohn-Sham equation into an equivalent time-independent generalized Floquet eigenvalue problem. Moreover, we have developed an exterior-complex scaling (ECS) – generalized pseudospectral (GPS) method for accurate solution of the non-Hermitian Floquet-TDDFT Hamiltonian [15]. The ECSGPS technique appears very useful in TDDFT-Floquet calculations where the exchange-correlation potentials may exhibit quite complicated behavior as functions of the electron coordinates and cannot be easily treated by means of the conventional uniform-complex-scaling techniques. We have applied this procedure to the study of one-photon detachment and two-photon dominant above-threshold detachment of Li^- negative ions [15]. In the one-photon case, the photodetachment cross section has been calculated as a function of the photon energy with results in good agreement with the experimental data. In the two-photon case, both the partial detachment rates and electron angular distributions for the dominant and above-threshold channels are presented for a range of laser field frequencies and intensities. Dramatic transformations of the angular distributions in the vicinity of the two-photon threshold are observed and analyzed.

c) High-Order Above-Threshold Multiphoton Detachment of H^- : Time-dependent Non-Hermitian Floquet Approach

The Floquet approaches developed in the past involved the determination of the complex quasienergies from a *time-independent* non-Hermitian Floquet matrix [11]. For more complex quantum systems, the dimensionality of the Floquet matrix can become very large and the problem can be either intractable or additional development of special numerical algorithms is needed to manage the ultralarge size of complex matrix eigenvalue problem. Recently we have presented an alternative method, the *time-dependent* non-Hermitian Floquet approach [16], for overcoming some of the ultralarge complex eigenvalue problems. The procedure involves the complex-scaling generalized pseudospectral (CSGPS) spatial discretization of the time-dependent Hamiltonian and non-Hermitian time propagation of the time-evolution operator by means of the split-operator technique in the *energy* representation. The approach is designed for effective treatment of multiphoton processes in very intense and/or low-frequency laser

fields, which are generally more difficult to treat using the conventional *time-independent* Floquet matrix techniques. We have applied this new procedure to a nonperturbative quantum study of high-order above-threshold detachment of H^- in intense laser fields [16]. Detailed exploration of the electron energy and angular distributions is pursued for the laser field intensities 10^{10}–10^{11} W cm^{-2} and wavelength 10.6 μm. We found the electron energy spectrum exhibits a second plateau region in the higher energy part. Transformation of the electron angular distributions in the plateau region is analyzed in detail. Extension of the approach to the molecular systems is in progress.

Future Research Plans

In addition to continuing the ongoing researches discussed above, we plan to initiate the following several new project directions: (a) Development and extension of the Floquet formulation of TDDFT to the molecular systems. (b) Development and extension of self-interaction-free TDDFT to diatomic molecular systems including the vibrational degrees of freedom for the study of the ionization mechanism and HHG phenomena in strong fields. (c) Further exploration of the quantum-fluid dynamics/DFT approach for the investigation of multiphoton processes of complex many-electron quantum systems in strong fields. (d) Attosecond phenomena.

References Cited (* Publications supported by the DOE program in the period of 2002-2004.)

[1] X. M. Tong and S. I. Chu, Phys. Rev. A**57**, 452 (1998).
[2] X. M. Tong and S. I. Chu, Int. J. Quantum Chem. **69**, 305 (1998).
[3] X. M. Tong and S. I. Chu, Phys. Rev. A**64**, 013417 (2001).
[4] X. Chu and S. I. Chu, Phys. Rev. A**63**, 023411 (2001).
[5] X. Chu and S. I. Chu, Phys. Rev. A**64**, 063404 (2001).
[6] E. A. Gibson, A. Paul, N. Wagner, R. Tobey, S. Backus, I. P. Christov, M. M. Murnane, and H. C. Kapteyn, Phys. Rev. Lett. **92**, 033001 (2004).
[7] X. M. Tong and S. I. Chu, Chem. Phys. **217**, 119 (1997).
*[8] J. Carrera, X. M. Tong, and S. I. Chu, Phys. Rev. Lett. (submitted).
*[9] X. Chu and S. I. Chu, Phys. Rev. A (submitted).
*[10] A. K. Roy and S. I. Chu, Phys. Rev. A**65**, 043402 (2002).
*[11] S. I. Chu and D. Telnov , Physics Reports **390**, 1-131 (2004).
[12] D. Telnov and S. I. Chu, Chem. Phys. Lett. **264**, 466 (1997).
[13] D. Telnov and S. I. Chu, Phys. Rev. A**63**, 012514 (2001).
*[14] S. I. Chu and D. Telnov, J. Chinese Chem. Soc. **49**, 737 (2002).
*[15] D. Telnov and S. I. Chu, Phys. Rev. A**66**, 043417 (2002).
*[16] D. Telnov and S. I. Chu, J. Phys. B **37**, 1489 (2004).

Coherent Control of Multiphoton Transitions in the Gas and Condensed Phases with Ultrashort Shaped Pulses

DOE Grant No. DE-FG02-01ER15143

Marcos Dantus
Department of Chemistry and Department of Physics, Michigan State University, East Lansing MI 48824
dantus@msu.edu

1. Program Scope

The proposed research has the general goal of controlling electronic and vibrational quantum state excitation in the gas and condensed phases. In particular, the goal is to achieve selectivity in multiphoton transitions for systems with increasing degrees of complexity, ranging from isolated diatomics to complex nanoparticle clusters. The projects are divided as follows:

I. High fidelity coherent reading, writing and manipulation of information in the vibronic states of isolated molecules
II. Control of multiphoton excitation of large molecules in condensed phase

2. Results

2.1. Manipulation of multiple quantum mechanical states in small isolated molecules

We have continued to fine tune our work on four wave mixing (FWM) and photon echo for the manipulation of quantum mechanical states of small isolated molecules. One of the most important impediments for the coherent manipulation of quantum states is decoherence. We carried out femtosecond photon echo measurements of electronic coherent relaxation between the $X(^1\Sigma g+)$ and $B(^3\Pi_{0u+})$ states of I_2 in the presence of He, Ar, N_2, O_2, C_3H_8. We found that the cross section for decoherence was greatest between two iodine molecules and it was on the order of 2.2 nm, several times larger than the Van der Waals radius. This finding revealed the very long-range interactions involved in electronic decoherence. The experimentally determined cross section radii for different buffer gases are shown in the figure. We were surprised to find that despite all the degrees of freedom available in propane, the decoherence cross section is similar to that of nitrogen.

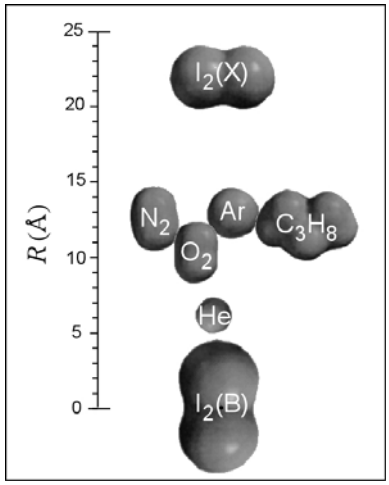

Our work has expanded to study the rotational and vibrational dynamics of larger systems. We have worked on NO_2 and N_2O_4. Our most interesting finding is that contrary to all calculations, N_2O_4 does not appear to have D_{2h} symmetry in our measurements. We are in the process of refining our data to determine the nature and extent of the deformation observed at room temperatures.

2.2. Control of multiphoton excitation of large molecules in condensed phase

This part of our work involves the use of very accurately shaped pulses for controlling the multiphoton excitation of large chromophores. The work has resulted in the development of a very accurate and practical method for characterizing the spectral phase of femtosecond laser pulses, and for correcting the distortions in order to obtain transform limited (TL) pulses. The figure shows the SHG-frequency resolved optical gating (FROG) and the multiphoton intrapulse interference phase scan (MIIPS) scan of 18 fs TL pulses. In our group we now work routinely with 11 fs pulses. The MIIPS technique

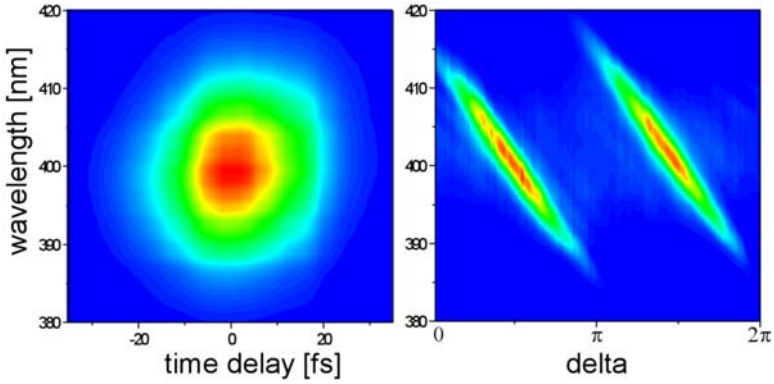

automatically corrects the phase distortions and renders TL pulses at the sample. One can easily then introduce well-calibrated phases for coherent control experiments. This development has resulted in articles in trade journals, it is now patented and being promoted for commercialization.

We have looked at the effect of spectral phase on nonlinear optical excitation and found very efficient strategies for controlling the excitation of large molecules. This work has now been applied to selective two-photon microscopy. We are very excited about results from our group where we show that we can use these coherent control principles to achieve functional imaging through scattering biological tissue. These experimental results are shown in the figure on the right. A and B correspond to pictures of the setup without and with biological tissue in front. C and D correspond to images obtained with TL pulse. Figures E and F correspond to images obtained using phase optimized pulses for the excitation of the fluorophore in acidic (red) and in basic (blue) environments. To obtain the functional images we subtracted the image obtained with the phase optimized for acidic environment from the one obtained from the shaped pulses optimized for basic environment. The coloring was artificially added; positive values (red) and negative values (blue) Notice that despite the presence of 1 mm of biological tissue one observes selective two-photon excitation. A finding that is somewhat surprising because of the scattering and loss of coherence experienced by the laser beam as it transmits through the biological tissue. We think these findings will have an impact in biomedical applications of femtosecond lasers.

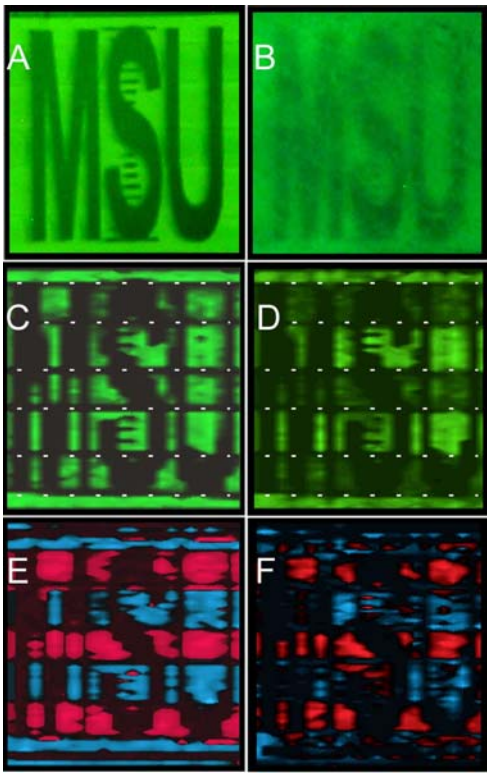

3. Future Work

We are presently setting up a microscope for carrying out selective excitation experiments on single molecules. The aim of this work is to probe the microchemical environment of these molecules. We hope to explore influences from acidic sites as well as amplification of electric fields by metallic nanoparticles near the chromophore.

The fundamental goal of our work is to control multiphoton nonlinear optical transitions in the gas and condensed phases. The specific projects range from the high-finesse experiments required for information storage in the vibronic levels of isolated diatomics, to the coherent and incoherent multiphoton excitation pathways in nanoparticles. These experiments will further the experimental methods available for coherent manipulation of electronic states, and the general understanding about the required electric fields.

Publications Resulting from this Grant 2002-2004:

1. V. V. Lozovoy, M. Comstock and M. Dantus, “Four-Wave Mixing and Coherent Control,” in Laser Control and Manipulation of Molecules, A.D. Bandrauk, Y. Fujimura and R.J. Gordon, ACS Publishing p. 61(2002)

2. I. Grimberg, V. V. Lozovoy, M. Dantus and S. Mukamel, “Femtosecond three-pulse spectroscopies in the gas phase: density matrix representation,” J. Phys. Chem. Feature 106, 5, 697 (2002) Our results featured in the cover.

3. V. V. Lozovoy and M. Dantus, “Photon echo pulse sequences with femtosecond shaped laser pulses as a vehicle for molecule-based quantum computation,” Chem. Phys. Letters, 351, 213 (2002)

4. K. A. Walowicz, I. Pastirk, V. V. Lozovoy, and M. Dantus, “Multiphoton intrapulse interference I; Control of multiphoton processes in condensed phases,” J. Phys. Chem. 106, 41, 9369, (2002) Our results are featured in the cover.

5. M. Comstock, V. V. Lozovoy and M. Dantus, “Femtosecond photon echo measurements of electronic coherence relaxation between the $X(^1\Sigma g+)$ and $B(^3\Pi_{0u+})$ states of I_2 in the presence of He, Ar, N_2, O_2, C_3H_8,” J. Chem. Phys. 119, 6546 (2003)

6. V. V. Lozovoy, I. Pastirk, M. Comstock, K. A. Walowicz, and M. Dantus, “Femtosecond four-wave mixing for molecule based computation,” Ultrafast Phenomena XIII, Eds. R.J.D. Miller, M. Murnane, N. F. Scherer and A. M. Weiner. Springer-Verlag, Berlin Heidelberg p.97 (2003)

7. V. V. Lozovoy, I. Pastirk, K. A. Walowicz, and M. Dantus, “Multiphoton intrapulse interference II. Control of two- and three-photon laser induced fluorescence with shaped pulses,” J. Chem. Phys. 118, 3187, (2003)

8. J. M. Dela Cruz, I. Pastirk, V. V. Lozovoy, K. A. Walowicz and M. Dantus, "Multiphoton Intrapulse Interference 3: probing microscopic chemical environments," J. Phys. Chem. 108, 1, 53 - 58, Our results are featured in the cover.

9. I. Pastirk, J. M. Dela Cruz, K. A. Walowicz, V. V. Lozovoy, and M. Dantus, "Selective two-photon microscopy with shaped femtosecond pulses", Optics Express, 11, 1695 (2003)

10. V. V. Lozovoy, I. Pastirk, M. Dantus, "Multiphoton intrapulse interference 4; Characterization and compensation of the spectral phase of ultrashort laser pulses", 29, 7, 775-777, Optics Letters (2004)

11. M. Dantus, V. V. Lozovoy, I. Pastirk, "Measurement and Repair: The femtosecond Wheatstone Bridge", OE Magazine 9 (September) 15, (2003)

12. J. Dela Cruz, I. Pastirk, V.V. Lozovoy, K.A. Walowicz, and M. Dantus, “Control of nonlinear optical excitation with multiphoton intrapulse interference,” Ultrafast Molecular Events in Chemistry and Biology, M. M. Martin and J.T. Hynes Eds. Elsevier (2004)

13. V.V. Lozovoy, M. Comstock, I. Pastirk, and M. Dantus, “Femtosecond Photon Echo Measurements of Electronic Coherence Relaxation of I_2 in the presence of He, Ar, N_2, O_2, C_3H_8,” Ultrafast Molecular Events in Chemistry and Biology, M. M. Martin and J.T. Hynes Eds. Elsevier (2004)

14. M. Dantus and V.V. Lozovoy, "Experimental Coherent Laser Control of Physicochemical Processes", Chem. Reviews, Special Issue on Femtochemistry, A. H. Zewail and M. Dantus Eds. 104, 1813-1860, (2004)

15. M. Comstock, V. V. Lozovoy, I. Pastirk, and M. Dantus, "Multiphoton intrapulse interference 6; binary phase shaping",12, 6, 1061-1066, Optics Express (2004)

16. V. V. Lozovoy and M. Dantus, “Systematic control of nonlinear optical processes using optimally shaped femtosecond pulses. Multiphoton Intrapulse Interference 7,” Chem. Phys. Chem. Invited Review Submitted 2004.

17. J. M. Dela Cruz, I. Pastirk, M. Comstock, and M. Dantus, “Coherent control through scattering tissue, Multiphoton Intrapulse Interference 8,” Optics Express, (accepted for publication 2004)

18. J. M. Dela Cruz, I. Pastirk, M. Comstock, V. V. Lozovoy, and M. Dantus, “Can coherent control methods be used through scattering biological tissue to achieve functional imaging?” Proceedings of the National Academy of Sciences, (in revision 2004)

GENERATION AND CHARACTERIZATION OF ATTOSECOND PULSES

L. F. DiMauro[1], K. C. Kulander[2], I. A. Walmsley[3,4] and R. Boyd[4]
[1] Brookhaven National Laboratory, Upton, NY 11973
[2] Lawrence Livermore National Laboratory, Livermore, CA 94551
[3] Oxford University, Oxford, UK OX1 3PU
[4] University of Rochester, Rochester, NY 14627

PROGRAM SCOPE

The objective of this program is the complete optical characterization of high harmonics, which might be exploited in the production of an attosecond pulse, and to demonstrate the formation of such a pulse. The program exploits a scaled interaction approach at long wavelengths for mimicking the behavior of an atom interacting with intense visible light. The proposal has two parallel efforts (BNL/LLNL and Rochester) with the ultimate aim of generating and measuring an attosecond pulse.

RECENT PROGRESS

High harmonic (HHG) radiation, which results from atoms interacting with an intense laser field, has the potential to produce pulses of light with unprecedented durations approaching the attosecond (1 as = 10^{-18} s) time-scale. Moreover, with high conversion efficiencies (~ 10^{-5}) [1] in the XUV range and ~ 10 A [2] spectral content, HHG exhibits attractive traits for coherent XUV research. Recently, two separate confirmations [3,4] of attosecond pulse formation from HHG have been reported. High harmonics are commonly generated by the interaction of intense, near visible (0.8 μm) laser field with high binding energy atoms (rare gases). However, Keldysh [5] formulated that equivalent interactions can be achieved throughout the electromagnetic spectrum. Thus, an equivalent interaction can be experimentally realized by proper choice of the field parameters, e.g. intensity, and wavelength, and atomic binding energy. We have demonstrated that the lower binding energy alkali metal atoms excited by an intense mid-infrared pulse fulfills this condition. The Keldysh framework addresses one of the most fundamental principles in strong-field physics: the invariance of a scaled interaction. Consequently, our experiments are a critical paradigm in establishing this understanding.

An important practical aspect of the aforementioned scaled interaction is the study of attosecond (10^{-18} s) pulse formation by enabling experimental accessibility to well-developed metrology for characterization of high harmonic radiation. For example, harmonics generated by a 3.4 μm mid-infrared (MIR) fundamental field have a spectrum that extends from the near-visible to the near-ultraviolet. In this regime, superior optics and nonlinear materials exist for manipulation and measurement of the high harmonic light. Furthermore, the study of alkali atoms with MIR light not only provides the necessary Keldysh scaling but also yields optical accessibility to bound-bound and bound-continuum harmonic emission. All these points are essential for establishing the viability for using a comb of high harmonic light for generating light pulses on the attosecond time-scale and provide the major impetus for our investigations.

TEMPORAL AND SPECTRAL PROPERTIES OF HIGH HARMONICS

Temporal and spectral properties of the high harmonics were investigated using cesium atoms excited by a 3.4 μm fundamental field. The temporal measurements included both second harmonic generation (SHG) autocorrelation and coherence time measurements. Harmonic orders 5-17 were characterized for spectral content and coherence times. Autocorrelation measurements were performed only for orders 5-9.

For brevity, Fig. 1 shows the autocorrelation (a) and spectral measurements (b) of harmonic order 9. Similar measurements were also performed for the fundamental pulse and harmonic order 5 and 7. Evident in this trace is the excellent signal-to-noise of the autocorrelated signal, unequivocally demonstrating our ability to measure these pulses using nonlinear temporal metrology. It should also be noted that this study establishes a new record for autocorrelating the highest order harmonics ($q \leq 9$) and we believe that characterization of the higher-orders are attainable. Thus, these investigations not only provide a benchmark for establishing the formation of attosecond pulses but it contributes significantly to our basic understanding of the scaling laws in strong field physics.

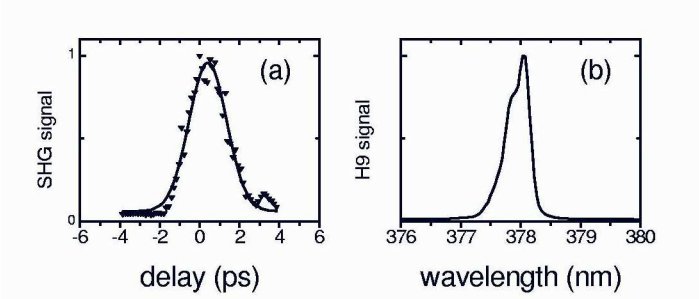

Figure 1: The (a) autocorrelation and (b) wavelength spectrum for the 9th harmonic order. Similar data was taken for the fundamental and harmonic orders 5 and 7. The harmonics are the result of an intense 3.6 μm pulse interacting with Cesium atoms.

ENHANCED HIGH HARMONIC GENERATION FROM EXCITED STATES

Besides providing a convenient method for fully characterizing attosecond pulses the scaled interaction approach also permits the exploration of novel schemes, not easily implemented on inert gas targets. We have performed the first experiments on high harmonic emission from an excited state atom. The scaled interaction approach enables these studies since the low binding energies of alkali atoms and their corresponding excited states are easily accessible to optical excitation. In our first study, harmonics are generated from optically prepared states of the Rb atom. Compared to an initial ground state, the excited states show large enhancement (factors of $10\text{-}10^4$) of the harmonic yield for orders 5 to 11 and depends on the pump intensity and excited state density.

The excited state is prepared by saturating the homogeneously broadened D_2 ($5s \rightarrow 5p_{3/2}$) transition in ^{85}Rb (72% abundance) using a FM-modulated diode laser. Figure 2 shows the harmonic spectrum resulting from 1 TW/cm^2, 3.5 μm excitation with (dark shaded) and without (light shaded) the diode laser. The difference between the two distributions is striking; clearly the presence of the diode laser greatly enhances the 5th and 7th harmonic (the higher orders, not shown, are also enhanced) production over the

ground state. The enhancement is order dependent and varies between 10-10^4 depending on the diode laser's frequency, the mid-infrared intensity and rubidium density.

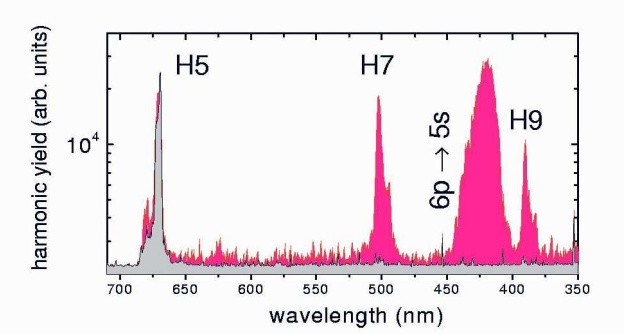

Figure 2: Harmonic spectra obtained by excitation of Rubidium atoms with 2.5 ps 3.5 μm pulses. The broad feature with diode laser on (also present with no mid-infrared laser) is the 6p⟶5s fluorescence line. Harmonic spectrum generated at 0.25 torr Rb vapor pressure and 1 TW/cm^2 MIR intensity, with the coupling laser on resonance (red), with the coupling laser off resonance (light gray).

The interpretation of this result is certainly more complex than originally conceived and needs more thorough investigations but the propensity for excited states to enhance the harmonic yield is clear and dramatic. More investigations are needed to understand the physics of this experiment but the unique character of our scaled interaction approach has opened a new avenue for investigating and possibly controlling the high harmonic process. This experiment establishes for the first time the ability to alter the harmonic process with the single atom response (quantum trajectories), as opposed to other studies that have focused on the macroscopic contributions.

FUTURE PLANS

Our plans for future high harmonic studies will have a broader scope while still exploiting the scaled interaction approach. The future program will be a new contract at Ohio State University since Dr. DiMauro will move his research effort to that institution.

The future scientific aims are as follows:

1. Utilize the scaled interactions approach to test fundamental concepts of attosecond generation and metrology.
2. Realize novel arrangements using the scaled interaction approach for advancing the development of high harmonic and attosecond generation.
3. Utilize the wavelength scaling of strong-field interactions to push high harmonic generation into kilovolt photon energies (x-rays) while defining new limits on attosecond pulse durations. The goal is the unprecedented development of light pulses that can achieve both the *atomic time* and *length scales*.
4. Develop advance metrology for short wavelength pulse characterization and provide fundamental tests of known metrology against direct measurements utilizing the scaled interaction approach.
5. Initiate a program in attophysics: applications of attosecond light pulses.
6. Establish and maintain a working attosecond source at OSU based on a carrier envelope phase (CEP) stabilized few-cycle near infrared laser system.

7. Advance the optical technology needed for the routine production of attosecond x-rays.

Items 1 and 2 are continuation of the scaled interaction concepts proposed and established in the current grant period. The viability, principles and novelty of this approach have been clearly demonstrated. Items 3-7 broaden the scope of this effort by proposing to establish a working attosecond source in the U.S. for conducting attophysics investigation, advance the metrology and develop new sources that could push both the time- and frequency-scales towards new limits.

REFERENCES

[1] E. Constant et al., *Phys. Rev. Lett*. **82**, 1668 (1999).
[2] H. Chang et al., IEEE J. Sel. Top. QEX, **4**, 266 (1998).
[3] P. M. Paul et al., *Science* **292**, 1689 (2001).
[4] M. Hentschel et al., *Nature* **414**, 509 (2001).
[5] L. V. Keldysh, *Zh. Eksp. Teor. Fiz.* **47**, 1945 (1964) [*Sov. Phys. JETP* **20**, 1307 (1965)].

PUBLICATIONS RESULTING FROM THIS RESEARCH

1. "Atomic Photography", L. F. DiMauro, Nature **419**, 789 (2002).
2. "Scaled Intense Laser-Atom Physics: The Long Wavelength Regime" T. O. Clatterbuck, C. Lyngå, P. Colosimo, J. D. D. Martin, B. Sheehy, L. F. DiMauro, P. Agostini and K. C. Kulander, *J. Mod. Optics* **50**, 441 (2003).
3. "Thirteen pump-probe resonances of the sodium D1 line" Vincent Wong, R. W. Boyd, C.R. Stroud Jr., R. S. Bennink, and A. Marino, *Phys. Rev. A* 68, 012502 (2003).
4. "Characterization of attosecond electromagnetic pulses" by E. Kosik, E. Cormier, C. Dorrer, I. A. Walmsley and L. DiMauro, in *Proceedings of the IV Ultrafast Optics Conference*, eds. I. A. Walmsley and P. B. Corkum (Springer, Heidelberg, 2003).
5. "Yield and Temporal Characterization of High Order Harmonics from a Tightly Focused Geometry: Intense Mid-Infrared Excitation of a Cesium Vapor", T. O. Clatterbuck, P. M. Paul, C. Lynga, L. F. DiMauro, M. Gaarde, K. J. Schafer, P. Agostini, K. C. Kulander and I. A. Walmsley, *Phys. Rev. A* **69**, 033807 (2004).
6. "The Physics of Attosecond Pulses" P. Agostini and L. F. DiMauro, *Reports on Progress in Physics* **67**, 813–855 (2004).
7. "Strong Field Atomic Physics" L. F. DiMauro and K. C. Kulander, in *Proceedings of the Erice Summer School*, ed. D. Batani (Italian Physical Society, Milan), in press.
8. E. Kosik, E. Cormier, C. Dorrer, I. A. Walmsley and L. F. DiMauro, "Characterization of attosecond electromagnetic pulses", in Ultrafast Optics IV, eds. F. Krausz, G. Korn, P. Corkum, I. A. Walmsley, (Springer, New York, 2004).
9. "Enhanced high harmonic generation from a optically prepared excited medium", P. M. Paul, C. Lynga, T. O. Clatterbuck, P. Colosimo, L. F. DiMauro, P. Agostini and K. C. Kulander, *Phys. Rev. Lett.*, submitted.
10. E. Kosik, A. Radunsky, I. A. Walmsley and C. Dorrer, "Spatially-encoded spectral shearing interferometry for characterization of ultrabroadband optical pulses", *Opt. Lett*., submitted.
11. E. Kosik, A. Wyatt, L. Corner, E. Cormier and I. A. Walmsley, "Characterization of Attosecond XUV Pulses", *J. Mod. Opt.*, submitted.
12. E. Cormier, I. A. Walmsley, E. M. Kosik, L. Corner and L. F. DiMauro, "Self-referencing spatially encoded spectral interferometry for the characterization of attosecond electromagnetic pulses", *Phys. Rev.*, submitted.

High Intensity Laser Driven Explosions of Homo-nuclear and Hetero-nuclear Molecular Clusters

Abstract (Summer 2004)

Principal Investigator:

Todd Ditmire
Department of Physics
University of Texas at Austin, MS C1600, Austin, TX 78712
Phone: 512-471-3296
e-mail: tditmire@physics.utexas.edu

Program Scope:

The nature of the interactions between high intensity, ultrafast laser pulses and atomic clusters of a few hundred to a few thousand atoms has come under study by a number of groups world wide. Such studies have found some rather unexpected results, including the striking finding that these interactions appear to be more energetic than interactions with either single atoms or solid density plasmas and that clusters explode with substantial energy when irradiated by an intense laser. It is now well established that the explosions of low-Z molecular clusters such as hydrogen or deuterium clusters explode mainly by a Coulomb explosion. Our program under the last three year cycle studied the interplay between a traditional Coulomb explosion description of the cluster disassembly and a plasma-like hydrodynamic explosion, particularly for small to medium sized clusters (<1000 atoms) and clusters composed of low-Z atoms. In this program we have started to extend these studies, particularly with an eye toward the optimization of cluster explosions for use in a high flux, laser driven neutron source. We are examining the details of the Coulomb explosion of molecular clusters and we are studying the temporal dynamics of the electron ejection and ion expansion through pump probe techniques. We have also started studying in detail the dynamics of explosions of mixed species clusters, such as methane (and deuterated methane) where it is now conjectured that dynamic effects play an important role in the ejection of the lighter ions. We are looking at a number of diagnostics but mainly have been concerned with examining ion energy spectra and fusion neutron yield in deuterated cluster plasmas. We are also studying, in collaboration with Mike Downer here in the department at UT, the explosion of the cluster by looking at the time resolved nonlinear optical properties of the cluster.

Recent Progress

Since the beginning of the current grant last fall, we have concentrated on two experiments. The first is a continuation of our previous work on fusion neutron generation from laser irradiated deuterated clusters. We are now concentrating on the physics of mixed species clusters, in particular, deuterated methane clusters. We have also derived new results using a two color pump probe experiment. This experiment is aimed at studying the time scale of the cluster explosion by measuring the time dependant nonlinear optical properties of the exploding cluster. The exploding cluster fusion experiments were conducted using the THOR laser in Austin which delivers 0.75 J, 35 fs pulses. The pump probe experiments were performed on the 5 TW CPA lasers which resides in Prof. Mike Donwers lab

1) Fusion with deuterated methane clusters and neutron angular distributions

During this the past year, we started studies of exploding mixed species CH_4 and CD_4 clusters. Heteronuclear clusters like deuterated methane are very interesting since these mixed ion clusters may

exhibit enhancements in ion energy through a dynamical effect in the Coulomb explosion. The Coulomb explosion of a single species cluster, like D_2 clusters, will eject deuterons with an energy given directly by the potential energy of the ion as it is initially in the fully stripped cluster. In exploding mixed ion clusters like CD_4 the light deuterons will outrun the heavier ions, explode in an outer shell with a higher average energy than would be expected from the naïve estimate of ion energy based on initial potential energy. This implies that the fusion yield could be substantially increased in plasmas formed from explosions of heteronclear clusters over that of neat D_2 clusters of the same size because of this kinematic enhancement of ion energies in the mixed ion case. We examined the explosion of CD_4 clusters and the fusion yield that results from these plasmas. Those experiments indicated that there was some enhancement of deuteron energies from CD_4 when compared to similar sized D_2 clusters.

This year, we followed up on these experiments motivated by a surprising result published recently by the LOA group in France. This group reported what seemed to be a rather large (>40%) anisotropy in the neutron emission from exploding CD_4 cluster plasmas. This is unexpected if the pure Coulomb explosion model is at work since the clusters should eject ions nearly isotropically. We examined the angular distributions from these clusters using the apparatus illustrated in figure 1. Here we examined the distributions of neutrons as a function of polarization angle in the laser polarization plan as well as a function of azimuthal angle in the plane of propagation. The French group reported a large peaking of the neutrons perpendicular to the laser propagation direction.

Our results are quite at odds with the French results. We find, first that there is nearly completely uniform neutron emission with polarization angle. We do observe a slight anisotropy in the azimuthal plane. This is illustrated with the data shown in figure 2. Here the neutron emission from a CD_4 cluster plasma, irradiated with 0.5 J of a 40 fs laser pulse is shown. The cluster sizes are around 10 nm per cluster. We see a small peaking of the neutron emission in the forward and backward direction (ie along and and back against the laser propagation axis). This anisotropy is much smaller than reported by the LOA group and is in a direction different than they see. We believe that our result is, in fact, completely in keeping with the Coulomb explosion picture of the cluster explosion, and that the slight neutron peaking can be explained by the cigar shaped plasma filament geometry of the plasma. A detailed explanation of these results as explained by detailed Monte Carlo particle simulations will be presented in a paper currently under preparation.

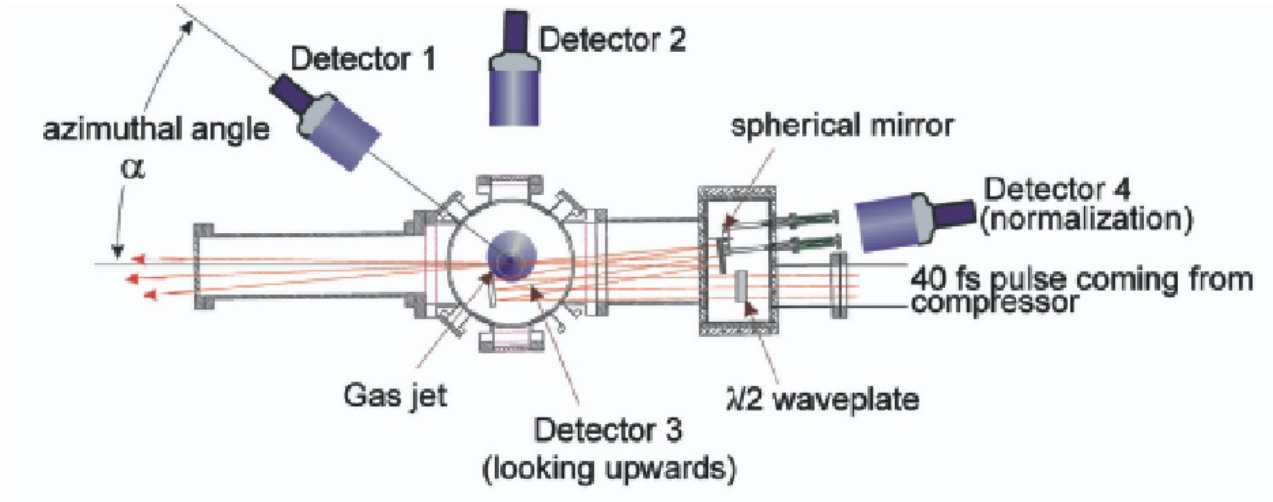

Figure 1: Experimental set-up used for measuring the neutron angular distribution on the UT THOR laser.

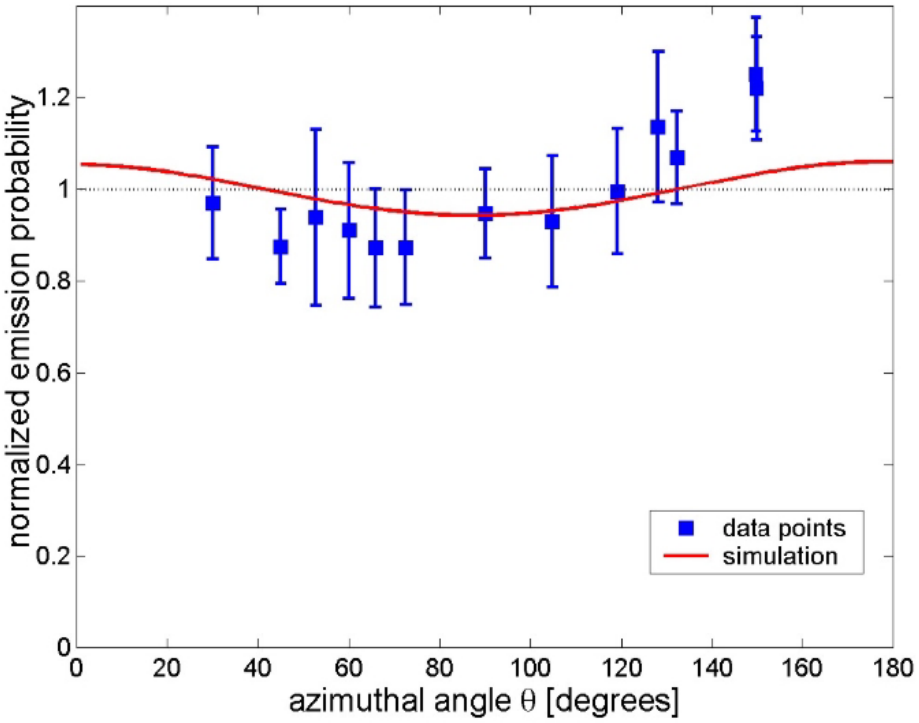

Figure 2: Azimuthal scan of neutron yield from CD_4 clusters carried out by an angular scan of 'Detector 1' shown in Figure 1.

2) Pump probe measurements of exploding cluster nonlinear properties

We have constructed an experiment to examine the third harmonic generation of 800 nm pulses in a gas of argon clusters as the clusters expand from the photoionization and heating of a an initial pump pulse (which has a wavelength of 400 nm). This pump-probe experiment is designed to yield information on the nonlinear oscillation dynamics of the electron cloud in an expanding cluster. This experiment follows on experiments conducted at LLNL on the linear absorption of a probe laser pulse in xenon clusters as a function of delay after an ionizing pump. The motivation of this experiment is to get information on the presence of collective motion of electrons in a cluster after the constituent atoms have been ionized but before the laser has completely removed the free electrons from the cluster. This "nanoplasma" situation is in contrast to the Coulomb explosion limit that we study in the exploding CD_4 and D_2 experiments described above. It represents the situation when larger, higher Z clusters are irradiated.

This experiment has been conducted on the 5 TW Ti:sapphire laser at UT and has been done in collaboration with Mike Downer. The experimental set-up is illustrated in figure 3. Here a femtosecond intense pulse is frequency doubled to produced a 400 nm "pump" pulse. This pulse initially ionizes the cluster and creates argon nanoplasmas. These plasmas expand on a fs time scale. As they expand, the collective resonance frequency of the bound electrons should change. At some time later, they come into resonance with the 800 nm probe pulse. We examine the third harmonic light that is generated by this time delayed 800 nm pulse. When a resonance occurs (or if it occurs), resonant enhancement of the third harmonic signal should be observed. Figure 4 illustrates the third harmonic signal that we see as a function of delay between the 400 nm and 800 nm pulse. At t=0, the two pulses overlap and we see enhanced signal from the frequency mixing of the two, nearly co-linear pulses. However, at about 250 fs after the pump pulse arrives, we see a second peak in the third harmonic signal. This we attribute to the collective electron

resonant enhancement of the harmonic generation. From this, since we know the frequency that resonance occurs, we can ascertain with some precision the expansion velocity of the cluster at these early times. This also confirms the formation of the nanoplasma and indicates that the electron could, does indeed, oscilate coherently in the laser field.

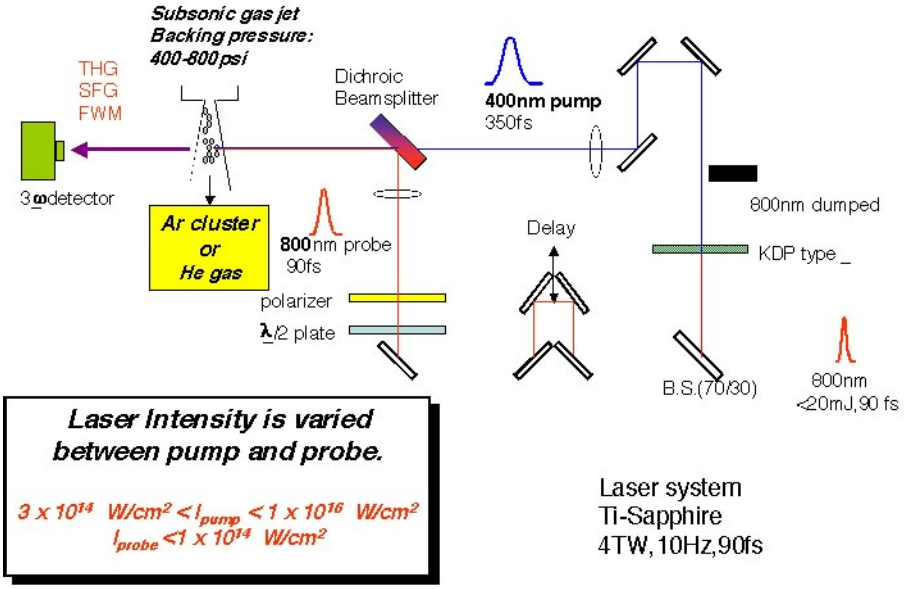

Figure 3: Experimental set-up for the two color pump probe experiment examining resonant enhancement of third harmonic generation by collective electron effects in the cluster.

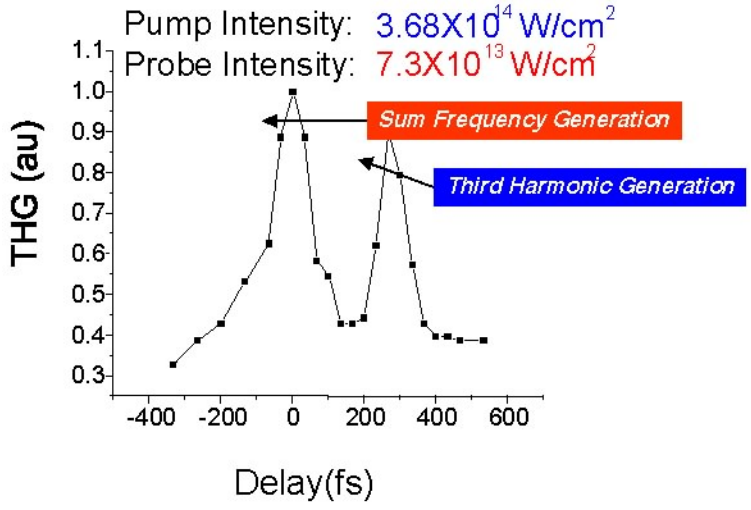

Figure 4: Measured 3ω signal from the 800 nm probe pulse as a function of delay after the 400 nm pump pulse.

Future Research Plans

Our future research plans are aimed mainly at studying heteronuclear clusters. In particular, we would like to search for definitive proof of the dynamic enhancement predicted in some mixed species clusters. Our plan for the coming year is the following:

1) Study ion energies from both CD_4 and CH_4 clusters. Because of the large difference in charge to mass ration between D^+ and H^+ we hope to observe a quantitative difference in the explosion energy of the light ions from the differing importance of the dynamic enhancement (which should be more pronounced for CH_4.) We will study angular distributions and perhaps electron energy spectra from these species.

2) Active the second compressor beam on the THOR laser. This will allow us to start "pump-pump" style experiments. These are experiments aimed at measuring the residual electron fraction remaining in the cluster after the passage of an intense pulse and will help us ascertain when the Coulomb explosion model breaks down and the nanoplasma model takes over.

3) Continue fusion neutron yield measurements in CD_4. In particular, we would like to examine, and manipulate the effects of laser propagation effects in the gas jet on the plasma production and ultimate neutron production. One idea that we will explore will be to use the second, compressed beam to "clean away" absorbing cluster gas in the leading edge of the gas jet. This should allow us to penetrate more deeply into the jet and reach higher density, where we expect a high fusion rate and higher yield.

Papers published on work supported by this grant and the preceding grant (2002-2004):

1) K. W. Madison, P. K. Patel, D. Price, A. Edens, M. Allen, T. E. Cowan, J. Zweiback, and T. Ditmire, "Fusion neutron and ion emission from laser induced explosions of deuterium and deuterated methane clusters" *Phys. Plas.* **11**, 270 (2004).

2) T. Ditmire, S. Bless, G. Dyer, A. Edens, W. Grigsby, G. Hays, K. Madison, A. Maltsev, J. Colvin, M. J. Edwards, R. W. Lee, P. Patel, D. Price, B. A. Remington, R. Sheppherd, A. Wootton, J. Zweiback, E. Liang and K. A. Kielty, " Overview of future directions in high energy-density and high-field science using ultra-intense lasers" *Rad. Phys. And Chem.* **70**, 535 (2004).

3) K. W. Madison, P. K. Patel, M. Allen, D. Price, T. Ditmire, "An investigation of fusion yield from exploding deuterium cluster plasmas produced by 100 TW laser pulses" *J. Opt. Soc. Am. B* **20**, 113 (2003).

4) J. W. G. Tisch, N. Hay, K. J. Mendham, E. Springate, D. R. Symes, A. J. Comley, M. B. Mason, E. T. Gumbrell, T. Ditmire, R. A. Smith, J. P. Marangos, M. H. R. Hutchinson, "Interaction of intense laser pulses with atomic clusters: Measurements of ion emission, simulations and applications" *Nuc. Inst. Meth. B – Beam Interactins with Materials and Atoms* **205**, 310 (2003).

5) J. Zweiback, T.E. Cowan, R. A. Smith, J. H. Hartley, R. Howell, G. Hays, K. B. Wharton, J. K. Crane, V. P. Yanovsky and T. Ditmire "Detailed Study of Nuclear Fusion From Femtosecond Laser-Driven Explosions of Deuterium Clusters" *Phys. Plas.* **9**, 3108 (2002).

Reaction and Fragmentation Interferometry

Department of Energy 2004-2005

James M Feagin

Department of Physics
California State University–Fullerton
Fullerton CA 92834
jfeagin@fullerton.edu

Our research remains part of a general effort in the AMO community to advance our understanding of collective few-body excitations. At the same time, we investigate the basic physics of nanoscale science based on our experience in the highly-evolved AMO industry of collision and few-body phenomena. In particular, we reconsider few-body reaction detection—a long-standing theme of the BES program—from the more general perspective of reaction imaging. We find there continues to exist unexplored opportunity to contribute to at least two nanoscience initiatives. We accordingly continue to pursue two parallel efforts, *detection interferometry* and *collective few-body excitations*. While we are keenly aware that most of the experiments we consider are difficult, we nevertheless maintain a strong interest in our long-time and productive relations with various experimental groups in this country and in Europe.

Fragmentation Entanglement

Although much has been achieved experimentally with quantum information and control with photons and quantum optics, there remains fundamental interest in establishing analogous tools with charged particles, especially correlated electrons and ions.[1] Key steps in this direction have been of course the successes with ion traps, for example not only in assembling a data bus with control gates[2] but in resolving diffraction patterns in differential charge-transfer cross sections[3] as well as a recent precision demonstration of Bell's theorem with a trapped ion pair.[4] Related directions include advances in atom interferometry—even fullerenes[5] and BEC fragments[6] can be diffracted with standing waves of light, technology akin to the recent remarkable confirmation of the Kapitza-Dirac effect with electrons.[7] One is thus motivated to consider few-body fragmentation detection from the more general perspective of reaction imaging.

In pioneering work on quantum correlation, Wootters and Zurek[8] analyzed how two-slit interference with photons changes when the recoil of a distant collimator slit is monitored.

---

[1] J. Ullrich et al., Rep. Prog. Phys. **66**, 1463 (2003); J. Ullrich and V. P. Shevelko, Eds., *Many-Particle Quantum Dynamics in Atomic and Molecular Fragmentation*, Springer, New York (2003).

[2] D. Bouwmeester, A. Ekert, and A. Zeilinger, Eds., *The Physics of Quantum Information*, Springer, Heidelberg (2001); M. A. Nielsen and I. L. Chuang, *Quantum Computation and Quantum Information*, Cambridge, New York (2000).

[3] X. Flechard et al., Phys. Rev. Lett. **87**, 123203 (2001); M. van der Poel et al., Phys. Rev. Lett. **87**, 123201 (2001).

[4] M. A. Rowe, D. Klelpinskl, V. Meyer, C. A. Sackett, W. M. Itano, C. Monroe, and D. J. Wineland, Nature **409**, 791 (2001); see also H. J. Metcalf and P. van der Straten, *Laser Cooling and Trapping*, Springer, New York (1999) and references therein.

[5] Nairz et al., Phys. Rev. Lett. **87**, 160401-1 (2001) and references therein.

[6] E. W. Hagley, L. Deng, W. D. Phillips, K. Burnett, and C. W. Clark, Optics & Photonics News, May (2001), p. 22, and references therein.

[7] D. L. Freimund, K. Aflatooni, H. Batelaan, Nature **413**, 142 (13 Sep 2001). See also P. H. Bucksbaum, Nature **413**, 117 (13 Sep 2001).

[8] W. K. Wootters and W. H. Zurek, Phys. Rev. D**19**, 473 (1979).

In the case of electrons, two-slit interference has been established[9] with Möllenstedt imaging, viz. a thin charged wire mounted between grounded walls that functions for electrons like a Fresnel biprism for photons. Discussions with R. Dörner and H. Schmidt-Böcking (Frankfurt) and L. Cocke (KSU) regarding plans to develop an experiment to collect photoionized electrons with Möllenstedt detection in coincidence with the momentum-analyzed recoil ions continue to motivate our interest in Wootters and Zurek.

As illustrated in Fig. 1, we have thus analyzed the two-slit detection of a scattered projectile with incident momentum $\mathbf{k}_p$ and with momentum components $\mathbf{k}_\pm$ towards the entrance ports of the interferometer resulting via momentum conservation in momentum fuzziness $\mathbf{K}_\pm = \mathbf{k}_p - \mathbf{k}_\pm$ of the recoiling target-atom center of mass.[10] Our projectile wavefunction is just one component of an entangled 'projectile + target' state required by momentum conservation,[11] as in the Wootters and Zurek analysis of photon diffraction.

We are working to extend our two-slit analysis to include modifications to Wootters and Zurek based on Fresnel diffraction along lines suggested some time ago.[12] We have also examined *multislit* interferometry and the notion of a *detection antenna* capable of extracting a selection of scattering-amplitude *multipoles*, somewhat in the spirit of our work on nondipolar effects mentioned below. Moreover, a stack of three gratings can be used to construct a Mach-Zehnder interferometer, an idea beautifully adapted by D. Pritchard's group at MIT to scatter single photons off an atom with amplitude shared between interfering paths inside the interferometer.[13] We have thus begun to extend our two-slit imaging to include target atoms *inside* their own interferometer.

Along these lines, we have also begun to apply our scattering interferometry to *trapped-ion* targets. The target states ψ_n would include the normal modes of vibrational motion of the trapped ions. In a swift, impulsive collision, the form-factor component $e^{i\,\mathbf{K}\cdot\mathbf{r}}\psi_0$ in the Born approximation would then describe a momentum-kicked oscillator ground state and therefore

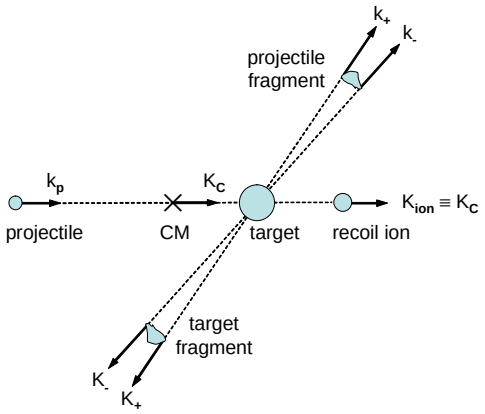

FIG. 1: A projectile with momentum $\mathbf{k}_p$ is scattered by a target at rest producing projectile and target fragments and a recoil ion. The recoil-ion momentum is postselected to match the system CM momentum, $\mathbf{K}_{ion} \equiv \mathbf{K}_c$, and thus to establish via momentum conservation perfect correlation between the projectile- and target-fragment momenta, $\mathbf{k} = -\mathbf{K}$. The pairs $\mathbf{k}_\pm = -\mathbf{K}_\pm$ are momentum components towards the entrance ports of projectile- and target-fragment interferometers.

---

[9] See A. Tonomura et al., Am. J. Phys. **57**, 117 (1989) and references therein.
[10] J. M. Feagin and Si-ping Han, Phys. Rev. Lett. **86**, 5039 (2001).
[11] J. M. Feagin and Si-ping Han, Phys. Rev. Lett. **89**, 109302 (2002).
[12] L. S. Bartell, Phys. Rev. D**21**, 1698 (1980).
[13] M. S. Chapman et al., Phys. Rev. Lett. **75**, 3783 (1995); D. A. Kokorowski et al., Phys. Rev. Lett. **86**, 2191 (2001) and references therein.

a vibrational *coherent state* of the ions, which facilitates a variety of familiar analytical tools. Zoller and coworkers have shown[14] that even in such a 'strong-excitation regime' the vibrational motion coupled with laser-excited *internal* states of the ions can be used to perform basic elements of a quantum computation. We are thus working to develop a protocol to teleport a preset, internal qubit of the ion to a scattered projectile imaged with two-slit interferometry.

Hardy Nonlocality

We have recently extended this work to the detection of a pair of recoiling reaction fragments, each by its own interferometer,[15] to demonstrate Hardy's contradiction between quantum mechanics and local hidden variables.[16] Hardy's theorem sidesteps Bell's inequality by establishing the contradiction with just four measurement outcomes on two system fragments. Whereas Bell's theorem involves fully statistical violations of the quantum description, the Hardy result is simpler and hinges on essentially perfect correlations to establish nonlocality. Our interferometry is based on the momentum entanglement depicted in Fig. 1 and is independent of the identity and internal state of the fragments. Although no doubt a very difficult experiment, our approach is thus relatively straightforward, at least conceptually.

Dichroism and Nondipolar Effects

Two-slit detection would also provide new probes of photoionization angular distributions. Even with the photo *single* ionization of an unoriented atom, we have demonstrated[17] that one could generate a circular dichroism analogous to the well established effect seen in photo *double* ionization[18] and thereby extract phase information on nondipolar amplitudes.

A related dichroism and nondipolar probe is expected in ordinary fluorescence in which a photon takes the role of the photoionized electron and is analyzed by two-port interferometry, as depicted in Fig. 2. Such an experiment is currently underway by T. Gay and coworkers at the University of Nebraska and interference fringes have been observed with rubidium fluorescence photons. Our preliminary calculations indicate the technique may provide a useful method for extracting electric and magnetic *quadrupole* contributions to dipole allowed transitions.[19]

Collective Coulomb Excitations

The coincident measurement of two continuum electrons[20,21,22] has been extended to the photo double ionization of molecular hydrogen in the isotopic form D_2,[23] and recently including coincident detection of the deuterons.[24] We have thus developed a description of the

---

[14] J. F. Poyatos, J. I. Cirac, and P. Zoller, Phys. Rev. Lett. **81**, 1322 (1998); see also J. J. Garcia-Ripoll, P. Zoller, and J. I. Cirac, Phys. Rev. Lett. **91**, 157901 (2003)
[15] J. M. Feagin, Phys. Rev. A **69**, 062103 (2004).
[16] L. Hardy, Phys. Rev. Lett. **71**, 1665 (1993)
[17] J. M. Feagin, Phys. Rev. Lett. **88**, 043001 (2002).
[18] V. Mergel et al., Phys. Rev. Lett. **80**, 5301 (1998) and references therein. (*Feagin is a coauthor on this paper.*)
[19] J. M. Feagin, Phys. Rev. A, in preparation.
[20] R. Dörner et al, Phys. Rev. A**57**, 1074 (1998). (*Feagin is a coauthor on this paper.*)
[21] A. Knapp et al, J. Phys. B: At. Mol. Opt. Phys. **35**, L521 (2002). (*Feagin is a coauthor on this paper.*)
[22] M. Walter, J. S. Briggs and J. M. Feagin, J. Phys. B: At. Mol. Opt. Phys. **33**, 2907 (2000) and references therein.
[23] T. J. Reddish et al., Phys. Rev. Lett. **79**, 2438 (1997); N. Scherer et al., J. Phys. B: At. Mol. Opt. Phys. **31**, L817 (1998); J. P. Wightman et al., J. Phys. B: At. Mol. Opt. Phys. **31**, 1753 (1998).
[24] R. Dörner et al., Phys. Rev. Lett. **81**, 5776 (1998). (*Feagin is a coauthor on this paper.*)

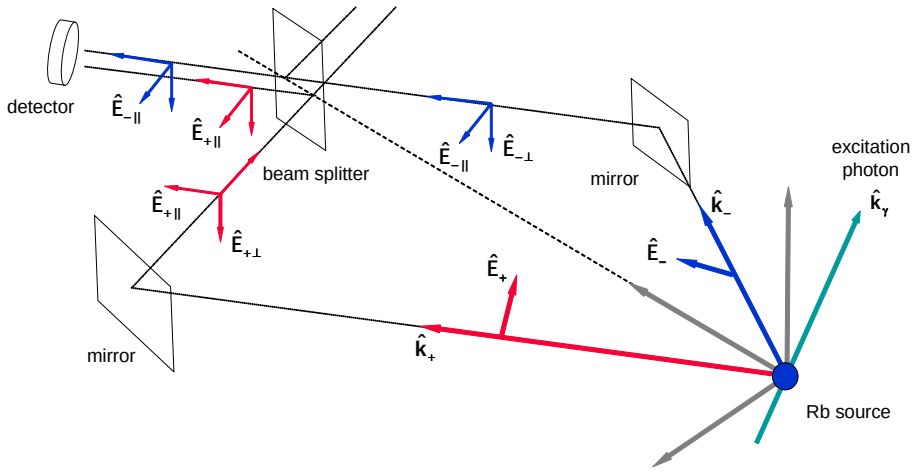

FIG. 2: Fluorescence photon interferometry with a single beam splitter. Here $\mathbf{k}_+$ and $\mathbf{k}_-$ are photon momentum components towards the two entrance ports (mirrors) of the interferometer with $\hat{\mathbf{E}}_+$ and $\hat{\mathbf{E}}_-$ the corresponding photon polarization directions. The trick is to resolve these polarization vectors into detector-frame components parallel and perpendicular to the plane of the interferometer, which we find must be tilted relative to the excitation photon momentum $\mathbf{k}_\gamma$ to see an effect.

photo double ionization cross section for diatomic molecules[25,26] based closely on the cross section for helium. We derive a dependence of molecular excitation amplitudes on electron energy sharing and dynamical quantum numbers labeling internal modes of excitation of the escaping electron pair. We consider both linear and circular polarizations. We have helped to compare our model to new and detailed D_2 *four-particle* fragmentation data Th. Weber has taken as part of his PhD work in Frankfurt in collaboration with L. Cocke (KSU) and M. Prior (LBNL).[27]

Publications

Hardy Nonlocality via Few-Body Fragmentation Imaging, J. M. Feagin, Phys. Rev. A**69**, 062103 (2004).

Fully Differential Cross Sections for Photo Double Ionization of Fixed-in-Space D_2, Th. Weber et al, Phys. Rev. Lett. **92**, 163001 (2004). (*Feagin is a coauthor on this paper.*)

Comment on Reaction Imaging with Interferometry, J. M. Feagin and Si-ping Han, Phys. Rev. Lett. **89**, 109302 (2002).

Energy Sharing and Asymmetry Parameters for Photo Double Ionization of Helium 100 eV Above Threshold, A. Knapp et al, J. Phys. B: At. Mol. Opt. Phys. **35**, L521 (2002). (*Feagin is a coauthor on this paper.*)

Circular Dichroism in Photo Single Ionization of Unoriented Atoms, J. M. Feagin, Phys. Rev. Lett. **88**, 043001 (2002).

Reaction Imaging with Interferometry, J. M. Feagin and Si-ping Han, Phys. Rev. Lett. **86**, 5039 (2001).

---

[25] J. M. Feagin, J. Phys. B: At. Mol. Opt. Phys. **31**, L729 (1998).
[26] T. J. Reddish and J. M. Feagin, J. Phys. B: At. Mol. Opt. Phys. **32**, 2473 (1999).
[27] Th. Weber et al., Phys. Rev. Lett. **92**, 163001 (2004). (*Feagin is a coauthor on this paper.*)

Studies of Autoionizing States Relevant to Dielectronic Recombination

T.F. Gallagher
Department of Physics
University of Virginia
P.O. Box 400714
Charlottesville, VA 22904-4714
tfg@virginia.edu

The scope of this program includes primarily phenomena which exist in two valence electron atoms but not in single valence electron atoms. The central focus has been dielectronic recombination (DR), the major source of recombination in high temperature plasmas. Ironically, the same physical processes which are important for DR are also important for zero kinetic energy (ZEKE) photoelectron spectroscopy, commonly used in the spectroscopy of small molecules. The notions of electric field enhancement of DR, and forced autoionization, developed under this program, have been particularly important for ZEKE spectroscopy.

In the past year we have worked primarily on DR from a continuum of finite bandwidth.[1] We have worked on three specific problems. First, we have examined the electric field enhancement for different entrance channels to show that using the field dependence of the DR it is possible to determine which of the nearly degenerate high ℓ states actually contribute to DR.[2] Second, we have carried out measurements of DR in very high frequency, 38 GHz, microwave fields. The original goal was to see resonant enhancement of well resolved intermediate states, which we hope will lead to microwave spectroscopy of autoionizing states. Finally, we have started to assemble the pieces for doing broadband microwave noise assisted DR.

True DR is the recombination of a continuum (free) electron with an ion via an intermediate autoionizing state. The example,

$$\mathrm{Ba}^+\ 6s_{1/2} + e^-\varepsilon\ell' \rightarrow \mathrm{Ba}\ 6p_{1/2}n\ell \rightarrow\ \mathrm{Ba}\ 6s_{1/2}n\ell + h\nu \quad , \tag{1}$$

shows that first the electron excites Ba^+ from the $6s_{1/2}$ to $6p_{1/2}$ state and is itself captured. Then, if radiative decay to the bound $6s_{1/2}\,n\ell$ state occurs, recombination has taken place.[3] In DR from a continuum of finite bandwidth we replace the true continuum with a broad $6p_{3/2}11d$ or $6p_{3/2}8g$ ionizing state straddling the Ba^+ $6p_{1/2}$ limit. We have examined the two processes

$$\mathrm{Ba}\ 6p_{3/2}11d \rightarrow \mathrm{Ba}\ 6p_{1/2}\,nd \rightarrow \mathrm{Ba}\ 6s\,nd + h\nu \tag{2a}$$

and

$$\mathrm{Ba}\ 6p_{3/2}8g \rightarrow \mathrm{Ba}\ 6p_{1/2}\,ng \rightarrow \mathrm{Ba}\ 6s\,ng + h\nu \quad . \tag{2b}$$

The $6p_{3/2}11d$ or $6p_{3/2}8g$ state makes the interchannel transition to the degenerate $6p_{1/2}nd$ or $6p_{1/2}ns$ state ($40 < n < \infty$). If it decays radiatively to the bound $6s_{1/2}nd$ or $6s_{1/2}ng$ state, DR has occurred. The primary attractions of this technique are the energy resolution of ~ 0.5 cm^{-1} (< 0.1 meV), the fact that the experiments can be done in zero field, and that the partial wave of the entrance channel is well defined. In the continuum of finite bandwidth experiments each $11d$ electron makes about twenty orbits and collides with the Ba^+ core twenty times before it autoionizes. In essence we are using the Ba $6p_{3/2}11d$ state as a storage ring for our DR experiment.[4]

In the first experiment we have compared the effects of electric fields on DR starting from the $6p_{3/2}11d$ and $6p_{3/2}8g$ continua of finite bandwidth. The motivation for this experiment

was that the quantum defects δ_d and δ_g of the intermediate $6p_{1/2}nd$ or $6p_{1/2}ng$ states are very different. In particular $\delta_d = 0.25$, while $\delta_g = 0.02$. The intermediate Ba $6p_{1/2}ng$ states are Stark mixed by a field a factor of ten smaller than the $6_{1/2}nd$ states.[5] Consequently, field enhancement of DR should occur at fields a factor of ten lower[6] using the Ba $6_{3/2}8g$ state as the continuum of finite bandwidth rather than the Ba $6p_{3/2}11d$ state. The experiment shows that, in fact, the field required for enhancement of DR via the Ba $6p_{1/2}ng$ states is a factor of ten lower than the field required for enhancement of DR via the $6p_{1/2}nd$ states. The significance of this finding is that it shows that the electric field dependence of DR via a set of nearly degenerate $n\ell$ states can be used to determine which ℓ states contribute. The autoionization rates (and thus the DR rates) decrease rapidly with ℓ, as do the quantum effects, which are non zero for any atom but H.[7,8] The field at which an $n\ell$ state joins the manifold is proportional to the quantum defect, and easily calculated.[5,7,8] The field at which the DR rate begins to increase is the field at which the ℓ state with an autoionization rate in excess of the radiative decay rate joins the Stark manifold.[2]

We have recently built a 38 GHz Fabry-Perot microwave cavity to explore DR in the presence of this microwave field. Previously we examined the DR process of Eq. (2a) in microwave fields of frequencies up to 12 GHz. We observed resonant enhancement when the microwave frequency satisfied

$$\omega = k / n^3 \quad , \tag{3}$$

i.e., when the microwave frequency matched the frequency of the $\Delta n = 1, 2, \ldots k$ transition in the atom.[9,10] The mechanism is resonant Stark mixing. For a 12 GHz field the $\Delta n = 1$ resonance at $n = 82$, is not resolved by our laser, which has a typical linewidth of 15 GHz. However, the 38.7 GHz $\Delta n = 1$ resonance, $n = 55$, should be resolved. The autoionization rates of the Ba $6p_{1/2}nd$ states are $\sim 0.05n^{-3}$, and we must drive the $\Delta n = 1$ transition before the atoms autoionize, which means that the microwave field must produce a Rabi frequency of ~ 2 GHz to have an effect. Since we do not have a high power 38 GHz source we have used a Fabry-Perot cavity with a Q of about 900. We have observed several fascinating phenomena. First, it is straightforward to observe well resolved $6p_{1/2}nd$ states, so with some modifications it may be possible to use this approach to do microwave spectroscopy of autoionizing levels. To our knowledge this has never been done. Second, we can observe resonance enhancement up to $\Delta n = 10$, whereas in the previous experiment we could only see resonances up to $\Delta n = 4$.[9,10] An interesting aspect of the higher k resonances, e.g., $\Delta n = 6$, is that it appears that it is $\Delta n = +6$, not $\Delta n = \pm 6$, although this feature must be examined more carefully. Such an asymmetry is possible since the higher n state is more likely to be Stark mixed. This phenomenon may be an interesting way to tag specific optically accessible states and could be useful in ZEKE spectroscopy.[11] The final and most interesting phenomenon we have observed is above threshold DR. In particular, we are able to see very strong (30% of the real zero field signal) DR signals at energies up to 5 cm^{-1} above the $6p_{1/2}$ limit. The observed DR signal exhibits a modulation at the microwave frequency and the modulation extends both above and below the limit. It is evidently DR via the $6p_{1/2}n\ell$ series dressed by the microwave field. In other words, the capture of the $11d$ electron occurs with the stimulated emission or adsorption of microwave photons. This process could be of interest for other experiments based on recombination.[12]

In the coming year we are planning to explore the fascinating avenues opened up by the 38 GHz experiment, initially using a cavity of lower Q which can be turned off more quickly. In some cases it may be possible to use a horn. We plan to explore the idea of tagging high lying Rydberg states, $n > 100$, with a well defined microwave frequency. Beyond these experiments

we plan to mimic the random time varying fields of electrons in a plasma using broadband microwave noise instead of a monochromatic microwave field. It should be possible to generate both linear, circular, and random, polarizations. We expect that noise will be more effective in enhancing DR than a static or monochromatic field.

References

1. J.P. Connerade, Proc. R. Soc. London, Ser. A, 362, 361 (1978).
2. E.S. Shuman, C.M. Evans, and T.F. Gallagher, Phys. Rev. A 69, 063402 (2004).
3. A.L. Merts, R.D. Cowan, and N.H. Magee, Jr., Los Alamos Report No. LA-62200-MS (1976).
4. T. Bartsch, S. Schippers, A. Muller, C. Brandau, G. Gwinner, A.A. Saghiri, M. Beutelspachier, M. Grieser, D. Schwalm, A. Wolf, H. Danared, and G.H. Dunn, Phys. Rev. Lett. 82, 3779 (1999).
5. M.L. Zimmerman, M.G. Littman, M.M. Kash, and D. Kleppner, Phys. Rev. A 20, 2251 (1979).
6. V.L. Jacobs, J. Davis, and P.C. Kepple, Phys. Rev. Lett. 37, 486 (1976).
7. B. Edlen, in *Spectroscopy I*, edited by S. Flugge, Handbuch der Physik, Vol. 27 (Springer, Berlin, 1964).
8. W.H. Clark and C.H. Greene, Rev. Mod. Phys. 71, 821 (1999).
9. V. Klimenko and T.F. Gallagher, Phys. Rev. Lett. 85, 3357 (2000).
10. V. Klimenko and T.F. Gallagher, Phys. Rev. A 66, 023401 (2002).
11. E.W. Schlag, *ZEKE Spectroscopy* (Cambridge University Press, Cambridge, 1998).
12. G. Gabrielse, N.S. Bowden, P. Oxley, A. Speck, C.H. Storry, J.N. Tan, M. Wessels, D. Grzonka, W. Oelert, G. Schepers, T. Sefzick, J. Walz, H. Pittner, T.W. Hänsch, E.A. Hessels, and (and ATRAP collaboration), Phys. Rev. Lett. 89, 213401 (2002).

Publications 2002-2004

1. H. Maeda and T.F. Gallagher, "Inner electron ionization of Sr 5s16ℓ states," Phys. Rev. A 65, 053405 (2002).
2. V. Klimenko and T.F. Gallagher, "Resonant enhancement of dielectronic recombination from a continuum of finite bandwidth," Phys. Rev. A 66, 023401 (2002).
3. C.M. Evans, E.S. Shuman, and T.F. Gallagher, "Microwave-induced dielectronic recombination above the classical ionization limit in a static field," Phys. Rev. A 67, 043410 (2003).
4. V. Klimenko, L. Ko, and T.F. Gallagher, "Enhancement of dielectronic recombination in crossed electric and magnetic fields," Phys. Rev. A 68, 012723 (2003).
5. E.S. Shuman, C.M. Evans, and T.F. Gallagher, "ℓ dependence of dielectronic recombination from a continuum of finite bandwidth in an electric field" Phys. Rev. A 69, 063402 (2004).

EXPERIMENTS IN MOLECULAR OPTICS

Robert J. Gordon

Department of Chemistry (m/c 111), University of Illinois at Chicago,
845 West Taylor Street, Chicago, IL 60607-7061, email address: rjgordon@uic.edu

1. Program Scope

The broad objective of this research program is to use the dipole force of an electromagnetic field to control the motion of neutral atoms and molecules. In these studies, the intensity gradient of a focused laser beam serves as a "molecular optic" that can be used to deflect, focus, and align a beam of particles.

The potential energy induced by a far off-resonant field is given by

$$U(r,q) = -me\cos q - \frac{1}{4}e^2(r)\left(\Delta a\cos^2 q + a_\perp\right),$$

where $e(r)$ is the electric field, μ is the dipole moment, $\Delta a = a_{//} - a_\perp$ is the polarizability anisotropy, $a_{//}$ and $a_\perp$ are the parallel and perpendicular components of the polarizability tensor, and q is the angle between the principle axis of the molecule and the e vector. For a rapidly oscillating, bipolar electric field, the dipole term averages to zero. If the atom or molecule is in its ground electronic state, the polarizability is positive and the potential energy is negative. In this case the particle experiences an attractive force that draws it into the field. The radial gradient of $e^2(r)$ thereby acts as a prism, which bends the trajectories of the particles. If in addition the polarizability is anisotropic, the $\Delta a\cos^2 q$ term induces a torque that aligns the molecules. If the field is asymmetric in sign so that the dipole term does not average to zero, the molecules may also be oriented by the field.

The ability to focus, align, and orient molecules has many potential applications. For example, a focused beam of molecules could be used to create nanostructures with novel electrical and optical properties. Aligned and oriented molecules could be used for stereospecific chemical reactions, to enhance high harmonic generation, and for isotope separation.

2. Recent Progress

Two projects currently running in our laboratory involve deflection of molecules with nanosecond lasers and alignment of molecules with ultrashort pulses. In order to conduct both sets of experiments simultaneously, we spent the past year constructing a second molecular beam imaging apparatus, which is shown schematically in Fig. 1. With this apparatus, a Nd:YAG laser is used to deflect molecules, and a dye laser ionizes molecules in specific quantum states. A key feature of this apparatus is an Einzel lens,

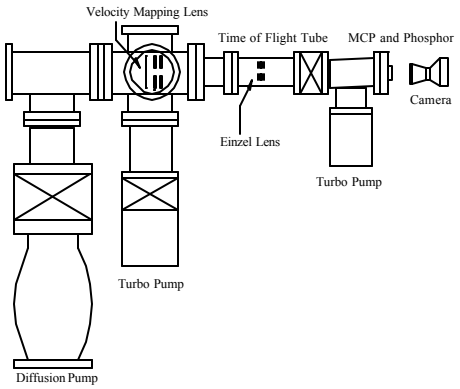

Figure 1

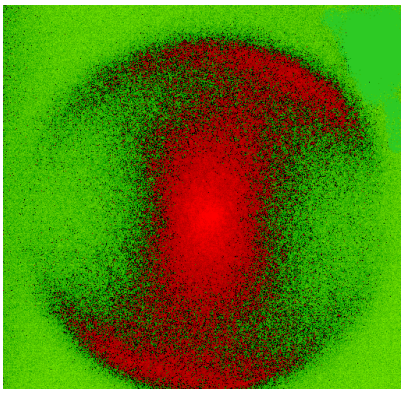

Figure 2

which was designed to enhance ion deflections by a factor of as much as 200. Other features include a motorized ion focusing assembly, which greatly simplifies positioning of the ion beam onto the microchannel plate detector, and an extendable flight tube. With the exception of the Einzel lens, which has been constructed but not yet installed, the apparatus is fully operational. A test image of I^+ produced by photoionizing iodobenzene at 532 nm is shown in Fig. 2. The central peak and vertical stripe are produced by multiphoton dissociative ionization, and the outer ring comes from a two-photon n,s* transition causing an energetic recoil of the I atom.

Concurrent with the apparatus construction, we have moved forward with the ultrafast alignment experiment. The output from a Ti:Sapphire (45 fs, 2 mJ, 1 kHz) laser was split into several beams, allowing one or two stretched pulses to be used for aligning molecules in a molecular beam, and an intense 45 fs pulse to be used as an ionizing probe. Alignment revivals may be observed either by imaging of the gated ions or by measuring the total ion signal collected by a boxcar as a function of delay between the pump and probe. In a test run we have used the second method to record the first half-revival of I_2 molecules.

3. Future Plans

During the coming year we plan to continue working on the deflection and alignment experiments. Once the Einzel lens has been installed, we plan to use the deflection apparatus to separate hydrogen halide molecules in different rotational M_J states. The idea behind this experiment is that molecules in different M_J states will experience different deflection potentials, depending on the angle between the molecular axis and the polarization vector of the laser field. In a second experiment, we plan to excite Kr atoms to high Rydberg states and to measure the deflection as a function of principle quantum number. Very large positive and negative polarizabilites are expected for such states. For the higher Rydberg states having negative polarizabilies, the focused laser beam should function as a molecular mirror.

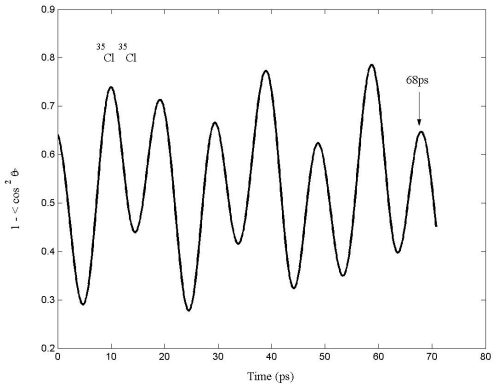

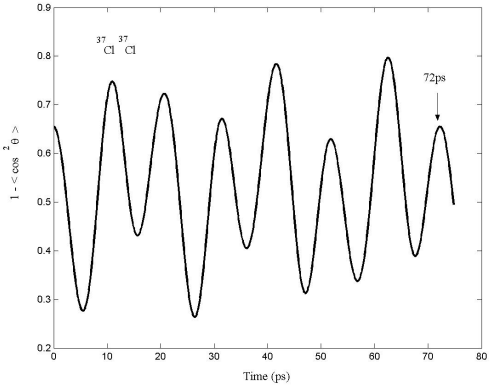

Figure 3a

Figure 3b

Two experiments are planned for the alignment apparatus. In the first we propose to utilize the mass dependence of the moment of inertia to separate different isotopomers. Figure 3 is a calculation of $1 - \langle \cos^2 \theta \rangle$ vs. pump-probe delay, showing the rotational revivals of $^{37}Cl^{37}Cl$ (panel a) and $^{35}Cl^{35}Cl$ (panel b). The revivals of the two isotopomers are separated by several ps, which should be easily resolvable. Maximum resolution should be achieved by measuring the total ion current from the parent ion. In a second experiment we propose to orient molecules by using a combination of a weak half-cycle pulse to kick molecules into a preferred hemisphere followed by a strong aligning pulse. The experiment will be preceded by a model calculation to determine the requisite field parameters.

4. Publications in 2002-2004

H. Yamada, N. Taniguchi, M. Kawasaki, Y. Matsumi, and R. J. Gordon," Dissociative Ionization of ICl Studied by Ion Imaging Spectroscopy," J. Chem. Phys. **117**, 1130 (2002).

R. J. Gordon, L. Zhu, W. A. Schroeder, and T. Seideman, "Nanolithography Using Molecular Optics," J. Appl. Phys. **94**, 669 (2003).

Experiments in Ultracold Collisions

Phillip L. Gould
Department of Physics U-3046
University of Connecticut
2152 Hillside Road
Storrs, CT 06269-3046
<gould@uconnvm.uconn.edu>

Program Scope:

Ultracold atoms have come to play an increasingly important role in atomic, molecular, and optical (AMO) physics. Such samples have proven useful in a variety of areas, including: Bose-Einstein condensation (BEC) and atom lasers; degenerate Fermi gases; photoassociative spectroscopy; ultracold molecule production; ultracold Rydberg atoms and plasmas; optical lattices; quantum optics and quantum computing; precision spectroscopy and improved atomic clocks; studies of photoionization, electron scattering, and ion-atom collisions; and fundamental atomic and nuclear physics experiments with radioactive isotopes. At the high densities (e.g., $n>10^{11}$ cm^{-3}) and low temperatures (e.g., $T<100$ μK) which are usually encountered in these studies, collisions between the ultracold atoms are important processes. They can be either detrimental or beneficial. As an example of the former, inelastic collisions can cause loss from atom traps. By contrast, the production of degenerate quantum gases (e.g., BEC) relies on elastic collisions for thermalization, and proposed neutral atom quantum computation schemes require a collisional interaction for producing entanglement. The main motivation of our experimental program is to not only improve our understanding of ultracold collisions, but also to devise ways to control them to our benefit.

Beyond the relevance of our studies to ultracold applications, there is significant fundamental interest in these extremely low energy (e.g., $\sim 10^{-8}$ eV) interactions. Since the angular momentum of the collision is usually small, quantum effects can be important. Also, the low collisional velocity allows the motion to be significantly altered by the long-range dipole-dipole interactions involving excited atoms. Collisions can thus be controlled, either enhanced or suppressed, with laser light. Furthermore, the dynamics occur on a slow time scale, allowing the collisions to be probed and manipulated in real time.

Our experiments use a magneto-optical trap (MOT) to capture, cool, and confine rubidium (Rb) atoms. Rb is our atom of choice because: 1) its resonance line is well-matched to readily available diode lasers at 780 nm; 2) there are two stable and abundant isotopes (^{85}Rb and ^{87}Rb) with different collisional properties; and 3) ^{87}Rb is the most popular atom for BEC studies. In our experiments, a phase-stable MOT is loaded from a slow atomic beam and the subsequent decay of atoms from the trap is monitored. The density-dependent atomic loss rate yields the inelastic collisional rate constant.

Recent Progress:

Our recent efforts have focused mainly on ultracold collisions induced by frequency-chirped laser light. Up until now, ultracold collision experiments involving excited atoms have used fixed-frequency light applied either continuously (cw) or in short pulses (e.g., 100 ns). A given frequency of light excites an atom pair to the attractive molecular potential at a particular internuclear separation R. By "chirping" the light, i.e., sweeping its frequency in time, atom pairs over a wide range of R can be excited and caused to collide. Chirping has the further advantage

that, if the laser intensity is sufficiently high, the population is transferred adiabatically to the excited state, making the process efficient and robust. We have observed that the rate of collisions induced by a positive (red-to-blue) chirp does indeed saturate with intensity, as expected for an adiabatic process. Also, the absolute collision rate is consistent with all collision pairs which are accessed by the chirp (and whose excitation survives to short range) undergoing an inelastic trap loss collision. We have also investigated the effect of the chirp rate. When the chirp occurs on the time scale of the atomic collisions, we observe a much larger collision rate than when the chirp is slow enough to be considered quasi-cw.

We have invested considerable effort in producing the frequency-chirped light required for these collision experiments. We start with an external-cavity diode laser and rapidly modulate its current to produce the chirp. Unfortunately, the desired frequency modulation is accompanied by significant amplitude modulation. This is eliminated by injecting a small amount of light from the chirped "master" laser into a separate free-running "slave" diode laser. The frequency of the injection-locked slave laser tracks the chirp of the master, while its output power remains essentially constant. Various heterodyne diagnostics allow us to characterize the chirp. Chirp rates up to 15 GHz/μs, with power modulations <1%, have been produced in this manner. The power available from the slave laser is also considerably higher than that from the master.

In collaboration with theorists here at UConn and in Armenia and Finland, we have developed a model for photoassociation of a BEC. Starting with a purely atomic BEC, light is adiabatically swept through a photoassociative resonance, thereby converting atoms into bound molecules. The situation is reminiscent of the well-known Landau-Zener model, where two coupled curves cross and the probability of making a transition from one curve to the other depends exponentially on the rate at which the crossing is traversed. In the case of BEC photoassociation, however, the system is nonlinear due to the fact that it takes two atoms to make a molecule. Surprisingly, we find that in this nonlinear case, the no-transition probability is linearly proportional to the rate at which the crossing is traversed. This analytical result, which has been tested numerically, will apply to any field theory involving these nonlinear terms.

Future Plans:

Our plans for the coming year involve two ultracold collision experiments. First, we will continue our work with frequency-chirped collisions. We will investigate the influence of the direction of the chirp (red-to-blue vs. blue-to-red) and the frequency range covered by the chirp. We will also vary the delay between successive chirps and look for cooperative effects. For sufficiently short delays, we expect that the atom pairs available for a given chirp will be depleted by the preceeding chirp. Under some conditions, we expect enhancement of one chirp's collision rate by its predecessor. This will occur if long-range collisional flux is excited by the first chirp, but the excitation decays before an inelastic trap-loss collision occurs. This enhanced flux is then available to be re-excited by the second chirp. So far, we have used linear current ramps to produce simple linear chirps. We will attempt to produce more sophisticated chirps and vary these chirps to optimize collision rates. Finally, we will apply a separate fixed-frequency laser, tuned to a photoassociative resonance, and use the frequency chirp to transiently enhance the flux available for photoassociation.

In our second planned experiment, we will simultaneously trap ^{85}Rb and ^{87}Rb and study collisions involving the two species. Interactions between mixd species of ultracold atoms are of interest for many reasons: sympathetic cooling of one species by another, mixed Bose-Einstein condensates and degenerate Fermi gas systems, and the formation of polar heteronuclear molecules. In terms of ultracold collisions, the ground-excited potential between two atoms at long range differs depending on whether the atoms are identical (R^{-3}) or different (R^{-6}).

Therefore, some of the trap-loss processes in mixed isotopes should be suppressed by the shorter range of the potential. The measurements will be carried out by observing how the trap-loss rate of one species is modified by the presence of the other.

Recent Publications:

"Measurement of the Rb($5D_{5/2}$) Photoionization Cross Section Using Trapped Atoms", B.C. Duncan, V. Sanchez-Villicana, P.L. Gould, and H.R. Sadeghpour, Phys. Rev. A **63**, 043411 (2001).

"A Frequency-Modulated Injection-Locked Diode Laser for Two-Frequency Generation", R. Kowalski, S. Root, S.D. Gensemer, and P.L. Gould, Rev. Sci. Instrum. **72**, 2532 (2001).

"Landau-Zener Problem for Trilinear Systems", A. Ishkhanyan, M. Mackie, A. Carmichael, P.L. Gould, and J. Javanainen, Phys. Rev. A **69**, 043612 (2004).

"Frequency-Chirped Light from an Injection-Locked Diode Laser", M.J. Wright, P.L. Gould, and S.D. Gensemer, Rev. Sci. Instrum., accepted for publication.

Physics of Correlated Systems

Chris H. Greene
Department of Physics and JILA
University of Colorado, Boulder, CO 80309-0440
chris.greene@colorado.edu

1. Program scope and overview

The general goal of this research project is to study the interactions of different degrees of freedom in an atom, molecule, or cluster, in an effort to gain an understanding of how energy can be interconverted among them. The systems studied are primarily of small or modest scale, and they are predominantly systems that show strong correlations between the various degrees of freedom. For these systems, which are microscopic and therefore necessitate the use of a quantum mechanical description in most cases, perturbative techniques are inadequate. The following paragraphs describe the areas of our concentration during the past year.

2. Energy interconversion between the electronic and nuclear degrees of freedom in an electron collision with a polyatomic molecule

Recent work by our group developed the first quantitative theoretical description of dissociative recombination for a polyatomic molecule, the for H_3^+ ion, which includes all degrees of freedom quantum mechanically.[1-5] A key result of this work was a confirmation of an earlier suggestion that this electron-impact-induced dissociation process is triggered by Jahn-Teller coupling. The first quantitative DR calculations that emerged from this treatment [4,5] were in general agreement with the newest storage ring experiment, over much of the incident energy range from 0-2 eV. However, there were some discrepancies, such as the energy range from 0.7-2 eV, where our calculation was more than an order of magnitude lower than experiment. One of the developments within the past year was our realization that the region where the electron beam is merged into the circulating ion beam in the experiments results in higher-energy collisions than in the parallel beam region. This results in a "toroidal correction" that had only been approximately accounted for in the published experimental data. When we reanalyzed this correction, and applied it directly to our theoretically calculated spectrum, most of the discrepancies between theory and experiment in the 0.7-2 eV range disappeared.[2]

One of the extensions that was underway last year, mentioned in the 2003 abstract of this project, was a calculation of the photoionization cross section of the metastable state of H3, studied extensively over a decade ago by H. Helm and his collaborators. This was a crucial test of the wavefunctions produced by the new theoretical approach developed to describe the dissociative recombination process. Since that time, these calculations were completed,[1] and they show very encouraging agreement between theory and experiment, significantly improved over the calculations carried out in the early 1990s by the P.I. with J. Stephens. This test permitted a detailed study of some resonance features prominent in two very different experiments, and it adds to our confidence in the validity of the approximations employed. Some discrepancies for the higher-energy photoionization resonances remain unexplained, however, and deserving of further study.

A set of calculations for the recombination rate of the isotopomers of H_3^+ is nearly completed and is expected to be published within the coming year.[3] A longer-term project, for which we have made good headway during the past twelve months, is a study of the dissociative recombination of HCO^+ triggered by an electron collision. This will be an important test of whether our method has general applicability to other species of chemical interest. A specific question that we hope to answer is whether the Renner-Teller effect controls the DR rate for linear molecular ions, analogous to the now-demonstrated importance of Jahn-Teller coupling for H_3^+. V. Kokoouline at the University of Central Florida continues to be an important collaborator on this project.

One thing required in most photoionization and electron-molecule collision calculations is a reliable method to compute the clamped-nuclei electron scattering amplitudes. A graduate student supported by this project, Stefano Tonzani, continued to develop the capability to carry out such calculations. A paper presenting a fully three-dimensional electron-molecule scattering code, using finite-element technology at the static-exchange level, has been submitted for publication.

3. Properties of metastable alkaline-earth atoms

Robin Santra has worked on a number of projects [6-8] involving the metastable states of the alkaline-earth atoms, since joining the group in the autumn of 2003. His first studies[7,8] probed the long-range interaction between two excited, anisotropic strontium atoms. These papers appear to have been significant in persuading some experimental groups that this system and other anisotropic systems of the same class will in most cases have too much inelastic decay to permit the creation of a long-lived condensate. Nevertheless, interest in the metastable states of Group II elements continues for applications related to atomic clock technology. This generated our interest in extending our two-electron codes to calculate many properties, such as the decay rates of quasi-forbidden transitions, and anisotropic interaction coefficients.[6]

4. Atoms, ions, and clusters in an intense VUV laser field

Another project that Robin Santra spearheaded has been a theoretical description of xenon clusters that are exposed to intense VUV radiation, of the type provided by the free-electron laser at the TESLA Test Facility (TTF) in Hamburg. This is a new regime of strong photon-cluster interactions, very different from the physics of infrared lasers that are directed at such clusters. Our theoretical treatment [9] showed that linear physics is able to explain why approximately 30 photons per atom are absorbed, in a 100 femtosecond pulse of intensity 7.3×10^{13} W/cm^2. [The experimental research was published by H. Wabnitz *et al.*, Nature **420**, 482 (2002).] Our calculations suggest that this absorption of this many VUV photons, one at a time, can be understood once realistic screened potentials are used to describe the behavior of the electrons, in addition to plasma screening effects. The energy absorption is dominated by free-free radiative absorption or inverse bremsstrahlung, but it is important to go beyond the level of simple Debye-screened hydrogenic potentials for the electron-ion interactions. A PhD student who began working in the group this year, Zachary Walters, is studying improvements to the initial calculations reported in [9], in an attempt to develop a more complete and quantitative description of this new regime of laser-cluster interaction dynamics. Calculations with Robin Santra are also underway to treat multiphoton ionization of single xenon atoms and ions, in order to interpret a new experimental measurement at the TESLA Test Facility.

5. Other miscellaneous projects completed since 2002

Papers [10-16] below discuss other results published during the past three years, which were described in detail in past abstracts submitted for this project.

Papers published since 2002 that were supported at least in part by this grant

[1] *Photofragmentation of the H_3 molecule, including Jahn-Teller coupling effects,* V. Kokoouline and C. H. Greene, Phys. Rev. A **69**, 032711-1 to -16 (2004).

[2] *Dissociative recombination of polyatomic molecules: A new mechanism,* C. H. Greene and V. Kokoouline, Phys. Scr. **T110**, 178-182 (2004).

[3] *Triatomic dissociative recombination theory: Jahn-Teller coupling among infinitely many Born-Oppenheimer surfaces,* V. Kokoouline and C. H. Greene, Faraday Discuss. **127**, xxx-yyy (2004). (in press).

[4] *Theory of dissociative recombination of D_{3h} triatomic ions applied to H_3^+*, V. Kokoouline and C. H. Greene, Phys. Rev. Lett. **90**,133201-1 to -4 (2003).

[5] *Unified theoretical treatment of dissociative recombination of D_{3h} triatomic ions: Application to H_3^+ and D_3^+*, Phys. Rev. A **68**, 012703-1 to -23 (2003).

[6] *Properties of metastable alkaline-earth-metal atoms calculated using an accurate effective core potential*, R. Santra, K. V. Christ, and C. H. Greene, Phys. Rev. A **69**, 042510-1 to -10 (2004).

[7] *Tensorial analysis of the long-range interaction between metastable alkaline-earth-metal atoms*, R. Santra and C. H. Greene, Phys. Rev. A **67**, 067213-1 to -15 (2003).

[8] *Multichannel cold collisions between metastable Sr atoms*, V. Kokoouline, R. Santra, and C. H. Greene, Phys. Rev. Lett. **90**, 253201-1 to -4 (2003).

[9] *Xenon clusters in intense VUV laser fields*, R. Santra, and C. H. Greene, Phys. Rev. Lett. **91**, 233401-1 to -4 (2003).

[10] *Nonclassical paths in the recurrence spectrum of diamagnetic atoms*, B. E. Granger and C. H. Greene, Phys. Rev. Lett. **90**, 043002-1 to -4 (2003).

[11] *Phase modulation of ultrashort light pulses using molecular rotational wave packets*, R.A. Bartels, T.C. Weinacht, N. Wagner, M. Baertschy, C.H. Greene, M.M. Murnane, and H.C. Kapteyn, Phys. Rev. Lett. **88**, 013903-1 to 013903-4 (2002).

[12] *Phase matching conditions for nonlinear frequency conversion by use of aligned molecular gases*, R.A. Bartels, N.L. Wagner, M.D. Baertschy, J. Wyss, M.M. Murnane, and H.C. Kapteyn, Optics Letters 28, 346-348 (2003).

[13] *Excitation of the $3p^4(4s,3d,4p)$ Ar^+ states during Ar photoionization: Intensity, alignment, and orientation*, H.W. van der Hart and C.H. Greene, Phys. Rev. A **65**, 062509 (2002).

[14] *Regularities and irregularities in partial photoionization cross sections of He*, H.W. van der Hart and C.H. Greene, Phys. Rev. A **66**, 022710 (2002).

[15] *Multiphoton processes in a two-dimensional model of helium, in "Correlations, Polarization, and Ionization in Atomic Systems"*, C.H. Greene, M. Baertschy, A.L. Young, and B.E. Granger, in , AIP Conference Proceedings, **604**, pp.1-5, (2002),. edited by D.H. Madison and M. Schulz.

[16] *Time-dependent close-coupling calculations of the triple-differential cross section for electron-impact ionization of hydrogen*, J. Colgan, M. S. Pindzola, F. J. Robicheaux, D. C. Griffin, and M. Baertschy, Phys. Rev. A **65**, 042721 (2002).

Chemistry with Ultracold Molecules

Dudley Herschbach
Department of Chemistry and Chemical Biology,
Harvard University, Cambridge, MA 02138
herschbach@chemistry.harvard.edu

This project aims to develop simple and versatile means to generate slow and cold molecules and manipulate their trajectories. The chief goal is to achieve the capability to explore energy transfer and chemical reactions of ultracold molecules, in the "nanomatterwave" domain. There molecular translation becomes so slow as to endow the molecules with deBroglie wavelengths larger than the size of the molecules. A key requisite for launching such studies is a means to lower markedly the molecular translational kinetic energy, to well below 1 K and thereby enable us to trap the molecules by static or radiative fields.

We have previously developed a device for producing intense beams of molecules with low kinetic energy [1]. This employs a supersonic nozzle near the tip of a hollow high-speed rotor, into which a permanent gas is feed continuously. Spinning the rotor with peripheral velocities of several hundred meters/sec, contrary to the direction of gas flow from the nozzle, markedly reduces the velocity of the emerging molecular beam in the laboratory frame.

Recent Progress: During the past year, we have pursued several ingredients of our program with generally encouraging results. This work has been carried out by new personnel: two postdoctoral fellows, Tim McCarthy and Mike Timko, who joined our group in January and March '04; and three undergraduates, Sunil Sheth, Rameez Qudsi, and Nilam Shah, working for various portions of the year.

(1) Scattering of slow molecules by background gas had proved a serious limitation of our method [1]. Much of the background came from the inevitable leaking of gas where the stationary feed line enters an orifice in the rapidly spinning rotor. That leakage has now been drastically reduced by adding an auxilary differentially pumped chamber. In recent runs using inverse seeding in Xe, our rotor device has now produced a beam of O_2 molecules with kinetic energy of 3 K, corresponding to a deBroglie wavelength exceeding 3 A.

(2) An auxilary apparatus has been constructed and applied to development of a supersonic C atom beam source employing laser ablation and cooling by a concurrent flow of rare gas.

(3) Our efforts begun last year to employ a silver-coated surface as a means to detect beams containing halogen or oxygen molecules were carried further. A protocol was evolved to read the images by means of a microscope backed up by a CCD camera. The sensitivity obtained for an HBr beam corresponds to a monolayer of molecules. Attempts to record diffraction patterns produced by sending the beam through a transmission grating (slits 50 μm wide, spaced 100 μm) gave results we do not yet understand. Although the overall width of the profile agrees well with the predicted diffraction pattern, the profile does not show the expected interference structure even though other tests of the detector indicate the angular resolution is sufficient.

(4) As a means to guide molecules into traps or storage rings and to separate them from the diluent gas used in the supersonic expansion, we have constructed an "E-H balance" apparatus. This device, originally employed by Bederson and colleagues in early studies of atomic polarizability [2], makes use of congruent electric and magnetic Stern-Gerlach deflecting fields. As a first application, we intend to use this to separate O_2 molecules from the diluent Xe. In trapping experiments, this will enable us to accumulate O_2 from many cycles of our rotor source, without disruption from Xe flying through the trap. We have carried out extensive computer simulations that demonstrate the resolution of this "filter" is very effective for molecules with low kinetic energy, because deflections are inversely proportional to the kinetic energy. When the balance condition is fulfilled (by adjusting the current in the magnet coils and voltage applied to the pole tips), $\alpha E(\partial E/\partial z) = \mu_{eff}(\partial H/\partial z)$. Here α is the molecular polarizability, which produces an attractive interaction deflecting towards the higher-field region; μ_{eff} is the effective low-field seeking component of the magnetic moment, E and H the electric and magnetic field strengths.

References: [1] M. Gupta and D. Herschbach, Slowing or Speeding Molecular Beams by Means of a Rapidly Rotating Source, *J. Phys. Chem. A* **105**, 1626 (2001).

[2] A. Salop, E. Pollack, and B. Bederson, *Phys. Rev.* **124**, 1431 (1961); E. Pollack, E.J. Robinson, and B. Bederson, *Phys. Rev.* **134**, A1210 (1964).

Future Plans: (1) With further improvements of the rotor apparatus, we anticipate producing intense molecular beams with laboratory kinetic energies below 0.5 K, low enough to permit trapping. (2) With the aid of the E-H balance, we will seek to demonstrate cumulative trapping of O_2 molecules and C atoms. (3) Exploit the E-H filtering to try evaporative cooling of the trapped molecules. (4) Undertake study of ultracold C + O_2 collisions, monitoring formation of CO + O by observing the CO product spectroscopically. (5) If things go unreasonably well, study also C + NO to form CN + O or CO + N.

Publications: B.K. Zhao, M. Castillejo, D.S. Chung, B. Friedrich, and D. Herschbach, A Cool Pulsed Molecular Micro-Beam, *Rev. Sci. Inst.* **75**, 146-150 (2004); B.K. Zhao, S.H. Lee, H.S. Chung, S. Hwang, B. Friedrich, and D.S. Chung, Separation of a Benzene and Nitric Oxide Mixture by a Molecule Prism, *J. Chem. Phys.* **119**, 8905 (2003); B. Friedrich and D. Herschbach, Stern and Gerlach: How a Bad Cigar Helped Reorient Atomic Physics, *Physics Today*, **56**, 53-59 (December, 2003)--this is a historical paper but also contains a brief description of the genesis and development of our work on a silver-surface imaging detector. In preparation, three papers: a treatment of tunneling in the Wigner limit, by D. Herschbach; more detail about the silver-surface imaging detector, by S. Sunil, D.S. Chung, B. Friedrich, and D. Herschbach; and work demonstrating the efficacy of the E-H balance filter for slow molecules, by T. McCarthy, S. Sunil, M. Timko, and D. Herschbach.

Exploring Quantum Degenerate Bose-Fermi Mixtures

Deborah Jin
JILA, UCB440
University of Colorado
Boulder, CO 80309
jin@jilau1.colorado.edu

In this project we are exploring a dilute gas mixture of bosonic ^{87}Rb atoms and fermionic ^{40}K atoms in the quantum degenerate regime. This combination of atomic species is convenient for the initial laser cooling stage, which uses a two-species vapor cell magneto-optical trap [1]. In addition, the collisional interaction between ^{87}Rb and ^{40}K atoms at ultralow temperature is relatively strong and attractive [2]. Strong interactions are favorable for the second stage of cooling. Here the gas mixture is loaded into a purely magnetic trap where the bosons are cooled via forced rf evaporation, while the Fermi gas is cooled indirectly through thermal contact with the Bose gas.

We can cool $2x10^5$ Rb atoms and $5x10^4$ K atoms into the quantum degenerate regime. The cooling cycle takes roughly 1.5 minutes, after which the gas is probed using absorption imaging. We can take images of the either gas independently with the appropriate choice of probe light frequency. Absorption images can either be taken in the trap or after release from the trap followed by a period of expansion. Using time-of-flight (TOF) expansion images, we now have the capability to take images of both the Rb and K gases for a single cooling cycle.

In the last year we have concentrated on studies of the interactions between the bosonic and fermionic atoms. These interactions are extremely important in determining properties of the quantum gas mixture, such as equilibrium density profiles, collective excitation frequencies and damping rates, and even mechanical stability. The s-wave scattering length, which characterizes the interactions at ultralow temperature, for interactions between ^{87}Rb and ^{40}K atoms, a_{RbK}, was reported by the LENS group in Florence to be very large and negative; and furthermore, evidence of mechanical collapse due to the strong attractive interactions was presented [G. Modugno *et al.*, Science **297**, 2240 (2002)]. In our experiment we have been unable to observe this collapse phenomenon.

To better understand the system, and at what densities mechanical instability would be theoretically predicted, we performed a collisional measurement to more precisely determine the all-important interaction parameter a_{RbK}. In a collisional measurement, the elastic collision cross-section, which is proportional to square of the scattering length, is determined from the time dependence of thermal relaxation following a perturbation of the gas. Ultimately this type of measurement suffers from a relatively large systematic uncertainty due to the difficulty in accurately determining the gas density. For the case of a fermion-boson mixture, we have introduced a technique that eliminates this large systematic uncertainty in the final value of a_{RbK}. Basically, we precisely determine the ratio of the intraspecies (boson-fermion) scattering length a_{RbK} to the interspecies (boson-boson) scattering length a_{RbRb}, by performing rethermalization measurements for K with Rb as well as for Rb alone. Since the boson-boson scattering length a_{RbRb} is already precisely known from previous measurements, we can convert our measured ratio into a new measurement for the interspecies scattering length a_{RbK}. Figure 1 shows a typical relaxation curve for K with Rb.

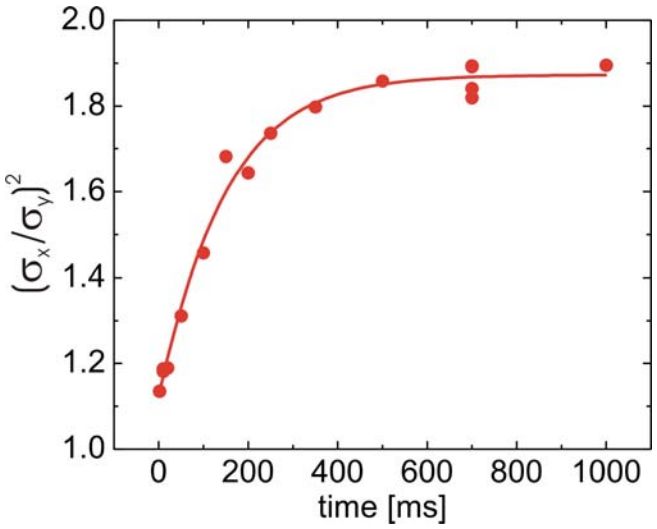

Figure 1. Measurement of the cross-dimensional thermal relaxation of a ^{40}K gas in thermal contact with a ^{87}Rb gas. Starting with the gas mixture at T ≈ 1 μK, energy is added selectively in the radial direction by rapidly compressing the cylindrically symmetric trap. The rethermalization rate is determined from the time dependence of the aspect ratio of the ^{40}K cloud, σ_x/σ_y, measured after 5 ms of expansion. The solid line is a fit that assumes exponential relaxation of the energy anisotropy.

With this new technique we found that $|a_{RbK}| = 250 \pm 30\ a_0$, where a_0 is the Bohr radius. This magnitude is significantly lower then the value reported by the LENS group [G. Modugno *et al.*, Science **297**, 2240 (2002)] and correspondingly, with this weaker interaction strength current theories would predict that the onset of mechanical instability requires higher densities that have been achieved in current experiments.

Our new value of a_{RbK} also helps to refine the predictions for interspecies Feshbach resonances. Magnetic-field Feshbach resonances have given experimenters the amazing ability to change the interactions in an ultracold gas in real time. This tool would be immensely useful for further investigation of interaction driven phenomena in an ultracold Bose-Fermi mixture and would open up new avenues for study such as the creation of ultracold, fermionic, heteronuclear molecules. We have recently submitted a paper [3] reporting the observation of three distinct magnetic-field Feshbach resonances between ^{87}Rb and ^{40}K. Along with a preprint from the MIT group, this is the first observation of heteronuclear Feshbach resonances.

To look for predicted magnetic-field Feshbach resonances [A. Simoni *et al.*, Phys. Rev. Lett. 90, 163202 (2003)] we loaded the ultracold gas mixture into a far-off resonance optical dipole trap formed by a single focused YAG beam. We then used adiabatic rapid passage to transfer the ^{40}K and ^{87}Rb atoms into their lowest energy Zeeman states. With these states we observed three loss features as a function of the applied magnetic field corresponding to heteronuclear Feshbach resonances (see Figure 2 below). Collaborating with the theoretical group of John Bohn, we identified these resonances as two s-wave resonances and one p-wave resonance. Since submitting a manuscript describing these results, we have recently observed a fourth resonance that was predicted by Bohn's group.

Observation of the first heteronuclear Feshbach resonances opens up exciting new possibilities. Future work will concentrate on characterizing these resonances and their utility for controlling interaction effects in the quantum Bose-Fermi dilute gas mixture. For example, we will explore the possibility of creating heteronuclear molecules using these Feshbach resonances. Characterizing inelastic collision rates near the resonances will also be important for future work. Ultimately we plan on using the interaction

control afforded by a magnetic-field Feshbach resonance to investigate strongly interacting Bose-Fermi mixtures.

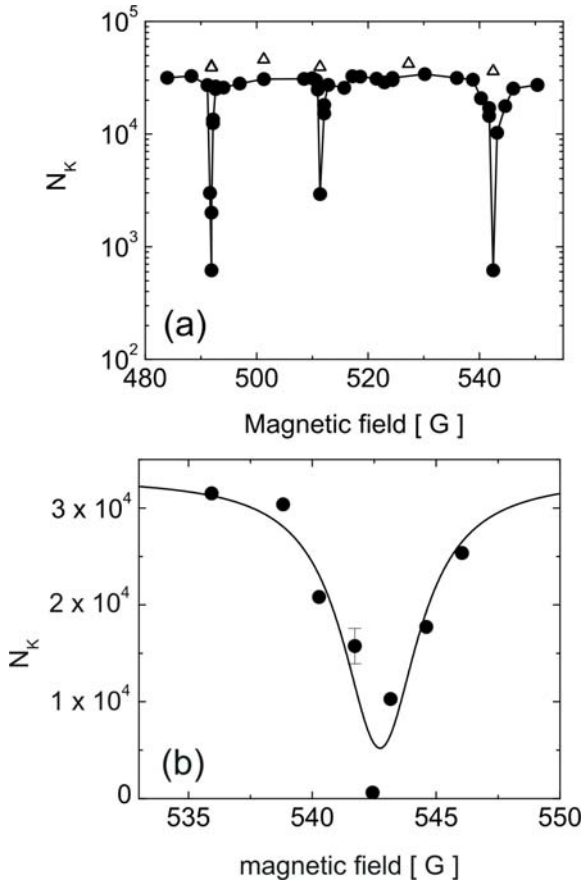

Figure 2. Observation of three interspecies Feshbach resonances for ^{40}K and ^{87}Rb atoms in their lowest energy spin-states. We plot the number of ^{40}K atoms (solid circles) after a 1 second hold at various values of the magnetic field. The open triangles show that we observe no appreciable loss when the experiment is repeated with all the ^{87}Rb gas removed from the trap. This verifies that the loss is due to interspecies interactions. The loss features are presumed to be due to the greatly enhanced three-body inelastic processes near Feshbach resonances

1. J. Goldwin, S. B. Papp, B. DeMarco, and D. S. Jin, "Two-species magneto-optical trap with K-40 and Rb-87," Phys. Rev. A **65**, 021402 (2002).
2. J. Goldwin, S. Inouye, M. L. Olsen, B. Newman, B. D. DePaola, and D. S. Jin, "Measurement of the interaction strength in a Bose-Fermi mixture with ^{87}Rb and ^{40}K", Phys. Rev. A **70**,021601R (2004).
3. S. Inouye, J. Goldwin, M. L. Olsen, C. Ticknor, J. L. Bohn, and D. S. Jin, "Observation of Heteronuclear Feshbach Resonances in a Bose-Fermi Mixture", cond-mat/0406208 (2004).

Using Intense Short Laser Pulses to Manipulate and View Molecular Dynamics

Robert R. Jones, Physics Department, University of Virginia,
382 McCormick Road, P.O. Box 400714, Charlottesville, VA 22904-4714
rrj3c@virginia.edu

I. Program Scope

The primary goal of this program is to explore and control fundamental physical phenomena associated with non-perturbative laser/molecule interactions. It is well-known that an intense non-resonant laser can radically affect molecular motion, both in internal and external degrees of freedom. By monitoring the electrons, ions, and/or photons emitted from irradiated molecules, one can obtain significant insight into the molecules' dynamical response to the laser field. Moreover, ionization, fragmentation, and/or high harmonic generation yields can be controlled by manipulating or "shaping" the time-dependent field to which the molecule is exposed. This picture is complicated by the fact that the molecule's alignment with respect to the laser polarization vector is a critical parameter in determining the effect of the field. Furthermore, the angular distribution of electrons, ions, or photons emitted relative to a molecule fixed axis may contain key information regarding a particular process, yet this information can only be recovered if the molecular axis has a well-defined direction in the laboratory frame. Thus, the random alignment/orientation of molecules in a typical gaseous sample poses a significant obstacle to understanding and controlling strong-field molecular dynamics.

Fortunately, intense short laser pulses can be used to transiently align molecules for use in strong field experiments [1,2]. The short laser pulse drives a sequence of Raman transitions, producing a rotational wavepacket whose evolution is characterized by periodic molecular alignment. In classical physics terms, the linearly polarized alignment laser induces a dipole along a preferred molecular axis. The time-averaged interaction of the dipole with the laser field gives the molecule an angular impulse, such that the molecular axis rotates toward the laser polarization vector. In practice, the non-zero rotational temperature of the molecular sample limits the achievable alignment. From the classical physics perspective, the rotational energy distribution in the molecular ensemble ensures that different molecules have different initial angular velocities, and will align at different times. Quantum mechanically, non-zero temperature molecules are initially in an incoherent superposition of rotational states so that the alignment pulse cannot produce a pure, coherent superposition state. A key aspect of our program is the development of improved methods to transiently align molecular targets. For example, we will employ a laser pulse shaper [3] and genetic learning algorithm in a closed-loop optimal control scheme [4,5] to search for the laser pulse "shape" to optimize the alignment of a specific target molecule.

In related work we intend to demonstrate transient, field free orientation of polar molecules by subjecting them to sub-picosecond half-cycle electric field pulses (HCPs) [6]. In a short, optical frequency laser pulse, rotational wavepackets are created via a second-order coupling that induces Raman transitions between rotational states of the same parity. However a unipolar HCP directly drives $\Delta J = \pm 1$ transitions between rotational levels of opposite parity, producing wavepackets with a time-dependent dipole moment. Classically speaking, the HCP gives the molecule an angular kick such that the positive end of the dipole rotates in the HCP field direction while the negative end moves against the field. Following the HCP, the molecule continues to rotate, such that the molecular dipole periodically aligns parallel or anti-parallel to the kick.

Ultimately, we plan to use aligned/oriented molecular targets to explore precisely why, and to what extent, intense field processes such as tunneling ionization and high harmonic generation differ between atoms and diatomic molecules with similar ionization potentials [7]. There have been numerous suggestions that, in diatomic molecules, electron ejection and/or scattering from the two distinct ionic cores will lead to interferences that affect the total and angularly resolved electron and harmonic yields [8-11]. Since the internuclear separation and relative orientation of the ion cores determines the precise form of the interferences, the use of aligned targets should provide the clearest experimental signature of these effects. Moreover, we will explore the possibility of exploit the interference effects as time-resolved probes of molecular dynamics with sub-Angstrom spatial resolution and temporal resolution equal to the laser pulse duration [11].

II. Recent Progress

A) Transient Alignment

We have used 100 fsec and 30 fsec 780 nm laser pulses to transiently align N_2. In both cases the alignment was probed using time-delayed circularly polarized 30 fsec 780 nm pulses [2]. The intense probe pulses rapidly remove multiple electrons from the neutral molecules so that they explode due to the Coulomb repulsion of the remaining positive ions. During this Coulomb explosion, the initial angular distribution of the N_2 molecule is mapped onto that of the outgoing N^{m+} ion fragments. The vector momenta of the ion fragments are measured using a multi-hit, wire-grid anode micro-channel plate detector. Use of the 100 fsec alignment pulses required that we seed our 2 mJ 100 fsec and 1.8 mJ 30 fsec amplifiers from a single 20 fsec mode-locked oscillator, enabling synchronization of their outputs to a precision of much less than 100 fsec. In the next stage of our experiments, the alignment pulses from the 100 fsec amplifier will be shaped as part of a closed feedback loop aimed at optimizing the alignment. To implement the feedback loop we have also modified the data collection software for the wire grid anodes to enable rapid determination of the average molecular alignment from the ion momenta [4,5].

B) Transient Orientation

Achieving transient molecular orientation will require that the product of the peak HCP field and the molecular dipole moment be as large as possible. In addition, if initial state incoherence is not to wash out the effect, the initial rotational population distribution must be restricted to a small number of levels. Due to its large dipole moment (7.1 Debye) and moderate rotational constant ($0.71\ cm^{-1}$) LiCl is an excellent candidate for our initial experiments. We have constructed a molecular beam apparatus in which LiCl molecules from a resistively heated oven will be carried and rotationally cooled in a skimmed, supersonic noble gas expansion. In the event that we are unable to obtain sufficient quantities of rotationally cold LiCl molecules, we will continue the experiments using SO. While the dipole moment of SO is a factor of 4 smaller than that of LiCl, we should be able to cool it extremely well by mixing it with the cooling gas prior to expansion through the pulsed nozzle. As in the alignment experiments, we intend to use Coulomb explosion, induced by an intense, time-delayed 30 fsec laser pulse, to probe the molecular orientation. The ion fragments will be detected using a new TOF ion spectrometer that is currently being tested.

HCPs will be generated by exposing a biased GaAs photoconductive switch to ~100 fsec laser pulses [12]. The HCP field is proportional to the bias voltage on the switch. We have made several attempts to increase the bias voltage (previously ~30 kV maximum) on our photoconductive switches. The associated HCP field increase will be necessary to excite the broad range of rotational states that is required to achieve strong orientation, particularly in molecules with

smaller dipole moments at non-zero temperature [6]. Unfortunately, due to electrical discharge problems we have had limited success scaling up the bias voltage. However we now believe the discharge problems may be alleviated by coating the switch with a high dielectric optical cement that has good transparency in the visible and far infrared. In addition, in the next few weeks we will test a new pulsed voltage source that will allow us to generate ~100 nsec, 100 kV bias pulses.

C. Numerical Modeling of Molecular Alignment and Orientation

We have developed numerical codes for calculating the time-dependent angular distribution within a sample of linear molecules following an arbitrarily shaped laser alignment and/or orientation pulse or pulse sequence. The calculations include the incoherent rotational distribution of the non-zero-temperature molecular ensemble as well as the lowest order effects of centrifugal distortion. The availability of these codes will help us identify appropriate parameter regimes for maximizing alignment and orientation, and for understanding the effectiveness or ineffectiveness of particular experimental schemes. For example we find, as in the case of transient alignment, that the use of multiple appropriately timed HCPs should lead to significant enhancements in the degree of orientation. Hence, sequences of lower amplitude HCPs might be effectively applied to orient molecules. We intend to explore this possibility experimentally.

D. High Harmonic Generation

We have constructed a hollow fiber harmonic generation apparatus [13] and, using our 30 fsec 780 nm laser, have very recently observed harmonic generation (up to the 41st harmonic) in Argon. We are currently characterizing the emission into different orders as a function of gas pressure and laser intensity. We intend to use this source to explore harmonic emission from molecules in the near future.

III. Future Plans

A. Molecular Alignment

We will soon begin experiments exploring the use of laser pulse-shaping [3-5] to optimize molecular alignment [14]. After finding the best alignment pulse or pulse sequence, we hope to use pre-aligned molecules in a systematic investigation of the role of interference in molecular ionization.

B. Molecular Orientation

Using the new high-voltage switches mentioned above, we hope to generate HCP fields approaching 1 MV/cm. Because the laser fluence required to saturate our large area (4” diameter) GaAs switches cannot be generated using our 1 kHz amplifiers, the HCP orientation experiments will be performed using our 30 mJ 130 fsec laser system which operates at 15 Hz. To ensure rapid Coulomb explosion of the oriented molecules, we will update the mode-locked oscillator and add a 30 fsec amplifier to this low repetition rate system. We then hope to insert the HCP source into the interaction chamber and begin the molecular orientation experiments.

C. High Harmonic Generation

We intend to characterize the harmonic emission from N_2 and O_2 in a hollow fiber. We will then use a Michelson interferometer to introduce two time-delayed pulses into the fiber to explore the effects of molecular alignment on high harmonic generation. In addition, we plan to explore quasi-phase matching methods for enhancing the harmonic yield and extending the emission to shorter wavelengths [15].

IV. Publications from DOE Sponsored Research (2002-2004)

i) E. Wells, I. Ben-Itzhak, and R.R. Jones, "Ionization of Atoms by the Spatial Gradient of the Pondermotive Potential in a Focused Laser Beam," Physical Review Letters **93,** 23001 (2004).

ii) E. Wells, M.J. DeWitt, and R.R. Jones, "Comparison of Intense Field Ionization of Diatomic Molecules and Rare Gas Atoms," Physical Review A **66**, 013409 (2002).

iii) S.N. Pisharody and R.R. Jones, "Phase-Controlled Stair-Step Decay of Autoionizing Radial Wavepackets," Physical Review A **65**, 033418 (2002).

iv) R.R. Jones, S. Pisharody, and R. van Leeuwen, "Laser Manipulation of Differential Autoionization Yields: Pump-Dump Control Through Coupled Channels," *Laser Control and Manipulation of Molecules*, ACS Symposium Series **826**, A. Bandrauk, R.J. Gordon, and Y. Fujimura, Eds. (2002).

V. References

1. T. Seideman, Phys. Rev. Lett. 83, 4971 (1999); F. Rosca-Pruna and M.J.J. Vrakking, Phys. Rev. Lett. 87, 163601 (2001).
2. I.V. Litvinyuk et al., Phys. Rev. Lett. 90, 233003 (2003).
3. A.M. Weiner et al., Opt. Lett. 15, 326 (1990); M.M. Wefers and K.A. Nelson, Opt. Lett. 18, 2032 (1993).
4. R.S. Judson and H. Rabitz, Phys. Rev. Lett. 68, 1500 (1992).
5. B. Pearson, J.L. White, T.C. Weinacht, and P.H. Bucksbaum, Phys. Rev. A 63, 063412 (2001).
6. M. Macholm and N.E. Henriksen, Phys. Rev. Lett. 87, 193001 (2001).
7. A. Talebpour, et al., J. Phys. B 29, L677 (1996); C. Guo, et al., Phys. Rev. A 58, R4271 (1998); M.J. DeWitt, E. Wells, and R.R. Jones, Phys. Rev. Lett. 87, 153001 (2001).
8. J. Muth-Bohm, A. Becker, and F.H.M. Faisal, Phys. Rev. Lett. **85**, 2280 (2000).
9. X. M. Tong, Z. X. Zhao, and C. D. Lin, Phys. Rev. A **66**, 033402 (2002).
10. M. Lein et al., Phys. Rev A **66**, 023805 (2002).
11. H. Nikura et al., Nature 417, 917 (2002).
12. D. You, R.R. Jones, P.H. Bucksbaum, and D.R. Dykaar, Opt. Lett. 18 290 (1993).
13. A. Rundquist et al., Science 280, 1412 (1998).
14. I.Sh. Averbukh and R. Arvieu, Phys. Rev. Lett. 87, 163601 (2001); C. Bisgaard et al., Phys. Rev. Lett. 92, 173004 (2004).
15. E. Gibson et al., Phys. Rev. Lett. 92, 033001 (2004).

Physics of Low-Dimensional Bose-Einstein Condensates, Grant No. DE-FG02-01ER15203

Eugene B. Kolomeisky (PI)
Department of Physics
University of Virginia
382 McCormick Road
P.O. Box 400714
Charlottesville, Virginia 22904-4714
ek6n@virginia.edu

The project consists in investigating fundamental properties of low-dimensional superfluids (Bose-condensed alkali gases in strongly anisotropic traps, for example) and related systems within a wider scope of the DOE Nanoscale Science, Engineering, and Technology Initiative.

Recent Progress

During the period of September 2003 - September 2004 we have been working on several (mostly completed projects) described below in more detail:

• E. B. Kolomeisky, J. P. Straley, and R. M. Kalas, **Ground-state properties of artificial bosonic atoms, Bose interaction blockade and the single-atom pipette**, published in Phys. Rev. A (2004). We analyzed the ground-state properties of an artificial atom made out of repulsive bosons attracted to a center for the case that all the interactions are short-ranged. Such bosonic atoms could be created by optically trapping ultracold particles of alkali vapors; we presented the theory describing how their properties depend on experimentally adjustable strength of "nuclear" attraction and interparticle repulsion. The binding ability of the short-range potential increases with space dimensionality - only a limited number of particles can be bound in one dimension, while in two and three dimensions the number of bound bosons can be chosen at will. Particularly in three dimensions we found an unusual effect of enhanced resonant binding: for not very strong interparticle repulsion the equilibrium number of bosons bound to a nuclear potential having a sufficiently shallow single-particle state increases without bound as the nuclear potential becomes *less attractive*. As a consequence of the competing nuclear attraction enhanced by the Bose statistics and interparticle repulsions, the dependence of the ground-state energy of the atom on the number of particles has a minimum whose position is experimentally tunable. This implies a staircase dependence of the equilibrium number of bound bosons on external parameters which may be used to create a single-atom pipette - an arrangement which allows the transport of atoms into and out of a reservoir, one at a time.

This paper constitutes a foundation for the future research activity.

• T.J. Newman, E.B. Kolomeisky, and J. Antonovics, **Population dynamics with global regulation: The conserved Fisher equation**, published in Phys. Rev. Lett. (2004). We introduced a conserved version of the Fisher equation. Within a population biology context, this model describes spatially extended populations in which the total number of individuals

is fixed due to either biotic or environmental factors. We found a rich spectrum of dynamical phases including a pseudo-traveling wave, and in the presence of the Allee effect, a phase transition from a locally constrained high-density state to a low-density fragmented state.

This work is not immediately related to the physics of low-dimensional quantum liquids except for the techniques used - virtually the same mathematics also describes Abrikosov flux line in a deformable medium (paper submitted for publication).

• E. B. Kolomeisky and M. Timmins, **Zel'dovich effect and evolution of atomic Rydberg spectra along the Periodic Table**, manuscript in preparation. In 1959 Ya. B. Zel'dovich predicted that the bound-state spectrum of non-relativistic Coulomb problem distorted at small distances by a short-range potential undergoes a peculiar reconstruction whenever this potential alone supports a low-energy scattering resonance. However the experimental evidence of this phenomenon has been lacking. We show that this effect manifests itself in systematic variation of Rydberg spectra with atomic number Z. The idea is that by varying Z along the Periodic Table the Nature effectively changes the depth of the inner part of the potential of the residual ion leaving the outer Coulomb tail intact. Therefore by analyzing the Rydberg spectra as function of atomic number Z it is possible to correlate them with the binding properties of the ionic core which consitutes the evidence of the Zel'dovich effect. Specifically, we demonstrate that the quantum defect of highly excited s state is an increasing function of $Z^{1/3}$ consisting of approximately equidistant rounded steps, and this dependence has its roots in the binding properties of the ionic core of the atom.

• E. B. Kolomeisky and R. M. Kalas, **Capacitance of a large Coulomb-blockaded quantum dot**, manuscript in preparation. We compute the capacitance of a quantum dot strongly coupled to a one-dimensional reservoir of interacting spinful electrons. We find that the capacitance is singular at the gate voltage degeneracy points, and these singularities have their origin in the discreteness of the electron spin. It is curious that in the regime studied the discreteness of electron charge is *irrelevant*.

Future Plans

Physics of Resonant Binding. One of our most interesting preliminary findings was prediction of a regime in which the equilibrium number of bosons bound by a short-range potential increases without bound as the potential is made *less attractive* - the opposite of the usual response. This occurs near the threshold energy for binding a single particle, where the scattering (or equivalently single-particle localization) length diverges, and one interpretation is that the wave function reduces to the product of the single particle wave functions of large spatial extent: the particle density has become so small that the repulsive interaction between particles is irrelevant. However, this argument is still at the level of the Hartree-Fock theory, that neglects correlations between the particles.

We are going to conduct complementary studies, both analytical and numerical, of the resonant binding to better understand its physics.

Physics of Artificial Bosonic Matter. Our previous work demonstrated that the ground-state properties of artificial bosonic atoms (bosons bound by short-range potentials) are

drastically different from their fermionic (electronic) counterparts found in nature. The unique feature of our systems is that all the interactions are short-range and tunable. We demonstrated that it is feasible to produce these objects in laboratory environment which in turn makes it relevant to conduct a comprehensive investigation of their properties. For example, what are the excited states? Can they be accessed by light the way electrons are probed in regular atoms? Many problems of conventional atomic and molecular physics have their "bosonic" counterparts and might be within experimental reach. For instance, how to solve the bosonic version of the H_2 molecule - two identical bosons bound by two short-range potentials? From atoms and molecules one can move to clusters and condensed matter.

Finite-Temperature and Arbitrary Tunneling Theories. In our previous work we restricted ourselves to the case of zero temperature and the effect of finite temperature of the Bose-Einstein condensate (BEC) was just estimated. Since it was found that tight traps and possibly the Feschbach resonance enhancement of interparticle repulsion is necessary to suppress finite-temperature effects, we are going to extend our results to finite temperatures to better understand future experimental findings. Moreover our tunneling theory was restricted to the limit of weak tunneling. We are going to generalize it to the case of arbitrary tunneling and finite temperature.

Transport Phenomena. The natural generalization of the BEC reservoir plus the pipette setup allowing for transport phenomena is to add another BEC reservoir to the right of the pipette. We will also need to be able to control the levels of chemical potentials in the reservoirs which can be accomplished by changing the BEC confining frequencies. When the chemical potentials of the reservoirs are slightly different, a superflow via the pipette will result. This setup is a bosonic version of the single-electron transistor, wherein the experimental ability to change the depth of the pipette potential is analogous to controlling the state of the transistor via the gate voltage. Then at zero temperature superflow is only possible if the population states of the pipette different by one particle are degenerate in energy. Otherwise the link between the BEC reservoirs will be insulating. Quantitatively this effect can be characterized by a *permeability* which can be defined as a ratio of the particle current to the chemical potential difference which caused it. Its electronic counterpart is the familiar conductance. The dependence of the permeability on the laser power will consist of a series of peaks broadened by finite tunneling and nonzero temperature. We are planning to compute the shape of these permeability resonances.

Time-Dependent Effects. Up to this point we restricted ourselves to phenomena in which the pipette is stationary as it is uploaded or downloaded by changing the laser power or interparticle interactions. This does not have to be the case as long as (i) the pipette does not enter the BEC (to avoid condensate excitation) and (ii) the pipette motion is slow enough (to allow for the reservoir/pipette tunneling to take place). This will lead to a series of associated time-dependent phenomena which can be recognized as dual counteparts of the ac Josephson effect. Below we restrict ourselves to describing an analog of the Shapiro steps.

Due to the Bose interaction blockade the flow through the pipette is limited to one boson at a time. This feature can be used to create a *single-boson turnstile*, a device which

passes one boson in every cycle of periodically changing external conditions. Consider a pipette sandwiched between two BEC reservoirs with different chemical potentials prompting superflow from left to right. We assume that the pipette is tuned so that it has a single-particle state which is higher in energy than the chemical potentials while the pipette is far away from both reservoirs. Now imagine moving the pipette periodically between the reservoirs with a frequency f which is slower than the tunneling rate of the particles on and off the pipette when the barriers are lowest. In the process of its motion toward the left reservoir two things happen: (i) the single-particle state moves down in energy and (ii) the tunneling barrier with the left condensate decreases. If at the leftmost pipette position the BEC chemical potential matches the pipette single-particle ground state, then exactly one particle enters the pipette. When the pipette is moved away from the left condensate droplet, they rapidly decouple which guarantees that the captured particle is prevented from escaping back to the left. As the pipette continues its "swing" to the right, the particle is carried along. If at the rightmost position the BEC chemical potential matches the pipette single-particle energy, then the particle tunnels into the right BEC droplet. When the pipette is moved away from the right reservoir, they rapidly decouple and no particle leaks into the pipette from the right. This completes the cycle returning the pipette to its original empty state. As a result exactly one boson is transfered between the reservoirs. The robustness of the operation is guaranteed by the Bose interaction blockade - the matching conditions near the BEC reservoirs do not have to be perfect.

These arguments can be generalized to allow for transferring of two, three or generally j bosons per cycle. For that the spatial amplitude of the pipette oscillation can be increased to permit larger number of bosons on the pipette. As a result the time-averaged current passing through the pipette must be equal to jf. Equivalently one can raise the chemical potential difference between the reservoirs keeping the pipette motion intact. This current quantization should manifest itself experimentally in series of plateaus on the dependence of the average current on the chemical potential difference between the BEC reservoirs. The transitions between neighboring plateaus will be rounded by finite tunneling and temperature, and we are planning to construct a quantitative theory of the effect.

DOE Sponsored Publications during 2002-2004

• J. P. Straley, E. B. Kolomeisky, and S. C. Milne, *The Bose molecule in one dimension*, Journal of Statistical Physics, to be published (2004).

• T.J. Newman, E.B. Kolomeisky, and J. Antonovics, *Population dynamics with global regulation: The conserved Fisher equation*, Phys. Rev. Lett. **92**, 228103 (2004).

• E. B. Kolomeisky, J. P. Straley, and R. M. Kalas, *Ground-state properties of artificial bosonic atoms, Bose interaction blockade and the single-atom pipette*, Phys. Rev. A **69**, 063401 (2004).

• E. B. Kolomeisky, X. Qi, and M. Timmins, *Ground-state properties of one-dimensional matter and quantum dissociation of a Luttinger liquid*, Phys. Rev. B **67**, 165407 (2003).

• E. B. Kolomeisky, R. M. Konik, and X. Qi *Quantum fluctuations of charge and phase transitions of a large Coulomb-blockaded quantum dot*, Phys. Rev. B **66**, 075318 (2002).

Program Title:

"Ion/Excited-Atom Collision Studies with a Rydberg Target and a CO_2 Laser"

Principal Investigator: Stephen R. Lundeen,
Dept. of Physics
Colorado State University
Ft. Collins, CO 80523
Lundeen@Lamar.colostate.edu

Program Scope:

The program involves three projects, two involving the interaction of multiply-charged ion beams with a Rydberg target, and one involving multiply-excited Rb atoms in a MOTRIMS target.

1) Studies of the fine structure of high-L Rydberg ions, in order to extract measurements of dipole polarizabilities and quadrupole moments of the positive ion cores.

2) Studies of X-rays emitted from the highly-excited Rydberg ions formed in charge capture collisions by highly-charged ions on Rydberg atoms.

3) Stepwise excitation of a Rb MOT to high Rydberg states within a MOTRIMS apparatus in order to study the n-dependence of charge capture cross sections.

Recent Progress and Immediate Plans:

Project 1) The eventual goal of this project is to measure the polarizability of Rn-like actinide ions, U^{6+} and Th^{4+}. We hope to do this using the RESIS/microwave technique in which the ion under study (e.g. U^{6+}) captures a single electron from our Rb Rydberg target to form highly excited Rydberg ions (e.g. U^{5+}(n=55)). Individual Rydberg levels (e.g. n=55, L=20) would then be selectively detected by excitation with a Doppler-tuned CO_2 laser, followed by Stark ionization. This would then allow detection of microwave induced transitions between Rydberg ion levels, revealing the fine structure pattern whose scale determines the polarizability of the core ion. During this year, we have made good progress towards this goal on two fronts.

Using the ECR ion source at Kansas State University, we have successfully applied this technique to measure the polarizability of Si^{2+} and Si^{3+}[1,2]. RESIS optical studies of Rydberg levels bound to Si^{4+} and Si^{5+} have also been made, but these systems are not well suited to microwave studies. In one case (Si^{4+}), this is because the polarizability is very small, and in the other case (Si^{5+}), it is because the presence of a permanent quadrupole moment leads to a much greater number of Rydberg levels. An additional difficulty with the higher charge ions is the gradual reduction in S/N that is expected as Q increases. This could eventually be ameliorated with a higher power CO_2 laser.

Also this year, using a Colutron ion source at Colorado State University, we have completed an optical RESIS study of n=9 and 10 Rydberg levels of the Barium atom.[3] This study determined improved values of the adiabatic dipole and quadrupole polarizabilities of the Cs-like Ba^+ ion. Table 1 compares our results with previous determinations [4], and with the most recent theoretical values[5]. The good agreement between measured and calculated dipole polarizability is only obtained with a very

careful relativistic calculation. Simple application of the Relativistic Hartree Fock method leads to predictions in error by about 40%[6]. We expect that accurate predictions for the actinide ions will require similar or greater theoretical effort. The measured quadrupole polarizability differs by more than a factor of two from the previous experimental determination, but is in fair agreement with theoretical predictions. The discrepancy between experimental values is related to the treatment of non-adiabatic contributions to the quadrupole polarization energies, a feature that we expect to be increasingly common in heavier Rydberg systems.

Table I. Comparison of measured dipole and quadrupole polarizabilities of Ba^+ with previous measurements and with theory.

	$\alpha_d(a_o^3)$	$\alpha_Q(a_o^5)$
This Work[3]	123.84(16)	5140(470)
Previous Ezpt.[4]	125.5(1.0)	2050(100)
Theory[5]	124	4130

In the year ahead, we plan to push the Rydberg ion studies to ions of higher charge, perhaps S^{5+}, using the KSU ECR source. This study should be comparable in difficulty to the actinide studies which are our eventual goal. If it is successful, we could begin the actinide studies as soon as a suitable source of actinide ions is obtained. In the meantime, we also plan to improve the precision of the Barium studies, using microwave techniques.

Project 2) In a paper published last year [7] we showed that the x-ray spectra emitted by H-like and He-like Rydberg ions was sensitive to very small (~ 10 - 20 V/cm) external electric fields. This is due to the onset of Stark mixing in the high Rydberg levels, which occurs in fields of $\left|\vec{E}\right| \cong 30000\left(\frac{Q}{n}\right)^5 V/cm$. For a typical case in our study, Q=14 and n=76, this is about 6 V/cm, much smaller that the field necessary to Stark ionize the level (~26,000 V/cm) or even mix it with neighboring levels (~ 1,600 V/cm). This year we completed a more extensive study of this effect, including a range of bare and H-like ions (Ne^{10+}, Si^{13+}, Si^{14+}, and Ar^{17+}) incident on a range of Rb Rydberg targets (n_T=8,9,10,12,14). This study confirmed the expected scaling of the field required to reach full Stark mixing. At full mixing, the ratio of x-rays emitted in transitions directly to 1S from the populated levels (e.g. 76 to 1) to the Kα x-ray (2 to 1) is sensitive to the degree of alignment of the Rydberg population along the collision axis. Our study confirmed that about 10% of the population formed in capture from the Rydberg target is formed in states with $|m| \leq 1$, in agreement with theoretical estimates obtained from CTMC. Our study also showed that multiple collisions with the Rydberg target were a significant factor, tending to reduce the degree of alignment. The exact nature of these secondary collisions is not yet clear, but the initial data indicated that their importance increases with the charge, Q, of the incident ion. A full report of this study has been submitted for publication[8].

During the next year, we plan to upgrade the x-ray apparatus so that it will be possible to apply fields perpendicular to the collision axis, as well as parallel to it. This

should lead to more robust measurement of the population alignment. In addition, we plan to extend and improve the studies of the effects of secondary collisions. We are hopeful that it will prove possible to extend the range of projectile charges to values greater than 17.

Project 3) Our interest in applying the MOTRIMS technique to study of ion-Rydberg collisions stems from the unique ability of the MOTRIMS to measure relative cross sections of capture from different n-levels without needing to establish the relative target thickness of each n. A paper describing this feature appeared this year in Physical Review Letters.[9] As of this date, we have not yet excited Rydberg levels within the MOTRIMS apparatus, but we expect to do so in the very near future. We are already exciting $4D_{5/2}$ levels in the Rb MOT, and we have just purchased a commercial diode laser which will make possible excitation from the $4D_{5/2}$ level to the $9F_{7/2}$ level. Eventually, we plan to use a TiSaphire laser to excite a range of Rydberg F levels, but excitation of the 9F level should give us an opportunity to make detailed plans for this broader study.

References

[1] R.A. Komara, M.A. Gearba, S.R. Lundeen, and C.W. Fehrenbach, Phys. Rev. A **67**, 062502 (2003)
[2] "Ion Properties from High-L Rydberg Fine Structure: Dipole Polarizability of Si^{2+}" R.A. Komara, M.A. Gearba, C.W. Fehrenbach, and S.R. Lundeen, to be published in J. Phys. B. At. Mol. Opt. Phys. (2004)
[3] "Determination of the dipole and quadrupole polarizabilities of Ba^{+} by study of the fine structure of high-L, n=9 and 10 Rydberg states of Barium" E.L. Snow, M.A. Gearba, W.G. Sturrus, and S.R. Lundeen, (in preparation)
[4] T.F. Gallagher, R. Kachru, and N.H. Tran, Phys. Rev. A **26**, 2611 (1982)
[5] Andrei Derevianko and Sergey Porsev (private communication)
[6] V.A. Dzuba, et. al Phys. Rev. A **63**, 062101 (2001) show in Table II that the 6s-6p dipole matrix element, which occurs squared in the dipole polarizability is 17% too large if calculated with Relativistic Hartree Fock code.
[7] M.A. Gearba, R.A. Komara, S.R. Lundeen, C.W. Fehrenbach, and B.D. DePaola, Phys. Rev. A **66**, 032705 (2002)
[8] "Study of Stark-induced x-ray emission by H-like and He-like Rydberg ions", M.A. Gearba, R.A. Komara, S.R. Lundeen, C.W. Fehrenbach, and B.D. DePaola, (submitted to Phys. Rev. A, August, 2004)
[9]X. Flechard, H. Nguyen, R. Bredy, S.R. Lundeen, M. Stauffer, H.A. Camp, C.W. Fehrenbach, and B.D. DePaola, Phys. Rev. Lett**. 91**, 243005 (2003)

Publications appearing or accepted during this grant period:

1) "State Selective charge transfer cross sections for Na^{+} with multiply excited rubidium: A unique diagnostic of MOT dynamics", X. Flechard, H. Nguyen, S.R. Lundeen, M. Stauffer, H.A. Camp, C.W. Fehrenbach, and B.D. DePaola, Phys. Rev. Letters **91**,

243005 (2003)

2) "Indirect spin orbit interaction in high *L* Rydberg states with $^2S_{1/2}$ cores", E.L Snow, R.A. Komara, M.A. Gearba, and S.R. Lundeen, Phys. Rev. A **68**, 022510 (2003)

3) "Ion Properties from High-L Rydberg Fine Structure: Dipole Polarizability of Si^{2+}" R.A. Komara, M.A. Gearba, C.W. Fehrenbach, and S.R. Lundeen, to be published in J. Phys. B. At. Mol. Opt. Phys. (2004)

Publications submitted and under review :

4) "Study of Stark-induced x-ray emission from H-like and He-like Rydberg ions", M.A.Gearba, R.A. Komara, S.R. Lundeen, C.W. Fehrenbach, and B.D. DePaola (submitted to Phys. Rev. A, August, 2004)

Theory of fragmentation and rearrangement processes in ion-atom collisions

J. H. Macek

Department of Physics and Astronomy,
University of Tennessee, Knoxville, Tennessee and
Oak Ridge National Laboratory, Oak Ridge, Tennessee
email:jmacek@utk.edu

1 Program scope

Structure in atomic cross sections relate to specific aspects of interactions between atomic species. Resonances are a notable example of this, however, other structures provide similar windows to the inner workings of atomic interactions. COLTRIMS measurements of electron energy and angular distributions, for example, find structure that reveals the role of electron motion on the top of potential barriers. One part of our project involves modelling this structure theoretically.

A second example is provide by structure in rearrangement cross sections. Quantitative calculations in the $10^{-4} - 10$ eV energy range of integral spin exchange in proton-hydrogen collisions show numerous oscillations. Some are due to resonances or to glory effects, but some are not identified by any standard mechanisms. We seek methods to completely classify the structure.

The projects listed in this abstract are sponsored by the Department of Energy, Division of Chemical Sciences, through a grant to the University of Tennessee. The research is is carried out in cooperation with Oak Ridge National Laboratory under the ORNL-UT Distinguished Scientist program.

2 Recent progress

The hidden crossing and two-center Sturmian theory of ionization have been used to analyze structure in doubly and singly differential cross sections for the species $\overline{p}$, H^-, H, and H^+ impacting on H and He targets[1-7]. In the singly differential cross section a distinct break in slope of $\frac{d\sigma}{dE_e}$ where E_e is the electron energy, is seen at the energy $E_e = E_M = m_e v^2/2$, where v is the relative velocity of the target and projectile and E_M is the matching

energy. This break is associated with two different ionization mechanisms that emerge in the hidden crossing analysis, namely, superpromotion, also call S-promotion, which produces electrons with $E_e > E_M$ and top-of-barrier promotion, also called T-promotion, which produces electrons with $E_e < E_M$. It is noteworthy that both components give comparable contributions to the total ionization cross section.

That there are two contributions to ionization has long been suspected, however, a theory of electron distributions for T-electrons has proved elusive. By using a analytic treatment of electron motion near the top-of-barrier we were able to obtain reliable singly differential cross sections for both S and T electrons. COLTRIMS measurements of doubly differential cross sections, showed however, that the theoretical electron angular distributions of the T-electrons were too concentrated near the top-of-barrier compared with observations. This discrepancy has now been resolved by using a more exact analytic description of electron motion near the top-of-barrier when the nuclei are separated by distances greater than 50 au. With this development, the approximate uncoupled two-center Sturmian theory gives an accurate representation of ionization in low energy ion-atom collisions.

The exact theory[1,5.6], where the two-center Sturmian channels are coupled, has also been used to compute total cross sections for proton impact on atomic hydrogen. Our results are in exact agreement with observations over a range from less than 1 keV to about 200 keV impact energy. Similar agreement, although over a more limited energy range, is found for the collisions of composite species such as neutral atoms and negative ions [2,5,6]. We conclude that the two-center Sturmian theory gives a correct and complete treatment of one electron atomic collision processes.

A wave version of the hidden crossing theory has also been developed to treat collisions with energies below 1 keV. The theory has been applied to collisions of anti-protons with atomic hydrogen [7]. No unusual structures in cross sections are found. Our simple analytic representation is well adapted to modeling of protonium formation for applications involving slow protons in dilute backgrounds of atomic hydrogen.

Calculations of rearrangement collisions at energies below a few eV must employ a completely wave treatment. We have recently made very accurate calculations of spin exchange in proton-hydrogen collisions in the 10^{-4}- 10 eV energy range for benchmark purposes [8]. The integral cross section, *i. e.* the cross section integrated over scattering angles show much structure. One purpose of these benchmark calculations is to classify all of the structure.

We identify features that correspond to conventional shape resonances and zero angle glory oscillations. In addition, we find structures that cannot be identified with these two well-understood features. To analyze these features we separate a part of the cross section that has semiclassical glory oscillations from a part that relates explicitly to quantum mechanics. This leads to an identification of the oscillations with Regge trajectories and we relate the structure to appropriate eigenstates. This allows us to classify the "Regge oscillations".

3 Future plans

We have found an unexpected source of oscillatory structure in low energy ion atom collisions for a particular species. The theory of this structure is quite general, thus it should be present in many other collision processes where the relative energy is of the order of 10^{-4} to 1.0 eV. We will use the theory we have developed to see if such structure is present for other processes of interest where experimental data is or may become available. More specifically, we will examine the capture of electrons from atomic hydrogen by N^{++} since the reaction has been studied over an energy range that includes the low energy region where the "Regge oscillations" might be present.

Our two-center Sturmian calculations of total ionization cross sections for one electron species involves a routine, but rather time consuming, step that greatly reduces the efficiency of the method. We will examine techniques to make this step more efficient. In particular we will change an integration contour so that regions where the integrand is highly oscillatory are avoided. If we can improve the efficiency, our computer programs will then be modified to provide a better human interface so that they can be readily used for applications by other workers.

At present there is a 20% discrepancy between benchmark LTDSE ionization cross sections, experiment, and our two-center Sturmian results for proton-hydrogen collisions. This discrepancy may be due to differing estimates of the population of states with $n > 4$ in the different calculations. We will adapt the two-center Sturmian theory to the computation of such high Rydberg states to see if this is indeed the source of the discrepancy. It is important to resolve this issue since cross sections with accuracies in the 1% range are needed for diagnostic purposes.

4 References to DOE sponsored research that appeared in 2002-2004

1. Exact electron spectra in collisions of two zero-range potentials with non-zero impact parameters, S.Yu. Ovchinnikov, D.B. Khrebtukov, and J.H. Macek, *Phys. Rev. A* **65**, 032722 (2002).

2. Electron Emission in $H^- - He, H_2$ Collisions, G. N. Ogurtsov, S. Yu. Ovchinnikov, and V. M. Mikoushkin, in (23rd International Conference on Photonic Electronic and Atomic Collisions, invited talks, July 2003 Stockholm, Sweden), *Physica Scripta* **T110**, 370 (2004).

3. Ionization of atoms by antiproton impact, J. H. Macek in *Electron Scattering From Atoms, Molecules, Nuclei and Bulk Matter*, Ed. by C.Whelan, (Kluwar Scientific 2002).

4. Annihilation of Low Energy Antiprotons in Hydrogen, S. Yu, Ovchinnikov and J.H. Macek, in (17th International Conference on the Application of Accelerators in Research and Industry, November 2002, Denton TX), *AIP Conference Proceedings*, **680**) (2003).

5. Ionization Dynamics in Atomic Collisions, S. Yu. Ovchinnikov, J. H. Macek, Yu. S. Gordeev, and G. N. Ogurtsov, in *Atomic Processes* Ed. by S. Shevel'ko, (Springer, 2003), Ch. 25.

6. Dynamics of Ionization in Atomic Collisions, J. H. Macek, Yu. S. Gordeev, and G. N. Ogurtsov, *Physics Reports*, **389**, 119-159 (2004).

7.Energy and angular distribtutions of electrons ejected from atomic hydrogen by low energy proton impact, J. H. Macek and S. Yu. Ovchinnikov, *Phys. Rev. A*, accepted for publication.

8. Computations of elastic scattering and spin exchange in $H^+ + H$ collisions for impact energies between 10^{-4} and 10 eV, Predrag Krstić, J. H. Macek, and S. Yu. Ovchinnikov, *Phys. Rev. A*, accepted for publication.

PROGRESS REPORT

ELECTRON-DRIVEN PROCESSES IN POLYATOMIC MOLECULES

Investigator: Vincent McKoy

A. A. Noyes Laboratory of Chemical Physics
California Institute of Technology
Pasadena, California 91125

email: mckoy@caltech.edu

PROJECT DESCRIPTION

The focus of this project is the application and development of accurate, scalable methods for the computational study of low-energy electron–molecule collisions, with emphasis on larger polyatomics relevant to materials-processing and biological systems. Because the calculations required are highly numerically intensive, efficient use of large-scale parallel computers is essential, and the computer codes developed for the project are designed to run both on tightly-coupled parallel supercomputers and on workstation clusters.

HIGHLIGHTS

We have continued to focus on electron interactions with larger polyatomic molecules, especially those relevant to biological systems and to industrial applications. Principal accomplishments in the past year are:

- Published results for plasma processing gas SF_6
- Intensive study of resonant electron-collision processes in the RNA base uracil nearing completion
- Study of elastic scattering by C_{60} nearing completion
- Studies of DNA bases continuing
- Continued development of computational methods

APPLICATIONS

During 2004, our focus in applications was biological systems. Having completed a survey of low-energy electron collisions with the DNA bases, we decided to make an intensive study of uracil, which is a constituent of RNA. Not only has uracil been the subject of a number of recent experimental studies [1–4], it has a slightly simpler structure than the corresponding DNA bases, facilitating computational studies. Our calculations addressed two principal issues: (1) What level of calculation is necessary to obtain good resonance (temporary anion) energies for uracil, and (2) Can calculations clarify the nature of the resonance process that appears to drive dissociative attachment to uracil?

One aspect of our study of the first question involved varying the one-electron basis set used to represent the molecular orbitals. In particular, we experimented with diffuse functions in pursuit of a better representation of the low-energy virtual orbitals that, in our square-integrable formulation of the collision problem, form the nonresonant background. A second aspect involved varying the number and type of many-electron functions used to represent the wavefunction of the electron–molecule system. Here, we found a significant effect from including, in addition to the usual terms

representing relaxation of the target molecule in the presence of the extra electron, closed-channel terms arising from the low-lying $^3A''$ excited states of uracil. We are currently writing up these results for publication. The lessons learned with uracil will be applied in similar studies of the DNA bases.

We are also in the final stages of the study of C_{60} begun last year. This work involved special-purpose modifications to our computer codes to exploit the high symmetry of the fullerene molecule while carrying out numerical quadratures for the "off-shell" portion of the Green's function that occurs in our Schwinger-type variational expression. As the calculation progressed, it became apparent that further code development would be needed in the "on-shell" portion of the calculation. Because of the large geometric size of C_{60}, relatively high partial waves become important at low collision energies, imposing a need for efficient means of achieving high accuracy in the description of the angular dependence of the scattering amplitude. We addressed this need by replacing products of one-dimensional quadratures with two-dimensional spherical (Lebedev) quadratures in the on-shell phase of the calculation. Though we routinely use Lebedev quadratures off-shell, applying them on-shell entailed writing a completely new program for evaluating the laboratory-frame differential cross sections. However, the new differential cross section program is not specific to C_{60} and is already being used in our studies of biological and plasma-processing molecules.

A few years ago, we computed elastic and inelastic electron cross sections for C_2F_4 as part of a collaborative effort to develop a cross section set for use by plasma modelers. At that time, almost no other electron cross section data for C_2F_4 were available. Very recently, both experimental [5] and theoretical [6] results for the elastic cross section were reported. Comparison of these recent results with those of our earlier study reveals broad areas of agreement but also some unexpected differences. In order to understand these differences, we are briefly revisiting C_2F_4 with a focus on obtaining thoroughly converged elastic results at key energies.

PROGRAM DEVELOPMENT

We continue to focus on the issue of scaling, that is, the rate of increase in computational difficulty with molecular size, because it is rapid scaling that poses the principal barrier to more accurate studies of electron collisions with polyatomic molecules. While we believe that the approach we pursued over the past several years continues to hold promise, it has not yet proven fully satisfactory, and we have begun development of an alternative approach to polarization effects in elastic scattering, in which different sets of molecular orbitals are employed to represent the isolated molecule and the electron–molecule collision complex. Evaluating matrix elements between different orbital sets poses some challenges, but we believe these can be resolved using standard techniques. This approach appears to capture the correct physics and offers extremely favorable scaling.

PLANS FOR COMING YEAR

We will wrap up the C_{60} and and uracil studies and publish those results. The experience gained from uracil will be applied to refine our existing results for the DNA bases by carrying out more detailed calculations, with better treatments of polarization effects. In the area of processing gases, we will complete the re-examination of C_2F_4 now under way. As described above, code

development will focus on means of representing polarization effects in elastic collisions that exhibit superior scaling.

REFERENCES

[1] G. Hanel, B. Gstir, S. Denifl, P. Scheier, M. Probst, B. Farizon, M. Farizon, E. Illenberger, and T. D. Märk, Phys. Rev. Lett. **90**, 188104 (2003).

[2] A. M. Scheer, K. Aflatooni, G. A. Gallup, and P. D. Burrow, Phys. Rev. Lett. **92**, 068102 (2004).

[3] S. Denifl, S. Ptasińska G. Hanel, B. Gstir, M. Probst, P. Scheier, and T. D. Märk, J. Chem. Phys. **120**, 6557 (2004).

[4] S. Feil, K. Gluch, S. Matt-Leubner, P. Scheier, J. Limtrakul, M. Probst, H. Deutsch, K. Becker, A. Stamatovic, and T. D. Märk, J. Phys. B **37**, 3013 (2004).

[5] S. J. Buckman, private communication.

[6] C. S. Trevisan, A. E. Orel, and T. N. Rescigno, Phys. Rev. **70**, 012704 (2004).

PROJECT PUBLICATIONS AND PRESENTATIONS, 2001–2004

1. "Low-Energy Electron Scattering by C_2HF_5," M. H. F. Bettega, C. Winstead, and V. McKoy, J. Chem. Phys. **114**, 6672 (2001).

2. "Electron Cross Section Set for CHF_3," W. L. Morgan, C. Winstead, and V. McKoy, J. Appl. Phys. **90**, 2009 (2001).

3. "Electron Collisions with Octafluorocyclobutane, c-C_4F_8," C. Winstead and V. McKoy, J. Chem. Phys. **114**, 7407 (2001).

4. "Electron–Molecule Collisions in Processing Plasmas," V. McKoy and C. Winstead, First International Symposium on Advanced Fluid Informatics, Sendai, Japan, 4–5 October, 2001 *(invited talk)*.

5. "Electron Collisions with Hexafluorocyclobutene, c-C_4F_6," C. Winstead and V. McKoy, Fifty-Fourth Gaseous Electronics Conference, State College, Pennsylvania, 9–12 October, 2001.

6. "Electron-Molecule Collisions in Processing Plasmas," V. McKoy and C. Winstead, Forty-Eighth International Symposium of the American Vacuum Society, San Francisco, California, 28 October–2 November, 2001 *(invited talk)*.

7. "Low-Energy Electron Scattering by CH_3F, CH_2F_2, CHF_3, and CF_4," M. T. do N. Varella, C. Winstead, V. McKoy, M. Kitajima, and H. Tanaka, Phys. Rev. A **65**, 022702 (2002).

8. "Electron Collisions with Tetrafluoroethene, C_2F_4," C. Winstead and V. McKoy, J. Chem. Phys. **116**, 1380 (2002).

9. "Electron Transport Properties and Collision Cross Sections in C_2F_4," K. Yoshida, S. Goto, H. Tagashira, C. Winstead, V. McKoy, and W. L. Morgan, J. Appl. Phys. **91**, 2637 (2002).

10. "Electron Collision Cross Sections for Tetraethoxysilane (TEOS)," W. L. Morgan, C. Winstead, and V. McKoy, J. Appl. Phys. **92**, 1663 (2002).

11. "Developing Cross Section Sets for Fluorocarbon Etchants," C. Winstead and V. McKoy, *Proceedings of the Third International Conference on Atomic and Molecular Data and Their Applications, Gatlinburg, Tennessee, 24–27 April, 2002*, AIP Conf. Proc. **636**, 241 (2002) *(invited talk)*.

12. "Quickly Generating Databases," C. Winstead, Third International Conference on Atomic and Molecular Data and Their Applications, Gatlinburg, Tennessee, 24–27 April, 2002 *(panelist)*.

13. "Electron Collisions with SF_6 (Sulfur Hexafluoride)," C. Winstead and V. McKoy, Fifty-Fifth Gaseous Electronics Conference, Minneapolis, Minnesota, 15–18 October, 2002.

14. "Parallel Computations of Electron–Molecule Collisions in Processing Plasmas," V. McKoy, Ninth International Conference on High-Performance Computing, Bangalore, India, 18–21 December, 2002 *(Keynote Lecture)*.

15. "Electron–Molecule Collisions in Processing Plasmas," V. McKoy, Applied Materials, Santa Clara, California, 7 February, 2003 *(invited talk)*.

16. "Electron–Molecule Collisions in Processing Plasmas," V. McKoy, Colloquium, Departments of Physics and Materials Science, University of Southern California, 28 April, 2003.

17. "Electron–Molecule Collision Calculations on Vector and MPP Systems," C. Winstead and V. McKoy, Cray Users' Group Conference, Columbus, Ohio, 12–16 May, 2003.

18. "Low-Energy Electron Scattering by Methylsilane," M. H. F. Bettega, C. Winstead, and V. McKoy, J. Chem. Phys. **119**, 859 (2003).

19. "Low-Energy Electron Collisions with Sulfur Hexafluoride, SF_6," C. Winstead and V. McKoy, J. Chem. Phys. (in press).

20. "Electron Collision Cross Section Set for SF_6," W. L. Morgan, C. Winstead, and V. McKoy, (in preparation).

21. "Low-Energy Electron Collisions with Buckminsterfullerene, C_{60}," C. Winstead and V. McKoy (in preparation).

22. "Elastic Collisions of Low-Energy Electrons with Gas-Phase Uracil," C. Winstead and V. McKoy (in preparation).

Ultrafast Atomic and Molecular Optics at Short Wavelengths

P.I.s: Henry C. Kapteyn and Margaret M. Murnane
Department of Physics and JILA
University of Colorado at Boulder, Boulder, CO 80309-0440
Phone: (303) 492-8198; FAX: (303) 492-5235; E-mail: kapteyn@jila.colorado.edu

PROGRAM SCOPE

The goal of this work is to study of the interaction of atoms and molecules with intense and very short (<20 femtosecond) laser pulses, with the purpose of developing new short-wavelength light sources, particularly at short wavelengths. We are also developing novel optical pulse shaping techniques to enable this work. In the past year, we have made a number of new advances that will increase the utility of short wavelength sources for applications in spectroscopy and imaging.

RECENT PROGRESS

1. **Self-compression of ultrashort pulses through ionization-induced spatio-temporal reshaping (Ref. 13):** We recently discovered and demonstrated a new mechanism for temporal compression of ultrashort light pulses that operates at high (i.e. ionizing) intensities for the first time. By propagating pulses inside a hollow waveguide filled with low-pressure argon gas, we demonstrate a self-compression from 30fs to 13fs, without the need for any external dispersion compensation. Theoretical models show that 3-D spatio-temporal reshaping of the pulse due to a combination of ionization-induced spectral broadening, plasma-induced refraction, and guiding in the hollow waveguide are necessary to explain the compression mechanism. The propagation of intense femtosecond duration light pulses in materials, gases and plasmas is important for many areas of high field science.

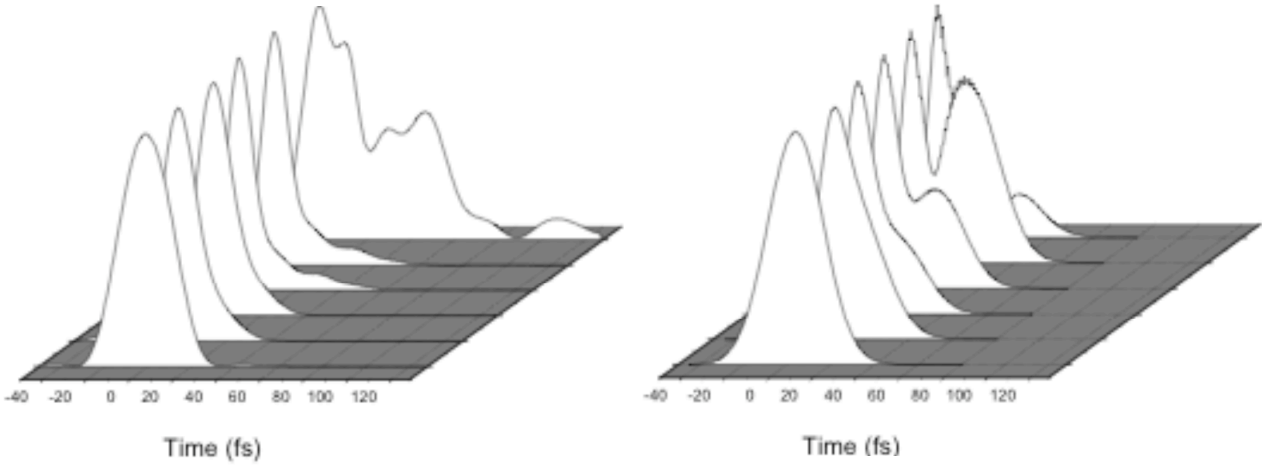

Figure 1: Comparison between the experimentally observed and theoretically predicted pulse envelopes as a function of pressure for 0, 2, 4, 6, 8 and 9 torr. (Left) Theoretically predicted pulse shapes. (Right) Experimentally measured pulse shapes The pulse compression and pulse splitting behavior are seen both experimentally and theoretically, with excellent agreement between experiment and theory.

In past work, nonlinear self-phase modulation (SPM) experienced by a pulse as it travels through a medium has been used to spectrally broaden a light pulse. This broadened pulse bandwidth can then be compressed by applying appropriate dispersion to the pulse

subsequent to the spectral broadening. Typically, a pulse is self-phase modulated by propagation through an optical fiber or a gas-filled hollow optical waveguide, and dispersion compensation is provided by pairs of prisms or gratings, or using "chirped mirrors" to induce a negative chirp. These schemes have been employed to compress pulses to < 4fs pulse duration; however, they are also relatively complex and lossy. A variety of other schemes for pulse compression have been demonstrated or proposed; for example, phase modulation of a light pulse induced by molecular phase modulation using vibrational or rotational motion. However, these schemes are also limited to low laser intensities below the dissociation threshold of the molecule.

In this work, we discovered a new and unanticipated regime of ultrashort pulse compression that operates at high laser intensities, where the pulse is ionizing the medium, and where 3-D effects dominate the compression mechanism. We show that an intense 800nm wavelength pulse propagating through a short gas-filled hollow waveguide, can reshape and self-compress in time without the need for subsequent dispersion compensation. Theoretical models show a new mechanism for pulse compression that cannot be explained by 1-D models, where 3-D spatio-temporal reshaping of the pulse occurs by ionization-induced spectral broadening, plasma-induced refraction, and guiding in the hollow waveguide. Therefore, this new technique is fundamentally different from previous mechanisms that broaden the spectrum of a short pulse in a waveguide, and then subsequently compress it using dispersion. This high field pulse compression is unique in its ability to shorten the duration of intense light pulses with high efficiency and with excellent pulse fidelity. Because this new mechanism can operate at intensities that are significantly higher than in other schemes, it may be scalable to much higher pulse energies, with implications for the design of many high field science experiments. Finally, our work is the first to demonstrate both experimentally and theoretically that it is possible to take advantage of 3-D pulse evolution to compress a light pulse in a way that is not predicted in 1-D simulations. Thus, our work provides unique insight that that fundamentally new physical phenomena can be found using 3-D simulations that has important implications for understanding many high field and plasma science experiments using either plasma or fiber-based guided geometries.

2. **High harmonic generation from ions (Ref. 7, 11, 12):** In recent work shown in Fig. 1, we experimentally demonstrated very high order harmonic generation of up to 250eV from Argon ions for the first time. Using a hollow waveguide filled with low-pressure gas, we can guide a laser beam in a highly-ionized plasma, to reduce the effect of ionization induced laser defocusing. As a result, we can extend the highest harmonic orders observable using 800nm driving-laser radiation by a factor of 2.5 compared with previous work. This corresponds to an extension of the cutoff by 150eV or 100 harmonic orders. These are higher photon energies than have previously been observed using either Argon or Neon gas under any conditions. At the laser intensities required to generate these harmonics, no neutral atoms remain. Thus, the harmonic emission originates from ionization of Ar^+.

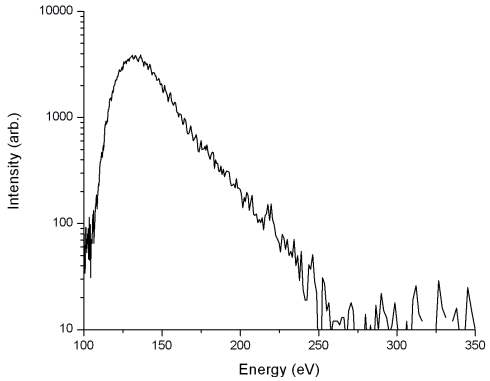

Figure 2: Harmonic emission from a 150μm diameter, 2.5cm long, fiber filled with low-pressure 7 Torr of Ar, excited by an 18fs pulse at a peak intensity of $\approx 1.3 \times 10^{15} Wcm^{-2}$.

The significance of this work is threefold. First, we have shown that high harmonic generation from ions can be used to greatly extend the coherent photon energies obtainable using HHG. Second, we demonstrated that large ions such as Argon, with high nonlinear susceptibilities compared to Helium, can be used to generate high-energy harmonics. This is of potential significance for developing useful coherent EUV and soft x-ray sources for many applications in science and technology. Finally, we demonstrated that the hollow waveguide geometry can generate higher photon energies than otherwise possible using a conventional gas jet or cell geometry. This work was recently published in Physical Review Letters.

3. **Using learning algorithms to study attosecond science (Refs. 9):** In work in collaboration with Herschel Rabitz and Ivan Christov, we demonstrated that the data generated using a learning algorithm to optimize a quantum system is useful in helping to understand the physics behind the process being optimized. In its optimization process, the learning algorithm naturally finds a particularly interesting region of parameter space and probes it extensively. Analyzing the statistical behavior of the solutions found by the algorithm confirms our theoretical models of the process. In particular, by optimizing high harmonic emission using a learning algorithm, and then analyzing the data resulting from the optimization process, we can verify our understanding of the temporal dynamics of the process. This work will soon be published in Physical Review A.

4. **Other work (Refs. 8, 10):** In other work in collaboration with Keith Nelson at MIT, we demonstrated the use of EUV light for time-resolved measurements of the photothermal and photoacoustic response of materials. By using wavelengths that are x20 shorter than visible light, we demonstrate the potential for dramatically increased sensitivity and signal levels, in some cases by almost two orders-of-magnitude compared with visible light. This approach will enable probing of surface acoustic dynamics on nano-scale spatial dimensions of 50nm and below, using a small-scale coherent EUV sources employing high-harmonic generation. This work was recently published in Applied Physics Letters.
   We also demonstrated a high-power laser system employing a new scheme where pulses with negative chirp are amplified, then recompressed using dispersion in a block of transparent material. This scheme has significant advantages for amplification of intermediate energy pulses at very high average power, including insensitivity to small misalignments of the pulse compressor, elimination of compressor gratings and their thermal loading issues, low compressor energy and bandwidth throughput losses, and a simplified optical design. Using this scheme, we demonstrate the highest average power single-stage, Ti:sapphire amplifier system to date with 11 W compressed output. This work will soon be published in Optics Letters.
   Finally, we have developed a phase stabilized, high power, ultrafast laser-amplifier system, for use in the study absolute-phase sensitive nonlinear optics, enhancement of EUV generation using pulse shaping, and for the study and manipulation of electronic and molecular wavepackets.

Publications (refereed) as a result of DOE support since 2002

1. R. Bartels, T. Weinacht, N. Wagner, M. Baertschy, C. Greene, M. Murnane, H. Kapteyn , “Phase Modulation of Ultrashort Light Pulses using Molecular Rotational Wavepackets”, Physical Review Letters **88**, 019303 (2002).
2. C. Durfee, L. Misoguti, S. Backus, R. Bartels, M. Murnane and H. Kapteyn, “Phase Matching in Cascaded Third-Order Processes, JOSA B **19** (4): 822-831 (2002).
3. S. Christensen, H.C. Kapteyn, M.M. Murnane, and S. Backus , "Simple, high power, compact, intracavity frequency-doubled Q-switched Nd:YAG laser," Review of Scientific Instruments **73** (5): 1994-1997 (2002).

4. R.A. Bartels, N.L. Wagner, M. Baertschy, J.Wyss, M.M. Murnane, H.C. Kapteyn, "Phase-matching conditions for nonlinear frequency conversion by use of aligned molecular gases," Optics Letters **28**, 346 (2003).
5. Ariel Paul, Randy Bartels, Ivan Christov, Henry Kapteyn, Margaret Murnane, Sterling Backus, "Multiphoton photonics: quasi phase matching in the EUV", *Nature* **421**, 51 (2003).
6. Emily A. Gibson, Ariel Paul, Nicholas Wagner, Ra'anan Tobey, Ivan P. Christov, David T. Attwood, Eric Gullikson, Andy Aquila, Margaret M. Murnane, and Henry C. Kapteyn, "Generation of coherent soft x-rays in the water window using quasi phase-matched harmonic generation", *Science* **302**, 95 (2003).
7. Emily A. Gibson, Ariel Paul, Nicholas Wagner, Ra'anan Tobey, Ivan P. Christov, Margaret M. Murnane, and Henry C. Kapteyn, "Very High Order Harmonic Generation in Highly Ionized Argon", Physical Review Letters **92**, 033001 (2004).
8. R. Tobey, E. Gershgoren, M. Siemens, M. M. Murnane, H. C. Kapteyn, T. Feurer and K. A. Nelson, "Photothermal and Photoacoustic Transients probed with Extreme Ultraviolet Radiation", Applied Physics Letters **85**, 564 (2004).
9. Randy A. Bartels, Margaret M. Murnane, Ivan P. Christov, Herschel Rabitz, and Henry C. Kapteyn , "Using learning algorithms to study attosecond dynamics", to be published in Phys. Rev. A (2004).
10. David M. Gaudiosi, Amy L. Lytle, Pat Kohl, Margaret M. Murnane, Henry C. Kapteyn, Sterling Backus, "Ti:sapphire amplifier system with 11 watt average power using downchirped pulse amplification," to be published in Optics Letters.
11. E. Gibson, X. Zhang, T. Popmintchev, A. Paul, A. Lytle, I.P. Christov, M.M. Murnane, H.C. Kapteyn, "Extreme Nonlinear Optics: Attosecond Photonics at Short Wavelengths", to be published in IEEE JSTQE (2004).
12. E.A. Gibson, I.P. Christov, M.M. Murnane, and H.C. Kapteyn , "Quantum Control of High-Order Harmonic Generation: Applied Attosecond Science", to be published in Applied Physics B (2004).

Publications (refereed) submitted as a result of DOE support

13. Nick Wagner, Emily Gibson, Tenio Popmintchev, Ivan Christov, Margaret M. Murnane, Henry C. Kapteyn, "Self-compression of ultrashort pulses through ionization-induced spatio-temporal reshaping", submitted to Physical Review Letters (2004).

Theory and Simulations of Ultrafast Nonlinear X-ray Spectroscopy of Molecules

Shaul Mukamel and Luke Campbell
Department of Chemistry, Rowland Hall,
University of California, Irvine 92697, USA
email: smukamel@uci.edu

August 12, 2004

X-ray Absorption Near Edge Spectroscopy (XANES) investigates the transitions of a selected deep core electron to a bound, unoccupied valence orbital using an x-ray beam tuned to just above (0 to 10 eV) the absorption threshold of a target element. These transitions only involve final orbitals with a significant amplitude near the core orbital, thus, this technique is a probe of the local unoccupied density of states in the vicinity of the absorbing atom.

The advent of picosecond to attosecond x-ray pulses has opened the door to time resolved x-ray spectroscopies [1]. In optical pump/x-ray probe measurements [2], an ultrafast optical laser pulse prepares the system in a transient state, which is then monitored by the x-ray probe pulse. Shifts in atomic positions due to transient geometry changes will affect the final state energies and the intensity of the transitions, and can thus be seen in XANES as shifts in peak positions and intensities. The change in charge distribution upon electronic excitation will also affect the final state energies. Further, when the electronic excitation moves electrons between orbitals, the allowed transitions of the system change. These effects were demonstrated in recent optical pump/x-ray probe experiments on organometallic complexes such as nickel tetraphenylporphyrin dipiperidine [3] and ruthenium tris-2,2'-bipyrinide [4].

Existing codes can calculate the XANES for the electronic ground state of an arbitrary atomic geometry, examples are the real space multiple scattering Green's function code FEFF [5] and the transition state density functional theory code StoBe-deMon [6]. We have recently used the former code to simulate the XANES of photodissociation of piperidine ligands from nickel tetraphenylporphyrin [7]. However, simulations of time resolved optical pump, x-ray probe experiments will also require calculating XANES of electronic excited states. In addition, it will be necessary to determine the time evolution of the atomic geometries in order to investigate changes in conformation, vibrations, photodissociation, and relaxations to the optimized excited state configuration subsequent to photoexcitation.

By neglecting core-valence exchange, we are able to separate the all electron wavefunctions of a molecule into products of a core electron and a valence electron wavefunction, with the final state valence orbitals computed self consistently under the influence of the core hole potential. We start with the molecule in an initial state with energy E_i and a valence N-electron wavefunction $|\Phi_i^N\rangle$. The possible final states after photoexcitation have energies E_f and final valence wavefunctions $|\Phi'_f{}^{N+1}\rangle$, with the prime indicating that the valence electrons are subject to the potential of the core hole. Introducing a core hole lifetime broadening Γ, and averaging over x-ray polarizations, the absorption cross section is

$$\sigma_{\rm abs}(\omega) = \frac{4\pi}{3\omega c}\sum_f \sum_{b,lm} \sum_\nu \mu_{lb}^\nu \mu_{bm}^\nu \frac{\langle\Phi_i^N|c_l|\Phi'_f{}^{N+1}\rangle\langle\Phi'_f{}^{N+1}|c_m^\dagger|\Phi_i^N\rangle\Gamma}{(\omega+E_i-E_f)^2+\Gamma^2}$$

where μ_{bl}^ν is the matrix element of the dipole operator in direction ν between valence orbital l and core orbital b, and c_l ($c_l^\dagger$) is the annihilation (creation) operator for an electron in orbital l. This expression involves only the total energies and the valence electronic properties of the molecule. By recasting the problem in terms of valence wavefunctions alone, we avoid the difficult problem of calculating deep core excitations. The low lying excited states of molecules are routinely calculated using quantum chemistry codes. By calculating large numbers of valence excited states of the molecule under the influence of a selected core hole potential, we are thus able to calculate the XANES.

We applied this method to the L_3 edge XANES of the ground state and the long lived (μs) triplet metal to ligand charge transfer (MLCT) state of ruthenium tris-2,2'-bipyridine ($Ru(bpy)_3{}^{2+}$). Recent experimental XANES measurements [4] show a 1 eV valence shift of the primary XANES peak and the appearance of a new XANES peak corresponding to the optical hole when $Ru(bpy)_3{}^{2+}$ is photoexcited to the MLCT state.

A singlet ground state calculation of $Ru(bpy)_3{}^{2+}$ using the 3-21G basis set was carried out with the Becke 3-parameter density functional [8] and the Lee-Yang-Par correlation functional [9] using the GAUSSIAN03 code. Time dependant density functional theory (TDDFT) was used to compute the electronic structure for the triplet MLCT state. To describe the core excited state we used the same basis set and density functionals as for the ground state, but included the core hole potential approximated as a point charge at the ruthenium nucleus, equivalent to replacing the ruthenium atom by rhodium (known as the Z+1 approximation). The first 50 excitations were calculated with TDDFT. Taking these as our set of final states and either the ground state the MLCT states as our initial state, we computed the XANES spectrum. Our results reproduced the 1 eV valence shift of the primary peak and the appearence of the new XANES transition to the optical hole of the MLCT state as seen by experiment [4].

Electronic excited states typically have a different geometry than the ground state. Short x-ray pulses can follow the time resolved geometry changes of a molecule after electronic excitation. To simulate such measurements, we plan to start with the ground state geometry but the excited state electronic structure.

A molecular dynamics simulation will then be performed to follow the trajectories of the atoms with time, and the XANES should be computed on the fly from these different configurations.

The present procedure is useful for transitions to and from the lowest lying electronic valence excited states. At present, we only include single excitations in our TDDFT calculations; as a result only a select class of initial electronic states can be calculated. Arbitrary low lying excited states could be described once double or higher particle-hole excitations are included - one excitation to represent the optically induced transition, and a second excitation that accounts for the photoelectron.

The limiting factor in our calculations is the computation of the excited states. It may thus be desirable to avoid such calculations altogether. By treating the core hole potential as a perturbation on the ground state system, we obtain an exactly soluable model for non-interacting systems [10]. A new set of orbital eigenvectors can be found by diagonalizing the valence Hamiltonian with the core hole potential, the excitations will be to these orbitals with energies given by the orbital energy eigenvalues. The x-ray spectrum immediately follows without the need for laborious calculations of excited states. For interacting systems, the non-interacting case could be solved, for example, at the Hartree-Fock level, and this could be used as the beginning of a perturbative calculation of the transitions using, for example, the GW method [11]. This method will also easily allow the treatment of an extended core hole.

The linear absorption is given by the Fourier transform of the time-time correlation function of the dipole operator. Higher order optical processes can be expressed in a similar fashion, in terms of higher order correlation functions of the dipole operator [12]. When one or more of the interactions is with an x-ray photon, our method could be extended to these non-linear spectroscopies.

References

[1] R. W. Schoenlein, S. Chattopadhyay, H. H. W. Chong, T. E. Glover, P. A. Heimann, C. V. Shank, A. A. Zholents, and M. S. Zolotorev Science **287** 2237-2240 (2000)

[2] C. Bressler and M. Chergui Chem. Rev. **104** 1781-1812 (2004)

[3] L. X. Chen, W. J. H. Jäger, G. Jennings, D. J. Gosztola, A. Munkholm, and J. P. Hessler Science **292** 262 (2001)

[4] M. Saes, C. Bressler, R. Abela, D. Grolimund, S. L. Johnson, P. A. Heimann, M. Chergui, Phys. Rev. Lett. **90** 047403 (2003)

[5] A. L. Ankudinov, B. Ravel, J. J. Rehr, and S. D. Conradson, Phys. Rev. B **58** 7565-7576 (1998)

[6] L. Triguero, L. G. M. Pettersson, and H. Ågren, Phys. Rev. B **58** 8097-8110 (1998)

[7] L. Campbell, S. Tanaka, and S. Mukamel, Chem. Phys. **299** 225-231 (2004)

[8] A. D. Becke, J. Chem. Phys. **98** 5648 (1993)

[9] C. Lee, W. Yang, and R. G. Parr, Phys. Rev. B **37** 785 (1988)

[10] G. D. Mahan *Many-Particle Physics* (Plenum Press, New York and London, 1990).

[11] L. Hedin, Phys. Rev. **139** A 796-A 823 (1965)

[12] S. Mukamel *Principles of Nonlinear Optical Spectroscopy* (Oxford University Press, New York and Oxford, 1995).

Ultrafast Coherent Soft X-rays: A Novel Tool for Spectroscopy of Collective Behavior in Complex Materials

Keith A. Nelson
Department of Chemistry, Massachusetts Institute of Technology
Cambridge, MA 02139
Email: kanelson@mit.edu

Henry C. Kapteyn, Margaret M. Murnane
JILA, University of Colorado and National Institutes of Technology
Boulder, CO 80309-0440
E-mail: kapteyn@jila.colorado.edu

Program Scope

Nonlinear time-resolved spectroscopy of condensed matter using coherent soft x-rays is being developed. Femtosecond pulses at soft x-ray wavelengths with nanojoule energies and high spatial coherence and focusability are produced through high harmonic generation in a hollow-waveguide geometry. These are to be used for excitation and probe pulses in time-resolved four-wave mixing, or transient grating, experiments. The primary experimental objective is to obtain direct access to both femtosecond time resolution and mesoscopic length scale resolution. A broader objective is to enable nonlinear time-resolved x-ray spectroscopy of condensed matter generally.

Although standard time-resolved spectroscopy techniques at optical wavelengths provide access to femtosecond time scales, they do not provide direct information on mesoscopic length scales since the wavelengths involved are tenths of microns. This exceeds almost all structural correlation lengths of interest in complex materials. In time-resolved four-wave mixing measurements, the experimental length scale is defined by the transient grating spatial period. Using soft x-ray pulses, this can be as short as a few tens of nanometers. Thus soft x-ray transient grating measurements open a window directly onto mesoscopic correlation lengths and fast correlation times. Our primary objectives are to determine both of these, and so explore any association between them, in complex materials such as polymers, supercooled liquids, glasses, and partially disordered crystals including mixed ferroelectrics.

The central experiments are aimed at excitation and characterization of high-wavevector surface acoustic waves whose behavior is mediated by mesoscopic structure, on the length scale of the acoustic wavelength, and by fast relaxation dynamics, on the time scale of the acoustic oscillation period. In particular, for acoustic waves with frequency ω and wavevector magnitude q, anomalous acoustic features (strong scattering and/or damping and dispersion) are expected in the regimes of $\omega\tau \sim 1$ and $qd \sim 1$, where τ is a relaxation (i.e. correlation) time scale and d a correlation length scale characteristic of the material. With soft x-ray wavelengths, transient grating measurements will provide access to acoustic wavelengths of tens to hundreds of nanometers and acoustic frequencies of tens to hundreds of gigahertz. Both of these regimes are of central interest in understanding complex behavior in disordered and partially ordered materials, since these typically show correlation length and time scales of nanometers and picoseconds respectively. Structural heterogeneity and relaxation dynamics are coupled strongly to acoustically induced density and shear distortions, so the acoustic behavior to be measured will be highly sensitive to the properties of interest.

Recent Progress

1. Transient acoustic responses of heterogeneous structures probed at soft x-ray wavelengths

A detailed study of soft x-ray (or extreme ultraviolet, EUV) diffraction from optically induced surface acoustic waves has been conducted and the results reported in Applied Physics Letters. [1] These first experiments were performed using nano-structured "damascene" grating patterns consisting of alternating copper and oxide strips on silicon wafers. These samples allow surface acoustic waves to be generated by uniform illumination with a single 800-nm pulse, since this gives rise to different extents of absorption and thermal expansion at the different regions. The experimental setup is illustrated schematically in Figure 1.

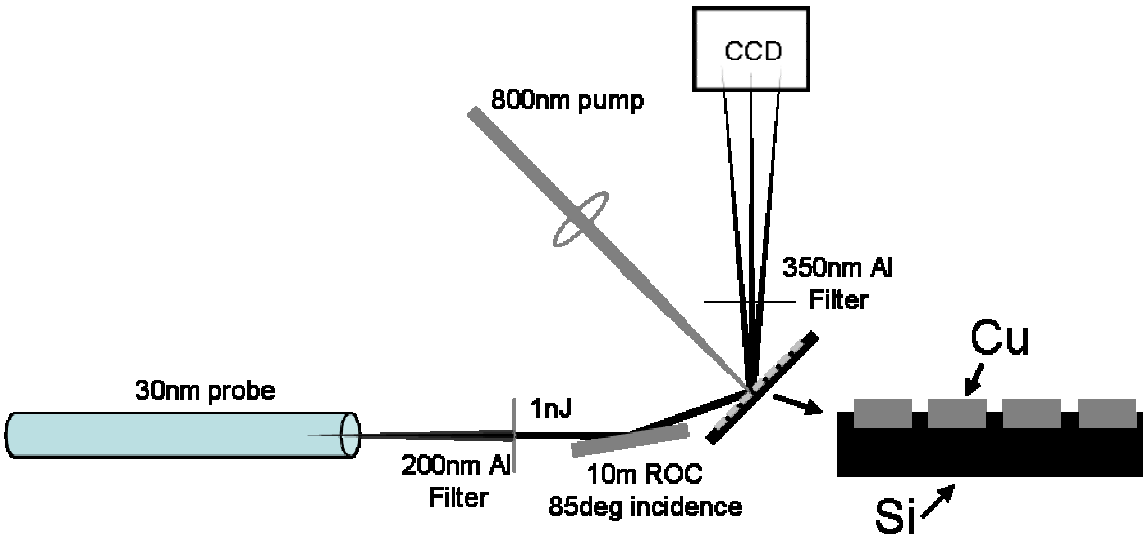

Figure 1: Experimental setup for optical pumping and EUV probing of thermal and acoustic transients. Part of the laser output is up-converted to generate the EUV probe beam. Optical excitation of the sample induces thermal expansion and acoustic oscillations that are detected by measuring the time-delayed, diffracted EUV probe. The sample is shown in detail.

A typical transient response of the damascene, probed by measuring the integrated first-order diffracted soft x-ray signal as a function of time, is shown in Figure 2. The induced acoustic oscillation frequency is grating-period-dependent and persists for up to 7 ns after excitation. In the data of Figure 2, the acoustically induced change in diffracted signal intensity (relative to the diffraction due to the unperturbed damascene grating pattern) is larger than 10% over the entire range of probe wavelengths (25nm – 33nm) for the highest pump fluence. For comparison, the signal from the same sample under the same pumping conditions but probed with visible light gives a measured change in diffraction of about 0.2%. Therefore, the EUV signal change is 1-2 orders of magnitude higher than what can be obtained using visible light, depending on the particular damascene grating spacing used. The increased sensitivity arises directly from the shorter EUV wavelength, at which surface acoustic displacements give rise to correspondingly larger phase modulations. Figure 3 shows the diffraction efficiencies recorded as a function of pump fluence. Both the time-dependences and the intensities of signals recorded with different damascene spatial periods and different pump fluence values were in agreement with theoretical expectations. Note that surface displacements as small as 0.02 nm were observed, with prospects for further improvement as the soft x-ray pulse stability is improved.

This new approach will enable probing of surface acoustic dynamics on nanoscale wavelength dimensions of 50 nm and below and in acoustic frequency ranges of 50 GHz and above.

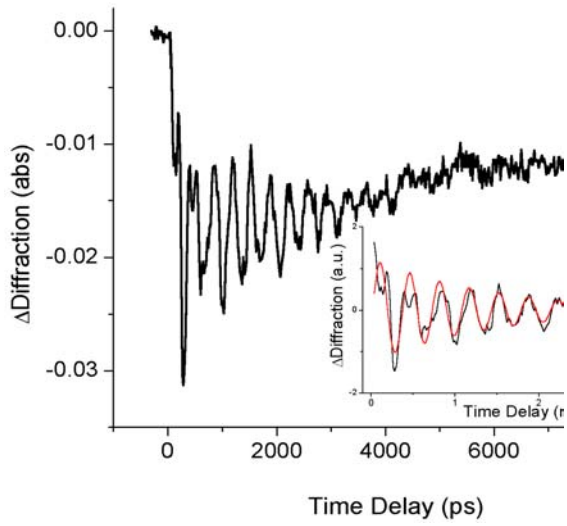

Figure 2: Integrated first-order diffraction signal following optical excitation of a damascene sample consisting of 500 nm Cu/500 nm SiO_2 stripes. Acoustic oscillations are evident with a decay time of 1.5 ns. Inset shows single 2.87-GHz frequency fit to the data. Other samples of varying periodicities gave qualitatively similar results, differing only in the acoustic frequencies measured.

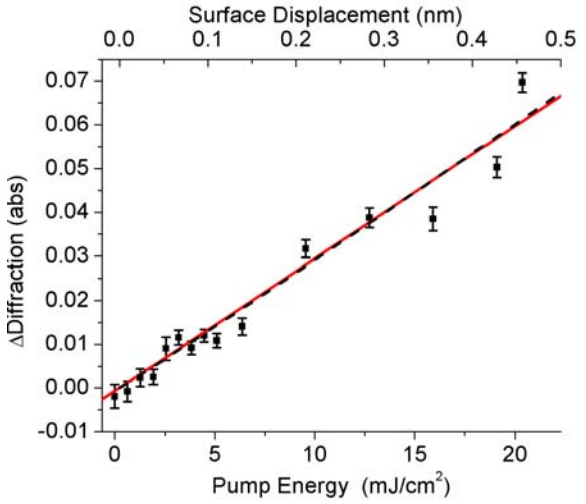

Figure 3: Measured change in EUV diffraction efficiency as a function of pump fluence (lower x-axis). Changes in diffraction exhibit linear behavior throughout the entire region of pumping fluence. The dashed line shows the calculated change in diffraction efficiency as a function of maximal surface displacement (top x-axis). The two lines overlap almost exactly.

2. Optical pump, soft x-ray probe transient grating measurements

While the measurements on damascene permitted progress in experimental optimization and theoretical calculation of soft x-ray diffraction, our more general experimental approach requires transient grating excitation of unpatterned surfaces. In recent work yet to be published, we succeeded in demonstrating *the first transient grating experiments using crossed visible pump pulses and an EUV probe pulse.* The experimental setup resembled that shown in Figure 2, except that crossed 800-nm excitation pulses were generated and delivered to the sample through the use of a binary phase mask. The diffracted signal as a function of time is shown in Figure 4. This preliminary experiment did not make use of any focusing of the EUV probe onto the CCD camera, and the transient grating wavelength Λ was quite long (5 μm), resulting in a very small EUV diffraction angle that permitted only partial separation of diffracted signal from reflected

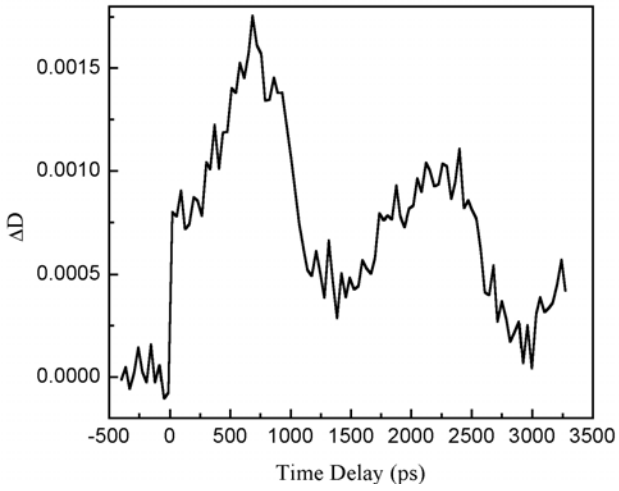

Figure 4: ISTS data recorded with 800 nm pump pulses and EUV probe pulses from an aluminum mirror surface. Surface acoustic wave oscillations are apparent.

EUV radiation. Improvement in the experimental geometry should lead to very substantial improvements in the signal intensity and signal/noise ratio. Nevertheless the data clearly demonstrate soft x-ray measurements of acoustic responses induced through transient grating excitation of unpatterned surfaces. The measured frequency and diffraction efficiency again compare well to theoretical expectations. This constitutes a major step toward our experimental objective of high-wavevector transient grating measurements of acoustic waves on unpatterned surfaces.

3. Novel optical apparatus for time-domain probing of high-frequency acoustic responses

Through EUV and ultimately hard x-ray transient grating measurements, we expect to gain direct access to acoustic responses at the highest wavevectors and frequencies. It is important to connect these measurements to those at lower acoustic frequencies. We have developed a method to permit this through narrowband photoacoustic spectroscopy with multiple-cycle, tunable acoustic waves. [2] An optical pulse sequence is generated with repetition rate set equal to the desired acoustic frequency. This is used to irradiate a thin metal film that acts as a transducer, sending an acoustic response into a substrate that is the sample of interest. The acoustic wave is detected interferometrically after passing through the substrate and a second metal film at the opposite side from the first. Measurements of acoustic responses in silica glass as a function of temperature have been conducted in this fashion, and measurements on polymer films are currently under way. This method depends on suitable sample configuration and on acoustic wave transmission through the multilayer sample, but within these constraints it can provide a useful window into high-frequency longitudinal acoustic wave behavior.

Future plans

Our next step will be to extend our recent visible pump, soft x-ray probe transient grating measurements to UV and finally soft x-ray excitation wavelengths. Experiments with UV excitation wavelengths can be conducted in the same manner as with 800-nm wavelengths, generating the two excitation beams using binary phase masks and projecting the beams to the sample through a 2-lens telescope. For soft x-ray excitation wavelengths, we plan to use wire grating patterns in close proximity to the sample surface, in a shadow-masking configuration that we have demonstrated previously for soft x-ray photolithography of permanent grating structures in polymer samples. This will enable our central experimental measurements of high-wavevector, high-frequency acoustic responses in disordered and partially ordered solid samples.

References to publications of DOE sponsored research

1. R. I. Tobey, E. H. Gershgoren, M. E. Siemens, M. M. Murnane, H. C. Kapteyn, T. Feurer, and K. A. Nelson, "Nanoscale Photothermal and Photoacoustic Transients Probed with Extreme Ultraviolet Radiation," Applied Physics Letters **85**, 564-566 (2004)
2. J.D. Beers, M. Yamaguchi, T. Feurer, B.J. Paxton, and K.A. Nelson, "Ultrahigh frequency acoustic phonon generation and spectroscopy with Deathstar pulse shaping," in Ultrafast Phenomena XIV, K.A. Nelson, S. DeSilvestri, T. Kobayashi, T. Okada, and T. Kobayashi, eds. (Springer-Verlag, 2004), in press.

Localized Photoemission from Gold Nanostructures and Electromagnetic Friction

Lukas Novotny (novotny@optics.rochester.edu)
University of Rochester, The Institute of Optics, Rochester, NY, 14627.

1 Program Scope

We study the local interaction between a laser-irradiated local probe, such as a metal tip, and a sample placed in close proximity. Under certain conditions, the local probe is able to confine and enhance the incoming radiation. For metal tips it has been theoretically predicted that the enhancement factor can be three to four orders of magnitude, i.e. the intensity at the metal tip is a factor $10^3 - 10^4$ stronger than the intensity of the incoming radiation. The enhanced field at the tip acts as a highly confined light source for a local, spectroscopic interaction with the sample surface. The field enhancement originates from a combination of electrostatic lightning-rod effect (quasi-singularity at the tip) and surface plasmon resonances which are strongly material and geometry dependent. The experimentally determined enhancement factors are not as strong as the theoretically predicted ones and it is the focus of our project to understand the critical parameters for maximizing the enhancement effect.

By moving the sample underneath the laser-irradiated metal tip and acquiring an optical response for different tip-sample positions we are able to record an optical raster-scan image with a resolution that solely depends on the tip sharpness. The principle of this *tip-enhanced spectroscopy* is shown in Fig. 1. So far, we were able to demonstrate resolutions better than 20nm using 1) two-photon excited fluorescence [1], 2) second-harmonic generation [2], and 3) Raman scattering [3]. Our work has enabled systematic studies of single molecule fluorescence in inhomogeneous environments and of defects and dopants in single-walled carbon nanotubes.

While studying the electromagnetic response of laser-irradiated gold tips we discovered that the tips emit radiation over a broad range of frequencies when excited with femtosecond laser pulses. We have further investigated the origin of this radiation and determined that it is due to second-harmonic generation [2] and broadband photoluminescence [4]. It was found that in both cases the emission originates from the tip end and hence it constitutes a highly confined light source. The yield of photoluminescence was found to be a good indicator for the strength of local field enhancement and we performed a study on metal nanoclusters to demonstrate this effect [5].

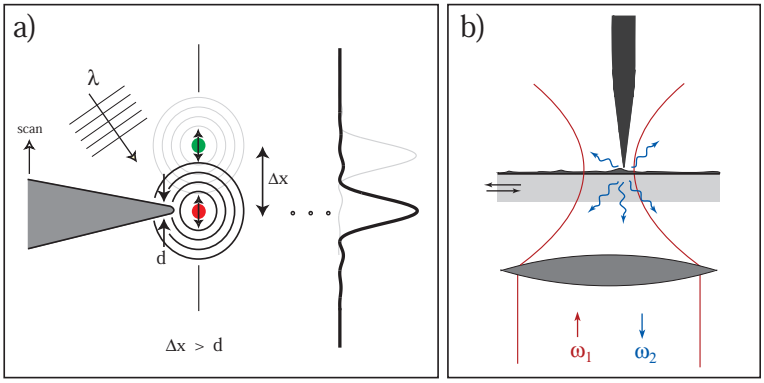

Figure 1: *Principle of the local field-enhancement technique. A laser-irradiated metal tip (polarization along tip axis) enhances the incident electric field near its apex thereby creating a localized photon source. a) Schematic of the method. b) Practical implementation: a higher-order laser beam is focused on a sample surface and a sharply pointed metal tip is positioned into the laser focus. The enhanced fields at the tip locally interact with the sample surface thereby exciting a spectroscopic response that is collected by the same objective and directed on a detector.*

2 Recent Progress

In the past year, we have investigated the photoluminescence from laser-irradiated metal tips. We have determined that the luminescence intensity is an indirect measure for the strength of field enhancement and we developed a technique for the characterization of so-called hot-spots associated with aggregates of metal particles [5]. In a parallel effort, we have investigated theoretically the nature of friction between tip and sample [6]. This study led to some remarkable predictions associated with so-called electromagnetic friction: 1) strong friction is associated with dielectric bodies in relative motion, and 2) electromagnetic friction is even present in for a single body if it interacts with thermal background radiation. This means that any object will ultimately come to rest. However, typical friction forces are in the range of atto-Newtons which makes it difficult to be observed at ambient conditions. Both projects, locally excited photoluminescence and electromagnetic friction, will be described in the following separate sections.

2.1 Localized photoluminescence

The optical properties of metal nanoparticles are strongly influenced by their size, their shape, and by their environment such as the proximity to other particles. When the dimensions of nanoparticles becomes smaller than the wavelength of the exciting light, energy can be confined in small spatial regions through the local excitation of surface plasmon resonances. The enhanced fields in these regions are used in a wide range of applications including surface enhanced Raman scattering (SERS), near-field microscopy, and nanoscale optical devices. Direct experimental measurements of electromagnetic fields localized between closely spaced nanostructures are needed to validate theoretical predictions and to develop systems with improved properties. In our study, we investigated the three-dimensional spatial variation of the electromagnetic field as a function of the separation between a gold nanoparticle and a sharp gold tip. We took advantage of the intrinsic photoluminescence properties of gold nanostructures. Two-photon excited luminescence was found to be sensitive to the local field enhancement on rough metal films [4]. In our experiments, we localize regions of strong field enhancement by measuring the spatial distribution of the photoluminescence yield.

Individual nanoparticles deposited on a transparent substrate were excited by the field of a tightly focused femtosecond laser, similar to the situation shown in Fig. 1b. The high peak intensity ($\approx 110\,\mathrm{GW}\ /\ \mathrm{cm}^2$) associated with ultrashort pulses $\approx 120\,\mathrm{fs}$ excites electrons in the metal particles from the d band to the sp conduction band by two-photon absorption [4]. Subsequent photoluminescence is collected with the same objective as used for excitation and is directed toward either a sensitive avalanche photodetector for imaging purposes or to a CCD spectrometer to acquire luminescence spectra.

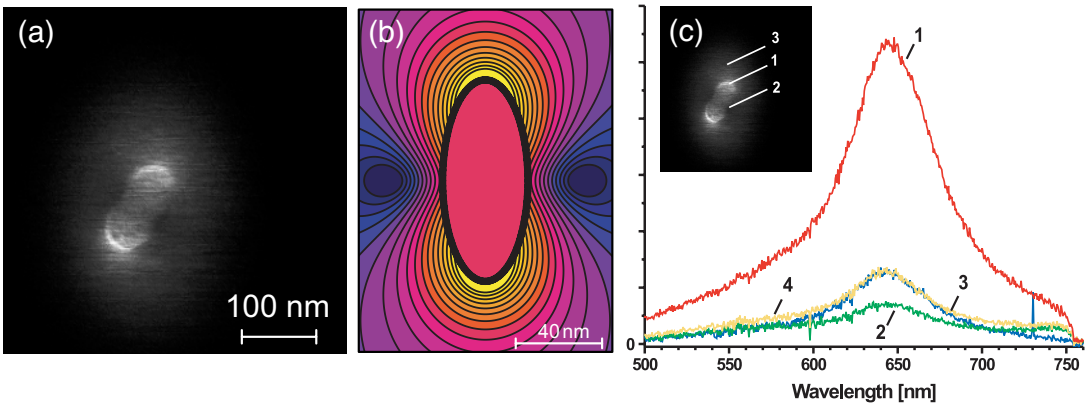

Figure 2: *(a) Two-photon excited photoluminescence image of an elliptical cluster of gold particles. The halo corresponds to the farfield luminescence. (b) Calculated intensity distribution of ellipsoid with the same dimensions excited near resonance* $\approx 650\,nm$. *(c) Photoluminescence spectrum (excitation at* $780\,nm$*) acquired for different tip positions.*

Fig. 2a shows the photoluminescence image originating from an elliptical gold particle as it is raster-scanned underneath the gold tip. The luminescence originates from the gold particle and not from the tip. The tip is used to locally scatter the near-field of the generated photoluminescence and hence to enable diffraction-unlimited imaging. As seen in Fig. 2a, the photoluminescence is strongly enhanced at the extremities of the ellipsoidal particle. On the other hand, the signal intensity is reduced at the two diametrically opposed points along the short axis. The photoluminescence image strongly resembles the calculated surface intensity distribution of an ellipsoid excited at resonance, as shown in Fig. 2b. The image demonstrates the dipolar character of the excited particle: charge accumulation at both ends along the long axis and charge depletion along the short axis. The calculation was based on the multiple multipole method (MMP) for an excitation wavelength of 650 nm and a dielectric constant of $\varepsilon_{Au} = -12.9 + 1.09i$.

We have determined that there is no resonant coupling between tip and particle. This is evidenced by the recorded spectra shown in Fig. 2c. The gray curve in represents the emission of the ellipsoidal particle without the tip present. The spectrum is peaked at 644 nm, in agreement with the calculated resonance. The particular shape of the spectrum originates from the convolution of the density of states available at these energies with the intrinsic surface plasmon resonance of the particle [4]. The spectrum was also recorded as a function of particle position (positions 1, 2, 3 and 4). No shift of the resonance peak is observed. Only the signal amplitude is affected by the tip and the overall shape of the spectrum is conserved. Therefore, the tip has a negligible influence on the intrinsic response of the particle. We thus have the analogous situation to two coupled oscillators, one of which is much weaker than the other. Because the tip can be regarded as a passive probe, we obtain a direct measurement of the field enhancement and thus of the local charge distribution on the surface of the dimer.

In conclusion, in this study we showed that local field enhancement at nanoscale metal structures leads to local photoluminescence excited by two-photon absorption. A direct map of the distribution of local fields (hot spots) can be recorded by locally scattering the photoluminescence intensity using a metal tip. The presented method is a promising approach for the characterization of field enhancing structures used in future plasmonic devices. It will also be useful in the study of hot spots responsible for the giant enhancement of Raman cross sections in SERS.

2.2 Electromagnetic Friction

To maintain a sharp metal tip at a distance of ≈ 1 nm from the sample surface a highly sensitive feedback mechanism is needed. A common approach is to oscillate the tip with an amplitude of less then $1\mathring{A}$ parallel to the sample surface and to measure the friction force as a function of tip-sample distance. Interestingly, this shear-force can even be measured in UHV conditions and at temperatures as low as 4 K [7]. There is no theory which would render an order-of-magnitude agreement with experimental measurements.

We performed a general study of electromagnetic friction arising from charge correlations between two bodies in relative motion [6]. It is well known that electromagnetic interactions between two charge-neutral objects give rise to an attractive force, known as the *dispersion force*. Our study shows that if the two objects are in relative motion to each other then there appears an additional non-conservative force which brings the motion ultimately to rest. We determined that the force is much stronger for dielectric objects than for metal objects. In addition, it was found that only fluctuations in the frequency range $0 \,..\, 100$ Hz contribute significantly to the force. This force has direct consequences for the development of future nanoscale systems and for various proposals in the field of quantum information. Dissipative interactions limit the performance of nano-electro-mechanical systems (NEMS) and will lead to increased decoherence in miniaturized particle traps such as ion-traps and atom chips.

A remarkable outcome of our theory is that friction is even present in empty space as long as the temperature is finite. Thus, an object moving in empty space comes ultimately to rest. This result is consistent with earlier existing theories. In another limit, for short distances between particle and surface, we can neglect retardation and find that friction becomes strongly material dependent, i.e. friction is many orders of magnitude stronger for dielectric materials than for conducting materials. Also important is the finding that only thermal fluctuations in the low-frequency range of $0 \,..\, 100$ Hz are significant.

3 Future Plans

In a continuation of our project we will investigate the possibility of performing absorption spectroscopy on single molecules using the localized emission near a metal tip as a photon source. We will explore metal tips of finite length to increase the field enhancement factor further by imitating concepts known from antenna theory.

References

[1] E. J. Sanchez, L. Novotny, and X. S. Xie, "Near-field fluorescence microscopy based on two-photon excitation with metal tips," *Phys. Rev. Lett.* **82**, 4014 (1999).

[2] A. Bouhelier, M. Beversluis, A. Hartschuh, and L. Novotny, "Near-field second-harmonic generation induced by local field enhancement," *Phys. Rev. Lett.* **90**, 13903 (2003).

[3] A. Hartschuh, E. J. Sanchez, X. S. Xie, and L. Novotny, "High-resolution near-field Raman microscopy of single-walled carbon nanotubes," *Phys. Rev. Lett.* **90**, 95503 (2003).

[4] M. R. Beversluis, A. Bouhelier, and L. Novotny, "Continuum generation from single gold nanostructures through near-field mediated intraband transitions," *Phys. Rev. B.* **68**, 115433 (2003).

[5] A. Bouhelier, M. R. Beversluis, and L. Novotny, "Characterization of nanoplasmonic structures by locally excited photoluminescence," *Appl. Phys. Lett.* **83**, 5041 (2003).

[6] J. R. Zurita-Sanchez, J.-J. Greffet, and L. Novotny, "Near-field friction due to fluctuating fields," *Phys. Rev. A* **69**, 022902 (2004).

[7] B. C. Stipe, H. J. Mamin, T. D. Stowe, T. W. Kenny, and D. Rugar, "Noncontact friction and force fluctuations between closely spaced bodies," Phys. Rev. Lett. **87**, 96801 (2001).

[8] J. R. Zurita-Sanchez and L. Novotny, "Multipolar interband absorption in a semiconductor quantum dot. II. Magnetic dipole enhancement," *J. Opt. Soc. Am. B* **19**, 2722 (2002).

[9] J. R. Zurita-Sanchez and L. Novotny, "Multipolar interband absorption in a semiconductor quantum dot. I. Electric quadrupole enhancement," *J. Opt. Soc. Am. B* **19**, 1355 (2002).

[10] A. Bouhelier, M. R. Beversluis, and L. Novotny, "Near-field scattering of longitudinal fields," *Appl. Phys. Lett.* **82**, 4596 (2003).

[11] A. Bouhelier, J. Renger, M. Beversluis, and L. Novotny, "Plasmon coupled tip-enhanced near-field microscopy," *J. Microsc.* **210**, 220 (2003).

[12] A. Hartschuh, H. N. Pedrosa, L. Novotny, and T. D. Krauss, "Simultaneous fluorescence and Raman scattering from single carbon nanotubes," *Science* **301**, 1354 (2003).

[13] A. Bouhelier, A. Hartschuh, M. R. Beversluis, and L. Novotny, "Near-field optical microscopy in the nanosciences," in *Microscopy for Nanotechnology*, N. Yao and Z. L. Wang (eds.), Springer Verlag, in print (2004).

[14] A. Hartschuh, M. R. Beversluis, A. Bouhelier, and L. Novotny, "Tip-enhanced optical spectroscopy," *Phil. Trans. R. Soc. Lond. A* **362**, 807 (2004).

DOE sponsored publications (2002-2004): Refs. [2], [4], [5], [6], [8], [9], [10], [11], [12], [13], [14].

Energetic Photon and Electron Interactions with Positive Ions

Ronald A. Phaneuf,
Department of Physics /220
University of Nevada
Reno NV 89557-0058
phaneuf@physics.unr.edu

Program Scope

This experimental program investigates processes leading to ionization of positive ions by photons and electrons. The objective is a deeper understanding of both ionization mechanisms and electron-electron interactions in atomic, molecular and cluster ions. Mononergetic beams of photons and electrons are crossed or merged with ion beams to selectively probe their internal electronic structure and the interaction dynamics. In addition to precision spectroscopic data for ionic structure, measurements of absolute cross sections for photoionization and electron-impact ionization provide critical benchmarks for the theoretical calculations that generate opacity databases. The latter are critical to models of astrophysical, fusion-energy and laboratory plasmas. Examples of particular relevance to DOE include the Z pulsed-power facility at Sandia National Laboratories, the world's brightest and most efficient x-ray source, and the National Ignition Facility at Lawrence Livermore National Laboratory, the world's most powerful laser. Both facilities are dedicated to high-energy-density science, fusion energy and defense-related research.

Recent Progress

The major thrust of this research program has been the application of an ion-photon-beam (IPB) research endstation to experimental studies of photoexcitation and photoionization of singly and multiply charged positive ions using synchrotron radiation. The high photon beam intensity and energy resolution available at ALS undulator beamline 10.0.1 make photoion spectroscopy a powerful probe of the internal electronic structure of atomic ions, permitting tests of sophisticated atomic structure and dynamics codes at unprecedented levels of detail and precision. Photon-ion measurements using the IPB endstation at ALS define the state of the art with respect to energy resolution in studies of photon-ion interactions by at least an order of magnitude. Specific accomplishments of the past year are highlighted below.

The emphasis has been the systematic investigation of photoionization of atomic ions of increasingly complex electronic structure, where theoretical approximations are less secure and essentially untested. Ions were selected for study in which the active electrons occupy the same shell, and consequently the electron-electron interaction is especially strong. For example, np – nd excitations have large oscillator strengths and dominate the photoionization of ions with partially filled nd subshells, giving rise to broad resonances that decay rapidly.

- A systematic study of photoionization of ions of the nitrogen isoelectronic sequence comprised the Ph.D. dissertation of A. Aguilar [12]. Absolute cross-section measurements were completed and analyzed for photoionization of metastable and ground-state O^+, F^{2+} and Ne^{3+}. A detailed paper that is nearly ready for submission

includes a quantum-defect analysis of four Rydberg series of resonances observed in this isoelectronic sequence and a comparison with both the TopBase astrophysics database and state-of-the-art R-matrix calculations for F^{2+} and Ne^{3+}.

- The potassium isoelectronic sequence, with 19 electrons and a single valence electron outside closed electron shells, was a topic of special interest. The ground-state configuration of K and Ca^{+} is $3p^{6}4s$ and the $3p^{6}3d$ configuration is metastable, whereas the reverse is true for Sc^{2+} and more highly charged members of the sequence. A comparison of photoionization of Sc^{2+} measured at ALS with its time-reversed analog, photorecombination of electrons with Ar-like Sc^{3+} measured by a group at the University of Giessen at the TSR storage ring in Heidelberg provided a definitive application of the principle of detailed balance, and demonstrated the synergy of photoionization and photorecombination measurements. A comparison made possible an experimental determination of the metastable content of the S^{2+} ion beam used for the photoionization measurements [4,8,11]. A broad 3p-3d 'giant' resonance in the photoionization of metastable Ca^{+} and ground-state Sc^{2+} was predicted on the basis of electron-ion recombination measurements made by the Giessen group to straddle the ionization threshold in Ti^{3+}, so that part of the resonance could be bound and part autoionizing. This was verified by recent measurements performed at ALS in collaboration with the Giessen group [14].
- The iron isonuclear sequence was targeted for study because of its significance in astrophysical and fusion plasmas, which has motivated a significant body of theoretical work under the auspices of the "Iron Project". The first seven ionization stages of iron are characterized by a partially filled 3d shell, giving rise to a complex energy level structures and strong configuration interaction. Absolute photoionization measurements were completed for Fe^{3+}, Fe^{5+} and Fe^{7+}. The latter is K-like and connects with the previous measurements on Ca^{+}, Sc^{2+} and Ti^{3+}. Photoionization of ions of the iron isonuclear sequence will constitute the Ph.D. dissertation of M. Gharaibeh, who held an ALS Graduate Fellowship in Residence during 2003-2004, and plans to graduate in December, 2004.

During the past year, a new research direction was initiated involving photoionization and photo-fragmentation of singly and multiply charged fullerene ions, also in collaboration with the Giessen group. The objective was to clarify the roles of collective versus localized electron excitations, to uncover new spectroscopic information and to perform the first absolute photoionization and photo-fragmentation cross-section measurements for fullerene ions. A broad resonance near 22 eV that dominates the photoionization of neutral C_{60} was also observed in photoionization of C_{60}^{+} C_{60}^{2+} and C_{60}^{3+}. This "giant plasmon resonance" in C_{60} is attributed to a collective excitation of the 240-q delocalized valence electrons on the surface of the C_{60} spherical cage. The cross-section data for these ions exhibit a second broader resonance feature near 39 eV, which has been interpreted by a group from the Max Planck Institute for Complex Systems in Dresden as a higher-order collective electron oscillation associated with a volume plasmon. A collaborative paper describing the experiment and theory has been submitted to Physical Review Letters. Absolute measurements have also been performed for photoionization and photo-fragmentation of C_{60}^{+} and C_{70}^{+} in the 280-310 eV range, which encompasses the carbon K-edge.

Future Plans

The energy range and high spectral resolution of ALS beamline 10.0 have been shown to be well suited to studies of photoionization and photofragmentation of C_{60}^{q+} and C_{70}^{q+} ions in the threshold energy region (17 – 70 eV), and in the vicinity of the carbon K-edge (280 – 310 eV). A systematic investigation of the role of the two giant plasmon resonances in single and multiple photoionization and in photofragmentation will be initiated. High-resolution measurements of 1s – 2p excitation of fullerene ions are of particular interest because of the distinct classes of bonding sites of C atoms in C_{60}^{q+} and C_{70}^{q+}, which should be manifested in high-resolution photoion-yield spectra.

The dominant feature ionization of ions of the Xe isonuclear sequence is the collapse of the 4f wave function as the ion charge is increased, leading to an increased relative importance of discrete 4d - nf resonances compared to the 4d - ϵf continuum "giant" resonance that dominates photoionization of neutral Xe. Guided by the photoionization data, electron-impact measurements are expected to elucidate the role of 4d - np and 4d - nf excitation-autoionization. ionization of Xe^{q+} ions. Photoionization and electron-impact ionization measurements for Xe^{3+} constituted the M.S. thesis of E. Emmons [15]. Photoabsorption by Xe^{4+}, Xe^{5+} and Xe^{6+} in the spectral region near 13.5 nm have application in light source development for advanced EUV lithography. Absolute photoionization measurements for these ions are planned in collaboration with NIST.

Complementary measurements of photoionization and electron-impact ionization of ions of the Kr isonuclear sequence will constitute the Ph.D. dissertation research of M. Lu. Ionization of the lower charge states, which have partially-filled 3d shells, is expected to be dominated by strong excitations due to 3p – nd, 3d – np and 3d – nf transitions. The FAC atomic structure code will guide the experiments and data analysis, as well as planned coincidence measurements of autoionization spectra due to electron-ion collisions.

References to Publications of DOE-Sponsored Research (2002-2004)

1. *Photoionization of Ne^+ using synchrotron radiation,* A.M. Covington, A. Aguilar, I.R. Covington, M.F. Gharaibeh, G. Hinojosa, C.A. Shirley, R.A. Phaneuf, I. Álvarez, C. Cisneros, I. Domínguez-Lopez, M.M. Sant'Anna, A.S. Schlachter, B.M. McLaughlin and A. Dalgarno, Phys. Rev. A 66, 062710 (2002).
2. *Formation of long-lived CO^{2+} via photoionization of CO^+,* G. Hinojosa, A.M. Covington, R.A. Phaneuf, M.M. Sant'Anna, R. Hernandez, I.R. Covington, I. Domínguez, J.D. Bozek, A.S. Schlachter, I. Álvarez and C. Cisneros, Phys. Rev. A 66, 032718 (2002).
3. *Photoionization of C^{2+} ions: time-reversed recombination of C^{3+} with electrons,* A. Müller, R.A. Phaneuf, A. Aguilar, M.F. Gharaibeh, A.S. Schlachter, I. Álvarez, C. Cisneros, G. Hinojosa and B.M. McLaughlin, J. Phys. B 35, L137 (2002).

4. *Experimental link of photoionization of Sc^{2+} to photorecombination of Sc^{3+}: an application of detailed balance in a unique atomic system,* S. Schippers, A. Müller, S. Ricz, M.E. Bannister, G.H. Dunn, J. Bozek, A.S. Schlachter, G. Hinojosa, C. Cisneros, A. Aguilar, A.M. Covington, M.F. Gharaibeh and R.A. Phaneuf, Phys. Rev. Lett. 89, 193002 (2002).

5. *Electron spectroscopy of Na-like autoionizing metastable ions,* M. Lu and R.A. Phaneuf, Phys. Rev. A 66, 012706 (2002).

6. *Photoionization of isoelectronic ions: Mg^{+} and Al^{2+},* A. Aguilar, J.B. West, R.A. Phaneuf, R.L. Brooks, F. Folkmann, H. Kjeldsen, J.D. Bozek, A.S. Schlachter and C. Cisneros, Phys. Rev. A 67 012701 (2003).

7. *Absolute photoionization cross section measurements of OII ions from 29.7 eV to 46.2 eV,* A. Aguilar, A.M. Covington, G. Hinojosa, R.A. Phaneuf, I. Álvarez, C. Cisneros, J.D. Bozek, I. Dominguez, M.M. Sant'Anna, A.S. Schlachter, S.N. Nahar and B.M. McLaughlin, Astrophys. J (Supplement Series) 146, 467 (2003).

8. *Photoionization of Sc^{2+} ions by synchrotron radiation: high-resolution measurements and absolute cross sections in the photon energy range 23-68 eV,* S. Schippers, A. Müller, S. Ricz, M.E. Bannister, G.H. Dunn, A.S. Schlachter, G. Hinojosa, C. Cisneros, A. Aguilar, A.M. Covington, M.F. Gharaibeh and R.A. Phaneuf, Phys. Rev A 67, 032702 (2003).

9. *Photoionization studies of the B^{+} valence shell: experiment and theory*, S. Schippers, A. Müller, B.M. McLaughlin, A. Aguilar, C. Cisneros, E.D. Emmons, M.F. Gharaibeh and R.A. Phaneuf, J. Phys. B: At. Mol. Opt. Phys. 26, 3371 (2003).

10. *Photoionization of C^{2+} ions*, A. Müller, R.A. Phaneuf, A. Aguilar, M.F. Gharaibeh, A.S. Schlachter, I. Álvarez, C. Cisneros, G. Hinojosa and B.M. McLaughlin, Nucl. Instrum. Methods Phys. Res. B 205, 301 (2003).

11. *Photoionization of Sc^{2+}: experimental link with photorecombination of Sc^{3+} by application of detailed balance*, S. Schippers, A. Müller, S. Ricz, M.E. Bannister, G.H. Dunn, J. Bozek, A.S. Schlachter, G. Hinojosa, C. Cisneros, A. Aguilar, A.M. Covington, M.F. Gharaibeh and R.A. Phaneuf, Nucl. Instrum. Methods Phys. Res. B 205, 297 (2003).

12. *Photoionization of positive ions: the nitrogen isoelectronic sequence*, A. Aguilar, Ph.D. Dissertation, University of Nevada, Reno (2003).

13. *Lifetime of a K-shell vacancy in atomic carbon created by 1s-2p photoexcitation of C^{+},* A.S. Schlachter, M.M Sant'Anna, A.M. Covington, A. Aguilar, M.F. Gharaibeh, E.D. Emmons, S.W.J. Scully, R.A. Phaneuf, G. Hinojosa, I. Álvarez, C. Cisneros, A. Müller and B.M. McLaughlin, J. Phys. B 37, L103 (2004).

14. *Threshold truncation of a 'giant' dipole resonance in photoionization of Ti^{3+},* S. Schippers, A. Müller, R.A. Phaneuf, T. van Zoest, I. Álvarez, C. Cisneros, E.D. Emmons, M.F. Gharaibeh, G. Hinojosa, A.S. Schlachter and S.W.J. Scully, J. Phys. B 37, L209 (2004).

15. *A complementary study of photoionization and electron-impact ionization of an atomic ion: Xe^{3+}*, E. Emmons, M.S. Thesis, University of Nevada, Reno (May 2004).

Note: Participation of those whose names are underlined was supported wholly or in part by this DOE grant.

Control of Molecular Dynamics: Algorithms for Design and Implementation

Herschel Rabitz and Tak-San Ho, Princeton University,
Frick Laboratory, Princeton, NJ 08540, hrabitz@princeton.edu, tsho@princeton.edu

A. Program Scope

This research is concerned with developing the concepts for photonic reagent control of quantum dynamics phenomena. A photonic reagent is an ultra-fast shaped laser pulse whose tailored structure is designed to manipulate the internal dynamics of atoms and molecules. Although a photonic reagent has a fleeting existence, it can have a permanent impact on the substrate it interacts with. The research in this program involves several interactive components aiming at (a) identifying the fundamental principles of quantum control, (b) better enabling laboratory control experiments, and (c) extracting as much information as possible from the resultant data. A summary of these activities is given below.

B. Recent Progress

1. Algorithm development for the enhanced design of quantum controls.

1.a A propagation toolkit to design quantum controls[1]. A toolkit of time-propagation operators, to be stored and recalled as needed, was incorporated into the algorithms for the optimal control of quantum systems. Typically, the control field $\varepsilon(t)$ revisits the same values many times during the full time evolution. This repetition may be utilized to enhance efficiency through a convenient toolkit of propagators where the propagators are computed and stored only at a small number of discrete electric-field values. The toolkit can reduce the cost of control field design by a factor scaling as $\sim N$ for quantum systems described in a basis set of N states.

1.b A local-time algorithm for achieving quantum control[2]. A local-time algorithm (LTA) was developed for designing electric fields to guide a quantum system toward a desired observable. The LTA is a noniterative forward marching procedure based on making a choice for the control field over the next immediate small time increment.

1.c Quantum control design via adaptive tracking[3]. An adaptive tracking algorithm was developed to achieve quantum system control field designs. The core of the adaptive tracking control algorithm is a self-learning track switch technique, which is triggered by monitoring of the evolving system trajectory.

1.d Solution algorithms for quantum optimal control equations in product spaces[4]. This work showed that the introduction of product spaces enables classification of several chemically/physically interesting cost functionals, including the time evolution of intermediate states during the control period. Monotonically convergent iteration algorithms are developed for the pulse design equations derived from these basic functionals.

1.e. Controlling quantum phenomena with photonic reagents[5]. Efforts at controlling molecular dynamics and other quantum phenomena with lasers have a history going back to the early 1960's. Recent years have seen dramatic successes beginning to emerge. This

work presented an overview of the basic operating principles behind the use of shaped laser pulses (photonic reagents) for manipulating quantum dynamics.

2. Algorithms for enhancing laboratory control of quantum phenomena

2.a Tying the loop tighter around quantum systems[6]. This work discusses several issues that lie ahead in the control of quantum phenomena, drawing on the ability to perform massive numbers of closed loop laser control experiments. Particular attention is given to the robustness of these experiments, the capability of deducing control mechanisms, and the introduction of special closed loop control techniques to reveal Hamiltonian information. All of these prospects point towards an increasing ability to control and understand quantum systems through closed-loop laboratory techniques.

2.b Closed loop learning control to suppress the effects of quantum decoherence[7]. This work explored the use of laboratory closed loop learning control to suppress the effects of decoherence in quantum dynamics. Simulations of the process are performed in multilevel quantum systems strongly interacting with the environment. The simulations suggest that decoherence may be optimally managed in the laboratory through closed loop operations with a suitable cost that is sensitive to the coherence of the dynamics.

2.c Quantum physics under control[8]. Thanks to the increasing ability to coherently control quantum systems, designer Hamiltonians can be created to explore new physics and to yield a better understanding of complex phenomena. This work presented an overview of this rapidly evolving field.

2.d Efficient algorithms for the laboratory discovery of optimal quantum controls[9]. The laboratory closed loop optimal control of quantum phenomena commonly use search algorithms as variants of genetic algorithms. An alternative direct deterministic algorithm is proposed in this work, which can outperform the existing approaches.

2.e Controlling quantum phenomena: why does it appear easy to achieve?[10]. This work explored the reason for the evident ease of finding effective quantum controls, revealing that the origin lies in the quantum system being controllable and undergoing unitary evolution. Under these conditions, the search space landscape for maximizing the probability of making a quantum transition is shown to have no false extrema.

2.f Quantum optimal control of ozone isomerization[11]. We presented a feasibility study of achieving ozone isomerization with photonic reagents based on a recent *ab initio* potential energy surface. An electric field was found that drives isomerization with a yield of 95% to the symmetric metastable triangular form of ozone.

3. Applications to the manipulation of chemical bonds

3.a Manipulating bond lengths adiabatically with light[12]. This work proposed a new method to manipulate bond lengths in molecules based on strong fields that prepare an artificial potential by controlling the mixing of electronic configurations.

3.b Light-induced trapping of molecular wave packets in the continuum[13]. A method to prepare molecules in nonequilibrium nuclear configurations was proposed, based on using strong laser fields to stabilize the dissociative continuum of an electronic potential. The dissociative potential can be shaped to continuously change the equilibrium bond position.

4. Quantum control mechanisms

4.a Revealing quantum-control mechanisms through Hamiltonian encoding in different representations[14]. Hamiltonian encoding is a means for revealing the mechanism of controlled quantum dynamics. In this context, the mechanism is defined by the dominant quantum pathways starting from the initial state and proceeding through a set of intermediate states to end at the final state. The nature and interpretation of the mechanism is shown to depend on the choice of the states to represent the dynamics and alternative representations may provide distinct insights into the system mechanism.

4.b Mechanism analysis of controlled quantum dynamics in the coordinate representation[15]. This work focuses on understanding mechanism in the coordinate representation, which is natural for many dynamical systems. The quantum amplitudes defining the mechanistic pathways are determined by a special procedure called Coding Hamiltonians to Access Mechanistic Pathways (CHAMP). Mechanism determination is illustrated for excitation of a model linear triatomic molecule.

5. Extracting Hamiltonian information from control dynamics data

5.a Optimal Hamiltonian identification: the synthesis of quantum optimal control and quantum inversion[16]. We introduced optimal identification (OI) as a collaborative laboratory/computational algorithm for extracting quantum Hamiltonians from experimental data specifically sought to minimize the inversion error. OI incorporates the components of quantum control and inversion by combining ultrafast pulse shaping technology and high throughput experiments with global inversion techniques to actively identify quantum Hamiltonians from tailored observations. The OI concept rests on the general notion that optimal data can be measured under the influence of suitable controls to minimize uncertainty in the extracted Hamiltonian despite data limitations such as finite resolution and noise.

5.b Error bounds for molecular Hamiltonians inverted from experimental data[17]. Inverting experimental data provides a powerful technique for obtaining information about molecular Hamiltonians. However, rigorously quantifying how laboratory error propagates through the inversion algorithm has always presented a challenge. This work we developed an inversion algorithm that realistically treats experimental error. This algorithm is built upon the formalism of map-facilitated inversion to alleviate computational expense and permit the use of powerful nonlinear optimization algorithms.

C. Future Plans

The research in the coming year aims to focus on further exploration of the fundamental principles of controlling quantum phenomena. A particular emphasis will be given to addressing the basic question of why it is proving to be rather easy to control quantum phenomena in the laboratory despite the fact that many tens or hundreds of phase and amplitude variables are

adjusted for this purpose. In addition, a new effort will be undertaken to explore the interrelationship between the controls for families of chemically and physically similar molecules, with the aim of establishing the systematic behavior behind the control of homologous quantum systems. Finally, new algorithms will be developed to identify the physically essential features in the laboratory control fields as well as extract mechanistic information from the controlled dynamics data.

D. References

[1] A propagation toolkit to design quantum controls, F. Yip, D. Mazziotti, and H. Rabitz, *J. Chem. Phys.*, **118**, 8168-8172 (2003).

[2] A local-time algorithm for achieving quantum control, F.L. Yip, D.A. Mazziotti, and H. Rabitz, *J. Phys. Chem. A*, **107**, 7264-7268 (2003).

[3] Quantum control design via adaptive tracking, W. Zhu and H. Rabitz, *J. Chem. Phys.*, **119**, 3619-3625 (2003).

[4] Development of solution algorithms for quantum optimal control equations in product spaces, Y. Ohtsuki and H. Rabitz, *Proceedings of CRM*, 33, (2003).

[5] Controlling Quantum Phenomena with Photonic Reagents, H. Rabitz, *Int. Rev Phys. Chem*. (2004) in press.

[6] Tying the loop tighter around quantum systems, H. Rabitz, *J. Mod. Opt.*, **50**, 2291-2303 (2003).

[7] Closed loop learning control to suppress the effects of quantum decoherence, W. Zhu and H. Rabitz, *J. Chem. Phys.*, **118**, 6751-6757 (2003).

[8] Quantum physics under control, I. Walmsley and H. Rabitz, *Physics Today*, **56**, 43-49 (2003).

[9] Efficient algorithms for the laboratory discovery of optimal quantum controls, G. Turinici, C. Le Bris, and H. Rabitz, *Phys Rev E* (2004) in press.

[10] Controlling quantum phenomena: Why does it appear easy to achieve?, H. Rabitz, special issue *J. Modern Optics*, (2004) in press.

[11] Quantum optimal control of ozone isomerization, M. Artamonov, T.-S. Ho, and H. Rabitz, *J. Chem. Phys.*, (2004) in press.

[12] Manipulating bond lengths adiabatically with light, I. R. Sola, B.Y. Chang, and H. Rabitz, *J. Chem. Phys.*, **119**, 10653-10657 (2003).

[13] Light-induced trapping of molecular wave packets in the continuum, B.Y. Chang, H. Rabitz, and I. R. Sola, *Phys. Rev. A*, **68**, 031402 (2003).

[14] Revealing quantum-control mechanisms through Hamiltonian encoding in different representations, A. Mitra, I. Solá, and H. Rabitz, *Phys. Rev. A*, **67**, 043409-1-9 (2003).

[15] Mechanism analysis of controlled quantum dynamics in the coordinate representation, R. Sharp and H. Rabitz, *J. Chem. Phys.* (2004) in press.

[16] Optimal Hamiltonian identification: The synthesis of quantum optimal control and quantum inversion, J.M. Geremia and H. Rabitz, *J. Chem. Phys.*, **118**, 5369-5382 (2003).

[17] Error bounds for molecular Hamiltonians inverted from experimental data, J.M. Geremia and H. Rabitz, *Phys. Rev. A*, **67**, 022711-1-11, (2003).

[18] Reproducing kernel Hilbert space interpolation methods as a paradigm of high dimensional model representations: Application to multidimensional potential energy surface construction, T.-S. Ho and H. Rabitz, *J. Chem. Phys.*, **119**, 6433-6442 (2003).

[19] Implementation of a fast analytic ground state potential energy surface for the $N(^2D) + H_2$ Reaction, T.-S. Ho, H. Rabitz, F.J. Aoiz, L. Banares, S.A. Vázquez, and L.B. Harding, *J. Chem. Phys.*, **119**, 3063-3070 (2003).

Cold Rydberg Atom Gases and Plasmas in Strong Magnetic Fields

G. Raithel, FOCUS Center, Physics Department, University of Michigan
500 East University, Ann Arbor, MI 48109-1120, graithel@umich.edu
http://quaser.physics.lsa.umich.edu/projects/highb/

Summary

We investigate cold plasmas and gases of cold Rydberg atoms in a high-magnetic-field (high-B) environment. An extension of low-B cold-plasma research into the high-B domain is desirable because strong magnetic fields occur in many astrophysical, terrestrial or man-made plasmas. A strong magnetic field will increase the plasma lifetime, alter the plasma dynamics, and change the nature of any Rydberg atoms contained within the plasma. Further, due to the pinning of free charges to **B**-field lines, the addition of a strong B-field to cold plasmas is likely to suppress collisional electron heating mechanisms, potentially opening an avenue to the generation of a strongly coupled electron component in a cold plasma.

In the experiments, an atom trap is used that operates at magnetic fields at least 15 times higher than previous high-B traps. We have measured the atom temperature, the atom number, the loading and the magnetic-trapping behavior of the trap. In electric-field ionization spectra of Rydberg atoms photo-excited in the high-B trap we have identified novel structures that reflect multiple, quantized ionization thresholds that are associated with free-electron Landau states. The lifetimes of quasi-bound Rydberg atoms above the photo-ionization threshold have been measured directly by observation of the electron current emanating from cold Rydberg gases excited in the trap. Lifetimes of positive-energy states of order 10 μs have been observed. Further, we have obtained evidence for collision-induced state redistribution in strongly magnetized Rydberg gases as well as Rydberg atom formation through recombination.

We have measured the stability of cold electron gases in a combined Ioffe-Penning trap, which is integrated in our system. This research relates to antihydrogen experiments elsewhere, in which antihydrogen is formed by recombination of positrons and antiprotons in trap setups similar to ours. Here, we use the Ioffe-Penning trap as a tool to enhance collision and recombination rates.

1 Laser-cooling and magnetic trapping at several Tesla

The main experimental tool in the described research is a unique high-B atom trap which can be used in two modes. In the optical-molasses mode, a slow atomic beam of ^{85}Rb atoms is laser-cooled in a magnetic field of up to 6 T. This reflects a 30x improvement over previous demonstrations. In the molasses mode, the atoms are cooled to temperatures near the Doppler limit (≈ 150 μK), but there is no restoring force towards the trap center. Therefore, in the molasses mode the cold atomic gas is short-lived due to diffusive escape of the cooled atoms from the molasses region.

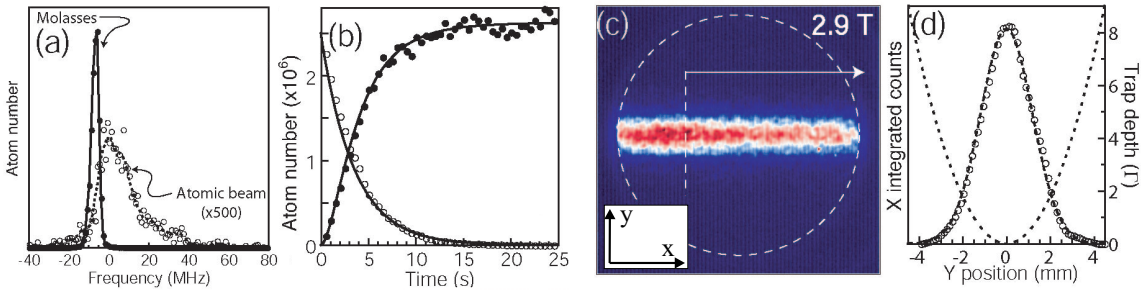

Figure 1: **a)** Number of atoms in the Ioffe-Pritchard laser trap (filled circles) versus detuning of the trap laser relative to the atomic transition frequency at the trap center. The reference curve (open circles, magnified 500×) shows the number of atoms detected in the atomic beam with the trap turned off. **b)** Loading (filled circles) and lifetime (open circles) curves for cooling and trapping in a 2.9 T Ioffe-Pritchard laser trap. **c)** Image of electrons streamed from the Ioffe-Pritchard laser trap onto the MCP and phosphor screen. **d)** The x-integrated spatial profile of the atom cloud versus y. The Gaussian fit is used to determine the temperature of the atoms. The trap depth is shown in units of the transition linewidth, $\Gamma = 6$ MHz.

We mostly operate the superconducting magnet system in a Ioffe-Pritchard laser trap mode. In this mode, atoms are continuously laser-cooled, accumulated and magnetically trapped in variable bias fields up to 3 T. This reflects a 15x improvement over previous demonstrations. In Fig. 1a, the number of atoms in the trap region, measured via photo-ionization and photoelectron detection, is plotted versus the frequency of the trap laser. The atom number obtained with the trap turned on exceeds the atomic-beam-only signal by about a factor 1000. Also, the spectral range over which large numbers of trapped atoms are obtained is only about one linewidth wide. Both observations demonstrate the effectiveness of the trap. Other important measures for trap performance are the loading rate, the time it takes to fill an initially empty trap up close to steady-state population, and the time it takes for the trap population to decay after blocking the loading beam. Loading rates, loading times and decay times can be extracted from the data shown in Fig. 1b. The number of atoms that can be trapped at 3 T has been found to be a few 10^6, and the density 10^7cm^{-3} to 10^8cm^{-3}. The atom temperature has been determined from measurements of the spatial distribution of the atoms in the trap (see Figs. 1c and 1d). We have found temperatures near the Doppler limit (about 140 μK). All measurements of trap performance are in agreement with detailed simulations of the trap.

So far, we have discussed the behavior of the trap with the trap laser being permanently on. The trap can also be used as a pure Ioffe-Pritchard magnetic trap by simply turning the trap laser off after a large number of cold atoms has been accumulated. We have measured a near 100% transfer efficiency from the laser trap into a pure magnetic trap. The magnetic-trap lifetime is about 80 s, limited by background pressure.

2 Electric-field ionization of strongly magnetized Rydberg atoms in low-m states

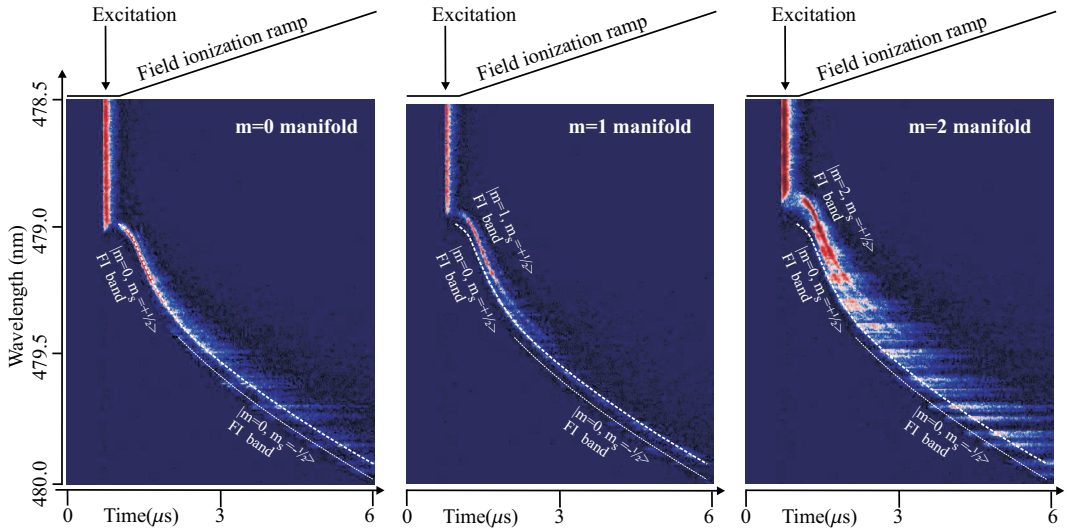

Figure 2: 2D representation of the field ionization behavior at 3 Tesla as a function of laser wavelength and ionization electric field. The latter is applied in form of a time-dependent field ionization pulse, as displayed in the top portions of the panels. Using the polarization of the photo-excitation, the $m = 0$ (left), $m = 1$ (middle) and $m = 2$ (right) manifolds of Rydberg states are excited. Four significant field ionization (FI) bands are identified, including one that is due to spin-orbit coupling ($|m = 0, m_s = -1/2\rangle$).

The demonstration of the high-B atom trap has set the stage for a variety of high-B cold-atom and cold-plasma experiments. The electric-field ionization spectra of slow, strongly magnetized Rydberg atoms have been studied for different polarizations of the Rydberg excitation laser. The results reflect an m-dependence of the photo-ionization thresholds associated with Landau channels, and an associated m-dependence of the ionization electric fields of the Rydberg atoms. The photo-ionization thresholds are given by the difference of the energy levels of free Landau states, $E_{n,m} = \hbar\omega_c(n + |m|/2 + m/2 + 1/2 + m_s)$, and the energy of the intermediate state, $E_{5P} = \hbar\omega_c(m_0/2 + m_{s0})$. There, ω_c is the cyclotron frequency, n is a radial quantum number of the Landau state, m and m_s are the azimuthal and spin quantum numbers of the Rydberg electron, respectively, and m_0 and m_{s0} are the azimuthal and spin quantum numbers of the $5P_{3/2}$ state that serves as an intermediate state of the two-step photo-excitation. A spin g-factor of 2 is assumed. All 5P-atoms present in the atom trap have $m_0 = 1$ and $m_{s0} = +1/2$. Further, due to considerable non-adiabatic coupling all Rydberg states contain a significant amount of $n = 0$ character and can therefore be assumed

to photo- and field-ionize at the threshold values that apply for $n = 0$. Assuming further that spin-orbit coupling is negligible, i.e. $m_s = m_{s0} = +1/2$, it is finally concluded that the photo-ionization thresholds observed in the spectra should be shifted with respect to the field-free ionization threshold by an amount of $\Delta E_m = \hbar\omega_c(|m|/2 + m/2)$. The photo-ionization thresholds observed in Fig. 2 follow this expectation. We have, in particular, confirmed that the threshold for $m = 0$ does not shift with the magnetic field.

The presence of well-defined, m-dependent photo-ionization thresholds is closely related to the presence of well-defined field ionization (FI) bands, which are clearly observed in Fig. 2 in the vicinity of the field-free photo-ionization threshold, $\lambda = 479.1$ nm. At low excitation energies, most of the field ionization signal occurs in the ionization band consistent with $m = 0$, even if the laser excitation has been into a manifold of larger m. This behavior may be due to m-mixing caused by a weak transverse component of the electric field of the field ionization ramp. The m-mixing causes the Rydberg atoms to field-ionize at the lowest possible ionization electric field, namely the one consistent with $m \leq 0$.

Close inspection of Fig. 2 reveals the presence of yet another field ionization band, namely a weak band below the $m = 0$ one. As seen in Fig. 2, this band becomes apparent mostly at low excitation energy. We also found that the continuum threshold associated with that band shifts at $\Delta E = -\hbar\omega_c$. We are quite certain that this band is caused by a combination of m-mixing and spin-orbit coupling of the excited Rydberg manifold $|m, m_s = +1/2\rangle$ to the manifold $|m + 1, m_s = -1/2\rangle$.

The effects of m-mixing and spin-orbit coupling progress as a function of evolution time, as seen in Fig. 3 for a case of linear laser polarization transverse to the magnetic field. In this case, the initially excited manifolds are, in equal parts, $m = 0$ and $m = 2$. In Fig. 3 it is observed that with increasing evolution time a more wide-spread pattern of FI-bands emerges, which reflects m-mixing caused by (quasi-)electric fields and, less likely, by radiative transitions. Also, the effect of spin-orbit coupling becomes more pronounced in time.

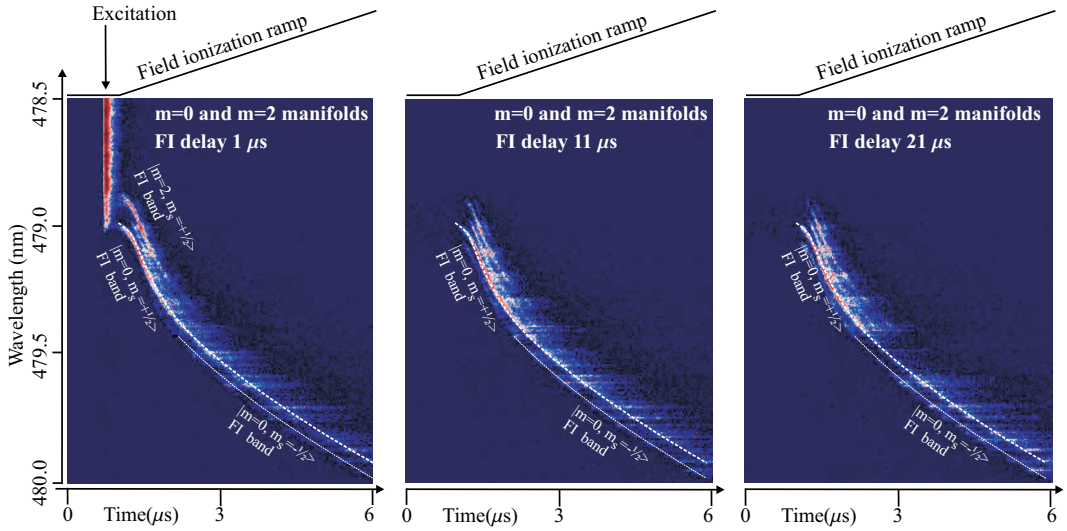

Figure 3: Field ionization behavior at 3 Tesla as a function of laser wavelength and ionization electric field for the indicated delay times of the FI pulses with respect to the photo-excitation. The $m = 0$ and $m = 2$ manifolds of Rydberg states are excited in equal parts. The figure demonstrates the progressive effects of m-mixing and spin-orbit coupling.

3 Lifetime of metastable Rydberg states

In similar data, we measure the spontaneous decay of Rydberg atoms excited above the photo-ionization threshold by monitoring the free-electron current emanating from samples of excited atoms. Quasi-bound positive-energy Rydberg atoms with lifetimes exceeding 10 μs are found. The decay mechanisms include spin-orbit coupling and m-mixing. Quantitative models describing our observations still need to be developed.

4 Ioffe-Penning trap

The setup incorporates a Ioffe-Penning trap, i.e. a trap that is suited for the simultaneous trapping of ions or electrons and neutral atoms. We have demonstrated the stability of such a trap by trapping neutral Rb atoms and by photo-ionizing them, thereby filling the Ioffe-Penning trap "from the inside" with photo-electrons. The electrons have been trapped in the Ioffe-Penning trap for 1/e time scales of up to 50 seconds. Using energy-selective extraction of the electrons from the Penning trap, it was also found that the electrons undergo significant cyclotron cooling.

5 Collision experiments

The effect of collisions between electrons contained in the Ioffe-Penning trap and subsequently excited high-B Rydberg atoms has been observed in field ionization spectra. A typical set of measurements is shown in Fig. 4. It is seen that long evolution times lead to a significant spread of the distribution of ionization electric fields. In particular, longer-lived, weakly bound Rydberg states with lower ionization electric fields become populated. Most notably, the presence of electrons in the Ioffe-Penning trap leads to a dramatic shift of Rydberg population into states with ionization fields that can be both lower or higher than that of the initially excited state (lower right panel in Fig. 4).

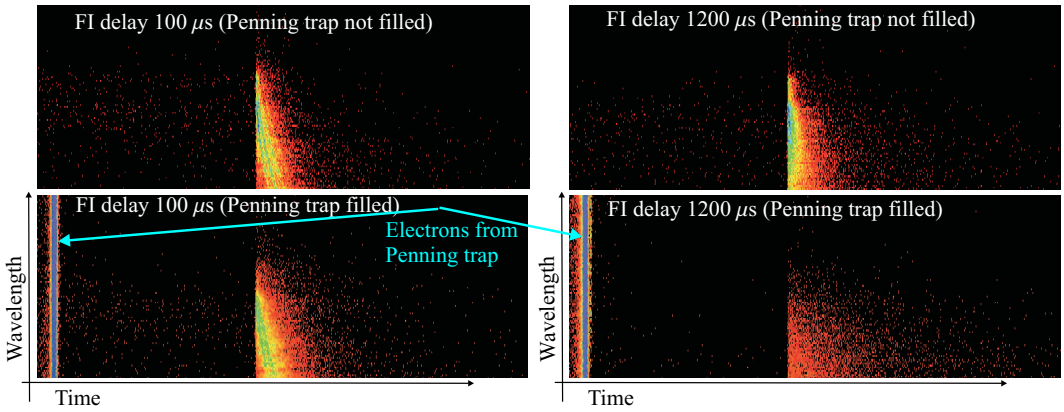

Figure 4: Collision-induced signal redistribution in field ionization spectra. The left (right) pair of panels shows FI spectra obtained 100 μs (1200 μs) evolution after the photo-excitation. Also, the upper (lower) pair of panels has been obtained without (with) pre-filling of the Ioffe-Penning trap overlayed over the Rydberg atom cloud with electrons. The free electrons in the Penning trap are extracted before the FI pulse is applied (see blue arrows).

Plans

We will spend significant time on the preparation of publications on existing results. More quantitative studies of Rydberg atom collisions will be performed, and the collision products will be analyzed with respect to lifetime. To increase cold-plasma and Rydberg-atom densities, more powerful lasers have been / will be installed.

Recent publications which acknowledge DoE support:

"Coulomb expansion of laser-excited ion plasmas," D. Feldbaum, N. V. Morrow, S. K. Dutta, G. Raithel, Phys. Rev. Lett. **89**, 173004 (2002).

"Decay rates of high-$|m|$ Rydberg states in strong magnetic fields," J. R. Guest, J.-H. Choi, G. Raithel, in print Phys. Rev. **A** (2003).

"High-m Rydberg states in strong magnetic fields," J. R. Guest, G. Raithel, Phys. Rev. **A 68**, 052502 (2003).

"Cold Rydberg Gas Dynamics," A. Walz-Flannigan, J. R. Guest, J.-H. Choi, and G. Raithel, Phys. Rev. **A 69**, 063405 (2004).

"Time Averaging of Multi-mode Optical Fiber Output for a Magneto-Optical Trap," A. P. Povilus, J. R. Guest, S. E. Olson, R. R. Mhaskar, B. K. Teo, G. Raithel, submitted (2004).

"Laser cooling and magnetic trapping at several Tesla," J. R. Guest, J.-H. Choi, E. Hansis, A. P. Povilus and G. Raithel, to be submitted (2004).

(see http://www-personal.umich.edu/~graithel)

A Dual Bose-Einstein Condensate:
Towards the Formation of Heteronuclear Molecules

Principal Investigator:

Dr. Chandra Raman
Assistant Professor
School of Physics
Georgia Institute of Technology Atlanta, GA 30332-0430
craman@gatech.edu

Program:

This program centers on the exploration of superfluidity in a single species sodium Bose-Einstein condensate and the pursuit of dual species BEC in sodium and rubidium gases. The apparatus produces large sodium condensates of up to 3×10^7 atoms by deploying a dark magneto-optical trap that has been loaded from a Zeeman-slowed atomic beam. The goal is to use the sodium gas to sympathetically cool rubidium and explore a new mixture of bosonic atoms. Such mixtures may prove fruitful for synthesizing polar molecules, which have sparked interest due to their possible application to tests of fundamental symmetries [1, 2] and quantum information schemes [3]. Moreover, they may eventually yield a heteronuclear molecular BEC, a novel superfluid with strong dipolar interactions [4, 5, 6].

Recent Progress:

In this first year of funding, we have completed the basic assembly of the apparatus. We have achieved a BEC of sodium atoms using a novel implementation of the "optically plugged" quadrupole magnetic trap (OPT), a hybrid of optical and magnetic forces. After improvements in the evaporation strategy, we can now produce condensates of up to 3×10^7 atoms [7]. This is a factor of 60 enhancement over previous work [8] and is the 3rd largest alkali BEC reported. The simplicity of the OPT (only one pair of electromagnets driven by a single power supply) should facilitate dual species condensation experiments that already possess a high degree of complexity due to the need for duplicate laser and optical setups.

The OPT employs the AC Stark shift of a blue-detuned laser beam (in our case, a 2.5 Watt, 532 nm laser focused to a $\sim 40\mu$m beam waist) to create an energy barrier that repels atoms from the vicinity of the magnetic field zero at the center of the coils. Near this field zero the atoms can be lost by Majorana transitions to an untrapped state. A simple estimate of the AC Stark shift required to suppress Majorana loss suggests that the barrier height U_0 should exceed $\frac{3}{2}k_B T_i$, where T_i is the temperature of atoms at the start of the evaporation process. While previous work [8] only examined barriers of approximately this height, about $k_B \times 350\mu$K, in our work [7] we could produce a BEC using considerably lower barriers of about 60μK (see Fig. 1). One explanation for this is that Majorana loss, which scales with temperature as T^{-2}, becomes significant only at low

T, when the cloud size is small and the atoms have a high probability of encountering the "hole". The small loss at higher temperatures can be overcome by the increase in phase space density due to evaporative cooling. Our results thus point to the versatility of the OPT, and suggest that the AC Stark shift barrier may not need to be as large as what one might expect. Future designs might be able to use a laser whose total power is less than 1 Watt.

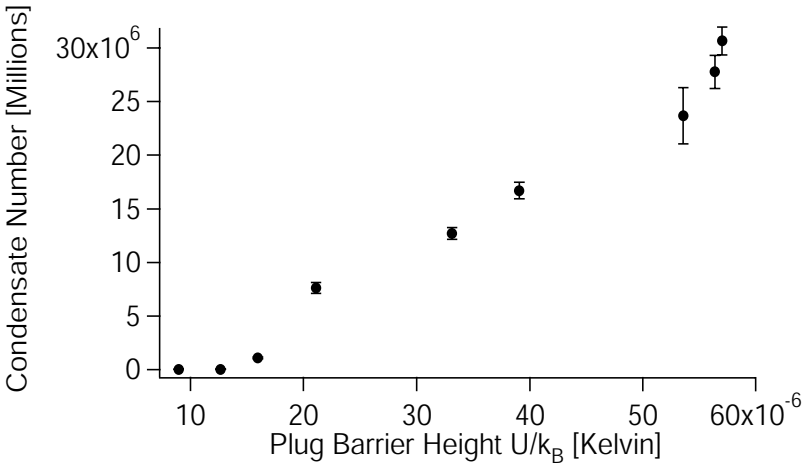

Figure 1: *The effectiveness of "plugging the hole" on evaporative cooling. The final condensate atom number is plotted versus the barrier height, which is proportional to the laser power used. Large condensates were obtained even when the plug is not completely capable of repelling atoms at the highest temperature of* $190\mu K$ *(taken from [7])* .

Finally, we addressed a drawback of the hybrid magnetic and optical trap–the exact potential energy surface depends on the precise laser beam alignment *and* its profile in the wings, parameters which are difficult to control. We demonstrated that the OPT can be used as a "cooling stage" to achieve quantum degeneracy, followed by transfer of atoms (in a procedure similar to [9]) into a purely optical trap formed by a single, focused infrared laser beam. Here the atoms are localized near the intensity *maximum*, where the potential energy surface is well-defined. We have succeeded in transferring nearly 10^7 atoms from the OPT into the optical trap in spite of a significant mode mismatch between the two potentials.

Future Goals:

Our goals are two-fold–to prepare the experiment for simultaneous trapping of sodium and rubidium mixtures, as well as to explore unique features of our sodium BEC in the optically plugged trap. Therefore, we will pursue the following directions:

- **Toroidal BEC**. Most trapping geometries have a harmonic variation about the trap minimum, resulting in a BEC shaped as an ellipsoid. An unusual feature of our OPT is the possibility to create a ring-shaped potential minimum if the laser beam is sufficiently round. We are working to purify the beam profile, and early results are encouraging [10]. We plan to study rotating BECs in a toroidal container, where superfluid flow is predicted to sustain persistent currents (individual quantized vortices which have been observed [11] are not generally stable).

- **Rubidium Trapping**. We plan to begin construction of diode lasers and optics for trapping rubidium, and pursue a dual-species trap. We are examining single, high power laser diodes capable of producing ~ 100 mW via injection locking as well as homemade amplified systems. The latter are based on a commercially available MOPA chip capable of delivering up to 1 Watt of laser power. Since sympathetic cooling with sodium should not involve a significant loss of rubidium, we expect this will be sufficient power to be able to trap $10^7 - 10^8$ Rb atoms in a magneto-optical trap. This will hopefully result in rubidium condensates with an atom number only 1 order of magnitude less than that of the sodium BEC.

Papers and presentations acknowledging DoE support:

- D. S. Naik and C. Raman: *An Optically Plugged Quadrupole Trap for Bose-Einstein Condensates.* Submitted to Physical Review Letters. Available as e-print cond-mat/0406341 (2004).
- Devang Naik, Patrick Bradley, Anthony Liang, and Chandra Raman: *Bose Einstein condensation in an Improved Optical Plug Trap*. Contributed talk at the 35th Meeting of the Division of Atomic, Molecular and Optical Physics, Tucson, Arizona , May 25-29, 2004 (2004 Bulletin of the American Physical Society).
- Devang Naik, Patrick Bradley, Anthony Liang, and Chandra Raman: *Optical Plug Trap*. Poster presentation at the 35th Meeting of the Division of Atomic, Molecular and Optical Physics, Tucson, Arizona , May 25-29, 2004 (2004 Bulletin of the American Physical Society).
- Devang Naik, Patrick Bradley, Anthony Liang, and Chandra Raman: *Bose-Einstein condensation in an Improved Optically Plugged Quadrupole Trap*. Poster presentation at the International Conference on Atomic Physics, Rio de Janeiro, Brazil, July 25-30, 2004 (2004 ICAP Proceedings).

References

[1] J. J. Hudson, B. E. Sauer, M. R. Tarbutt, and E. A. Hinds, Phys. Rev. Lett. **89**, 023003 (2002).

[2] G. Modugno, M. Inguscio, and G. M. Tino, Phys. Rev. Lett. **81**, 47904793 (1998).

[3] D. DeMille, Phys. Rev. Lett. **88**, 067901 (2002).

[4] L. Santos, G. V. Shlyapnikov, P. Zoller, and M. Lewenstein, Phys. Rev. Lett. **85**, 1791 (2000).

[5] S. Yi and L. You, Phys. Rev. A **61**, 041604(R) (2000).

[6] K. Gral, K. Rzazewski, and T. Pfau, Phys. Rev. A **61**, 051601(R) (2000).

[7] D. S. Naik and C. Raman, e-print cond-mat/0406341 (2004).

[8] K. B. Davis, M.-O. Mewes, M. R. Andrews, N. J. v. Druten, D. S. Durfee, D. M. Kurn, and W. Ketterle, Phys. Rev. Lett. **75**, 3969 (1995).

[9] D. M. Stamper-Kurn, M. R. Andrews, A. P. Chikkatur, S. Inouye, H.-J. Miesner, J. Stenger, and W. Ketterle, Phys. Rev. Lett. **80**, 2027 (1998).

[10] C. Raman, talk at DAMOP Conference, Tucson, Arizona 2004. (2004).

[11] J. R. Abo-Shaeer, C. Raman, J. M. Vogels, and W. Ketterle, Science **292**, 476 (2001).

"Atomic Physics Based Simulations of Ultra-cold Plasmas"

F. Robicheaux
Auburn University, Department of Physics, 206 Allison Lab, Auburn AL 36849
(robicfj@auburn.edu)

Program Scope

This theory project focuses on the study of atomic processes that occur in ultra-cold plasmas. We have investigated plasmas in strong magnetic fields and without magnetic fields. The results of our studies of atomic processes in strongly magnetized plasmas are of direct relevance to the two groups (ATHENA and ATRAP) that are attempting to create cold anti-hydrogen. The results of our studies of plasmas without magnetic fields were used to interpret the results from several experimental groups.

Typically, the plasmas (without magnetic fields) we study have electron temperatures between 1 and 100 K, sizes of a few 100 μm, and evolve over time scales of several 10 μs. The main interest is the non-linear interplay between atomic and plasma processes. For example, two free electrons can scatter near an ion so that one becomes captured by the ion and the other gains energy. Thus, a Rydberg atom is formed and energy is released to the free electrons. The Rydberg atom can serve as a heat source for the plasma because other electrons can scatter from the Rydberg atom and drive the atom to more deeply bound states. We find that the huge role played by the Rydberg atoms in the plasma is analogous to that played by dust in dusty plasmas: the evolution of the properties of the Rydberg atoms and the plasma are strongly linked. Our goal with this project was to understand some of the basic and peculiar properties of ultra-cold plasmas and demonstrate how they arise from the non-perturbative coupling of atomic and plasma physics.

During the past year, we have begun studies of ultra-cold plasmas in strong magnetic fields. The motivation for this study is the interplay between the atomic and plasma physics in strong magnetic fields. A further motivation is that recent experiments have claimed the formation of anti-Hydrogen by causing anti-protons to traverse ultra-cold positron plasmas; unfortunately, very little is known about the processes that lead to the anti-Hydrogen formation or about the properties of the anti-Hydrogen atoms. We are in the process of developing ideas and computer programs to understand the basic atomic processes in strong magnetic fields. The processes that will need to be understood include: three body recombination, electron-Rydberg atom scattering, photon emission from Rydberg atoms, motion of Rydberg atoms, and electron-proton scattering. Even crude estimates of some of these processes will greatly improve our understanding about the formation and evolution of Rydberg atoms in strong magnetic fields.

Recent Progress

Interest in the interaction of cold electrons with cold positive ions led us to investigate the phenomena discovered in ultra-cold, neutral plasmas. Experiments performed in S. Rolston's group (NIST), T. Gallagher's group (U of Virginia)/ P. Pillet's group (Orsay), and G. Raithel's group (U of Michigan) showed many

puzzling features; these features were fundamental and showed that often the basic processes were not well understood. Although these experiments did not use a strong magnetic field (like those in the anti-Hydrogen experiments), we felt this would be a good starting problem. Our theoretical studies of this problem resulted in 2 publications [1,2].

Our calculations were able to explain most of the puzzling features in the experiments through a proper understanding of the role played by the formation of Rydberg atoms and their subsequent interaction with electrons in the plasma. We were able to show that the anomalously fast expansion of the plasma at later times could be fully explained by three body recombination with subsequent scattering from the Rydberg atoms. We were able to explain the strange time evolution of the Rydberg atom binding energy in terms of a measurement effect and a rapid heating of the electron part of the plasma at early times. We predicted that the Coulomb coupling parameter (essentially the ratio of potential energy to kinetic energy) should not be high even for the plasmas that start very cold due to the heating from atom formation; this is important because if the Coulomb coupling parameter is large then highly correlated behavior is expected. Measurements, reported in PRL, confirmed our basic prediction. We were able to make detailed comparisons with several measurements: time dependence of the flux of electrons escaping the plasma, the distribution of binding energies for Rydberg atoms as a function of temperature, the time dependence of the number of Rydberg atoms. We predicted several other effects: ion acoustic waves should be frozen into the plasma at later times; there should be a correlation between the speed of the Rydberg atom and its binding energy; and the center of the plasma should be initially hotter than the edges and the time scale for equilibration is longer than would be expected.

We also attempted to simulate the conversion of a Rydberg gas into an ultra-cold plasma in order to understand experiments by Gallagher and Pillet. Our simulations did show a conversion on roughly the time scale seen in the experiments. However, the evolution of our Rydberg gas did not resemble that in the experiments. The Rydberg gas passed through a phase of mostly high angular momentum states that was not seen in the experiments. Recent measurements, published in PRL, are in agreement with our calculation.

We have recently started simulations of atomic processes in strong magnetic fields. We began with the simulation of three body recombination in a strong magnetic field. We have completed the first stage of this study which was published in Phys. Rev. A.[3] Glinsky and O'Neil computed the rate for this process in the limit that the magnetic field strength goes to infinity. In this limit, the electrons can only move along the field and the positive ion is fixed in space. They obtained a rate that was roughly a factor of 10 smaller than the B=0 rate. We noted that in the recent experiments to make anti-Hydrogen the magnetic fields are very large (3 or 5.4 T) but are not in the limit of Glinsky and O'Neil. We performed classical Monte Carlo simulations of the three body recombination rate including next order effects in 1/B. Our simulations allowed the proton to have its full motion while the electron motion was found using the guiding center approximation since the cyclotron orbit of the electron was by far the fastest time scale and smallest length scale. We found

that the recombination rate was roughly 60% higher than in the B=infinity limit for a proton moving slowly through an electron gas.

An important aspect of this project is to provide guidance and understanding for the anti-Hydrogen experiments. We investigated the properties of the atoms formed by three body recombination. Unfortunately, we found that the speed of the anti-atom across the magnetic field line was roughly the transverse speed of the anti-proton before the recombination (this means that the anti-atoms will have a tendency to fly out perpendicular to the trap) and we found that the anti-atoms did not have large dipole moments (this means that the ability to guide the motion of the anti-atoms will be reduced). We did find a feature that may aid the anti-hydrogen experiments: the recombination for an anti-proton moving with a substantial speed along the field becomes substantially reduced when the anti-proton speed becomes comparable to the positron thermal speed. Since the speed of the anti-proton perpendicular to the magnetic field is roughly 1/40 the positron speed, this may allow for a directionality of the recombined anti-Hydrogen.

A much more ambitious study tried to model the motion of the anti-proton through a realistic representation of the trap. In order to do this, we self-consistently solved for the electric potential with a cold positron plasma using the experimental trap geometries and voltages. The simulation included the slowing of the anti-proton due to interaction with plasma waves in the positron cloud, individual scattering with positrons, and capture of positrons and stripping in the trap electric fields. We identified the short time the anti-proton spends in the positron clouds as a dominant effect in the experiments. Detailed calculations are mostly in agreement with all experimental measurements. We were able to obtain additional information about the velocity distribution of the anti-hydrogen and the binding energy distribution. The results are published in Ref. [4]. The results of this study confirmed some of the expectations from Ref. [3]. However, we found that the short time spent in the positron plasma greatly reduced the binding energy compared to expectations. This has major implications for the experiments.

Future Plans

We plan to continue studies of ultra-cold plasmas with no magnetic field. Recent experiments reported by T. Killian's group (Rice Univ.) directly image the position and velocity distribution of the positive ions, setting the stage for detailed measurements. As with our previous studies, we prefer to focus our effort on explaining strange behavior in the experiments and predicting basic processes that could be measured with existing technology.

The main effort will be in understanding atomic and plasma processes in strong magnetic fields. There are several open atomic physics questions that we will address. (1) Classical and quantum mechanical positron scattering from anti-Hydrogen in a strong magnetic field. In both experiments, the anti-Hydrogen is formed in high Rydberg states and collisions with positrons drive it to more deeply bound states. Our current programs approximate this process using classical methods with drift velocity approximation for the positrons. These approximations become unsuitable at deeper binding energies. (2) Direct radiative recombination and radiative cascades in strong magnetic fields. The strong magnetic fields

qualitatively change weakly bound states and the low energy continuum. By performing quantum mechanical calculations, we will obtain the radiative decay rates and branching ratios for a large number of states. From this information, we will model the time required to reach the ground state only by radiative processes. This process is important since both experiments produce highly excited anti-Hydrogen. (3) We will simulate other methods for anti-Hydrogen formation. For example, anti-Hydrogen formation was reported using double charge exchange: a positron collides with a Rydberg atom giving positronium plus an ion then the positronium collides with an anti-proton to give anti-Hydrogen plus an electron. (4) We also hope for more direct interaction with the experimental groups for detailed comparison of calculations and measurements.

The goal for this project is to obtain some immediate results that can aid in the interpretation and understanding of atomic processes in strong magnetic fields. The source of anti-protons will be interrupted soon. There are several other projects for which we have long term plans.

DOE Supported Publications (2002-2004)

[1] F. Robicheaux and J.D. Hanson, Phys. Rev. Lett. **88**, 055002 (2002).
[2] F. Robicheaux and J.D. Hanson, Phys. Plasmas **10**, 2217 (2003).
[3] F. Robicheaux and J.D. Hanson, Phys. Rev. A **69**, 010701 (2004).
[4] F. Robicheaux, Phys. Rev. A **70**, Aug (2004).

Ultrafast Tabletop Laser Pump – X-ray Probe Measurement of Solvated $Fe(CN)_6^{4-}$

Taewoo Lee,[*] Frank Benesch,[**] Yan Jiang,[*] and Christoph G. Rose-Petruck[*]

** Department of Chemistry, Box H, Brown University, Providence, RI 02912*
*** Division of Engineering, Box D, Brown University, Providence, RI 02912*

phone: (401) 863-1533, fax: (401) 863-2594, Christoph_Rose-Petruck@brown.edu

Abstract

Ultrafast laser-pump XAFS-probe measurements of $Fe(CO)_6^{4-}$ in water were performed. $K_4Fe(CN)_6 \cdot 3H_2O$ was solvated in distilled water. The concentration was about 500 mM. An ultrafast laser pulse excited the sample solutions which was subsequently probed by ultrafast x-ray pulses generated in the laser-driven x-ray source. With the sample solution at the focus of an x-ray lens, the total transmission of the x-ray optics and spectrometer was 10^{-7}. With a CCD-camera detection efficiency of 50%, about 50 ph / s were detected behind the liquid sample beam within a 1-keV spectral range around the iron K-edge. The sample solution was excited by 100-μJ, 400-nm pulses with about 100-fs pulse duration. The focus diameter was about 50 μm. The resulting light intensity caused photo-excitation of the solute as well as ionization of the solution. Thus, the induced dynamics does not only comprise ligand substitution, but might also include higher fragmentation of the chemical system. While the chemical compositions of the products have not been determined, the measurements clearly demonstrate the feasibility of such experiments with a table-top x-ray source.

The current experimental setup depicted in Figure 1. An ultrafast laser pulse excited the sample solutions which was subsequently probed by ultrafast x-ray pulses generated in the laser-driven x-ray source. Such a table-top ultrafast x-ray source relies on the interaction of high-intensity laser pulses with a solid target. The laser system produced 4.5-mJ, 800-nm, 50-fs laser pulses on target and simultaneously 400-nm pulses for sample solution excitation. The high-intensity laser pulses were focused onto a brass-coated steel wire at an incidence angle of about 45 degree in p-polarization. The wire speed was 20 mm / s permitting the interaction of each laser pulse with an undamaged surface. The wire target was installed in a helium atmosphere at 1 bar that was rapidly circulated and HEPA-filtered. An off-axis F1.5-parabola was used to focus the laser beam

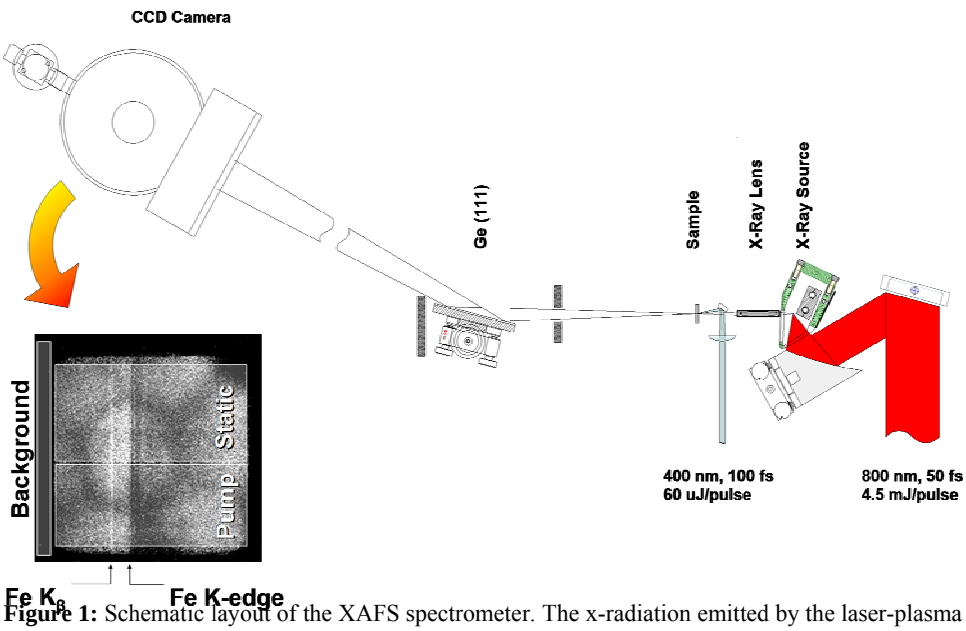

Figure 1: Schematic layout of the XAFS spectrometer. The x-radiation emitted by the laser-plasma is transmitted through the x-ray lens and imaged into the liquid sample. A flat Ge(111) crystal disperses the x-radiation, which is detected by the liquid nitrogen cooled x-ray CCD camera. The 400-nm pump laser pulse overlaps the x-ray beam in the sample jet. A typical CCD image and superimposed regions of interest are shown.

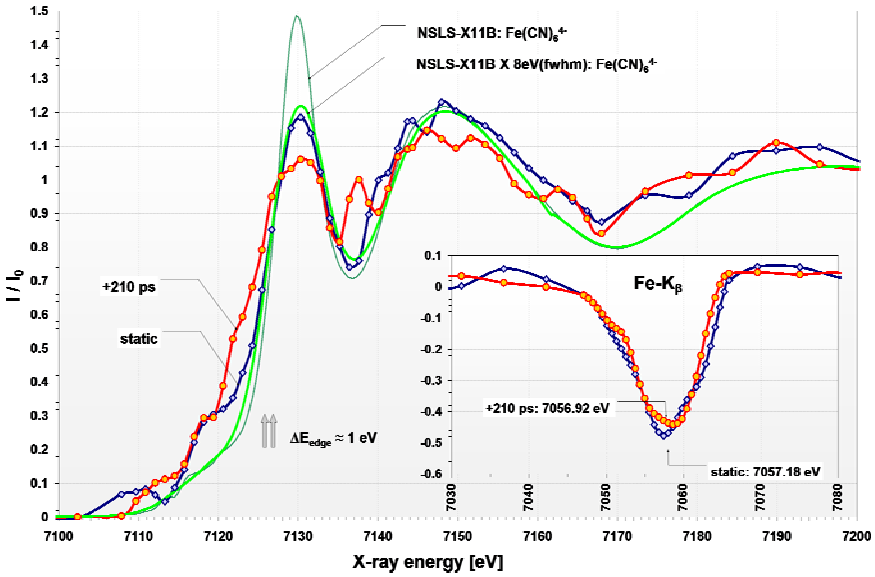

Figure 2: Diamonds: static XANES spectrum measured using the laser plasma x-ray source; Circles: XANES spectrum measured at 210 ps after photoexcitation. Thin solid line: $Fe(CN)_6^{4-}$-spectrum measured at NSLS, beamline X11B. Heavy solid line: $Fe(CN)_6^{4-}$-spectrum measured at NSLS, beamline X11B convoluted with the spectral resolution of the laser-driven x-ray spectrometer.

onto the target. An x-ray flux of 10^9 ph / s 4π within the spectral range from 7 keV to 8 keV was generated. With the sample solution at the x-ray lens focus, the total transmission of the x-ray optics and spectrometer was 10^{-7}. With a CCD-camera detection efficiency of 50%, about 50 ph / s were detected behind the liquid sample beam within a 1-keV spectral range around the iron K-edge. $K_4Fe(CN)_6 \cdot 3H_2O$ was solvated in distilled water. The concentration was about 500 mM. The sample solution was excited by 100-µJ, 400-nm pulses with about 100fs pulse duration. The focus diameter was about 50 µm. The resulting light intensity caused photo-excitation of the solute as well as ionization of the solution. Thus, the induced dynamics does not only comprise ligand substitution, but might also include higher fragmentation of the chemical system. The samples were kept in a light protected container prior to the measurements in order to prevent premature photochemical conversion.

Figure 2 shows the experimental XANES spectra before and 210 ps after photoexcitation. For comparison a XAFS spectrum measured at NSLS, beamline X11B is shown as well. It was convoluted with a Gaussian line shape with a width of 8-eV (fwhm). The resulting curve matches the laser measured spectrum, which implies that the spectral accuracy of our apparatus matches that of a synchrotron source while its precision is currently lower due to its lower spectral resolution. Photoexcitation changes the XANES spectrum. The iron K-edge measured after

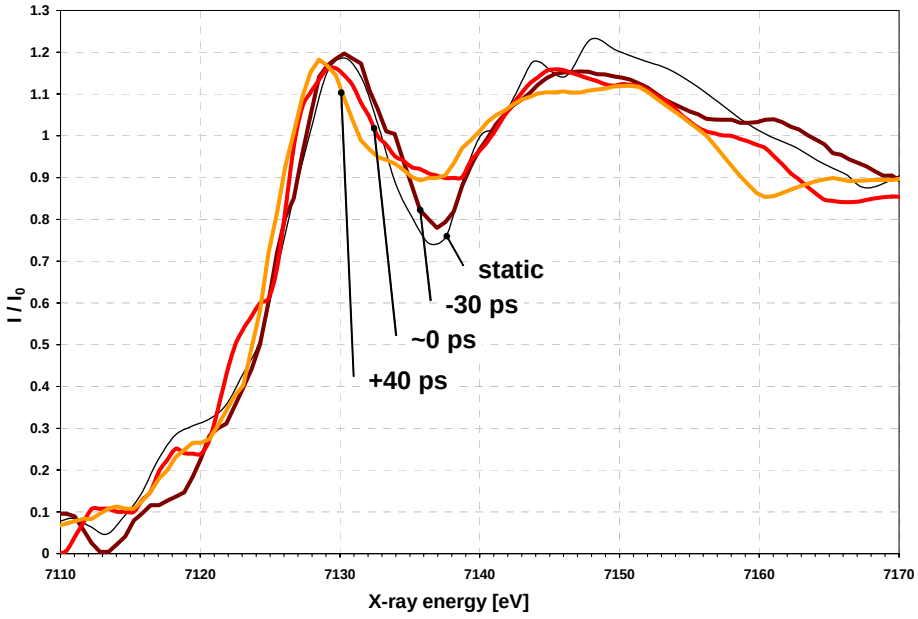

Figure 3: Ultrafast laser-pump XANES-probe spectra of iron hexacyanide (IHC) in water measured at 3 pump-probe delay times using the laser plasma x-ray source. For comparison the static (not-pumped) XANES spectrum is shown as thin line. Time-zero is currently known to within 10 ps.

photoexcitation is 1 eV lower than for that for $Fe^{II}(CN)_6^{4-}$. This observation is not caused by an accidental shift of the entire absorption spectrum as proven by the spectral stability of the iron K_β line. (See the insert of Figure 2) Furthermore, the depth of the XANES modulations decreases, which indicates the destruction of the octahedral symmetry of the iron complex. These measurements were repeated at several pump-probe delays. The results are shown in Figure 3. After photo-excitation, a systematic red-shift of the K-edge is observed as time progresses.

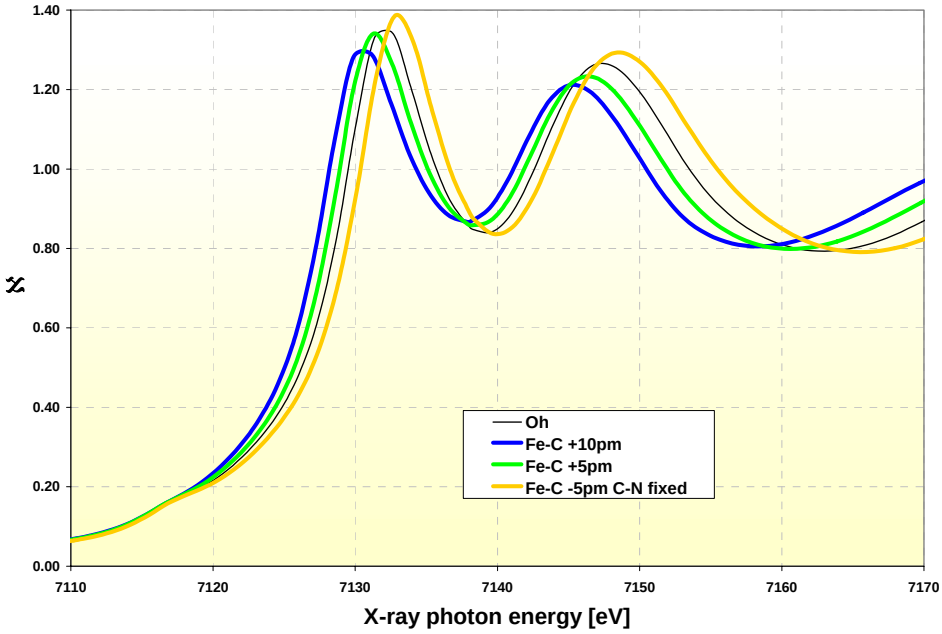

Figure 4: XANES spectra of $Fe(CN)_6^{4-}$ (thin line). Additionally, the XANES spectra at various iron-carbon distances are shown. The C-N distances were held constant.

The K-edge shift suggests that a substantial fraction of the products contains Fe^{I}. However, edge shifts in this system can be caused by oxidation state changes *as well as* metal-ligand bond length changes. As shown in

Figure 4, we simulated this shift through an increase of the iron-ligand distances by less the 10 pm which indicates that the observed XANES spectra reflect an average bond length increase within the excited complex by less then 5%. A conclusive distinction of the effects of oxidation stage and bond length change will be possible with future measurements that cover the entire x-ray spectrum including the EXAFS range. Nevertheless, the measurements clearly demonstrate the feasibility of such experiments with a table-top x-ray source.

The authors gratefully acknowledge partial funding and support for this work by the National Science Foundation, Grant No. CHE-9984890, the U.S. Department of Energy, Award No. DE-FG02-03ER15413, the Research Corporation, Award No. RI0455, and equipment support by Fastpulse Technologies, Inc. This research carried out in part at the National Synchrotron Light Source, Brookhaven National Laboratory, which is supported by the U.S. Department of Energy, Division of Materials Sciences and Division of Chemical Sciences, under Contract No. DE-AC02-98CH10886. The authors thank Dr. Peter Siddons for help during the measurements at NSLS and Ms. Emma Welch for her contributions and help.

D.O.E. grant DE-FG 03-00ER15084

Development and utilization of bright tabletop sources of coherent soft x-ray radiation

Principal Investigators:
Jorge J. Rocca,
Electrical and Computer Engineering Department, Colorado State University, Fort Collins, CO 80523-1373
Telephone: (970)-491- 8514/8371, Fax: 970 (491) – 8671, e-mail: rocca@engr.colostate.edu
Henry C. Kapteyn
JILA/Physics Department, University of Colorado, Boulder, CO 80309-0440
Telephone (303) 492-8198, Fax:(303) 492-5235 , e-mail: kapteyn@jila.colorado.edu
Carmen S. Menoni
Electrical and Computer Engineering Department, Colorado State University, Fort Collins, CO 80523-1373
Telephone: (970)-491- 8659, Fax: 970 (491) – 8671, e-mail: carmen@engr.colostate.edu

Program Description

This project investigates aspects of the development and utilization of compact XUV sources based on fast capillary discharges and high order harmonic up conversion [1,2-3]. These sources are very compact, yet can generate soft x-ray radiation with peak spectral brightness several orders of magnitude larger than a synchrotron beam lines. The work has included the characterization of some of the important parameters that enable the use of these sources in unique applications, such as the degree of spatial coherence and the wavefront characteristics that affect their focusing capabilities. In relation to source development, we have recently conducted preliminary work towards exploring the generation of high harmonics in a *pre-ionized* medium created by a capillary discharge. Since ions are more difficult to ionize than neutral atoms, the use of pre-ionized nonlinear media may lead to the generation of coherent light at > 1 KeV photon energy. Recent application results include the first study of the damage threshold and damage mechanism of XUV mirrors exposed to intense focalized 46.9 nm laser radiation, and the demonstration of nanopatterning of photoresist using a table-top capillary discharge 46.9 nm laser.

Generation of a discharge-ionized plasma channels for high harmonic generation from ions

We have conducted preliminary modeling and experimental work towards the generation of high harmonics in a *pre-ionized* medium created by a capillary discharge. Such pre-ionized nonlinear media may lead to the generation of coherent light at photon energies > 1 KeV. The use of ions as nonlinear media for x-ray generation was first proposed in 1973 [4] ,and HHG in the strongly ionizing regime has been discussed in several works. However, only very recent work at Colorado has both definitively demonstrated that high harmonics can be observed from further ionization of an already fully-ionized gas [2] and has demonstrated that it is possible to apply techniques of quasi-phase matching to the process of HHG [3] . A periodically corrugated hollow fiber was used avoid the destructive interference that would otherwise occur due to a phase-velocity mismatch between the driving laser and the short-wavelength light. Using this method, HHG was demonstrated in Ne at photon energies of ~300 eV, approaching the expected cutoff of 330 eV. This energy range is in the “water window,” of interest for imaging of biological samples. However, in all this work, the ultrashort-pulse laser is doing all the “work” in ionizing the gas. Since the initial ionization generates only low-energy HHG photons, the energy expended in ionization is wasted, reducing the potential conversion efficiency. Using the phase-matched waveguide geometry, ionization-induced absorption is often a very significant limiting mechanism, absorbing as much as 50% of the incident light. Furthermore, ionization-induced defocusing is an even more significant limitation. Also, since the waveguide is a hollow glass tube, at some point the intensity of the driving laser becomes too high to sustain in the waveguide without damaging the walls, ultimately limiting the maximum intensity of the driver beam that can be practically used. The use of a pre-ionized waveguide has the potential to circumvent many of these limitations. High-harmonic generation in laser-generated plasma channels was proposed [5], but not studied experimentally. We plan to investigate the generation and quasi-phase-matched generation of high harmonics of femtosecond Ti:Sa laser pulses (λ=

800 nm) in a plasma waveguide created using an electrical capillary discharge plasma columns with a tailored degree of ionization. In this scheme, an electrical discharge will create a totally ionized medium, where the degree of ionization is selected by the choosing the discharge current pre-ionized plasma channel, through which the high-harmonic driving laser will propagate. This provides access to significantly larger I_p values than those of neutral atoms, contributing to the generation of shorter wavelengths. The driver laser intensity can be significantly increased before tunnel ionization again becomes an important loss. This will result in an increase in the cutoff energy. Driver laser energy loss due to optically-induced ionization is dramatically reduced. This can result in an increase in the efficiency of HHG. Finally, the radial distribution of the electron density profile can be concave, generating an index guide. This allows for a reduced laser intensity at the walls of the capillary, making it possible to guide pulses at the higher intensities required for shorter wavelength HHG, without damage to the walls.

With this objective we have started the development and characterization of a discharge-ionized gas-filled capillary channel in which both the degree of ionization and the electron density profile can be tailored for propagation of an intense ultrashort laser pulse. The amplitude and shape of the discharge current pulse are selected to produce the desired degree of ionization. Also, the discharge is designed to create an electron density profile with minimum electron density on axis and maximum density near the capillary walls, that will constitute an index waveguide for the light. Model simulations and preliminary experiments show that in small capillaries of 150-250 μm diameter filled with gases at pressures of the order of 5-10 Torr, a modest short current pulse with an amplitude of 10-200 A is sufficient to create a plasma columns with mean degree of ionization Z ranging from 1 to 4.

Hydrodynamic simulations

Using a two- temperature one-dimensional Lagrangian code hydrodynamic/atomic code developed at CSU we have predicted the characteristics of the capillary plasmas and the discharge parameters that are required to optimize the degree of ionization and the guiding of intense light for high-harmonic generation. The atomic physics for the ionized gas of interest is self-consistently simulated by

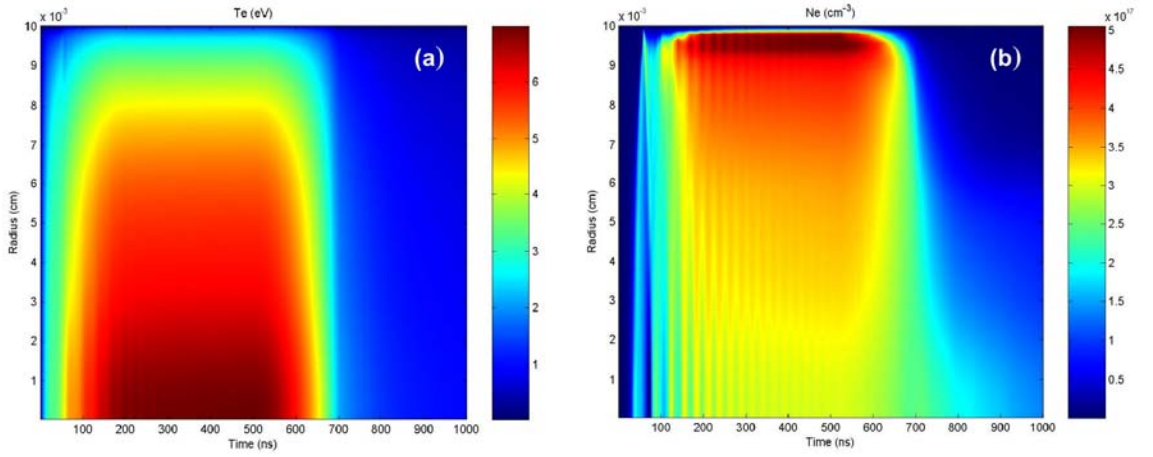

Figure1. Evolution of the radial profile of the electron temperature (a) and electron density (b) for a capillary plasma excited by the current pulse shown in Fig. 1. The capillary radius is 100 μm and the Ar gas pressure is 10 Torr.

computing the population rate equations using a collisional-radiative model that uses a cell approach to model the radiation transport. We have simulated the plasma columns that can be created in small-diameter argon-filled capillaries. Similar results could be obtained for neon and other noble gases of interest of HHG by properly adjusting the discharge parameters to compensate for the differences in ionization energy and transport coefficients. The results presented below correspond to a 200 μm diameter capillary channel filled with 10 Torr of Ar. These conditions are similar to what has been used in

past experiments demonstrating HHG from Argon ions [3]. The gas is assumed to be excited by a 100 A current pulse of 500 ns FWHM duration.The horizontal axis represents the micro- capillary axis and the top of the graph represents the capillary wall.

In this discharge, the ohmic dissipation produced by the current pulse heats the free electrons and creates an azimuthal magnetic field. If the self-generated magnetic field is large enough for the magnetic pressure to overcome the kinetic pressure of the electrons and ions, the plasma column compresses. However, in the relatively low current discharge of interest here, the dynamics of the plasma are dominated by ohmic heating and heat conduction losses.

Shortly after the initiation of the current pulse the plasma is observed to expand as a result of the of the larger temperature increase in the axial region of the plasma zones due to ohmic heating. The outer zones remain colder due to heat conduction to the capillary walls. This generates a radial electron temperature profile with maximum on axis and minimum at the capillary wall, as illustrated in Fig.1b. The electron temperature on axis is computed to approach 7 eV, while it remains several eV cooler in the periphery. With this temperature profile the plasma pressure of the inner zones exceeds the sum of the pressure of the outer most zones plus the magnetic pressure, resulting in the expansion of the plasma seen in Fig. 1b. Rapid initial radial oscillations in the plasma density are damped by the viscosity of the plasma. After about 300 ns the plasma reaches steady state, and the electron density distribution remain relatively constant until the end of the current pulse, when the plasma cools and recombines.

Figure 2 shows the radial lineout of the electron density 500 ns after the initiation of the current pulse when all plasma parameters have reached steady-state. This concave electron density profile with minimum electrons density on axis gives origin to an index of refraction distribution with maximum on axis, which guides the laser light. Fig. 3 shows the computed radial variation of the mean degree of ionization of the plasma for a 200 A discharge. The mean ion charge, Z, is predicted to increase with time to reach Ar IV (Z=3) at the axis about 300 ns after the beginning of the current pulse. Ar IV has an ionization potential of 59.8 eV. Moreover, the degree of ionization of the plasma can be tailored by changing the amplitude of the current pulse.

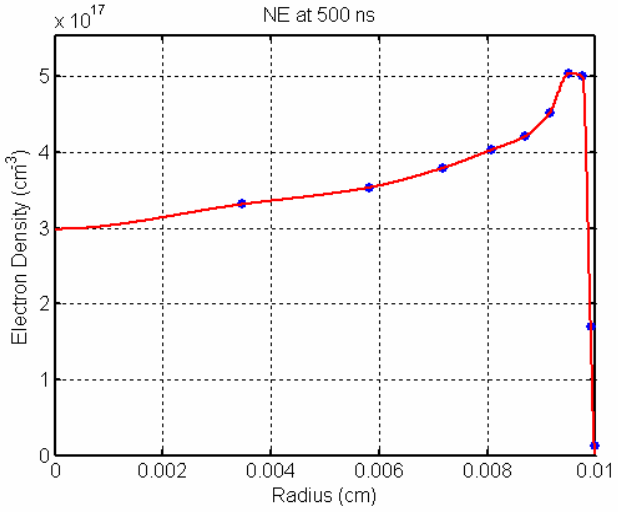

Figure2. Radial lineout of the electron density profile at 500 ns after the initiation of the current pulse. The concave nature of the profile constitutes an index waveguide that can guide the laser light with decreased interaction with the walls.

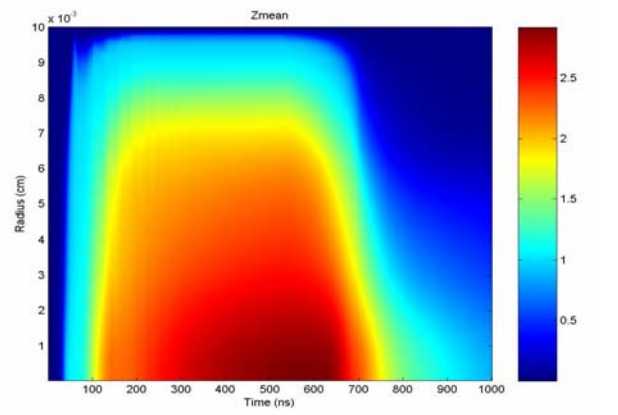

Figure 3. Computed variation of the mean degree of ionization as a function of time. The capillary diameter is 200 μm , and the gas is Ar at an initial pressure of 10 Torr. The shape of the current pulse is that shown in Fig. 1 and the peak amplitude 200A. At 500 ns after the beginning of the current pulse the dominant ions species are Ar III and Ar IV.

Preliminary experiment

While the discharge excitation parameters required are quite modest the generation of plasmas in such narrow capillaries with relatively fast current pulses can impose some challenges. We conducted a tests of plasma generation by pulse-discharge excitation into a 5 cm long capillary channel 200 micrometers in diameter, filled with Ar pressures between 5 and 10 Torr. Plasmas were excited by current pulses of about 500 ns duration and amplitudes ranging from 10 A to 100 A. The light emitted by the discharge over the visible and ultraviolet range was analyzed with a 0.6 meter spectrograph to characterize the degree of ionization. Figure XX shows the relative intensity of lines from Ar I, Ar II and Ar III spectra as a function of capillary discharge current for discharge currents of 50, 70 and 100 A. The data shows it is possible to select the degree of ionization by controlling the discharge current.

Future plans During the next year of the project we plan to develop a discharge capable of operating at a high repetition rate (> 100Hz, with the ultimate goal of reaching 1 KHz by the end of the project). We will subsequently explore the generation of high harmonic from ions in this waveguide.

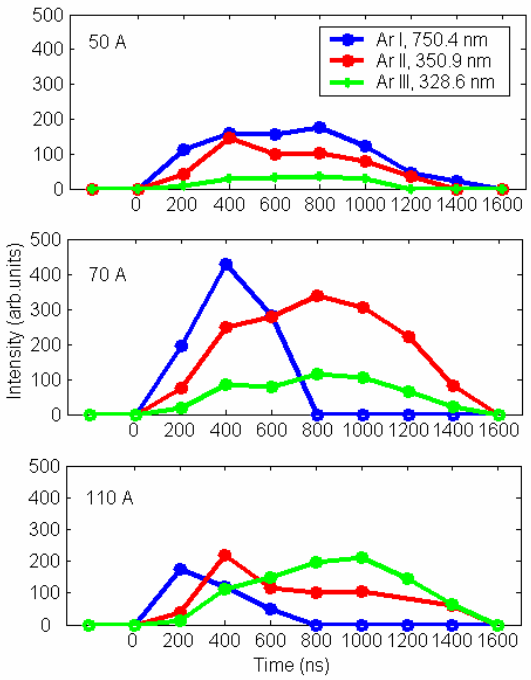

Fig 4. Temporal evolution of the intensity of Ar I, Ar II and Ar III lines in a 200 um diameter capillary discharge plasma for three different discharge currents. The data shows the degree of ionization can be selected by adjusting the discharge current.

References

1. B. R. Benware, C. D. Macchietto, C. H. Moreno, and J. J. Rocca, *Phys. Rev. Lett.* **81**, 5804 (1998); Y. Liu, M. Seminario, F.Tomasel, et al. *Phys. Rev. A***, 63** 033802, (2001).
2. E. A. Gibson, A. Paul, N. Wagner, et al., *Physical Review Letters*, vol. TBP, 2004.
3. E. A. Gibson, A. Paul, N. Wagner, et al., *Science*, vol. 302, pp. 95-98, 2003 ; A. Paul, R. A. Bartels, R. Tobey, et al., *Nature*, vol. 421, pp. 51-54, 2003.
4. S. Harris, *Physical Review Letters*, vol.31, 341-345, 1973
5. C. G. Durfee and H. M. Milchberg, *Phys. Rev Lett.* , vol. 71, pp. 2409-2412, 1993.

Publications

1. M. Grisham, G. Vaschenko, C.S. Menoni, J.J. Rocca et al. “Damage of Extreme Ultraviolet Sc/Si multilayer Mirrors Exposed to Intense 46.9 nm Laser Pulses”, *Optics Letters*, **26**, 620, (2004)
2. G. Vaschenko et al. “Damage threshold and damage mechanism of Sc/Si multilayer mirrors exposed to intense ns 46.9 nm laser pulses. “, in “X-Ray Lasers 2004”, Int.of Phys. (2004) , in press.
3. L. Juha et al. “Short –wavelength ablation of solids: pulse duration and wavelength effects”. SPIE vol 5534, (2004), in press.
4. Yu.P. Pershin et al. “Structural changes on Sc/Si multilayer mirror under irradiation with intense 46.9nm laser pulses”. Journal of Appl. Phys. submitted (2004)
5. S. Le Pape, Ph. Zeitoun, M. Idir, P. Dhez, J.J. Rocca**,** and M. François, “Electromagnetic field distribution measurements in the soft x-ray range: full characterization of a soft x-ray laser beam”, *Phys. Rev. Lett.* **88**, 183901 (2002)
6. Y. Liu, M. Seminario, F. G. Tomasel, C. Chang, J. J. Rocca and D. T. Attwood, “Achievement of Essentially Full Spatial Coherence in a High Average Power Soft X-Ray Laser,” *Phys. Rev. A*, **63,** 033802, (2001).

New Directions in Intense-Laser Alignment

Tamar Seideman
Department of Chemistry, Northwestern University
2145 Sheridan Road, Evanston, IL 60208-3113
seideman@chem.northwestern.edu

1. Program Scope

This is a new program, to be initiated in September 2004. The goal of the research is to introduce two new directions in the area of intense laser alignment and explore them theoretically and numerically. The first part of the research will extend the concepts of alignment and three-dimensional alignment from the isolated molecule limit to condensed phase environments. Potential applications of the extended scheme include the control of charge transfer reactions, the design of a new form of molecular switches, the introduction of a new approach for probing the properties of dissipative environments, and the development of an approach to guided molecular assembly, which could enhance the performance of devices such as field-effect transistors and nano-sensors.

The second part of the proposed research will extend the theory of rotational revivals from linear systems to molecules of arbitrary symmetry and explore implications to experiments that are currently being set up. Potential applications of the extended theory include a new route to racemate separation, a laser-based approach to nano-scale processing of surfaces, an improved technique for time-domain determination of molecular structure, and a route to coherently-driven molecular machines.

2. Background and Recent Progress

Aligning molecules has been an important goal of modern reaction dynamics for over 3 decades.[1] The intense laser approach to molecular alignment, proposed[2,3] in 1995, has been the topic of increasingly intensive experimental[4–14] and theoretical[2,3,11–26] interest in the past five years. A review of the theory underlying intense laser alignment, its experimental observation and its applications is given in Ref. 27. It is exciting to note that, although Ref. 27 has appeared only recently, the rapid development of the field makes the review nearly outdated.

The qualitative physics underlying intense-laser alignment is simple and general.[2] Consider a linear molecule subject to a linearly polarized, pulsed laser field and assume first

that the frequency is tuned near resonance with a vibronic (or a vibrational) transition. In the weak field limit, if the system has been initially prepared in a rotational level J_0, electric dipole selection rules allow J_0 and $J_0 \pm 1$ in the excited state. The interference between these levels gives rise to a mildly aligned excited state population. At nonperturbative intensities, the system undergoes Rabi-type oscillations between the two resonant states, exchanging another unit of angular momentum with the field on each transition. Consequently, a rotationally-broad wavepacket is produced in both states. The associated alignment is considerably sharper than the weak-field distribution, as it arises from the interference of many levels.[2,15] Rather similar coherent rotational excitation dynamics takes place at far-off resonance frequencies. In this case a rotationally-broad superposition state is produced via sequential Raman-type ($|\Delta J| = 0, 2$) transitions, the system remaining in the ground vibronic state.[18] Depending on the molecule and the frequency, both mechanisms may simultaneously contribute.

The properties of the rotational wavepacket are very similar in the near- and far-off-resonance frequency regimes. The crucial parameter that determines the wavepacket composition, and hence the ensuing alignment, is the duration of the pulse turn-on and turn-off.[18] In the case of a long pulse (long as compared to the rotational periods, $\tau_{\rm rot}$), each eigenstate of the field-free Hamiltonian is guaranteed to evolve adiabatically into the corresponding state of the complete Hamiltonian during the turn-on, returning to the original (isotropic) field-free eigenstate upon turn-off. Thus, in the long pulse limit laser alignment reduces to the problem of alignment in a strong DC field. An obvious drawback of adiabatic alignment is that the alignment is lost once the laser pulse is turned off. For the majority of applications one desires field-free aligned molecules.

Reference 2 proposed and illustrated theoretically and numerically the possibility of retaining the field-induced alignment after turn-off of the laser pulse, through nonadiabatic rotational excitation. A short laser pulse, $\tau < \tau_{\rm rot}$, leaves the system in a coherent superposition of rotations that is aligned upon turn-off, dephases at a rate proportional to the square of the wavepacket width in J-space, and subsequently rephases. Interestingly, under rather general conditions, the alignment is significantly enhanced after turn-off of the laser pulse.[15] A first experimental realization of the theory of Ref. 15, reported in Ref. 6, was followed more recently by quantitative experimental demonstrations in several laboratories.[7,8,12]

A third mode of alignment is introduced in Ref. 16 in the context of simultaneous alignment and focusing of molecular beams, potentially a route to nanoscale surface processing.[28] To that end the combination of a long turn-on with a rapid turn-off is necessary. During the turn-on the molecular system evolves into an eigenstate of the complete Hamiltonian—an aligned many-J superposition. Upon rapid turn-off the wavepacket

components are phased together to make the full Hamiltonian eigenstate but now evolve subject to the field-free Hamiltonian. The wavepacket dephases at a rate determined by the intensity and subsequently rephases. This third (in fact hybrid) mode of alignment was recently observed in two laboratories.[9,10]

Our recent research in this area has introduced the concept of rotational revivals,[15] extended alignment from one to three dimensions through use of elliptically polarized fields,[11] and developed and applied a formalism for study of nonadiabatic alignment of complex (asymmetric top) polyatomics.[12–14] Most of our work in the polyatomic domain has been carried out in collaboration with the experimental group of H. Stapelfeldt in Aarhus.[11–14]

3. Future Plans

One of our goals in future research in this field is to extend the concepts of alignment and three-dimensional alignment from the isolated molecule limit to dissipative media. Both the case of solutions and that of gas cells are of interest. Potential applications in the former environment include study and manipulation of charge transfer reactions with application to molecular switches, and guided molecular assembly with application in the design and fabrication of molecule-based devices. In the latter environment we envision applications including quantum storage and laser control of bimolecular collisions. In both media one may expect rotational coherences to furnish new views of the dissipative properties of interesting solvents, complementary to the insights gained through study of the dissipation of vibrational coherences.

A second goal of the research is to extend the concept of rotational revivals from linear molecules to systems of arbitrary symmetry. The fundamental interest in the revival structure of asymmetric molecules is immense; its richness traces to the instability of the rotations of asymmetric tops. Among many potential applications, several of which we hope this research will inspire, we mention the use of intense lasers to enhance the signals of rotational coherence spectroscopy and NMR spectroscopy, and the application of laser-oriented molecules to enable the realization of light-driven molecular rotors based on coherent two-pulse excitation.[30]

The first goal will be accomplished by means of a combination of standard classical molecular dynamics simulations with a quantum mechanical density matrix formulation, currently under development in our group. The second goal will be accomplished by application of our existing formalism of asymmetric top molecules subject to fields of arbitrary polarization,[12–14] requiring only numerical extension of the codes to make optimal use of supercomputers.

[1] See, for instance, (a)D. P. Pullmann, B. Friedrich and D. R. Herschbach, J. Chem. Phys. **93**, 3224 (1990); H. J. Loesch and J. Remscheid, J. Chem. Phys. **93**, 4779 (1990); M. Wu, R. J. Bemish, and R. E. Miller, J. Chem. Phys. **101**, 9447 (1994). (b) P. R. Brooks, J. S. McKillop, and H. G. Pippin, Chem. Phys. Lett. **66**, 144 (1979); S. Stolte in *Atomic and Molecular Beam Methods*, G. Scoles editor, (Oxford University, New York, 1988), p. 631; V. A. Cho and R. B. Bernstein, J. Phys. Chem. **95**, 8129 (1991). (c)V. Aquilanti, D. Ascenzi, D. Cappelletti, F. Pirani, Nature **371**, 399 (1994).
[2] T. Seideman, J. Chem. Phys. **103**, 7887 (1995).
[3] B. Friedrich and D. R. Herschbach, Phys. Rev. Lett. **74**, 4623 (1995).
[4] W. Kim and P.M. Felker, J. Chem. Phys. **107**, 2193 (1997).
[5] J. J. Larsen *et al.*, J. Chem. Phys. **111**, 7774 (1999).
[6] F. Rosca-Pruna and M. J. J. Vrakking, Phys. Rev. Lett. **87**, 153902 (2001).
[7] R. A. Bartels *et al.*, Phys. Rev. Lett. **88**, 013903 (2002).
[8] H. Sakai *et al.*, submitted for publication in Phys. Rev. Lett.
[9] I.V. Litvinyuk *et al.*, Phys. Rev. Lett. **90**, 233003 (2003).
[10] J.G. Underwood *et al.*, Phys. Rev. Lett. **90**, 223001 (2003).
[11] J. J. Larsen, K. Hald, N. Bjerre, H. Stapelfeldt and T. Seideman, Phys. Rev. Lett. **85**, 2470 (2000).
[12] E. Peronne, M.D. Poulsen, C.Z. Bisgaard, H. Stapelfeldt and T. Seideman, Phys. Rev. Lett. **91**, 043003 (2003).
[13] M.D. Poulsen, E. Peronne, C.Z. Bisgaard, H. Stapelfeldt E. Hamilton and T. Seideman, J. Chem. Phys. **121**, 783 (2004).
[14] E. Péronne, M.D. Poulsen, H. Stapelfeldt, C.Z. Bisgaard, E. Hamilton, and T. Seideman, submitted for publication in Phys. Rev. A
[15] T. Seideman, Phys. Rev. Lett. **83**, 4971 (1999).
[16] Z.-C. Yan and T. Seideman, J. Chem. Phys. **111**, 4113 (1999).
[17] T. Seideman, J. Chem. Phys. **111**, 4397 (1999).
[18] T. Seideman, J. Chem. Phys. **115**, 5965 (2001).
[19] C. M. Dion, A. Keller, O. Atabek, and A. D. Bandrauk, Phys. Rev. A **59**, 1382 (1999).
[20] J. Ortigoso, M. Rodriguez, M. Gupta and B. Friedrich, J. Chem. Phys. **110**, 3870 (1999).
[21] P. Van Leuven, M. Malvaldi and M. Persico, J. Chem. Phys. **116**, 538 (2002).
[22] C. M. Dion, A. D. Bandrauk, O. Atabek, A. Keller, H. Umeda and Y. Fujimura, Chem. Phys. Lett. **302**, 215 (1999).
[23] I. Sh. Averbukh and R. Arvieu, Phys. Rev. Lett. **87**, 163601 (2001).
[24] M. Machholm and N. E. Henriksen, Phys. Rev. Lett. **87**, 193001 (2001).
[25] N. E. Henriksen, Chem. Phys. Lett. **312**, 196 (1999).
[26] S. Guerin, L. P. Yatsenko, H. R. Jasulin, O. Faucher, and B. Lavorel, Phys. Rev. Lett. **88**, 233601 (2002).
[27] For a recent review of the theory underlying intense laser alignment, its experimental observation and its applications see H. Stapelfeldt and T. Seideman, Rev.Mod.Phys. **75**, 543 (2003).
[28] T. Seideman, Phys. Rev. A **56**, R17 (1997).
[29] T. Seideman, J. Chem. Phys. **113**, 1677 (2000).
[30] Y. Fujimura *et al.*, Chem. Phys. Lett. , submitted.

Inner-shell electron spectroscopy and chemical properties of atoms and small molecules

T. Darrah Thomas, Principal Investigator
T.Darrah.Thomas@oregonstate.edu

Department of Chemistry
153 Gilbert Hall
Oregon State University
Corvallis, OR 97331-4003

Program scope

Many chemical phenomena depend on the ability of a molecule to accept (or donate) charge at (or from) a particular site in the molecule. Examples are acidity, basicity (proton affinity), rates and regiospecificity of electrophilic reactions, hydrogen bonding, and ionization. Among these, inner-shell ionization spectroscopy (ESCA or x-ray photoelectron spectroscopy) has proven to be a useful tool for investigating how a molecule responds to added or diminished charge at a particular site. The technique is element specific and is applicable to all elements except hydrogen. It is, in many cases site specific. As a result, x-ray photoelectron spectroscopy (XPS) can probe all of the sites in a molecule and identify the features that cause one site to have different chemical properties from another. In addition, the inner-shell ionization energies, as measured by XPS, provide insight into the charge distribution in the molecule – a property of fundamental chemical importance.

During the last 35 years, inner-shell electron spectroscopy has been a source of much useful chemical information. Until recently, however, the investigation of the carbon 1s photoelectron spectra of hydrocarbons (or the hydrocarbon portion of molecules containing a heteroatom) has been hampered by lack of resolution. Carbon atoms with quite distinct chemical properties may have carbon 1s ionization energies that differ by less than 1 eV, whereas historically the available resolution has been only slightly better than this. In addition, the vibrational excitation accompanying core ionization adds complexity to the spectra that has made analysis difficult.

The availability of third-generation synchrotrons coupled with high-resolution electron spectrometers has made a striking difference in this situation. It is now possible to measure carbon 1s photoelectron spectra with a resolution of about half the natural line width (~100 meV), with the result that recently measured carbon 1s spectra in hydrocarbons show a richness of chemical effects and vibronic structure.

During the last seven years this program has endeavored to exploit this capability in order to investigate systems where new features can be revealed by high-resolution carbon 1s photoelectron spectroscopy. The primary goal has been to determine carbon 1s ionization energies not previously accessible in order to use the relationships between these energies and other chemical properties to elucidate the chemistry of a variety of systems. Early work focused on understanding the features of the spectra: line shape, line width, vibrational structure, and vibronic coupling, since understanding these features is essential to unraveling the complex spectra that are found for molecules having several carbon atoms. Now that these features are (more or less) understood, emphasis has shifted to investigation of chemically significant systems and to gaining further insights into the relationships between core-ionization energies and chemical properties.

Recent progress (2002-2004)

Inner-shell lifetimes. The ultimate factor that determines the highest possible resolution for inner-shell spectroscopy is the lifetime of the core hole. For 1s holes in first-row elements and 2p holes in second-row elements this is determined primarily by the Auger transition rate. In these cases, the Auger process involves valence electrons, and it is expected that chemical effects that influence the valence electron density will also influence the core-hole lifetime. For instance, theoretical calculations predict a significant difference between the carbon 1s lifetimes in CH_4 and CF_4 because of the difference in valence charge density at the carbon. The electronegative fluorine atoms withdraw valence electrons from the central carbon atom, making them less available for Auger decay. As a consequence, the Auger lifetime is expected to be longer and the natural linewidth narrower in CF_4 than in CH_4. Similar effects are predicted for CO and CO_2. Verification of these predictions has been a major goal during the first few years of this program. The results of a number of studies are summarized in a paper published in 2002.[1] The essential conclusion of these investigations is that the chemical effects on inner-shell lifetimes are significantly smaller than has been predicted by simple theory. For instance, the natural line widths of CH_4, HCCH, CH_3CH_3, CO, and CO_2 are all within about 5 meV of 100 meV (where 5 meV is approximately the uncertainty of the measurements). Only CF_4, with a measured linewidth of 77 meV, shows a significant chemical effect. The reason for the lack of a chemical effect is not understood and remains a problem for theoretical investigation.

By contrast, very pronounced chemical effects on the inner-shell linewidth are seen in the 2p photoelectron spectra of SiH_4 and SiF_4.[2] For SiH_4, the silicon 2p linewidth is found to be 38 meV, in approximate agreement with the predictions of simple theory, whereas for SiF_4 the linewidth is 79 meV, or about 5 times the predicted value. It is thought that this anomalously large linewidth for SiF_4 arises from the valence electrons on the fluorine atoms contributing to the Auger decay through interatomic transitions. Such effects were expected to be very small and were not included in earlier calculations of Auger transition rates.

Calibration of electron spectra. For accurate measurement of inner-shell ionization energies it is useful to have a set of accurately known ionization energies that can be used for calibration. A sample whose ionization energy is unknown can be measured simultaneously with one whose energy is known. Then effects due to uncertainty in the photon energy or variation in the plasma potential can be eliminated. For this purpose, measurements of carbon 1s ionization energies for nine compounds have been measured with an accuracy of 0.03 meV.[3] These range from ethane (290.545 eV) to tetrafluoromethane (301.898 eV) and encompass almost the full range over which carbon 1s ionization energies are found. Particularly useful are the measurements for carbon dioxide and tetrafluoromethane, since these have very simple spectra and have ionization energies that fall outside the range of those of most other carbon-containing compounds.

It is also necessary to have a convenient calibration source for the electron-energy analyzer, in order to know the absolute kinetic energy that is being measured, to know the accurate step size per energy interval, and to know the linearity of the energy scale. The xenon $L_{4,5}OO$ Auger spectrum provides 19 lines at low kinetic energy that are useful for this purpose. A paper reporting accurate energies for these lines was published in 2002.[4]

Inner-shell ionization energies and electronegativity. Inner-shell ionization energies reflect the charge distribution in a molecule. A ligand that withdraws electrons from the atom of interest causes an increase in the ionization energy. As a result, core-ionization energies correlate

well with ligand electronegativities. For instance, the carbon 1s ionization energies of the halomethanes ($C_{4-n-m}X_nY_m$; X, Y = F, Cl, Br, I) correlate nearly linearly with the sum of the electronegativities of the halogens.[5] Although a correlation is not surprising, linearity is. The linearity appears to result from a combination of effects, all relating to the size of the halogen, which in turn influences the effect of charge withdrawal by the ligand as well as the polarizibility of the ligand.

The linear correlation between core-ionization energies and electronegativity can be used to assign electronegativities to substituent groups. For instance, the carbon 1s ionization energy of CH_3CF_3 together with the carbon 1s ionization energies of CH_4 and CH_3F and the known electronegativities of hydrogen and fluorine can be used to give the electronegativity of CF_3. This technique has recently been used to investigate the electronegativities of CF_3, SF_5, and OSO_2F.[6,7]

Six-carbon cyclic hydrocarbons. The series of molecules cyclohexane, cyclohexene, 1,3- and 1,4-cyclohexadiene, and benzene illustrate a striking change in chemical properties. At one extreme, cyclohexane, the molecule is saturated and relatively unreactive. The intermediate members are unsaturated and reactive, and the final member, benzene, is aromatic and, again, relatively unreactive. With the high-resolution capabilities of the ALS it has been possible to measure carbon 1s photoelectron spectra of these molecules with sufficient resolution that the contributions from the chemically inequivalent carbons can be determined. A paper describing the vibrational structure in these spectra and reporting the carbon 1s ionization energies is in press.[8] A subsequent paper will deal with the chemical implications of these results.

1. T. X. Carroll, K. J. Børve, L. J. Sæthre, J. D. Bozek, E. Kukk, J. A. Hahne, and T. D. Thomas, *J. Chem. Phys.* **116**, 10221 (2002).

2. T. D. Thomas, C. Miron, K. Wiesner, P. Morin, T. X. Carroll, and L. J. Sæthre, *Phys. Rev. Lett.*, **89**, 223001 (2002).

3. V. Myrseth, J. D. Bozek, E. Kukk, L. J. Sæthre, and T. D. Thomas, *J. Electr. Spectrosc. Relat. Phenom.*, **122**, 57 (2002).

4. T. X. Carroll, J. D. Bozek, E. Kukk, V. Myrseth, L. J. Sæthre, T. D. Thomas, and K. Wiesner, *J. Electr. Spectrosc. Relat. Phenom.*, **125**, 127 (2002).

5. T. D. Thomas, L. J. Sæthre, K. J. Børve, J. D. Bozek, M. Huttula, and E. Kukk, *J. Phys. Chem.* A **108**, 4983 (2004).

6. J. E. True, T. D. Thomas, R. W. Winter, and G. L. Gard, *Inorg. Chem.* **42**, 4437 (2003).

7. C. Leibold, H. Oberhammer, T. D. Thomas, L. J. Sæthre, R. Winter, and G. L. Gard, *Inorg. Chem.* **43**, 3942 (2004).

8. V. M. Oltedal, K. J. Børve, L. J. Sæthre, T. D. Thomas, J. D. Bozek, and E. Kukk, *Physical Chemistry Chemical Physics PCCP*, in press, 2004.

Future plans

Focus during the future will be on measurements of carbon 1s photoelectron spectra that will give further insights into chemistry and, in particular, group electronegativity. Although the relationship between electronegativity and ionization energy is approximately linear, there is also a significant quadratic behavior that appears to reflect the polarizibility of the ligand. In addition, the presence of a second type of ligand modifies the effect of the first one. Some typical series of compounds that will be of interest are indicated below. Compounds that are underlined will be the target of new measurements, the others having been measured already.

Electronegativity of the methyl group: CH_4, CH_3CH3, $CH_3CH_2CH_3$, $(CH_3)_3CH$, $\underline{C(CH_3)_4}$.

Electronegativity of ethyl, ethenyl, and ethynyl groups and their interactions: $CH_3CH_2CH_3$, $(CH_3CH_2)_2CH_2$, $CH_2{=}CHCH_3$, $(CH_2{=}CH)_2CH_2$, $HC{\equiv}CCH_3$, $HC{\equiv}CCH_2CH_2CH_3$, $HC{\equiv}CCH_2CH{=}CH_2$.

Interaction of halogens with alkyl groups: $CH_2{=}CHCH_2F$, $CH_2{=}CHCH_2I$, $CH_3CH_2CH_2I$, CH_3CHICH_3, $CH_3CH_2CH_2F$, $CH_3CH_2CH_2CH_2F$, $CH_3CHFCH_2CH_3$, $(CH_3)_3CF$, $(CH_3)_3CCl$, $CH_3CF_2CH_3$, $CH_3CHBrCH_3$.

Transmission of inductive effects through a conjugated chain. $CH_3CH{=}CH_2$, $CH_3CH{=}CHCH{=}CH_2$.

Further studies of interactions of halogens: CF_3Br, CF_2Br_2, CF_2I_2, CI_4.

Further studies of CF_3: $CF_3CH_2CF_3$.

Substituents effects in benzene: benzene, toluene, xylene (o, m, and p), mesitylene, 1,2,4,5-tetramethylbenzene.

Publications involving DOE support, 2002-2004

Carbon 1s photoelectron spectroscopy of CF_4 and CO: Search for chemical effects on the carbon 1s hole-state lifetime, T. X. Carroll, K. J. Børve, L. J. Sæthre, J. D. Bozek, E. Kukk, J. A. Hahne, and T. D. Thomas, *J. Chem. Phys.* **116**, 10221 (2002).

Adiabatic and vertical ionization energies in representative small molecules, V. Myrseth, J. D. Bozek, E. Kukk, L. J. Sæthre, and T. D. Thomas, *J. Electr. Spectrosc. Relat. Phenom.*, **122**, 57 (2002).

Xenon $N_{4,5}OO$ Auger spectrum – a useful calibration source, T. X. Carroll, J. D. Bozek, E. Kukk, V. Myrseth, L. J. Sæthre, T. D. Thomas, and K. Wiesner, *J. Electr. Spectrosc. Relat. Phenom.*, **125**, 127 (2002).

Carbon 1s photoelectron spectroscopy of halomethanes. Effects of electronegativity, hardness, charge distribution, and relaxation, T. D. Thomas, L. J. Sæthre, K. J. Børve, J. D. Bozek, M. Huttula, and E. Kukk, *J. Phys. Chem.* A **108**, 4983 (2004).

Carbon 1s photoelectron spectroscopy of six-membered cyclic hydrocarbons, V. M. Oltedal, K. J. Børve, L. J. Sæthre, T. D. Thomas, J. D. Bozek, and E. Kukk, *Physical Chemistry Chemical Physics PCCP*, in press, 2004.

Quantum Dynamics of Ultracold Fermionic Vapors

Grant #DE-FG02-01ER15205
Report for the Period: 11/1/03-10/31/04

John E. Thomas
Physics Department, Duke University
Durham, NC 27708-0305
e-mail: jet@phy.duke.edu

1. Scope

The purpose of this program is to study collective quantum dynamics of a mechanically driven ultracold gas of ^{6}Li fermions, contained in an ultrastable CO_2 laser trap. In the vicinity of a Feshbach resonance, mixtures of the two lowest hyperfine states of ^{6}Li are strongly interacting: S-wave scattering interactions are magnetically tunable from zero to strongly attractive or strongly repulsive. Hence, this two-component mixture is particularly well suited for exploring fundamental interactions in Fermi gases. Pairing interactions in this system are predicted to lead to a Fermi superfluid phase which is an atomic gas analog of a very high temperature superconductor. Since the interaction strength and density can be experimentally controlled, the system is ideally suited to study fundamental new features of spin pairing and superconductivity.

2. Recent Progress

During the past year, we concentrated on collective excitations and achieved a major break through: We obtained the first evidence for superfluid hydrodynamics in a strongly interacting Fermi gas [1]. We excited the radial breathing mode in the gas and measured both the frequency of the mode and the damping time as a function of temperature and magnetic field. Prior to this work, we developed a simple theory of Pauli blocking in a Fermi gas with unitarity-limited collisional interactions. The results provide estimates of the maximum two-body scattering rates which can be used to restrict theories of collisional hydrodynamics in low temperature Fermi gases. These results are described briefly below.

Evidence for Superfluid Hydrodynamics in the Breathing Mode of a Strongly-Interacting Fermi Gas

Our experiments produce a highly degenerate, strongly interacting gas of ^{6}Li by all-optical methods: We use an ultrastable CO_2 laser trap to confine a mixture of the two lowest hyperfine states of ^{6}Li atoms, which is loaded from a standard magneto-optical trap (MOT) at a temperature of $\simeq 150\,\mu$K. A 50-50 mixture is produced by rate-equation radio-frequency pumping. Rapid evaporation to degeneracy is accomplished in a few seconds by applying a bias magnetic field near the Feshbach resonance at $\simeq 830$ G. High evaporation efficiency is achieved by maintaining a large ratio of trap depth to thermal energy, while lowering the trap depth by a factor of up to $\simeq 600$. The trap is then adiabatically recompressed to 4.6% trap depth. After this procedure, typically $N = 3 \times 10^5$ atoms remain at a temperature less then 0.1 of the Fermi temperature. The experiments achieve the conditions predicted for the onset of resonance superfluidity in a strongly interacting Fermi gas.

To excite the radial breathing mode, the trap is extinguished briefly (25 μs in our current experiments). The gas expands slightly during this period and then oscillates in the radial dimension after recapture, while the much slower axial oscillation is not excited. The gas is held for a variable time and then released from the trap. After 1 ms of expansion, the gas is imaged to determine the transverse radius of the cloud as a function of the hold time.

At magnetic fields near the Feshbach resonance, we find that the measured breathing mode frequencies are in very good agreement with recent predictions for a hydrodynamic gas with unitarity-limited mean field interactions. The results show that near resonance on either side, fermion pairs must be large, as the measured frequencies differ significantly from that of a molecular Bose-Einstein condensate.

At a magnetic field slightly above resonance, where the two-body physics does not support a bound state, we measured the temperature dependence of the damping time. In a collisionally hydrodynamic gas, one expects the collision rate to decrease as the temperature is lowered into the regime where Pauli blocking is effective. In that case, the gas becomes less hydrodynamic as the temperature is lowered, and the damping time decreases. We observe the opposite: The damping time increases strongly as the temperature is lowered, providing evidence of superfluid hydrodynamics.

Unitarity-Limited Elastic Collision Rate in a Harmonically Trapped Fermi Gas

A two-component atomic Fermi gas in the vicinity of a Feshbach resonance has an s-wave scattering length which is large compared to the de Broglie wavelength of the colliding fermions. Hence, the gas is unitarity-limited and the elastic scattering cross section takes the form $\sigma(k) = 4\pi/k^2$, where k is the relative de Broglie wavevector. Previous estimates of the collision rate in a Fermi gas are valid only for a constant,

energy-independent scattering cross section. Hence, there was a need for predictions in the unitary regime which is relevant to many current experiments.

We developed a simple two-body scattering model based on the Boltzmann equation. We assume that the effective range is small although the scattering length is large. The model determines the maximum elastic scattering rate and also the temperature dependence of the collision rate including Pauli blocking, which suppresses the scattering rate as the temperature is reduced below the Fermi temperature.

By incorporating these results in a relaxation approximation model, we find that the anisotropic expansion observed in our previous experiments may not be explained by collisional hydrodynamics. This is consistent with recent theory which predicts a large temperature increase during collisional hydrodynamic expansion of a low temperature gas, in contrast to our observations.

The results also determine the maximum damping time of the breathing mode for a collisionally hydrodynamic gas as well as providing an estimate of the temperature dependence. The predictions for a collisional gas are inconsistent with our observations.

3. Future Plans

Our immediate plans include a thorough study of the magnetic field dependence of the breathing mode frequency. This will help to resolve a discrepancy between our measurements and those of the Innsbruck group, who observe an abrupt jump in frequency and a large damping rate at a field of 910 G. Their measured frequencies near the Feshbach resonance are also substantially below the hydrodynamic predictions. Our preliminary measurements appear to confirm their results for the abrupt frequency jump and increased damping, but at a substantially higher magnetic field. At lower fields near resonance, our original results are reproduced.

We have developed an improved method of controllably increasing the temperature at fixed atom number, and have plans to make an improved measurement of the temperature dependence of the damping time. This will help to determine the precise shape of the damping time as a function of temperature for comparison to future theories in the strongly interacting regime.

We also plan a study of the scissors mode of the trapped gas, by abruptly twisting the optical trap through a few mrad. The scissors mode is a surface mode, in contrast to the breathing mode which is compressional. Observing the magnetic field and temperature dependence of the scissors mode will provide further tests of recent theories of superfluid hydrodynamics in the Feshbach resonance regime.

4. References to Publications of DOE Sponsored Research

1) J. Kinast, S. L. Hemmer, M. E. Gehm, A. Turlapov, and J. E. Thomas, "Evidence for Superfluidity in a Resonantly Interacting Fermi Gas," Phys. Rev. Lett. **92**, 150402 (2004).
2) J. E. Thomas, S. L. Hemmer, J. Kinast, A. Turlapov, M. E. Gehm, and K. M. O'Hara, "Dynamics of a Highly-Degenerate, Strongly-Interacting Fermi Gas of Atoms," Proceedings of the Quantum Fluids Conference 2003 (Albuquerque, NM, August 3-8, 2003); J. Low Temp. Phys. **104** (2003).
3) J. E. Thomas, S. L. Hemmer, J. M. Kinast, A. V. Turlapov, M. E. Gehm, and K. M. O'Hara, "Dynamics of a Highly-Degenerate, Strongly-Interacting Fermi gas," Proceedings of the 16$^{\text{th}}$ International Conference on Laser Spectroscopy, (Palm Cove, Australia, July 13-18, 2003).
4) M. E. Gehm, S. L. Hemmer, K. M. O'Hara, and J. E. Thomas, "Unitarity-Limited Elastic Collision Rate in a Harmonically Trapped Fermi Gas," Phys. Rev. A **68**, 011603(R) (2003).

AUTHOR INDEX

Beck, Donald....24
Becker, Kurt H....135
Belkacem, A....111
Ben-Itzhak, Itzik....47
Benesch, Frank....237
Berrah, Nora....20
Bohn, John....139
Boyd, R....149
Bucksbaun, P.H....2
Campbell, Luke....205
Chandler, David....49
Chang, Zenghu....93
Chu, Shih-I....142
Cocke, C.L....16
Cundif, Steven....60
Dalgarno, A....56
Dantus, Marcus....146
DePaolat, B.D....97
DiMauro, L.F....149
Ditmire, Todd....153
Doyle, John....51
Dunford, R.W....7, 78, 81
Ederer, D.L....7
Ellioff, Mike....49
Esry, B.D....103
Feagin, James....158
Gallagher, T.F....162
Gordon, Robert....165
Gould, Harvey....115
Gould, Phillip....168
Greene, Chris....171
Havener, C.C....79
Herschbach, Dudley....174
Hertlein, M....111
Ho, Tak-San....221
Holland, Murray....52
Jiang, Yan....237
Jin, Deborah....177
Jones, Robert R....181
Kanter, E.P....7, 78, 81
Kapteyn, Henry....201, 240
Klimov, Victor....67
Kolomeisky, Eugene....185
Krässig, B....7, 78, 81
Krausz, Ferenca....1
Kulander, K.C....149
Lee, Taewoo....237
Lin, C.D....8
Litvinyuk, Igor....101
Lundeen, Stephen....189
Macek, J.H....193
Manson, Steven....29
McCurdy, C.W....36
McKoy, Vincent....197
Menoni, Carmen....240
Mokler, P.H....78
Msezane, Alfred....74
Mukamel, Shaul....205
Murnane, Margaret....201
Nelson, Keith....209
Novotny, Lukas....213
Orel, A.E....34
Orlando, Thomas....40
Phaneuf, Ronald....217
Poliakaff, Erwin....28
Prior, M....111
Rabitz, Herschel....221
Raithel, G....225
Raman, Chandra....229
Reis, D.A....2
Rejoub, R....79
Reseigno, T.N....36
Richard, P....89
Robbins, D.L....71
Robicheaux, F....233
Rocca, Jorge....240
Rose-Petruck, Christoph G....237
Sanche, Léon....33
Schoenlein, Robert W....118
Schultz, David R....122
Seideman, Tamar....244
Smith, A.J....71
Southworth, S.H....7, 78, 81
Starace, Anthony....43
Stockman, Mark....63
Stöhlker, Th....78
Tarnovsky, Vladimir....135
Thomas, T. Darrah....248
Thomas, John E....252
Thumm, Uwe....107
Unstadter, Donald....12
Valentini, James....49
Walmsley, I.A....149
Young, L....7, 78, 81